University of Bath

PHD

Investigation into the role of the RNA methyltransferase NSun2 in neuroplasticity regulation

George, Harry

Award date:
2019

Awarding institution:
University of Bath

Link to publication

Alternative formats
If you require this document in an alternative format, please contact:
openaccess@bath.ac.uk

Copyright of this thesis rests with the author. Access is subject to the above licence, if given. If no licence is specified above, original content in this thesis is licensed under the terms of the Creative Commons Attribution-NonCommercial 4.0 International (CC BY-NC-ND 4.0) Licence (https://creativecommons.org/licenses/by-nc-nd/4.0/). Any third-party copyright material present remains the property of its respective owner(s) and is licensed under its existing terms.

Take down policy
If you consider content within Bath's Research Portal to be in breach of UK law, please contact: openaccess@bath.ac.uk with the details. Your claim will be investigated and, where appropriate, the item will be removed from public view as soon as possible.

Download date: 05. May. 2023

Investigation into the role of the RNA methyltransferase NSun2 in neuroplasticity regulation

Harry Samuel George

A thesis submitted for the degree of Doctor of Philosophy

University of Bath

Department of Biology and Biochemistry

August 2019

UNIVERSITY OF BATH

Copyright notice

Attention is drawn to the fact that copyright of this thesis/portfolio rests with the author and copyright of any previously published materials included may rest with third parties. A copy of this thesis/portfolio has been supplied on condition that anyone who consults it understands that they must not copy it or use material from it except as licenced, permitted by law or with the consent of the author or other copyright owners, as applicable.

Access to this thesis/portfolio in print or electronically is restricted until ……. (date).

Signed on behalf of the Doctoral College.....(print name)…….

Author’s declaration

I am the author of this thesis, and the work described therein was carried out by myself personally, except where indicated by specific reference in the text. Work done in collaboration with, or with the assistance of others, is indicated as such. The material presented here has not been submitted for any other academic award. Any views expressed in the dissertation are those of the author.

SIGNED: .....H.George..... DATE:.....07.08.2019.....

Acknowledgements

First and foremost, I would like to thank my supervisor Shobbir Hussain who entrusted me with his project, I am grateful for the opportunity and I hope I have made him proud. I would also like to thank Zafar Bashir, who agreed to take me into his lab for a couple of months; unfortunately for him, I ended up staying for a couple of years. I hugely appreciate both of your faith, guidance and support that has undoubtedly made this thesis possible. I would also like to thank everyone in the Bashir lab for their support and, more importantly, their friendship. To name but a few: Mahsa, Ola, Ben, Gareth, Clair, Paul, Jasmine, Marie and Ellen.

The biggest thanks must go to my Mum, Dad and brother, who are always there for me no matter what. Last but not least, my partner, Alex. Her unwavering support and ability to cheer me up after a difficult day in the lab has made this experience much easier. My family have always believed in me when sometimes I do not.

Abstract

Disruption of the NSun2 gene in humans is known to cause an intellectual disability syndrome. The clinical presentation of the disorder is similar to Fragile X Syndrome and Tuberous Sclerosis Complex, two diseases which have been strongly associated with deficits in synaptic plasticity formation. The NSun2 protein, which can regulate protein synthesis, is known to locate to the dendrites of neurons, thus raising the possibility that it too may play a role in postsynaptic modulation pathways. Utilising a transgenic NSun2-deficient murine model, this thesis work aimed to investigate whether disruption of NSun2 might lead to relevant synaptic plasticity defects known to be associated with impaired memory and learning. Thus e*x-vivo* field recordings were obtained from the CA1 hippocampus of NSun2-deficient mice via stimulation of the *schaffer collateral* pathway. Alongside these experiments, whole cell current-clamp recordings were used to investigate intrinsic properties and plasticity of Cornu Ammonis (CA) 1 pyramidal neurons. The field recordings demonstrated a deficit in N-methyl-D-aspartate (NMDA) receptor-dependent long-term potentiation (LTP) and long term depression (LTD) with no deficits observed in metabotropic glutamate receptor (mGluR)-LTD. The current-clamp recordings revealed that NSun2 mutant pyramidal cells fire action potentials at a faster rate and have a faster membrane time constant.

The work presented in this thesis suggest that the key neurological aspects observed in NSun2-deficiency syndromes may be caused by deficits in hippocampal synaptic plasticity mechanisms, with NMDA receptor signalling playing important, likely central, roles.

Table of contents

Abbreviations

ABP-GRIP	AMPA receptor-binding protein–glutamate receptor interacting protein
aCSF	Artificial cerebral spinal fluid
ADP	After-depolarisation
AHP	after-hyperpolarisation
AIS	Axon initial segment
AMPA	α-amino-3-hydroxy-5-methyl-4-isoxazolepropionic acid
ANO2	Anoctamin-2
BDNF	Brain-derived neurotrophic factor
BK	Big potassium channel
BP	Binding protein
CA	Cornu Ammonis
CACCs	Calcium-activated chloride channel
CaMKII	$Ca2^{+}$/calmodulin-dependent protein kinase
CHX	Cycloheximide
CNS	Central nervous system
Cm	Membrane capacitance
CYFIP1	Cytoplasmic FMR1-interacting protein 1
D-AP5	D-2-amino-5-phosphonovalerate
DG	Dentate gyrus
DSI	Depolarisation-induced suppression of inhibition
DTE	Dendritic targeting elements
E-LTP	Early-phase long-term potentiation
EC	Entorhinal cortex
EIF	Eukaryotic translation initiation factor
EPSC	Excitatory post-synaptic current
EPSP	Excitatory postsynaptic potential
ERK	Extracellular signal-regulated kinase
fEPSP	Field excitatory postsynaptic potential
FMRP	Fragile-X Mental Retardation Protein
FTO	Fat Mass and Obesity-Associated

FXS	Fragile X Syndrome
GABA	Gamma-aminobutyric acid
GFP	Green flourescent protein
GPCR	G-Protein coupled receptors
HCN	Hyperpolarisation-activated cyclic nucleotide-gated
HFS	High frequency stimulus
Ih	h-current
IM	M-current
IP3	Inositol 1,4,5-trisphosphate
L-LTP	Late-phase long-term potentiation
LFS	Low frequency stimulation
LTD	Long-term depression
LTP	Long-term potentiation
m5C	5-methylcytosine
m6A	N6-Methyladenosine
mAHP	Medium after-hyperpolarisation
MAPK	Mitogen-activated protein kinase
MCPG	α-methyl-4-carboxyphenylglycine
mGluR	Metabotropic glutamate receptor
miCLIP	Methylation individual nucleotide resolution crosslinking immunoprecipitation
mRNA	Messenger Ribonucleic acid
mTOR	Mammalian target of rapamycin
NF-kB	Factor kappa-light-chain-enhancer of activated B
NGF	Nerve growth factor
NMDA	N-methyl-D-aspartate
NPM-1	Nucleolar phosphoprotein-1
NSF	N-ethylmaleimide-sensitive factor
NSun2	NOP2/Sun domain family member 2
PAK	p21-activated kinase
PBS	Phosphate Buffered Saline
PCC	Pearson Correlation Coefficient
PCR	Polymerase Chain Reaction
PICK1	Protein interacting with C kinase 1

PK	Protein kinase
PLC	Phospholipase C
PN	Pyramidal neuron
PP	Protein phosphotase
PP-LFS	Paired pulse low-frequency stimulus
PPF	Paired-pulse facilitation
PPR	Paired pulse ratio
PSD	Postsynaptic density
PSI	Protein synthesis inhibitor
(RS)-3,5-DHPG	(RS)-3,5-Dihydroxyphenylglycine
RBP	RNA binding protein
Ri	Input resistance
Rm	Membrane resistance
RMP	Resting membrane potential
RNA	Ribonucleic acid
rRNA	Ribosomal ribonucleic acid
SC	Schaffer collateral
SEM	Standard error of mean
SFA	Spike frequency adaptation
SK	Small-conductance Ca^{2+}-activated K^{+}
SP-LFS	Single pulse low-frequency stimulus
STDP	Spike-timing dependent plasticity
STM	Short-term memory
SUnSET	Surface sensing of translation
svRNA	Small vault RNA
TAE	Tris-acetate EDTA
TAP	Temporoammonic Pathway
TARP	AMPA receptor Regulatory Protein TARP
TBS	Theta-burst stimulation
τm	Membrane time constant
TrkB	Tropomyosin receptor kinase B
tRNA	Transfer ribonucleic acid
UTR	Untranslated Region
VFD	Venus flytrap domain

VG	Voltage gated
Vm	Membrane potential
vtRNA	Vault RNA

List of figures and tables

Aims

The overarching aims of this research is to establish the underlying neurological mechanisms which may be responsible for the learning and memory deficits observed in human NSun2-deficiency syndromes. For this purpose, a transgenic mammalian model of NSun2-deficiency will be utilised for electrophysiological investigation. The primary hypothesis to be tested will be that NSun2 may play key roles in synaptic plasticity modulation in the hippocampus, a process which is known to be central for learning and memory formation within neural circuits. Intrinsic neurophysiological properties of relevant neuron types will also be investigated in order to further characterise any deficits that may be present. In order to provide some clues into relevant underlying molecular mechanisms, a basic characterisation of NSun2 protein behaviour within neuronal-like cells will also be performed. This additional work will be carried out via immunofluorescence imaging investigations *in vitro*.

Chapter 1. Introduction

Four introductory chapters are presented within this thesis. Chapter 1.1 describes the electrochemical properties of neurons during both sub- and supra-threshold states. These fundamental properties are vital in understanding the behaviour of a neuron at rest and when responding to stimuli. Discrepancies in these properties between different experimental models can be indicative of possible changes to aspects such as cell morphology or ion channels within the membrane, therefore affecting how information is encoded, an aspect that is regularly investigated in intellectual disability models. Alongside this, the chapter discusses relevant synaptic transmission, specifically the chemical synapse and some of the ionotropic and metabotropic glutamatergic receptors involved.

The majority of experiments in this thesis work were conducted in the CA3 region of the mouse hippocampus. Chapter 1.2 explores the hippocampus, a temporal lobe structure which is known to be involved in spatial cognition. A detailed anatomical description is provided in order to clarify terminology used for the rest of this thesis (as definitions of the hippocampal formation can vary). Current knowledge concerning the role of the mammalian hippocampus in memory and learning is also covered.

Chapter 1.3 explores both synaptic and intrinsic properties of neurons; these processes involve complex molecular mechanisms altering synaptic connections that are necessary for memory and learning. Within this chapter there is a focus on the current understanding of LTP and LTD, both of which are already strongly implicated in other intellectual-disability syndromes, and are investigated in relation to NSun2-deficiency in this thesis.

Chapter 1.4 examines our current knowledge of NSun2-deficiency and normal NSun2 function. An appreciation of the molecular roles of NSun2, such as being

an established regulator of protein synthesis, may indeed be particularly relevant to a potential role in synaptic plasticity modulation. Thus, a broader discussion of post-synaptic protein synthesis and its probable involvement in learning and memory is also provided.

1.1. Electrochemical properties of the neuron

Neural properties vary depending on the location of the neuron, its developmental stage and the neuronal type. Although these properties may differ between neurons, there are underlying principles that are shared by all. This chapter will discuss the resting membrane potential, sub-threshold and spiking properties as well as synaptic transmission and the receptors involved.

1.1.1. Resting membrane potential

A plasma membrane encases all living cells including neurons. This membrane consists of a rather dynamic phospholipid bilayer in which different proteins are embedded, such as ion channels, to provide a wealth of varied functionality. Being an efficient insulator, the membrane provides a barrier to charged molecules and separates the internal fluid of the cell from the extracellular media. This separation of fluid combined with specialised ion pumps provides a distribution of ions (Table 1.1) maintaining a concentration gradient and causing an electrical potential difference across the membrane. The resting membrane potential of neurons can fall between -40 to -90mV with the average sitting at around -65mV. The three ionic species contributing greatest to the resting membrane potential are K^+, Na^+ and Cl^-, with high intracellular concentrations of K^+ and low Na^+ and Cl^- (Table 1.1). Specialised proteins called ion pumps help to maintain the concentration gradient; the Na^+/K^+ pump exploits the energy released from ATP breakdown to ADP. This pump is electrogenic because, for

every cycle, 3 Na^+ ions are pumped out of the cell and 2 K^+ ions into the cell and therefore negatively charges the cell. Transporters also exist for Ca^{2+} and Cl^- ions.

Ion	Intracellular Concentration (mM)	Extracellular Concentration (mM)	Equilibrium Potential (mV)
K^+	140	5	-92
Na^+	10-15	145	+64
Cl^-	4	110	-88

Table 1.1. Approximate extracellular and intracellular concentrations for key ions for the average neuron

Another factor contributing to the negative resting membrane potential is the permeability of the membrane to each ionic species. An equilibrium potential can be calculated with both the intracellular and extracellular concentrations, which describes the membrane potential being at a state where ion influx is equal to ion efflux (net ion flux of 0). The negation of a net ion flux is caused by the fine balance of chemical and electrical driving forces and can be calculated with the Nernst Equation:

$$E_x = \frac{RT}{zF} \ln \frac{[X]_o}{[X]_i}$$

Where E is the equilibrium potential for the ion being considered (x), R for the gas constant, T for the temperature (Kelvin), z for the valence of ion, F is the Faraday constant and finally, $[x]_i$ and $[x]_o$ are the ionic concentration inside and outside the cell, respectively.

If, for example, the membrane of a neuron was only permeable to K^+ then the resting membrane potential would be equal to E_k (approximately -92mV). This is because K^+ will diffuse along its chemical concentration gradient resulting in K^+ exiting the cell resulting in a loss of positive charge inside the cell. When the membrane potential is equal to E_k then the net flux of K^+ will be equal to 0. However, neurons do not rest at E_k because they are not only permeable to K^+, but also Na^+ and Cl^-. It is the level of membrane permeability for each ion that dictates the extent of the ions' influence on the resting membrane potential. In a neuronal membrane, the greatest permeability is for K^+ and so the resting membrane potential sits closer to E_k than equilibriums for the other ion species. The Goldman Hodgkin Katz Equation is a modified Nernst equation and takes into account all the relative permeabilities of each ionic species to calculate the resting membrane potential. The Goldman equation is as follows:

$$V_m = \frac{RT}{F} \ln \frac{P_K[K^+]_o + P_{Na}[Na^+]_o + P_{Cl}[Cl^-]_i}{P_K[K^+]_i + P_{Na}[Na^+]_i + P_{Cl}[Cl^-]_o}$$

Where the symbol meanings remain unchanged from the Nernst equation, other than V_m for membrane potential and P for permeability of the ion under consideration.

1.1.2. Passive membrane properties

Passive membrane properties, also referred to as cable properties, have an essential role in neuronal signalling. They can influence the velocity of membrane potential changes as well as the magnitude over time of these changes. Three passive membrane properties exist:

1) Membrane resistance (R_m) influences the ability for ions to cross the membrane. The phospholipid bilayer membrane is a good insulator making it difficult for ions to cross the membrane, however, ion channels embedded within membranes offer a pathway for ions to pass into or out of the cell and therefore their presence lowers R_m. If more ion channels are open at rest, then R_m will be dramatically decreased. Another factor influencing the membrane resistance is the cell size; a larger cell will have a larger membrane and therefore a greater area for charge to leak leading to a lower R_m.

2) Membrane capacitance (C_m) is the membranes ability to store charge. Acting as an insulator, the membrane separates two conductive solutions: the intracellular and extracellular media. The specific capacitance of a membrane is approximately 1 $\mu F.cm^{-2}$. This fixed value means that the capacitance is directly proportional to the size of the neuron and a larger neuron with a higher capacitance needs more charge to alter V_m.

3) Internal axial/cytoplasmic resistance is the ability of charges to spread through the cell; it is the resistance presented by the cytoplasm. The smaller the diameter of the neuron, the higher the axial resistance.

It is possible to make estimations of passive membrane properties through measurements of voltage changes in response to square-wave current injections applied to individual neurons during electrophysiology experiments.

Any changes that ensue in response to an applied current cannot be instantaneous because of the capacitive and resistive properties of the membrane. The rise and decay of voltage changes will therefore be slower than the instantaneous current changes applied by the experimenter. As a current is applied, the membrane (capacitor) becomes charged and the current crossing the membrane (resistor) through the ion channels increases, gradually shifting the membrane potential to a steady state. The rate of the membrane potential change can be described by the membrane time constant (τm): the time taken to reach 63% of the final voltage (Kita et al., 1984).

Using square-wave current injections experimentally can lead to useful insights. Firstly, input resistance (R_i) can be measured from the steady state voltage response to a current injection and calculating it with Ohm's law (V = IR). A cell with a larger R_i requires less current injected into a given cell for the same membrane potential change. R_i can be a determinant of open channels, internal axial resistance and the cell size (Kandel, 2013). Secondly, the membrane time constant can be estimated by fitting an exponential curve to a voltage response prior to it reaching a steady state. As emphasised by W.Rall (1959), the application of current to a neural soma will cause it to spread across the cell body but a significant volume of current will flow axially through the axon and dendrites as well as through the membrane into the extracellular fluid. There are many factors that determine the spread of current: soma size, axon length, dendritic branching and cell diameter as well as electrical considerations such as the capacitive and resistive properties of the membrane and intra- and extra-cellular fluid resistivity.

Measurements taken from voltage transients at the soma, as done in the conventional "patch-clamp" technique, takes into account axial current flow to dendrites as well as current spread across the soma. For this reason, fitting a single exponential curve to a voltage response may underestimate the membrane time constant (Rall, 1957). However, the majority of publications do

in fact use a single exponential curve for analysing time constants and allows effective comparisons between experimental groups; a difference in τm can be an indicator of difference in soma size, diameter of the neuron as well as branching of dendrites and spine size or number. However, it is not possible to identify specific morphological changes in a neuron if a τm alteration was observed in an experimental model and would therefore require morphological investigations.

1.1.3. Subthreshold membrane conductance

CA1 pyramidal neurons (PNs) possess voltage gated ion channels activated when a neuron is in a lower voltage range than is required for action potentials to occur. Two prominent and well-studied channels are the K_V7/KCNQ channel and the hyperpolarisation-activated cyclic nucleotide-gated (HCN) channel. K_V7/KCNQ channels are mediators of the M-current (I_M) and HCN channels mediate the h-current (I_h). Both channels are integral to maintaining the resting membrane potential of a neuron among other physiological properties.

Two subunits from the KCNQ family, K_V7.2 and K_V7.3, are key contributors to the I_M, which is an outward current triggered approximately at potentials above -60mV and below the action potential-threshold. The channels are slow-activating and do not inactivate. They are also inhibited by G-Protein Coupled Receptors (GPCRs) activated by neurotransmitters and are integral to burst firing, spike-frequency adaptation (SFA) and after-spike potentials (Brown and Passmore, 2009).

HCN channels are activated at lower potentials than KCNQ channels, at under -60mV. Because they are active at potentials close to the resting membrane potential, they contribute to its maintenance. With permeability to K^+ and Na^+, HCN channels are inward-rectifying at a neuron's resting membrane potential and aid in depolarisation of the membrane due to having a reversal potential of -

20mV. The observation of I_h is possible with current-clamp recordings by injecting a negative current step to hyperpolarise the membrane. A distinctive "sag" potential occurs as the membrane potential deflects back towards a more depolarised potential before reaching a steady-state (Robinson and Siegelbaum, 2003). In CA1 PNs, both HCN1 and HCN2 channels are expressed in a gradient fashion throughout neurons with the highest density residing in distal dendrites. They are believed to be involved in SFA and after-hyperpolarising potentials (Magee, 1999) as well as restraining spatial memory in rodents (Nolan et al., 2004).

1.1.4. The action potential

The action potential was first analysed in the squid axon by Hodgkin and Huxley (Hodgkin and Huxley, 1952) where only two voltage-gated channels were observed. An axonal action potential has a primary purpose of propagating a signal over distance whereas action potentials in the cell body serves a vastly different function. Action potentials in cell bodies are more complex, they can encode information through frequency and pattern and can respond to minute changes in current injections resulting in substantial changes in firing frequency (Bean, 2007; Connors and Gutnick, 1990; Tateno et al., 2004). The greater complexity of mammalian cell body membranes compared to the poorly encoding squid axon is due to a richer expression of voltage-dependant ion channels (Bean, 2007). In fact, there have been reports of almost 500 ion channel genes in mammalian genomes (including their variants) (Ashburner et al., 2000).

Action potentials almost always initiate in the axon initial segment (AIS), which is found proximal to the soma, in the case of the CA1 PN, 30-50μm away (Bean, 2007). This region contains a high concentration of voltage-gated (VG) ion channels and integrates incoming potentials (Kole and Stuart, 2012). Once the AIS is depolarised to a threshold of around -50mV, VG-sodium channels open.

The inward current activates rapidly, on the scale of microseconds, and contributes to the rising phase of the action potential. The activation of these channels is self-perpetuating; as more sodium channels are activated, this causes yet more of them to activate. The influx of sodium causes the membrane potential to depart from its resting state and move towards, but not reaching, the sodium equilibrium potential (Hodgkin and Huxley, 1952). Two crucial mechanisms ensure the depolarisation is a brief process: the inactivation of the VG-sodium channels dramatically and rapidly decreasing sodium influx and the increase in potassium conductance via the opening of VG-potassium channels (the action potential time course with sodium and potassium channel permeability is shown in Figure 1.1). Following these two processes the membrane undergoes a refractory period where the membrane potential falls slightly below the resting membrane potential. This prevents the neuron from being able to fire an action potential during this time (order of milliseconds) (Purves D, 2001). The after-hyperpolarisation is observed more often than not but is not universal across all neuron types. Distinct phases can also be observed with slow, medium and fast components sometimes being distinguishable. Some of the specific channels that can contribute to the after-hyperpolarisation include small-conductance Ca2+-activated K+ (SK)-channels (Pedarzani et al., 2005) and Big Potassium (BK)-channels (Faber and Sah, 2003). The action potential initiated in the AIS is able to propagate along the axon because the sodium influx passively acts on neighbouring voltage-gated sodium channels, thereby triggering an action potential in that axonal region. This process continues and spreads through the axon until it reaches the terminal of the axon (Purves D, 2001).

The basic mechanics of action potentials are shared among all neurons, however, the hundreds of ions channels and ion channel isoforms that exist are differentially expressed in neurons and consequently provide different excitable properties. For example, channels can influence the probability of a neuron to fire in response to any given input, the pattern and frequency of action potential

firing as well as how they integrate information (Bean, 2007). Advances in genetics, pharmacology and whole-cell techniques has helped reveal the vast diversity of ion channels. This diversity serves a huge advantage by improving the computational power of a neural network.

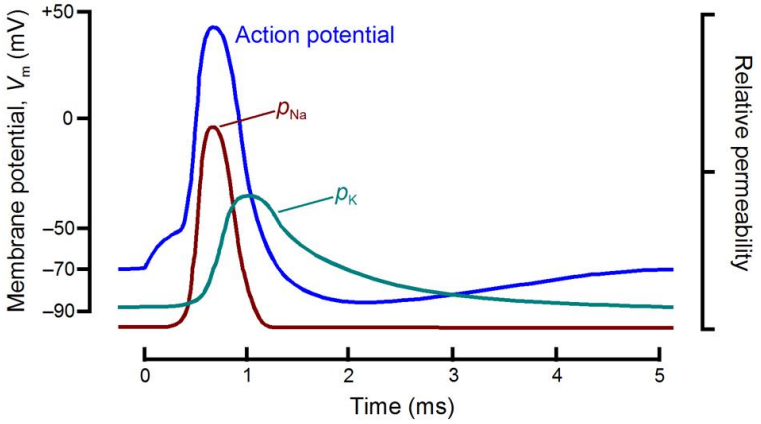

Figure 1.1. Time course of potassium and sodium permeability during an Action Potential

Sodium drives the upstroke of the action potential. The combination of sodium channel inactivation with the delayed-onset of potassium channel activation leads to an efflux of potassium ions resulting in the downward phase of the Action Potential (PhysiologyWeb, 2000).

1.1.4.1. After-spike potentials

Intuitively named, the after-spike potential describes potential changes after an action potential (also known as a spike). It is an important physiological occurrence that can influence firing patterns and therefore impacts the encoding of information. Blocking after-potentials pharmacologically has been shown to affect the firing patterns of neurons in response to current injections (Brown and Randall, 2009). After-spike potentials are bidirectional, in that it can both

depolarise (after-depolarisation (ADP)) and hyperpolarise (after-hyperpolarisation (AHP)) neurons and both occur in CA1 PNs.

After-spike potentials generally begin with a fast AHP, lasting for a few milliseconds instigated by BK channels (Gu et al., 2007). This is then followed by a fast ADP and if large enough, can push the membrane potential back to threshold level and instigate another spike. Evidence suggests the fast ADP is caused by a persistent Na^+ current (Azouz et al., 1996; Yue et al., 2005). A medium AHP follows, lasting up to 200ms, and is thought to be mediated by I_M and I_h (Gu et al., 2005). Finally, a slow AHP ensues lasting for several seconds.

1.1.5. Synaptic transmission

1.1.5.1. The chemical synapse

Throughout the 1930's to the 1960's the existence of chemical synapses was fiercely debated (Todman, 2008). The initial chemical synapse proposal by Henry Dale in the early 1920's was eventually accepted after synapses were investigated from many different angles from pioneers such as John Eccles. The chemical synapse is a specialised point of contact between neurons and allows the formation of neural networks by permitting connectivity. Estimates on the total number of synapses in the human brain fall at around 10^{15}, an astronomical value which perfectly encapsulates the complexity of neural circuits (Drachman, 2005). The chemical synapse can lead to either inhibitory and excitatory postsynaptic responses and has the capability to amplify signals. Activation of postsynaptic receptors can induce downstream metabolic changes of the postsynaptic cell that lasts far longer than the causative stimulus.

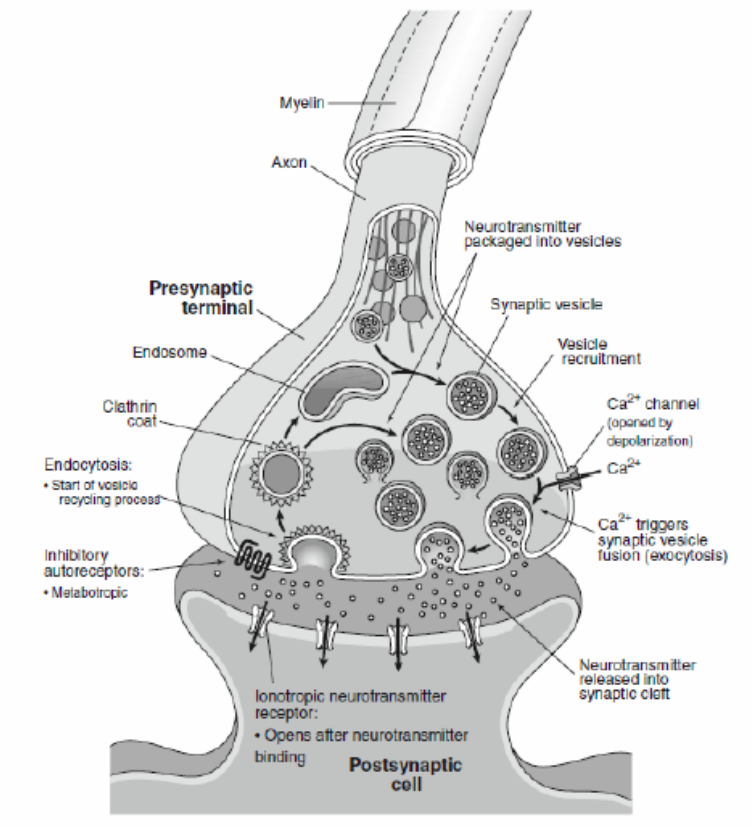

Figure 1.2. The chemical synapse

A chemical synapse is comprised of several components. 1) The vesicle-containing presynaptic terminal, the site of neurotransmitter release. 2) The synaptic cleft, which is situated between pre- and post-synaptic compartments where neurotransmitters diffuse through. 3) The postsynaptic region holding postsynaptic receptors in its membrane. Voltage-gated Ca^{2+} activation caused by the arrival of an action potential leads to vesicle docking and neurotransmitter release across the synaptic cleft. The neurotransmitter binds to its complimentary binding site on specific postsynaptic receptors that can influence the postsynaptic membrane potential. (Image from Conn, 2008).

1.1.5.1.1. Presynaptic neurotransmitter release

The presynaptic component, or “bouton”, of a synapse contains numerous neurotransmitter-containing vesicles that can be found either docked or

undocked within the Active Zone (the site of neurotransmitter release). The Active Zone is a region of the pre-synaptic terminal consisting of the pre-synaptic membrane and associated proteins involved in the release of vesicles across the synaptic cleft (Schikorski and Stevens, 1997). The vesicles that dwell within the Active Zone is called the Readily Releasable Pool.

The contents of a vesicle are largely determined by the cell type. If the cell were to be excitatory then the vesicle is likely to contain glutamate or another excitatory neurotransmitter whereas if the cell was inhibitory then gamma-aminobutyric acid (GABA) would likely reside within the vesicle. The excitatory and inhibitory characterisation of the neurotransmitter depends on the postsynaptic membrane response to said neurotransmitter; excitatory leads to depolarisation and inhibitory leads to hyperpolarisation of the membrane potential.

If the presynaptic terminal becomes sufficiently depolarised as a result of a propagated action potential, then Ca^{2+} will enter via VG-Ca^{2+} channels in close vicinity to the vesicles. The local increase in intracellular Ca^{2+} binds to specific proteins such as Synaptogamin triggering fusion of the vesicles to the presynaptic membrane (Katz and Miledi, 1968; Martens et al., 2007; Schikorski and Stevens, 1997). Its subsequent release into the synaptic cleft involves an intricate mechanism involving the formation of vesicle-presynaptic membrane fusion protein complexes (Chapman, 2008; Murthy and De Camilli, 2003). The majority of fusion reactions involve SNAREs, an essential fusogen that can overcome the energy barrier for the fusion of phospholipid membranes and allow exocytosis (Jahn et al., 2003). The SNARE complex formation (whereby v-SNARE and t-SNARE proteins combine from the separate membranes to form a SNAREpin, also known as a trans-SNARE complex) is widely accepted for its role in exocytosis. Information regarding aspects such as the specific dimerization of SNARE transmembrane domains and the regulatory proteins

involved, such as Munc18-1, has provided a detailed overview of the molecular mechanisms underpinning neurotransmitter release (Han et al., 2017).

An important characteristic of neurotransmitter release is the quantal release (discrete volume of neurotransmitter release), which is probabilistic by nature (approximately only 15% of action potentials result in neurotransmitter release (Dobrunz and Stevens, 1997). After release of the neurotransmitter, it diffuses across the synaptic cleft and activates postsynaptic receptors completing the transfer of information from one neuron to another.

1.1.5.1.2. Postsynaptic receptors

Postsynaptic neurotransmitter receptors are generally categorised into metabotropic and ionotropic receptors defined by their modes of action. Ionotropic receptors are ligand-gated ion channels that forms a pore allowing the passage of ions when activated from the binding of the neurotransmitter. These receptors form the fast component of synaptic transmission, usually in the order of milliseconds. On the other hand, metabotropic receptors generally belong to the GPCR family and so do not form ion pores upon activation but rather indirectly modify other proteins, including other ion channels. Upon the neurotransmitter binding to a metabotropic receptor, a cascade of events can occur with wide-ranging effects from phosphorylation to gene expression (Kandel, 2013). Excess neurotransmitter is swiftly cleared from the synaptic cleft through re-uptake by neurons and glia and enzymatic degradation that is a necessary to preserve the temporal fidelity of synaptic transmission (Amara and Kuhar, 1993; Kandel, 2013).

1.1.5.1.3. Ionotropic glutamate receptors

1.1.5.1.3.1. AMPA receptors

Forming the bulk of the fast component of excitatory synaptic transmission, the α-amino-3-hydroxy-5-methyl-4-isoxazolepropionic acid (AMPA) receptor is comprised of four subunits: GluA1–4 (Palmer et al., 2005). Each subunit shares a 68–73% sequence homology and consists of three transmembrane domains and a cytoplasmic re-entrant loop forming the channel pore (Hollmann and Heinemann, 1994). Alongside these structural features, the AMPA receptor has an intracellular C-terminal tail to allow interactions with other molecules and proteins, and a large extracellular N-terminus, possibly for the binding of a second ligand (Palmer et al., 2005). There are various combinations of the four subunits forming a tetramer and the subunit configuration can be determined by the brain region as well and the developmental stage of the animal (Palmer et al., 2005). To add a further layer of complexity, AMPA receptors with different subunit compositions are differentially regulated through synaptic plasticity as well having differing functional characteristics (Sheng and Kim, 2002; Song and Huganir, 2002).

Like many messenger ribonucleic acids (mRNAs), AMPA receptor transcripts are subject to modifications; having a large impact on AMPA receptor functionality is RNA editing at the Q/R site residing in the GluA2 subunit located specifically in the re-entrant loop area. In this site (amino acid 607), the RNA encodes a glutamine (Q) residue, however over 99% of cerebral GluA2 subunits express arginine (R) (Bredt and Nicoll, 2003; Palmer et al., 2005, 1997). Importantly, this modification creates AMPA receptors that are impermeable to Ca^{2+} and with a linear rectification (GluA2-negative AMPA receptors are inwardly rectifying). The explanation of what seems an over-representation of modified GluA2-containing receptors could be attributed to the increased retention of GluA2 in the endoplasmic reticulum (Bredt and Nicoll, 2003). Other

possible transcript modifications can occur at the R/G site of the other AMPA receptor subunits and can also be influenced by alternative splicing (Palmer et al., 2005).

1.1.5.1.3.2. NMDA receptors

Similar to AMPA receptors, N-methyl-D-aspartate (NMDA) receptors are also tetramers with a variety of possible subunit compositions limited to either two obligatory GluN1 subunits combined with either two GluN2 or -3 subunits (of which there are four GluN2 subunits, GluN2A, -B, -C and –D, and two GluN3 subunits, GluN3A and –B varieties) (Paoletti et al., 2013). Unlike AMPA receptors, NMDA receptors are not only gated by glutamate, but are also co-gated by glycine via GluN1 and GluN3 subunits as well as D-serine via GluN1 and GluN3 (Paoletti et al., 2013).

The slower activation and deactivation kinetics of NMDA receptors are responsible for the slow component of excitatory transmission (in contrast to the AMPA receptor-mediated fast component). Comparable to AMPA receptors, NMDA receptor functional properties are influenced by its sub-unit composition (Dingledine et al., 1999; Paoletti et al., 2013). GluN2 subunits have been identified as having a huge impact on not only the conductance of channel but also its probability of opening as well as its deactivation kinetics (Paoletti et al., 2013). Regulation of NMDA receptors is multifaceted as numerous factors can influence its functionality and trafficking. For example, phosphorylation, numerous allosteric modulators and pH can affect NMDA receptors (Dingledine et al., 1999). As explained in the previous section, AMPA receptors are largely impermeable to Ca^{2+} (due to the Q/R editing) which is in stark contrast to NMDA receptors which readily allow the flux of Ca^{2+}. A distinctive trait of NMDA receptors is the presence of a Mg^{2+} block in the channel pore when the cell is at its resting membrane potential (Coan and Collingridge, 1985) providing a detector of pre- and post-synaptic activity. The reason being that the Mg^{2+} block

can only be removed upon depolarisation which then allows Ca^{2+} influx once glutamate binds to the NMDA receptor (Bliss and Collingridge, 1993). Ca^{2+} entry into the cell via NMDA receptors leads to a host of changes within the cell and underlines forms of plasticity that are explained in more depth in section 1.3.

1.1.5.1.3.3. Nicotinic acetylcholine receptors

Nicotinic receptors are ionotropic receptors, also known as cholinergic receptors, and are activated by the neurotransmitter acetylcholine which leads to an influx of cations, mainly Na+, into the neuron (Yakel, 2012). They are widely expressed in numerous brain regions including the hippocampus where they aid in the regulation of neural excitability and plasticity (Levin, 2002). The primary cholinergic input to the hippocampus is the medial septum and aids is sustaining network oscillations required for cognition (Cobb and Davies, 2005). Hippocampal GABAergic interneurons also contain nicotinic receptors and their activation is thought to induce rhythmic inhibition of pyramidal neurons (Griguoli and Cherubini, 2012).

It should be mentioned that nicotinic receptors are not the only form of cholinergic receptors; muscarinic receptors are also widely expressed in the brain and respond to acetylcholine leading to modulation of neural function and plasticity. However, muscarinic receptors are metabotropic and therefore their activation leads to intracellular changes via a second messenger, rather than opening a pore in the membrane.

1.1.5.1.4. Metabotropic glutamate receptors

Metabotropic glutamate receptors are named due to their activation by glutamate that leads to indirect metabotropic processes. They are all GPCRs, specifically members of the group C family. They can provide a huge number of functions and are broadly split into three groups: Group I, II and III. Group II

(mGluR2 and 3) and Group III (mGLuR4, 6, 7 and 8) receptors inhibit cAMP formation by activating a G protein causing the inhibition of adenylyl cyclase (Niswender and Conn, 2010)

Activation of Group II and III receptors has been associated with decreased NMDA receptor activity (Ambrosini et al., 1995) as well as involvement in forms of long-term synaptic plasticity (Bellone et al., 2008). Although research into these groups of receptors has been growing in recent years, they will not be discussed in this thesis; the below section will focus on the Group I metabotropic glutamate receptors.

1.1.5.1.4.1. Group 1 mGluRs

Group 1 metabotropic glutamate receptors (mGluRs) are a type of membrane-bound metabotropic receptor found within the peripheral membrane of post-synaptic densities of excitatory neurons as well as presynaptic regions (Lüscher and Huber, 2010). They are comprised of mGluR1 and mGluR5, both of which are linked to the heterotrimeric G protein, Gq, which allows the receptor to transmit signals from the receptor to intracellular domains. The widespread existence of mGluRs suggests they have a multitude of functions and have been targeted for pharmacological treatment of many different disorders including neurodevelopmental (Dölen et al., 2010) and neurodegenerative disorders (Kumar et al., 2015). mGluRs are members of the class C GPCRs and so have a large extracellular N-terminal domain, named the Venus flytrap domain (VFD) where the ligand-binding site is found (Pin et al., 2003). The VFD has three configurations: open-open which is stabilised by antagonists and the open-closed and closed-closed confirmations formed by ligand-binding. Many different ligands permit group1 mGluR activation, such as L-Glutamate, Dihydroxyphenylglycine (DHPG) and L-Quisqualic acid. DHPG is an exogenous compound that is deemed to be the most specific agonist of group 1 mGluRs (Niswender and Conn, 2010) as most other group 1 mGluR agonists also

activate alternative groups of mGluRs or activate ionotropic receptors (Schoepp et al., 1999). Interestingly, the VFD also has the ability to bind divalent cations such as calcium and magnesium, both of which can activate the receptor (Francesconi and Duvoisin, 2004). Once the ligand is bound to the VFD, the conformational change is propagated to the C-terminal tail.

Group 1 mGluR's couple to Gq/G11 which activates Phospholipase C (PLC). This activation results in phosphotinositide hydrolysis and the generation of diacyl-glycerol and Protein Kinase C (PKC) activation and the generation of inositol 1,4,5-trisphosphate (IP3) triggering Ca^{2+} release from intracellular stores. However this is by no means the only pathway initiated, as group 1 mGluRs also activate other pathways that stem from Gi/o, Gs and molecules that act independently to G-proteins (Hermans and Challiss, 2001). Upon activation several intracellular signalling mechanisms take place that can lead to synaptic plasticity as well as changes to intrinsic excitability; In the hippocampus, specific activation of mGluR5 can lead to the aforementioned PLC/IP3 pathways but evidence has also implicated both p38 mitogen-activated protein kinase (MAPK) and extracellular signal-regulated kinases (ERKs) in protein translation resulting in synaptic plasticity. This will be discussed in more detail in chapter 1.3.

Group 1 mGluR's have been extensively characterised in hippocampal pyramidal cells through decades of research. Their activation has been implicated in many neurophysiological alterations such as alterations to VG-ion channels (Charpak et al., 1990), a prime example being the modification to the K^+ activated Ca^{2+} current, otherwise known as I_{AHP}. Using whole cell recordings in a voltage clamp configuration, Charpack *et al.* (1990) injected square current pulses combined with fura-2, a calcium sensitive dye, in order to investigate a relationship between neuronal spiking and changes in calcium levels. The injected current elicited a train of action potentials which decreased in frequency over time, a process known as adaptation/accommodation. During this period

VG-Ca^{2+} channels open instigating an influx of Ca^{2+} into the cell. The elevated Ca^{2+} levels intracellularly initiate the opening of K^+ channels in order to inhibit further generation of action potentials, potentially preventing excitotoxicity, by allowing K^+ to exit the cell. However, with the application of group 1 mGluR agonists the adaptive response is diminished causing a constant generation of action potentials. The augmented firing frequency created a larger Ca^{2+} influx which has been attributed solely to a direct effect on I_{AHP} (Lancaster and Adams, 1986).

1.1.5.1.5. GABA receptors

Approximately 10-15% of neurons are categorised as GABAergic interneurons. These interneurons have a vast physiological and anatomical diversity and are found within every subfield of the hippocampus. The majority of their axons remain local to the subfield their cell bodies and dendrites reside, however some interneurons possess long ranging axons to ramify within the cortex. GABAergic interneurons can target well-defined post-synaptic regions as well as innervate widespread targets ensuring an extensive coverage of their principal cell targets (Pelkey et al., 2017).

By definition, interneurons release the inhibitory neurotransmitter, GABA, whose primary role utilises Cl^- influx or K^+ efflux via the activation of $GABA_A$ or $GABA_B$ (found in numerous cell types including pyramidal neurons and astrocytes) in order to hyperpolarise the cell membrane potential. For this reason, they not only regulate cell excitability but improve the temporal fidelity of networks through well-timed inhibitory input, thus shaping the timing of afferent and efferent information flow. They are also vital for the synchronization of oscillatory activity across different frequency domains between cortical circuits (Pelkey et al., 2017).

To emphasise the relevance of these receptors in intellectual disability disorders, such as Fragile X Syndrome, the FMR1 knock-out model has reduced GABA subunit receptors, overall GABA levels as well as overall decreased GABA input (Lozano et al., 2014). Recently a phase III trial has been completed with the use of Arbaclofen, a $GABA_B$ agonist; although the study did not meet the primary outcome of improved social avoidance (Berry-Kravis et al., 2017), the numerous investigations involving modulation of GABA receptors in intellectual disability disorders outlines its potential as a therapeutic target.

1.1.5.1.6. Monoaminergic receptors

Monoamine receptors are receptors whose activity is influenced by the binding of small-molecules with a monoamine structure. These receptors are generally all GPCRs and are important for neurophysiology and synaptic plasticity. Several of these receptor types are briefly discussed below.

1.1.5.1.6.1. Adrenergic

The mammalian hippocampus receives noradrenergic innervation originating at the principal site of the locus coeruleus (Sara, 2009). β-adrenergic receptors are known to be expressed in hippocampal neurons, including pyramidal and granule cells as well as interneurons (Guo and Li, 2007).

β-adrenergic signal via Gs protein, followed by the stimulation of adenylyl cyclase leading to the increase of intracellular cAMP and subsequent activation of PKA and indirect activation of ERK (mediated by β-arrestin, rather than a G-protein mechanism) (O'Dell et al., 2015). Both PKA and ERK are believed to have critical roles in synaptic plasticity with memory enhancement resulting from β-adrenergic receptor activation (Sweatt, 2004).

1.1.5.1.6.2. Dopaminergic

Dopamine receptors can be broadly split into two categories, D1-like and D2-like, categorised due to their reliance on different G-proteins and the resulting intracellular signalling pathways initiated. Both receptor types are found in the mammalian hippocampus in the molecular layer of the dentate gyrus and CA1 pyramidal cells and interneurons (Gangarossa et al., 2012).

Dopaminergic signalling has been established as having an important role in novelty related modulation of memory (Takeuchi et al., 2016). It was previously thought that dopaminergic modulation of the hippocampus was caused by innervation from the ventral tegmental area (Lisman and Grace, 2005), however later evidence suggests dopaminergic projections from the locus coeruleus also modulate hippocampal activity (Takeuchi et al., 2016). Optogenic activation of locus coeruleus fibres in hippocampal slices enhances schaffer collateral plasticity demonstrating the modulatory activity of dopamine in the hippocampus (Takeuchi et al., 2016).

Interestingly, a dopamine receptor falling under the D2-like receptor category, known as D4, has been implicated in the protein synthesis dependency of long-term potentiation. Pharmacological blockade of the D4 receptor in the hippocampus promoted a protein-synthesis dependent late phase of long-term potentiation and transformed early phase potentiation from protein-synthesis independent into a dependent form (Navakkode et al., 2017). This type of modulation could have implications in numerous protein synthesis deficient models.

1.1.5.1.6.3. Serotonergic

The final monoaminergic to be introduced is serotonin receptors. These receptors are split into 7 groups, 6 of which are metabotropic and 1 which is

ionotropic (5-HT_3). All of these subtype receptors have been identified in the hippocampus (Berumen et al., 2012) and are considered to be involved in plastic modifications of the hippocampus, particularly after exposure to stress (Joca et al., 2007).

The regulation of serotonergic systems has been of particular interest in disease states including, but not limited to, depression, anxiety, autism, mania and neurodegenerative disorders (Nordquist and Oreland, 2010). The vast number of behavioural, psychiatric and neurodegenerative disorders that have been associated with the serotonergic underscores the huge number of mechanisms that result from their activation and are outside the scope of this thesis. However, of note, a commonly used drug in western society to aid in mood disorders is selective serotonin reuptake inhibitors. These inhibitors have been tested clinically to improve “behavioural problems” in adults with intellectual disability and resulted in a significant reduction in aggression and self-harming behaviour (Sohanpal et al., 2007) and suggests the importance of understanding the serotonergic system in intellectual disability models.

1.1.6. Glia

Glia, or glial cells, were most likely discovered around the same time as neurons, sometime in the 19th century, however they were originally thought of as “glue” that holds neurons in place. It wasn’t until the mid-20th century that the importance of these cells became better understood. In the CNS glial cells can be broadly categorised into three groups: astrocytes, oligodendrocytes, and ependymal cells. Oligodendroytes provide insulation to neurons by creating a myelin sheath increasing action potential propogation whilst ependymal cells provide a neuro-epithelial lining of the ventricles of the brain as well as the central canal found in the spinal cord. Astrocytes are arguably the most studied type of glial cell in neurophysiology and the regulation of synapses and plasticity.

Astrocytes are vital for the regulation of synapse maintenance and is important for the overall architecture and activity of neural circuits and therefore animal behaviour. These non-neuronal cells provide direct contact onto synapses allowing their regulation and secrete soluble factors modulating the structure of pre- and post-synaptic regions and had led to the “tripartite synapse” concept (Araque et al., 1999). The doctrine proposes that neurotransmitters released from neurons have the ability to bind to nearby astrocyte processes. This binding activates astrocyte signalling pathways modulating synaptic plasticity and therefore behaviour (Papouin Thomas et al., 2017). Astrocytes not only contact neurons but also form gap junctions between other astrocytes allowing ions and nutrients to diffuse, increasing the synaptic regulation of neurons by astrocytes (Pannasch and Rouach, 2013). Astrocytes have been implicated in Down Syndrome, a genetic disorder causing intellectual disability. Research demonstrated an increase in astrocyte number and significant morphological changes as well as impaired Ca^{2+} signalling proteins within astrocytes (Dossi et al., 2018).

1.1.7. Summary

This introductory section described certain fundamental concepts of the neuron: the maintenance of the resting membrane potential, the ion channels determining sub-threshold properties and the generation of action potentials. Finally, synaptic transmission was discussed with a focus on the two types of postsynaptic channels, ionotropic and metabotropic, and how these receptors function.

1.2. The hippocampus

Located deep in the temporal lobe, the hippocampus is a major structure in vertebrate brains. Elongated, and resembling a seahorse, the hippocampus received its name based on this sea creature (genus Hippocampus). The first description of the structure is credited to the surgeon and anatomist Giulio Cesare Aranzio (c. 1530-1589) with further anatomical research conducted by Ramón y Cajal (1911) and Lorente de Nó (1934). For multiple reasons, not limited to the defined laminar cytoarchitecture and characterised information flow, the hippocampus is arguably the most researched brain structure in history. This chapter will focus on the hippocampal anatomy and its role in learning, memory and disease.

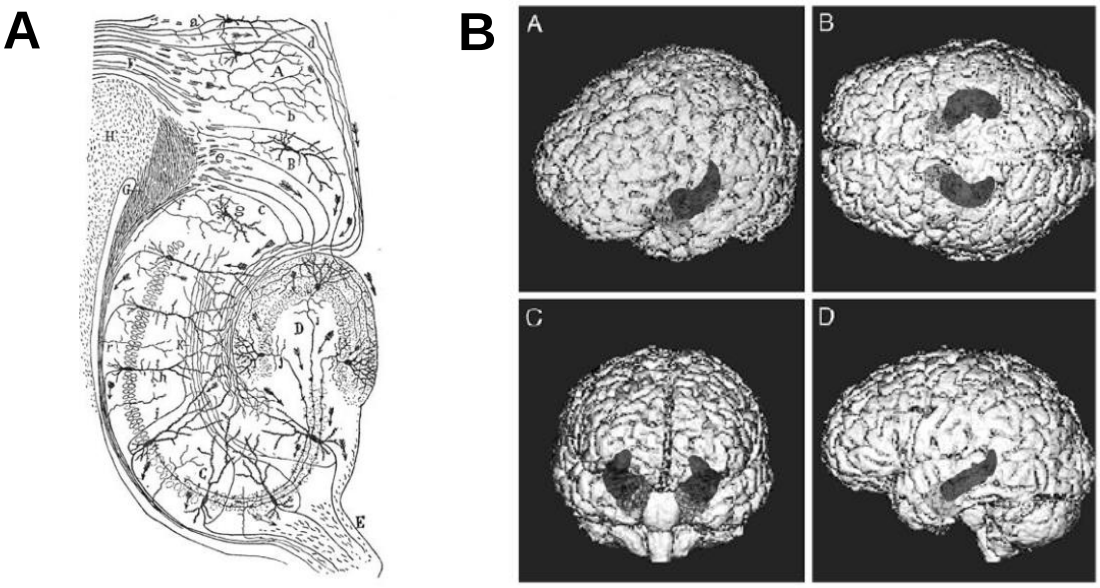

Figure 1.3. The human hippocampus

A) *Original drawing of the hippocampus by Santiago Ramon y Cajal from his 1911 book: Histologie de Système Nerveux. The arrows indicate his hypothesis for information flow within the hippocampus*
B) *MRI images depicting localisation of the hippocampus in the human brain. A: Oblique view. B: Dorsal view. C: Frontal view. D: Lateral view (from Anderson et al., 2007)*

1.2.1. Hippocampal formation anatomy

Analysing the cross-section of the hippocampus reveals the distinctive laminar architecture that is remarkably similar between different species, although not identical (Anderson, 2007; Insausti, 1993; O'Keefe, 1999). The term '*hippocampus'* usually refers to the brain structure as a whole, however more precise terminology should be considered when addressing the hippocampal sub-regions. There is no universally agreed upon definitions for these sub-regions but for the sake of continuity, the terminology outlined by Anderson *et al*. (2007) will be used for this thesis. A hierarchy of sub-regional groups exists: The *Hippocampus Proper* (also known as the *hippocampus*) is comprised of three CA sub-fields: CA1, CA2 and CA3. The *Hippocampus Proper* when combined

with the *Entorhinal cortex* (EC), *Dentate Gyrus* (DG), *parasubiculum*, *presubiculum* and the *subiculm*, is deemed the *Hippocampal Formation*. The precise anatomy and elaborate connectivity is tremendously complex, and for this reason, full examination of the hippocampus is outside the scope of this chapter. In order to focus on what is most relevant to this thesis, a brief summary regarding key features, characteristics and connections of what has been traditionally called the “tri-synaptic circuit” consisting of connections between EC, DG and CA sub-fields will be presented.

The EC is a mediator between the hippocampus and cortical regions allowing reciprocal communications between the two areas. It is divided into medial and lateral regions, consisting of six layers with fibres projecting from the EC to form excitatory glutamatergic synapses onto principal cells of the DG, CA1, CA2, CA3 and subiculum depending on which EC layer the fibres reside.

The *Perforant path* afferents emerge largely from Layer II of the EC, both laterally and medially. Fibres projecting from Layer III of the EC largely synapses onto CA2 and CA1 distal dendrites, as well as the subiculum, via the *Temporoammonic Pathway (TAP).* The *perforant path* fibres synapsing in the DG do so in the molecular layer (the most superficial DG layer) via dendrites of granule cells. These granule cells are innervated differentially by the lateral *perforant path* and medial *perforant path* with the former connecting to the outer third of the molecular layer (distal dendrites) whilst the latter connects to the middle third (more proximal dendrites). This anatomical distinction is conserved as the fibres continue towards the CA2/3 sub-region as the lateral *perforant path* synapses onto distal apical dendrites of pyramidal cells in the superficial layer of stratum lacunosum-moleculare whilst the medial *perforant path* projects deeper (but in the same layer).

The granule cell layer contains a high density of dentate granule cell bodies which extend unmyelinated mossy fibre axons. These axons pass through the

polymorphic cell layer (the deepest DG layer) and innervate CA3 pyramidal cells. Cajal coined the term ‘mossy fibre’ due to their characteristic appearance. These axons form unusually large presynaptic boutons that create synapses with dendritic spines of CA3 pyramidal cells within the *stratum lucidum*, where proximal areas of the pyramidal cell apical dendrites reside. The mossy fibre axons innervate only CA3 and not CA2, which aids in characterisation of the CA2 sub-field because CA2 and CA3 pyramidal cells are otherwise similar. CA2 is a hippocampal region that has been relatively neglected when compared to the other well-studied subfields, particularly CA1, however it has been undergoing somewhat of a renaissance with new methods to define and manipulate its neurons (Dudek et al., 2016; Hitti and Siegelbaum, 2014).

All CA sub-fields share the same laminar structure (Figure 1.4). At its most superficial layer, into which pyramidal cell dendrites reach, the CA sub-fields are again divided into two or three layers: the stratum *lacunosum-moleculare* at the furthest edge, the more deeply sitting *stratum radiatum*, the *stratum lucidium (*exclusively in the CA3*)*, next to that layer is the *stratum pyramidale* (the cell body layer) and finally, the deepest layer is the *stratum oriens*. This deepest layer contains basal dendrites of the pyramidal cells as well as some afferent fibres and inhibitory interneurons. A border around the *stratum oriens* can be identified, known as the *alveus*, which is formed by the aggregation of myelinated efferent pyramidal axons. In addition to the pyramidal neurons, there are a variety of GABAergic interneurons inhabiting the numerous laminae that largely create local synaptic connections but also project between sub-regions within the hippocampus.

Perhaps the most comprehensively studied synaptic connection in the brain is the CA3 to CA1 projection, termed the *Schaffer collateral* (SC) pathway. This pathway is aptly named due to the greatly divergent nature of CA3 pyramidal neuron axons. The many collateral fibres given off pass through the CA3/2 sub-fields and terminate onto CA1 dendrites in the *stratum radiatum* and *oriens* to

form excitatory glutamatergic synapses. Some of these collateral fibres form recurrent associational connections by remaining within the CA3/2 region. As well as the receiving inputs from the SC Pathway, the CA1 receives inputs from layer III of the EC through direct projections, known as the previously mentioned TAP. Fibres making up the TAP project to the distal apical dendrites of CA1 pyramidal neurons in the *stratum lacunosum-moleculare*.

Closure of the 'tri-synaptic' circuit occurs through CA1 pyramidal neuron projections to both the *subiculum* and layer V/VI of the EC. Dissimilar to the CA3 projections, very few CA1 pyramidal neuron axons form recurrent associational connections within its own region and instead the majority pass through the *stratum oriens* to reach the EC. The *subiculum* also projects to the EC but also to various other cortical and subcortical areas (O'Mara, 2006).

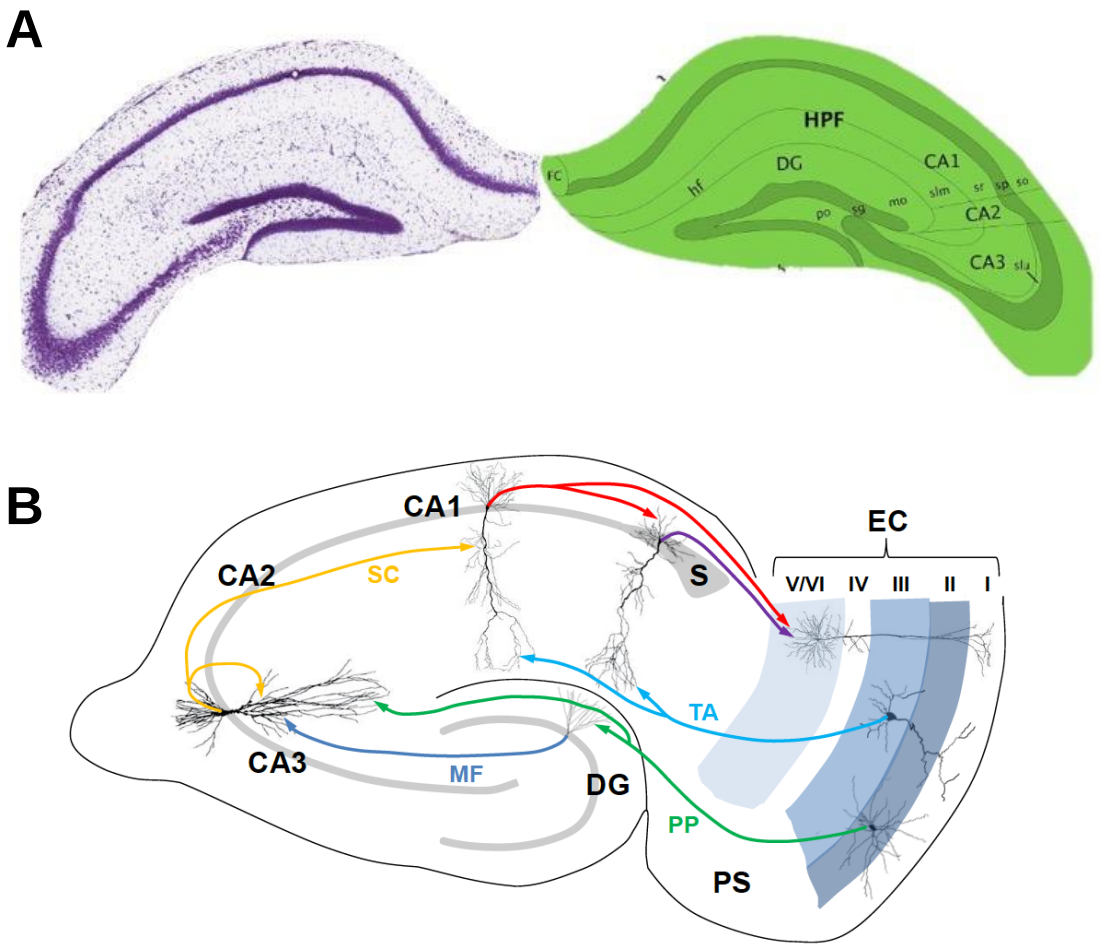

Figure 1.4. The mouse hippocampus

A) *Bilateral coronal cross section of p56 mouse hippocampus: Left - Nissl stained, right – labelled regions (so = straum oriens, sp = pyramidale layer, sr = stratum radiatum, slm = stratum lacunosum-moleculare, mo = molecular layer, sg = granule cell layer, po = polymorph layer, slu = stratum lucidium). Image modified from Allen Brain Atlas.*
B) *Schematic of hippocampal connectivity. Blue shaded areas depict EC layers and grey for cell body layers of DG, subiculum and CA fields. Coloured arrows demonstrate unidirectional flow of information (TAP = Temporoammonic pathway. MF = Mossy Fibre pathway. PP = Perforant Path)*

1.2.2. Role of the hippocampus in learning and memory

Generally, memory can be characterised into two classifications: declarative memory which involves facts and events, otherwise known as explicit memory, and non-declarative memory which encompasses physiological and behavioural responses in the absence of conscious thought (Dickerson and Eichenbaum, 2010). The initial link between the hippocampus and a role in memory was suggested by Scoville and Milner whose case study of patient Henry Molaison in 1957 described amnesia resulting from bilateral medial temporal lobe resection. The patient suffered uncontrollable seizures and, with the intention to treat his condition, underwent surgical removal of the majority of the *hippocampus*, *amygdala* and *entorhinal cortex*. Although successfully improving his epilepsy, Henry Molaison could no longer create new long-term memories, a term called *anterograde amnesia* (he also presented with a mild form of retrograde amnesia). Importantly, while his capacity to form long-term declarative memories was severely impacted, his general intelligence, working memory and ability to learn new tasks and motor skills (non-declarative memory) remained unaffected (Scoville and Milner, 1957).

Much research in the succeeding decades focused on animal models carrying hippocampal lesions. A prevalent test for hippocampal damage has been, and still is, the Morris water maze. In essence, the rodent is placed in a pool of water and must swim and search to find a submerged platform that allows the animal to halt swimming. Due to the local cues, the animal should be relying on a spatial map strategy. Rodents with hippocampal lesions have a reduced performance in this task (Bolhuis et al., 1994).

The examination of performances in various spatial learning tasks from multiple studies has led to the suggestion that spatial learning requires the connections between the hippocampus and other cortical areas (Lynch, 2004). Bilateral lesions to the medial temporal lobe in monkeys resulted in severe difficulties

completing the delayed nonmatching sample task (Mishkin, 1978). Similar, but less dramatic decreases in performance were observed when the lesion was localised to parahippocampal cortical and entorhinal regions (Zola et al., 1989, 2000).

Temporal components of hippocampal-dependent memory have been previously demonstrated through the visual paired-comparison task, which evaluates the subjects' preference for exploring a new, over a familiar, object. Studies involving amnesic patients with hippocampal damage revealed no deficits when a delay was absent between presenting the first and second stimuli, but there was a deficit when a delay was introduced (McKee and Squire, 1993). However, studies involving rats resulted in conflicting outcomes (Mumby et al., 1996) and suggests that further research is required to fully understand the role of the hippocampus in recognition memory.

Although great emphasis has been given to the hippocampus' role in spatial memory, there are other instances of its importance in non-spatial memory tasks. For example, Clark *et al.* (2002) demonstrated that subiculum and hippocampus lesions caused deficits in the social transmission of food preference task in mice.

The first physiological correlate between the hippocampus and spatial memory was provided by O'Keefe and Dostrovsky (1971). By implementing single-unit *in vivo* hippocampal recordings in freely moving rats, they contributed to the concept of the 'place cell'; the notion that pyramidal neurons in the hippocampus display spatially selective firing fields in the CA1 and CA3 (McNaughton et al., 1983), in the DG (Jung and McNaughton, 1993) and also in the subiculum (Sharp and Green, 1994).

Discoveries that the spatially selective firing of place cells in the CA1 remained in the presence of lesions to the CA3 (Brun et al., 2002) or DG (McNaughton et

al., 1989) suggested that spatial information to the CA1 is supplied through a direct projection from the EC (Moser et al., 2008). Subsequent research has shown that medial EC principle neurons display spatially selective firing, however they differed from place fields as these cells fired spikes in more than one location creating a grid-like pattern (Figure 1.5) (Fyhn et al., 2008). As the medial EC dorsal-ventral axis increases, so does the grid cell's firing and spacing (Fyhn et al., 2008). Also, removal of layer III medial EC affected CA1 place cell firing (Brun et al., 2002), yet grid cells were unchanged (Fyhn et al., 2008), therefore providing validation that the EC directly feeds the CA1 with spatial information. In layers III, V and VI of the EC, specialised grid cells exist known as head direction cells that fire action potentials in a grid-like formation, but only when the animal is facing in a certain direction (Sargolini et al., 2006).

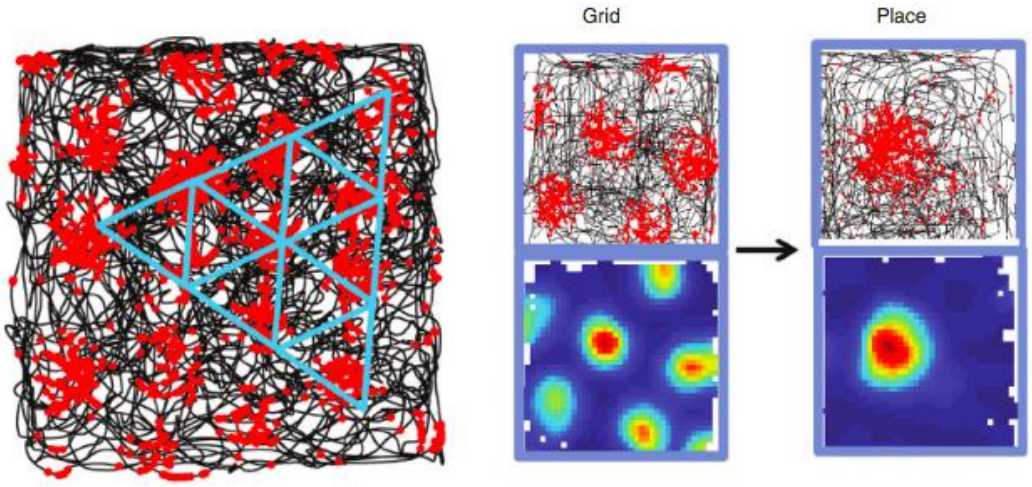

Figure 1.5. Grid cells and place cells

Left: Example of grid cell firing from EC of rat brain. Black trace represents the rats' trajectory as it explores a square enclosure. Spike locations are depicted in red, with one ret dot equalling one spike (blue lines have been drawn to illustrate the hexagonal structure of the grid pattern. Right – Grid and place cell from EC. Bottom is a heat map with a colour scale ranging from red to blue with red portraying high activity and blue low activity, and the top image displays the animals trajectory, with red dots demonstrating the spike locations (May-Britt Moser, 2015).

1.2.3. Summary

The hippocampus is a distinct brain region located within the temporal lobe. Its anatomy is amazingly complex but also remarkably uniform and similar between many different species. Place and Grid cells form vital components of the hippocampus and demonstrates its importance in encoding spatial information.

1.3. Neural plasticity

1.3.1. Synaptic plasticity

The brain is essential for the process of learning and memory, and due to the plastic nature of neural networks and individual neurons, external stimuli (i.e. experience) are able to modify neurons and their connectivity with one another; this process is called synaptic plasticity.

Hebb first conceptualised the notion of plastic neural networks approximately 70 years ago; he postulated that if Cell A repeatedly excited cell B within close proximity, changes will take place to either or both cells in a way that would increase the cells efficiency to communicate with one another (Hebb, 1950). Since his proposal, enormous global efforts have been expended resulting in a greater, but far from complete, understanding of neuronal plasticity. Such efforts have revealed key findings, such as the existence of many distinctive forms of plasticity, differing by aspects such as induction methods, molecular mechanisms or duration of plasticity to name a few. One such form of plasticity is LTP, first discovered in anaesthetised rabbits with a high frequency stimulus (HFS) applied to the perforant path that caused a potentiation of synaptic responses in a population of neurons in the dentate gyrus (Bliss and Lømo, 1973). Many years after the first detection of LTP, it was found that synaptic strength can also be weakened leading to a depression of the excitatory postsynaptic potential (EPSP) induced by a low frequency stimulation (LFS) (Dudek and Bear, 1992). This finding by Dudek and Bear was discovered in populations of CA1 pyramidal cells in rat brain slices by applying a 1-3Hz stimulation to the Schaffer Collateral pathway. This bi-directionality of EPSP changes displayed by hippocampal neurons has formed the basis of how mammals encode neural information dependent on synaptic weights.

1.3.1.1. Measuring synaptic plasticity in the laboratory

Numerous laboratory methods are utilised allowing the measurement of synaptic plasticity. Many are based on extracellular field recordings (described in detail in the Materials and Methods chapter) as they are an efficient way of recording plasticity changes from a field of neurons, rather than from individual cells. During these experiments the current sink is recorded (known as the field EPSP (fEPSP)) from the extracellular region of neurons that are in close proximity to the recording electrode. A baseline is acquired in all such experiments and is essential to analyse the change in fEPSP response post-plasticity induction. Successful plasticity results in a change in fEPSP response that is maintained for at least 60 minutes. The reasons for these long-lasting changes and the protocols used to elicit them are discussed in more detail in the sections below.

1.3.1.2. LTP

Since Bliss and Lømo's pioneering LTP experiment in 1973, LTP has become one of the most extensively probed neurophyisological phenomena, particuarly in the context of the SC pathway. The succeeding years provided fundamental breakthroughs that helped set the foundations for the field of synaptc plasticity, namely the properties of "associativity", "input specificity" and "cooperativity" (Levy and Steward, 1979; McNaughton et al., 1978). In essence, a weak input with few tetanised synapses will not induce LTP, on the other hand, LTP can be reliably induced with a strong input (cooperativity), however LTP will only be induced in the stimulated pathway (input specificity). Furthermore, activating two inputs simultaneously, one of which is too weak to induce LTP independently, but can become strong enough to induce LTP when stimulated together (associativity). Another requirement was then found for LTP inducton: synaptic stimulation coupled with postsynaptic depolarisation (Kelso et al., 1986; Malinow and Miller, 1986).

It was at least a decade since the discovery of LTP before significant headway was made in understanding the function and possible underlying mechanisms of LTP. This was largely due to technological advances and the advent of *in vitro* hippocampal slice preperations allowing biophysical studies in the 80's. A combination of work from Collingridge *et al.* (1983) who uncovered the requirement of NMDA receptors for LTP induction but not for mediation of synaptic transmission, Nowak *et al.* (1984) who uncovered the Mg^{2+} block in NMDA receptors and Dale and Roberts (1985) who showed a fast AMPA receptor and slow NMDA receptor component. Finally Lynch *et al.* (1983) demonstrated that chelating Ca^{2+} blocks LTP induction. To briefly summarise the typical (but not sole) form of LTP inducton: glutamate released presynaptically activates AMPA receptors leading to an influx of cations causing the postsynaptic cell to depolarise and therefore displace the Mg^{2+} block in NMDA receptors. Ca^{2+} then enters the neuron via the NMDA receptors leading to a complex cascade of events eventually leading to the insertion of more AMPA receptors into the postynaptic membrane increasing the synaptic strength (Malinow, 2003). There is debate as to whether postyanptic or presyantpic mechanism alterations lead to the excitatory postsynaptic current (EPSC) enhancement in NMDA receptor-dependent LTP. Substantial evidence supporting presynaptic changes were provided by glutamate release and paired-pulse facilitation (PPF) studies. For example, an increase in extracellular glutamate concentrations have been detected *in vivo* in the dentate gyrus (Dolphin et al., 1982) and an increase in release probability deduced by a decreases in PPF during LTP induction in the hippocampus of rats (McNaughton, 1982) (discussed further in chapter 4). On the other hand, there is extensive evidence suggesting postsynaptic alterations are the major component to LTP. Such experiments include Diamond *et al's.* study (1998) who measured transporter currents from glial cells to analyse changes to glutamate levels, made possible because of the electrogenic nature of glutamate uptake. They revealed that there were no changes in glutamate levels post-LTP

induction indicating no presynaptic changes, which has been further verified (Lüscher et al., 1998). Furthermore, the concept of silent synapses provides further postsynaptic evidence for LTP. Postsynaptically silent synapses contain NMDA receptors but lack AMPA receptors, and therefore no EPSCs can be found at negative membrane potentials. These synapses can be unsilenced through LTP induction protocols in the CA1 region of the hippocampus (Liao et al., 1995). Changes to postsynaptic AMPA receptors also provide further evidence; the probaility of the receptor opening in response to glutamate, how long the receptor is open for and its unitary conductance can change as a result of LTP-induction protocols (Bliss and Collingridge, 2013). Moreover, the enrichment of AMPA receptors in postsynaptic membranes through various mechanisms is required for LTP. Evidence for this has come in the form of immunhistochemistry experiments demonstrating increased GluA1-containing AMPA receptors inserted in neural membranes with glycine treatment (Lu et al., 2001) as well as analysing green flourescent protein (GFP)-tagged AMPA receptors in response to glutamate uncaging (Patterson et al., 2010).

The molecular alterations resulting from Ca^{2+} influx are multifarious, complex, and are yet to be fully resolved. Some of the molecules proposed to be involved in LTP include Ca^{2+}/calmodulin-dependent protein kinase (CaMKII), protein kinase A (PKA), protein kinase C (PKC), tyosine kinases and mitogen-activated protein kinases (MAPKs) (Bliss and Collingridge, 1993; Malenka and Nicoll, 1999; Salter and Kalia, 2004). Aruguably the most extensively studied downstream signalling molecule is CaMKII. CaMKII remains inactive at resting conditions (Coultrap and Bayer, 2012), however the Ca^{2+} entry through NMDA receptors activates Calmodulin (CaM) which in turn, binds to CaMKII alleviating its autoinhibitory state. This allows autophosphorylation of CaMKII and permits its kinase activity (Lisman et al., 2002). Preventing this action can lead to deficits in fear conditioning (Rodrigues et al., 2004) and spatial learning in rodents (Giese et al., 1998). Interestingly, the mis-regulation of CaMKII has been implicated in Angleman’s disease, another form of intellectual disability (Weeber

et al., 2003). As a kinase, activated CaMKII has the ability to add phosphate groups to other molecules such as Stargazin (Tomita et al., 2005), a Transmembrane AMPA receptor Regulatory Protein (TARP) that is essential for the synaptic translocation and stability of AMPA receptors necessary for LTP. There is evidence that CaMKII activity leads to protein synthesis and degradation (Lisman et al., 2012) but further research is needed for clarification of these mechanisms. It is important to mention that NMDA receptors are by no means the only receptor involved in LTP induction with kainate receptors (Bortolotto et al., 2005) and Group 1 mGluRs (Balschun et al., 1999) among others implicated in LTP.

Another important consideration for the induction and influence over LTP is Brain-derived neurotrophic factor (BDNF). BDNF is a part of the neurotrophin family of signalling proteins and is an agonist for Tropomyosin receptor kinase B (TrkB) found at glutamatergic synapses. BDNF is endogenously synthesised and released from glutamatergic neurons (Lessmann et al., 2003) where TrkB also resides, both pre- and post-synaptically (Drake et al., 1999). BDNF-TrkB signalling acts through three pathways: MAPKs, PLC and PI3K that regulates both gene transcription and protein translation (Yoshii and Constantine-Paton, 2010) and has been heavily implicated in LTP, specifically L-LTP, through abundant pharmacological and genetic knock-out model research (Korte et al., 1995; Minichiello et al., 1999; Pang et al., 2004). Coinciding with this, further studies indicate an activity-dependent increase in endogenous BDNF (Castrén et al., 1993), however exogenous application of BDNF does not seem to instigate LTP (Kramár et al., 2004). It is clear that BDNF is a vital component to LTP and has been linked to hippocampal dependent learning in rodents; deletion of the TrkB receptor reduced performance in a Morris water maze and radial arm maze task (Minichiello et al., 1999).

1.3.1.2.1 Protein synthesis in LTP

The first indication of protein synthesis involvement in memory and learning originated from Flexner *et al.* (1963) who reported memory impairments in mice instigated by a temporal lobe injection of the protein synthesis inhibitor (PSI), puromycin. Since that first experiment there has been a large number of reports investigating protein synthesis in LTP and memory and has arguably produced the most variable and conflicting data within the field of synaptic plasticity.

In the 1960's and 70's, a substantial number of behavioural studies utilised PSIs. Examples include puromycin decreasing shock-avoidance behaviour in goldfish (Springer et al., 1975) and acetoxycycloheximide diminishing spatial memory in mice (Barondes and Cohen, 1967). Nonetheless, there were immediate challenges, namely the off-target effects of the compounds used. Puromycin can lead to epileptogenic action among other side-effects which may interfere with memory (Cohen et al., 1966). Cycloheximide (CHX), another PSI, may also lead to toxicity due to the relatively high doses required for protein synthesis inhibition and memory impairment (Bull et al., 1976). On the other end of spectrum, there are multiple reports that over 90% inhibition of protein synthesis doesn't impact encoding and retention of memories such as in colour-discrimination learning (Wittstock and Menzel, 1994), olfactory conditioning (Wittstock et al., 1993) and spatial learning in mice (Flexner and Flexner, 1966).

An essential argument linking protein synthesis with learning and memory involves the temporal phases of LTP. There have been suggestions that LTP time frames can be temporally separated dependent on distinct molecular mechanisms and also that the entire duration of LTP varies depending on the stimulation protocol (Bliss and Collingridge, 1993; Racine et al., 1983; Reymann et al., 1985). LTP is frequently divided into an early phase (E-LTP) and a late phase (L-LTP). E-LTP time-frames vary hugely with a time-course anywhere between 1 and 5 hours being reported (Abbas et al., 2009a). This phase of LTP

has been described to involve an increase in trafficking and insertion of AMPA receptors into the postsynaptic membrane from a readily-releasable AMPA receptor pool (Bredt and Nicoll, 2003; Song and Huganir, 2002) as well as their direct phosphorylation (Barria et al., 1997; Lee et al., 2003; Soderling and Derkach, 2000), both of which are protein translation-independent processes. Although there is no specific definition, there are suggestions that the transition from E-LTP to L-LTP occurs around the 1 hour mark where the maintenance of potentiated responses requires the synthesis of proteins (Aakalu et al., 2001; Johnstone and Raymond, 2011; Kang and Schuman, 1996; Schuman et al., 2006). However, the seldom cited research disputing this model indicates otherwise (Abbas et al., 2009a; Villers et al., 2012). How and why these discrepancies occur are not known but nor are they uncommon. Differences such as the animal species, age of animal, strain of animal to the minute differences in solution preparation, incubation period of slices, temperature of recordings and even how the animal is handled prior to sacrifice may instigate huge differences in outcomes when in combination. An incredibly detailed and thorough review on this subject from Abbas *et al.* (2015) utilised meta-analysis in an attempt to clarify decades of research but failed to find a decisive conclusion. One argument postulated that the ‘critical window’ of LTP is determined at the induction time-point where the protocol used influenced protein synthesis dependency. Remarkably, Fonseca *et al.* (2006) established that the frequency of neural stimulation can be an essential determinant of protein synthesis in both E- and L-LTP and could explain the many inconsistencies in this area. Recording fEPSPs from CA1 PNs, the group showed that E-LTP was more readily blocked with the PSI, anisomycin, at higher frequency stimulation. This suggests that increasing the LTP-induction frequency increases the reliance of the neural network on protein synthesis for potentiation in the E-LTP phase.

As it seems protein synthesis is a requirement under certain conditions, the question concerning input specificity remains. A neuron has one nucleus but

potentially thousands of synapses, only a few of which may be required to undergo changes. Steward and Levy (1979) discovered polysomes localised to dendritic regions suggesting that translation of proteins can occur locally. Ostoroff *et al. (*2010) added to this claim by demonstrating the accumulation of polysomes in dendrites with the use of a fear-conditioning paradigm indicating that protein synthesis increases during learning. Clearly another requirement for local translation is mRNAs. Many mRNA's such as MAP2 and ARC transcripts have been identified in dendritic regions using in situ hybridization, (Garner et al., 1988; Lyford et al., 1995). The trafficking of dendritically localised mRNA can be determined by the presence of specific sequences known as dendritic targeting elements (DTE's) (Bramham and Wells, 2007). The DTE's are thought to be recognised by RNA binding proteins (RBPs), such as MARTA1 which associates with the MAP2-DTE (Rehbein et al., 2002) and allows the shuttling of mRNA from the nucleus to the dendritic site of plasticity. The above evidence suggests there is a molecular capacity involving protein synthesis permitting input specificity for LTP.

Alongside the research providing evidence for the existence of translational machinery within dendritic regions, much work has gone into understanding the molecular pathways involved in protein synthesis. NMDA receptor activity, a vital component of electrically-induced LTP, has been shown to lead to increased translation within dendrites via mammalian target of rapamycin (mTOR) activation. Activated mTOR can phosphorylate 4E-Binding Proteins (BPs) causing them to dissociate from eukaryotic translation initiation factor (eIF)-4E improving its availability for translational processes resulting in increased translation levels (Gong et al., 2006). NMDA receptor activation can also lead to ERK-dependant Mnk1 activation which increases eIF4E phosphorylation and consequently translation (Banko et al., 2004). These two studies demonstrate that both ERK and mTOR pathways are activated by NMDA receptor activation and may be required for LTP induction and maintenance. However, a more comprehensive view of which mRNAs are regulated during LTP induction as

well as how they are regulated is necessary. The majority of the research is heavily *in vitro* focused and ideally a shift in focus to *in vivo* based experimentation would help improve understanding of protein synthesis in plasticity. Techniques for live-cell imaging studies could be particularly useful as demonstrated by Wong *et al.* (2017) who tracked endogenous RNA *in vivo* to visualise RNA docking and the formation of B-actin hotspots prior to branch formation.

There is ample evidence to suggest protein synthesis is involved in certain contexts of LTP demonstrated with the use of PSIs, the localisation of translational machinery to dendritic regions and the activation of translational pathways (mTOR and ERK) from NMDA receptor activation. However, there remains some strong scepticism within the field regarding the involvement of protein synthesis in LTP, and the perceived dichotomy of E-LTP and L-LTP (and its reliance on protein synthesis) awaits validation.

1.3.1.2.3. LTP and learning correlates

One of the crucial goals within cellular and molecular neuroscience is to establish a causal link between the physiological process of LTP and the behaviour presented as a result of learning and memory. *In vivo* experiments using animal models have offered demonstrable evidence of an intimate link between LTP and memory. One such example of this physiological link involving the hippocampus has been given by Whitlock *et al*. (2006) who recorded local field potentials in the CA1 region of the hippocampus of freely moving animals. The field potentials recorded were increased after inhibitory avoidance learning and was reversed with the application of a cell-permeable protein kinase inhibitor. Importantly, alongside this reversal, the inhibitory avoidance behaviour was severely disrupted suggesting that altering the change in field potential amplitude affects learning, and the potentiation in responses is a requirement for

some forms of learning. Other significant research showed a reversal of LTP through inhibition of PKMz, which is an active isoform of PKC, by using a PKMz inhibitor that coincided with a persistent loss of spatial information in rats (Pastalkova et al., 2006). The kinase is now established as a vital component of memory maintenance by enhancing AMPA receptor responses (Kwapis and Helmstetter, 2014).

1.3.1.2.4. LTP in disease

Over the past decade and half, aberrant plasticity, including LTP, has been connected with numerous brain disorders and as a consequence, efforts are being undertaken to investigate neural plasticity in disease models (Bliss et al., 2014). Arguably the most pressing disorder requiring attention is Alzheimer's disease due to its prevalence, severity and lack of any effective treatment placing a large socio-economic burden on society. Initial findings that Amyloid Beta protein (a component of amyloid plaques found in patients with Alzheimer's Disease) application inhibited LTP in the hippocampus indicated a link between Alzheimer's disease and LTP (Klyubin et al., 2012). Multiple Sclerosis is a demyelinating disease that has also been linked to LTP with plasticity deficits found in a Multiple Sclerosis model (Nisticò et al., 2014). Also, LTP insufficiencies have been observed in models of intellectual disability, including Fragile X syndrome (FXS) (Shang et al., 2009; Zhao et al., 2005), Tuberous sclerosis (von der Brelie et al., 2006) and Rett syndrome (Moretti et al., 2006) providing a substantial link between intellectual disability and LTP. These are just a few neurological disorders that demonstrates how aberrant synaptic plasticity may lie at the centre of many brain disorders.

1.3.1.2.5. Depotentiation of LTP

Depotentiation can be defined as the reversal of LTP, first demonstrated in the CA1 hippocampus by Bashir and Collingridge (1994). The experimental observation of this phenomenon has usually been observed in hippocampal slices with the application of a low frequency stimulus (between 1 – 3Hz) that perfectly demonstrates the plastic nature and bi directionality of neural connectivity. Depotentiation has not received much attention compared to other forms of plasticity such as LTP (Bashir and Collingridge, 1994; Miguéns et al., 2011; Sanderson et al., 2012; Woo and Nguyen, 2003). Despite the relatively low levels of interest, some molecular mechanisms underlying depotentiation have been uncovered as well as potential links to disease such as schizophrenia, due to depotentiation deficits found in a schizophrenia model (Sanderson et al., 2012), however the unknown aetiology of the disease renders information extrapolated from animal models difficult to interpret.

Understandably, depotentiation has similarities to LTD; in both cases a reduction in EPSPs are observed. Although there are similar molecular mechanisms between the two, there are distinctions that have been found such as the requirement of NR2A NMDA receptor subunits in depotentiation rather than NR2B that has been reported in LTD (Zhu et al., 2005). Depotentiation signalling pathways are thought to involve adenosine due to adenosine receptor antagonists decreasing depotentiation in hippocampal slices (Liang et al., 2008). Later research indicated that this mechanism involved the triggering of cAMP efflux and its extracellular conversion to adenosine where adenosine A1 receptors coupled to $G_{i/o}$ proteins leading to an independence of PKA signalling (Liang et al., 2008). The involvement of PP1, PP2A and CamKII are also deemed to be integral mechanisms of depotentiation (Sanderson et al., 2012). Another downstream effector of the A1 receptor my involve G-protein-activated inwardly rectifying K^+ channels due to a report that genetically knocking out this channel in an animal inhibited depotentiation (Chung et al., 2009)

1.3.1.3. LTD

LTD describes a decrease in postsynaptic strength that can be maintained for an extended period of time. The first report regarding the existence of LTD was published in 1992, Dudek and Bear applied an LFS amounting to 900 pulses between 1 – 3Hz to the SC pathway (from this point on will be referred to as LFS-LTD). This novel finding led to the understanding that the plastic nature of synaptic connections is bidirectional. Dudek and Bear (1992) established that their LTD discovery relied upon NMDA receptor activation because applying an NMDA antagonist blocked the depressive effect. At the time, the knowledge that LFS-LTD required NMDA receptor activation as well as subsequent Ca^{2+} influx (Mulkey and Malenka, 1992) caused a conundrum; these mechanisms are very similar to that of the more established LTP. The ensuing years teased some answers to this problem and revealed that differences may arise from the temporal characteristics of the Ca^{2+} flux and its magnitude (Cummings et al., 1996; Dan and Poo, 2006; Oliet et al., 1997) as well as possible roles for specific NMDA receptor subunits (Bartlett et al., 2007). Although the full characterisation of LFS-LTD currently remains elusive, the control of AMPA receptor internalisation is understood to involve the activation of kinases and phosphatases such as calcineurin and protein phosphatase (PP) 1 (Mulkey et al., 1994, 1993).

Similar to LTP, LTD consists of different forms and can be induced via diverse protocols that involve varying molecular mechanisms, not solely the NMDA receptor-dependent form induced via LFS as originally found by Dudek and Bear. These forms will be discussed in more details in the following sections.

1.3.1.3.1 NMDA-LTD

NMDA receptor-dependent LTD has received the most research focus within the LTD family and can be initiated via a LFS (described above) or with a brief application of NMDA (Lee et al., 1998). The mutual occlusion between these two forms of plasticity suggests it is likely they share common mechanisms (Lee et al., 1998). Importantly, there do seem to be differences between the chemically and electrically induced varieties, for example, chemically-induced NMDA-LTD has been associated with an increase in dephosphorylation of the AMPA receptor subunit, GluR1 (Lee et al., 1998) whereas electrically-induced NMDA-LTD requires postsynaptic PP1 (Morishita et al., 2001).

It is likely that various subtypes of NMDA receptors trigger LTD that is dependent on factors including the induction protocol, environmental conditions, developmental stage, animal strain and brain region investigated (Vasuta et al., 2007; Weiler et al., 1997). An example of this is provided by Woo *et al.* (2005) who demonstrated that young adult mice have enhanced GluN2B levels caused by the BDNF precursor, proBDNF, that may lead to a GluN2B-sensitive NMDA-LTD. Intriguingly, NMDA-LTD seems to be more pronounced in early development as shown in *in vitro* hippocampal electrophysiology studies and can be enhanced if the animal is exposed to novelty (Bashir and Kemp, 1997) or mild stress (Kim et al., 1996) prior to sacrifice. The latter is particularly important as different methods can be used to sacrifice the animal, such as a schedule 1 method consisting of a cervical dislocation that may involve different methods of animal handling or a non-schedule 1 method involving anaesthetising the animal prior to decapitation.

The majority of expression mechanisms for NMDA-LTD are likely postsynaptic, although changes to presynaptic glutamate release has been reported; a decrease in release probability was observed after NMDA-LTD induction caused by alterations to retrograde messengers such as nitric oxide (Stanton et al.,

2003). On the postsynaptic side, glutamate uncaging studies have shown that the removal of AMPA receptors from postsynaptic membranes are a major cause for a decrease in glutamate sensitivity (Collingridge et al., 2004). There is also evidence supporting a decrease in receptor conductance that may contribute to NMDA-LTD (Lüthi et al., 2004).

The molecular mechanisms underpinning the induction and expression of NMDA-LTD begins with Ca^{2+} entering NMDA receptors where it binds to calmodulin activating PP2B. PP2B then dephosphorylates inhibitor-1 causing activation of PP1 which in turn dephosphorylates the AMPA receptor subunit, GluA1, at site ser845. Alongside this pathway, the Ca^{2+} entering from NMDA receptors also liberates Ca^{2+} from intracellular stores, further raising intracellular Ca^{2+} levels. A more detailed description of the intracellular cascades resulting in LTD from NMDA receptor activation can be seen in Figure 1.6.

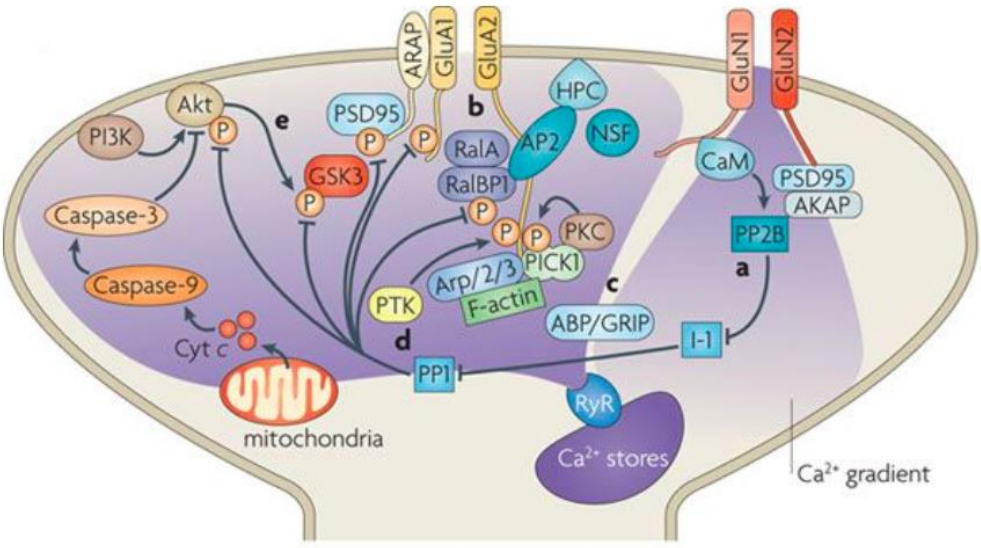

Figure 1.6. Signalling mechanisms of NMDA-LTD

a) *Ca^{2+} enters NMDA receptors and is detected by calmodulin leading to protein phosphatase cascade and activating PP1. PP1 acts by dephosphorylating numerous targets such as GluA1 and PSD95.* ***b)*** *GluA2-containing AMPA receptors are maintained at the synapse through an interaction with N-ethylmaleimide-sensitive factor (NSF). NSF is displaced as hippocalcin, the calcium sensor, targets adaptor protein 2 to GluA2 initiating the endocytosis of AMPA receptors.* ***c)*** *Protein interacting with C kinase 1 (PICK1) aids in the dissociation of AMPA receptor from AMPA receptor-binding protein–glutamate receptor interacting protein (ABP-GRIP) via GluA2 phosphorylation by protein kinase C. PICK1 also binds to actin-related proteins negatively regulating actin polymerisation. d) phosphorylation of GluA2 helps exchange PICK1 for ABP-GRIP. e) GSK3β is activated by PP1 and is required for NMDA-LTD (Collingridge et al., 2010).*

The pathways described above do not involve protein synthesis although evidence does point to a protein synthesis component. Kauderer and Kandel (2000) used anisomycin to block protein synthesis in organotypic hippocampal slice cultures recordings which in turn blocked NMDA-LTD in what they classed as a late form of LTD. It must be noted that the same group used another PSI, CHX, in acute hippocampal slices which did not reduce NMDA-LTD. The authors suggest that this variation may be caused by an increase in model

stability in organotypic slices due to the increased recovery period after slicing. The possibility of protein synthesis pathways existing within the NMDA-LTD process requires further investigation to enable clarification.

1.3.1.3.2. mGluR-LTD

As well as NMDA-LTD, LTD can also be induced through the activation of mGluRs, known as mGluR-LTD. mGluR-LTD has been observed via activation of many mGluRs, including: mGluR1, mGluR2, mGluR3, mGluR5 and mGluR7 (Bellone et al., 2008), however, only group 1 mGluR's (encompassing mGluR1 and mGluR5) will be explored in more detail. The other receptors are outside the scope of this thesis.

The first evidence supporting the existence of mGluR-LTD in the hippocampus arose from Bashir and Collingridge (1994) (previously described in the cerebellum by Ito *et al.* (1986)); they demonstrated how the application of an LFS protocol caused depotentiation of potentiated synapses that was blocked by α-methyl-4-carboxyphenylglycine (MCPG) (a group I/II mGluR antagonist) and was independent of NMDA receptor involvement (Bashir and Collingridge, 1994). Following this discovery, *de-novo* mGluR-LTD was shown to be inducible in rat hippocampal slices using a paired-pulse LFS (PP-LFS) consisting of 900 paired pulses separated with a 50ms interval and delivered at 1Hz (Bashir and Kemp, 1997). In the same year, a Group I mGluR agonist, DHPG, was first used in a bath application to trigger LTD in the hippocampal CA1 region (Palmer et al., 1997). This form of mGluR-LTD has been coined 'DHPG-LTD' and has been more commonly used to investigate the molecular mechanisms of mGluR-dependent LTD then the electrically induced version (Gladding et al., 2009).

Reports indicate distinct mechanisms exist between mGluR-LTD and the NMDA counterpart (Fitzjohn et al., 1999; Gladding et al., 2009). For example, evidence

has proposed a Ca^{2+} independent mechanism required for mGluR-LTD, which is in contrast to NMDA receptor-LTD (Fitzjohn et al., 2001). However, it is important to note that Ca^{2+} dependency in mGluR-LTD is a controversial subject as González-Sánchez *et al*. (2017) demonstrated the importance of Ca^{2+} influx in cortical neurons for regular mGluR-LTD (González-Sánchez et al., 2017). Another contrasting feature is the requirement for certain phosphatases and kinases in the two mechanisms, such as PKA and PKC in NMDA-LTD (Peineau et al., 2009) and tyrosine phosphatases in mGluR-LTD (Moult et al., 2008).

Group 1 mGluRs are postsynaptically expressed, though they are located outside of the postsynaptic density, and as a result they rely on glutamate spill-over for their activation (Lujan et al., 1996). Methods regularly used to investigate DHPG-LTD revolve around knock-out models, with a previous $mGluR5^{-/-}$ model shown to have completely abolished DHPG-LTD whilst an $mGluR1^{-/-}$ model only partially reduced the depressive effect (Huber et al., 2001; Volk et al., 2006). The broad consensus is that the cooperation of both receptors likely induces LTD. Conversely, strain differences of mice and slight differences in experimental methodology may be a contributory cause.

The molecular mechanisms underpinning DHPG-LTD are yet to be fully defined, however pathways downstream of mGluR activation are gradually being unearthed (Figure 1.7). ERK and MAPK pathways are believed to be heavily involved in DHPG-LTD (Gallagher et al., 2004; Huber et al., 2001, 2000; Moult et al., 2008) and involves signalling molecules such as CaMKII, PKC, eIFs, Staufen 2 and PI3K, however there is some dissonance between studies regarding the importance of these molecules (Hou and Klann, 2004; Huang et al., 2004; Lebeau et al., 2011; Mockett et al., 2011; Moult et al., 2008; Schnabel et al., 1999). The large discordance between results in this area likely reflects the precise regulation of the mechanisms with the strain, species, age and gender of animals possibly having a huge impact on results. For example, a developmental switch has been proposed whereby neonatal animals rely upon a

presynaptic protein synthesis independent form of mGluR-LTD and adult animals utilise a postsynaptic and protein synthesis dependent form (Nosyreva and Huber, 2005). Age has also been deemed a determining factor for protein tyrosine phosphotase involvement (Kumar and Foster, 2007).

A strong case for the involvement of protein synthesis in DHPG-LTD has been supplied by Di Prisco *et al.* (2014) who used a genetic murine model with reduced eIF2a phosphorylation which is thought to be required for protein translation. AMPA receptors could not be internalised in these mice and as a result DHPG-LTD could not be induced and object-place learning was severely reduced. Further evidence for the involvement of protein synthesis has been contributed in the pursuit of understanding FXS which is further discussed in section 1.3.1.3.4.

DHPG-LTD is a complex phenomenon with characteristics and mechanisms that are not agreed upon. Although there are a large number of conflicts, some molecular models are more popular than others such as that reviewed by Sanderson *et al.* ((Sanderson et al., 2016) depicted in Figure 1.7.

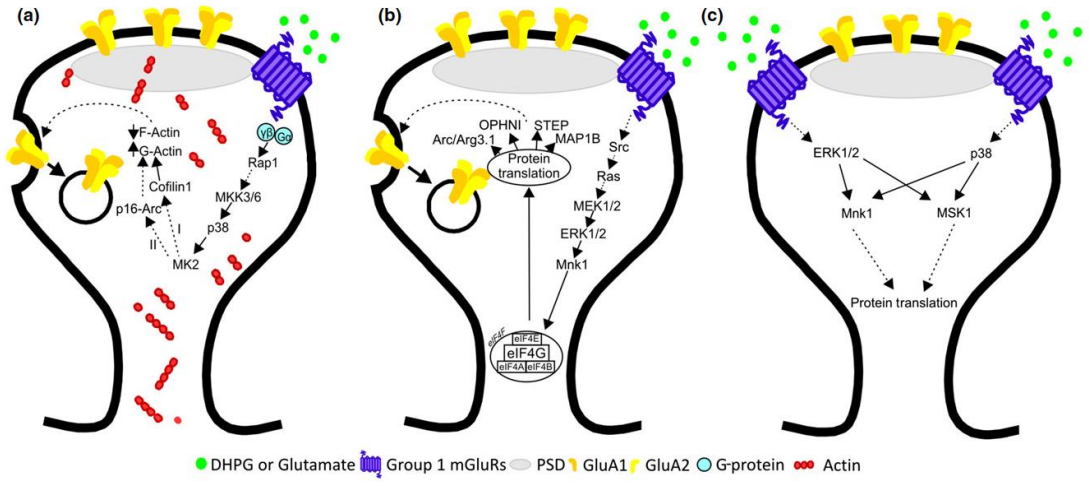

Figure 1.7. Putative model depicting mGluR-LTD cascade of events

a) *DHPG or glutamate activates mGluRs leading to the detachment of $G\alpha_q$ from the βγ subunits of the GPCR. This causes activation of RAP1 which activates MKK 3/6 and subsequently p38, allowing it to phosphorylate MK2. The now activated MK2 can influence two different downstream cascades (I) It can dephosphorylate and activate coflin1 to alter spine morphology (Eales et al., 2014) and trigger AMPA receptor internalisation and lower F-actin levels whilst increasing G-actin (II) p16-Arc becomes directly phosphorylated by MK2 to regulate AMPA receptor internalisation.*
b) *The link between ERK1/2 and mGluR activation are not yet known. However, mGluR activation can lead to the phosphorylation of eukaryotic initiation factors and MnK1 which controls protein translation, regulating the expression of proteins important in AMPA receptor internalisation such as MaP1B, Arc/Arg3.1 and striatal-enriched protein phosphatase.*
c) *ERK1/2 and p38 can activate Mnk1 and MSK1 (Thandi et al., 2002). These can also have an influence on translational control resulting in endocytosis of AMPA receptors.*

Distinctions in mechanisms have been identified between the chemical and synaptic forms of mGluR-LTD. For example, *in vivo* recordings within the dentate gyrus of freely moving rats revealed a reliance of LFS-LTD exclusively on mGluR1 activation with no involvement of mGluR5, whereas DHPG-LTD relies on both receptors to some extent. DHPG-LTD has also been shown to

have a relatively small NMDA receptor component that is not found in LFS-LTD, however the strong Ca^{2+} influx through L-type VG-Ca^{2+} channels is vital for both LTD types (Naie et al., 2007).

1.3.1.3.3 LTD in learning and memory

As previously described, there is evidence linking synaptic plasticity to learning and memory. However, the extent to which mGluR-LTD contributes specifically to hippocampal-dependent learning is not fully clarified. Meaningful indications linking memory and mGluRs can be found in the literature, for example, the use of an $mGluR5^{-/-}$ rodent model showed a significant reduction in the extinction of contextual and auditory fear (Xu et al., 2009), and pharmacological blockade of mGluR5 reduces performance in radial arm experiments (Manahan-Vaughan and Braunewell, 2005). Also, LFS given *in vivo* to exploring rats increased levels of LTD in the ipsilateral hippocampal CA1 region compared to when the animals were not exploring a novel environment (Balschun et al., 1999). Finally, as was mentioned in the previous section, inhibiting mGluR-LTD via eiF2a phosphorylation reduced object-place learning (Di Prisco et al., 2014). NMDA-LTD has been linked to hippocampal-dependent learning. A genetic mutation of the NR2B NMDA receptor subunit in a murine model inhibited NMDA-LTD as well as spatial learning. However, whether the LTD inhibition led to the deficient learning is difficult to determine, especially as NMDA-LTP was slightly reduced and could have contributed to the deficits in the behavioural tasks (Brigman et al., 2010). Another transgenic mouse model inhibited PP2 activity which reduced NMDA-LTD and disrupted learning in a water maze and T-maze task (Nicholls et al., 2008). Alongside these findings, it was found that potentiating hippocampal NMDA-LTD with D-serine (an NMDA receptor co-agonist) improved spatial reversal learning (Duffy et al., 2008).

1.3.1.3.4 LTD in disease

Perhaps the most renowned pathology linked to mGluR-LTD is FXS, the most common form of monogenic intellectual disability and monogenic autism in society. The clinical symptoms include moderate-severe intellectual disability, autistic behaviours, decreased attention and short-term memory and patients can also present with facial dysmorphia and epilepsy (Gallagher and Hallahan, 2012). FXS is caused by the loss of Fragile-X Mental Retardation Protein (FMRP) due to a silencing mutation of the Fmr1 gene that encodes FMRP (Bassell and Warren, 2008). To summarise FMRPs functionality, it can bind to a subset of mRNAs and inhibit its translation by halting the ribosome and preventing reading of the mRNA (Darnell et al., 2011). The FMRP knock-out mouse model has demonstrated exaggerated mGluR-LTD (Bear et al., 2004; Huber et al., 2002). The general theory for this effect is that without FMRP inhibiting mRNAs, there is no 'brake' on translation and an excess of proteins are translated that are involved in the internalisation of AMPA receptors, such as Arc and MAP1B (Darnell et al., 2011; Zalfa et al., 2003). ERK1/2 could be involved in the disease pathway as excessive protein levels observed in the FXS mouse model can be reduced with ERK1/2 inhibition (Osterweil et al., 2010). Also, ERK1/2 mRNA is a target of FMRP (Darnell et al., 2011) resulting in an increased response from protein synthesis machinery (Osterweil et al., 2010). As of yet, clinical trials involving the modulation of mGluR5 receptors have been unsuccessful (Dölen et al., 2010) and this could be for reasons such as the heterogenic nature of FXS that contains subpopulations (resulting from differing responses to the treatments) and the lack of biomarkers to accurately detect those patients that are most likely to benefit from the treatments (Jacquemont et al., 2014).

Alzheimer's disease has also been linked to mGluRs. Hippocampal atrophy occurs early in the disease and progressively deteriorates (Sabuncu et al., 2012). As previously discussed, LTP deficits have been detected in Alzheimer's

disease animal models (Klyubin et al., 2012) however the role of LTD requires much more attention. Previously, both inhibition and deletion of mGluR5 rescued severe spatial learning deficits in an Alzheimer's disease model (with reduced Aβ plaque load) (Hamilton et al., 2014).

1.3.2. Short-term synaptic plasticity

The previous sections discussed forms of long-term synaptic plasticity. Short-term changes occurring at synapses, also known as short-term synaptic plasticity, refers to alterations to synaptic efficacy over a period of time that reflects the history of presynaptic activity. Two types of short-term plasticity currently exist, facilitation and depression and can be measured *in vitro* by applying a pair of pulses to a neural pathway whilst recording the EPSPs from a synapsing neuron.

PPF is a feature of CA1 PNs (Lee et al., 2017; Leung and Fu, 1994) and is regularly used as a measurement of release probability of vesicles (Manita et al., 2007). The PPR is widely regarded as an indicator of release probability with the residual calcium hypothesis, introduced by Katz and Miledi (1968), remaining the most established and accepted theory. The doctrine proposes that PPF, as witnessed in CA1 PNs, is a sign of low release probability from presynaptic terminals. Residual calcium within the presynaptic terminal builds up after the first pulse leading to an increase in probability of release on the second pulse and therefore a greater release of neurotransmitter and a larger post-synaptic response. A decrease in PPR could indicate an increase in presynaptic vesicle release probability and an increase in PPR could indicate a decrease in release probability. It must be mentioned that the link between PPR and release probability has been profoundly challenged by Manita *et al.* (2007) who attributed release probability to astrocyte calcium signalling.

1.3.3. Intrinsic properties

In contrast to the extensive efforts made to understand synaptic plasticity, research into the plasticity of intrinsic properties of neurons has only begun to be considered in depth over the past couple of decades. The features of intrinsic properties involve the modulation of functional properties and/or expression of the hugely diverse number of ion channels embedded in the plasma membrane. This type of modulation can have an impact on action potential generation, waveform and passive properties of membranes, all of which can influence how a single neuron may respond to an input. The backpropagation of action potentials in dendrites is also influenced by intrinsic properties and is important for spike-timing dependent plasticity (STDP) (Daoudal and Debanne, 2003). A study showed that an STD-LTP was complemented with a decrease in excitability of the cell as well as a reduction in R_i. The intrinsic changes were revealed to be caused by the regulation of HCN channels (Fan et al., 2005).

The intrinsic excitability of a neuron is plastic and is therefore subject to alterations that can be determined by its physiological history, such as previous synaptic and intrinsic activity (Daoudal and Debanne, 2003; Zhang and Linden, 2003). The location, gating properties and number of the hugely diverse array of voltage-gated ion channels determine the intrinsic excitability of each cell (Bean, 2007) and governs action potential after-potentials (after-depolarisations and after-hyperpolarisations) (Brown et al., 2011). The ionic conductances causing the after-potentials are imperative for the rate and pattern of repetitive neural firing and interestingly many of these conductance's are altered in response to mGluR activation (Anwyl, 1999).

N-type calcium channels are a type of high voltage activated channel found amply in the hippocampus tending to localise presynaptically and have been associated with neurotransmitter release and synaptogenesis (Su et al., 2012). Previous research has demonstrated that the whole mGluR family can

individually inhibit the N-type channel through a membrane delimited process (Choi and Lovinger, 1996) which is therefore independent of diffusible intracellular messengers. In the CA1, suppression of this calcium channel through mGluR activation has been shown to reduce inhibitory postsynaptic currents and abolish depolarisation-induced suppression of inhibition (DSI) (Lenz et al., 1998). DSI can be summarised as a transient decrease in GABAergic transmission following brief postsynaptic depolarisation i.e. the decrease in inhibition seen with DSI is facilitated presynaptically through reduced GABA release. Another calcium channel inhibited by mGluR activation is the L-type calcium channel; it is likely that the downregulation of this channel (via mGluR activation) is caused by a slow mechanism consistent with the time frame of intracellular messenger involvement and has subsequently been linked to intracellular calcium release (Kato et al., 2012).

As mentioned, mGluR activation has many effects on the cell that alter its intrinsic excitability such as SFA, also known as accommodation. The term “accommodation” was first used in the context of neurons by Nernst over a century ago and can be used to describe the decrease in action potential firing frequency over time resulting from supra-threshold current injections. The role of potassium currents has long been ascribed to spike accommodation, such as voltage-gated and calcium-sensitive potassium currents (Ha and Cheong, 2017). Group 1 mGluR activation has been shown to enhance the inward current of such channels that may contribute to the decrease in SFA (Chuang et al., 2000). A more recently identified channel deemed to be involved in SFA is anoctamin-2 (ANO2), a protein found in both CA1 PNs (Huang et al., 2012) as well as thalamocortical neurons among others (Ha and Cheong, 2017). ANO2 is a calcium-activated chloride channel (CACCs) and is dependent on the intracellular Cl^- concentration, their activation can either induce hyperpolarisation or depolarisation. Due to the high expression of K^+/Cl^- cotransporters in mature central nervous system (CNS) neurons, a low intracellular Cl^- concentration is

maintained leading to hyperpolarisation of a cell when ANO2 is activated (Ha and Cheong, 2017).

CA1 pyramidal cells are examples of adaptive neurons and the adaptation process is largely contributed to by the inactivation of closed Na^+ channels as well as an outward K^+ current termed I_{AHP} that is known to inactivate with mGluR activation. The I_{AHP} has slow activating and inactivating kinetics that is activated by a rise in intracellular calcium levels (Anwyl, 1999). The current is mediated by the SK channels which have a characteristic low conductance. The inhibitory action of mGluRs on SK channels has been shown in CA1 pyramidal cells (Gereau and Conn, 1995), dentate gyrus (Abdul-Ghani et al., 1996) and Purkinje cells located in the cerebellum (Netzeband et al., 1997). In the CA1, the effects of group 1 mGluRs is likely to be dependent on G-proteins as the I_{AHP} inhibition was blocked dose-dependently by RGS4, a G-Protein signalling regulatory protein (Saugstad et al., 1998) (RGS proteins act as effector antagonists). The evidence of calcium levels being a vital element in mGluR depression of I_{AHP} have been contradictory; using Egtazic acid (calcium buffer) reduced the inhibitory action of mGluR agonists (Abdul-Ghani et al., 1996) yet the measurement of intracellular calcium levels using fura-2 showed no increase in calcium levels intracellularly with mGluR activation (Anwyl, 1999). The intracellular molecular pathway is generally accepted to involve PKC activation and in fact, PKC activators have been used to inhibit the slow AHP in CA1 pyramidal cells (Nouranifar et al., 1998). The evidence is substantial enough to attribute I_{AHP} as a major contribution to spike accommodation, however there are other currents causative to this neural feature such as I_M, an outward-rectifying potassium current activated in response to depolarising stimuli that is also inhibited by mGluR activation (Shirasaki et al., 1994).

Other intrinsic alterations caused by mGluR activation include peak amplitude changes. Past evidence has proposed an interaction of fast transient Na^+ currents with group 1 mGluRs via PKC. mGluR activation via DHPG application

leads to a decrease in this Na^+ current which in part determines the upstroke phase of the action potential and therefore the peak action potential (Carlier et al., 2006). Other mGluR-mediated modifications include input resistance; a determining factor of input resistance is the extent in which ion channels within the membrane are open; the lower the resistance, usually the more channels are open. DHPG has been shown to increase input resistance (Ireland and Abraham, 2002) and has been attributed to closure of constitutively active channels such as TRPC (El-Hassar et al., 2011) found in the hippocampus (Chung et al., 2006) . Depolarisation of the resting membrane caused by mGluRs altering cellular properties that contribute to determining the resting membrane potential, such as the release of intracellular Ca^{2+} (El-Hassar et al., 2011), is another mGluR-mediated intrinsic alteration. Finally, Park *et al*. (2010) have previously presented results specifying an elimination of a post-burst AHP which could be due to a complex upregulation of R-type channels involving PLC activation as a result of mGluR5 activation.

1.3.3. Summary

Synaptic plasticity involves the modulation of neural connections that is maintained over an extensive period of time leading to changes in how information is encoded. The two most significantly investigated forms of synaptic plasticity are LTP and LTD and are required for learning and memory. This chapter described several aspects of synaptic plasticity such as the possibility of protein synthesis involvement and the receptors required for its induction and maintenance. Intrinsic properties are also susceptible to modulation that involves changes to a neuron's ion channels and is also a vital component of learning and memory.

1.4. NSun2, RNA methylation and regulated translation in neurons

1.4.1. NOP2/Sun domain family member 2 (NSun2)

The NSun2 protein was first described as a downstream Myc target (a well-known proto-oncogene) that induces proliferation (Frye and Watt, 2006). Research since Frye and Watts' initial publication has helped elucidate the role of the protein as a key cellular RNA modification enzyme. Thus NSun2 specifically catalyses the addition of methyl groups to target cytosines in RNAs resulting in a stable modification known as a 5-methylcytosine (m5C). NSun2-mediated m5C modifications were initially detected in highly abundant cellular RNAs such as ribosomal RNAs (rRNAs) and transfer RNAs (tRNAs). Subsequent reports, which leveraged more sensitive sequencing-based approaches, have further identified hundreds of candidate m5C sites in both non-coding RNAs and mRNAs (Amort et al., 2017; Hussain et al., 2013a; Khoddami and Cairns, 2013; Squires et al., 2012), which are expected to be enriched in regions immediately downstream of translation initiation sites (Yang et al., 2017). NSun2 is found in multiple tissue types with an abundance found in numerous brain regions with particularly high densities detected in cell bodies of the hippocampal formation (DG, CA1, CA2, CA3) as illustrated in the Allen Brain Atlas.

1.4.1.1. NSun2-deficiency in humans

Since 2012, whole exome sequencing studies have revealed NSun2 gene mutations in 15 individuals from 6 families of Middle Eastern and Pakistani descent (Abbasi-Moheb et al., 2012; Fahiminiya et al., 2014; Khan et al., 2012; Komara et al., 2015; Martinez et al., 2012) . The condition resulting from these mutations has been likened to known genetic disorders such as Noonan

syndrome (Fahiminiya et al., 2014) and Dubowitz syndrome (Martinez et al., 2012) due to the clinical presentation of intellectual disability that has been identified in all current cases of NSun2-deficiency. Abbasi-Moheb *et al.* (2015) reported a long face, large nose and high nasal bridge in all 8 of the patients analysed in their report as well as the majority of patients being of short stature with microcephaly. Another prominent feature was the muscular hypotonia present. Khan *et al.'s (*2012) report was similar, although a broad gait was also identified and delayed puberty in one of the patients. Martinez *et al.* (2012) described axial hypotonia along with the prominent facial dysmorphia as the only neurological deficit and intellectual disability characteristics seen in the previous cases. Fahiminiya *et al.* (2014) reported a patient suffering from blepharophimosis (a horizontally narrow palpebral fissure) but no other facial dysmorphia was reported, but similarly to Martinez *et al's* study, did present with axial hypotonia. Finally, Khan *et al. (*2015) stated microcephaly, short stature, facial dysmorphia, broad gate and delayed puberty in their study of an NSun2-deficient patient with below average levels of testosterone and luteinising hormones detected. Autistic behaviours were also noted in the study.

Difficulties in understanding this neurodevelopmental disorder stems from its heterogeneous origin, lack of available biomarkers and an inability to translate findings from animal studies to real-world strategies to help those affected. Efforts have recently been made to generate different NSun2 knock-out models in both mice and drosophila, as well as obtaining samples from NSun2 deficient patients, in order to improve the current knowledge of the gene in neuronal function and cognition.

1.4.1.2 NSun2 transgenic models

Initially, a drosophila model was created using a Flippase-mediated trans-deletion of NSun2 and was subject to an aversive olfactory conditioning

paradigm in order to identify potential short-term memory (STM) deficits (Abbasi-Moheb et al., 2012) . The results indicated severe STM impairments that could be rescued through restoring NSun2 expression. Although the clinical reports of NSun2-deficient patients do not seem to investigate STM deficits, low IQ scores (40-50) have been reported in an affected Pakistani family (Khan et al., 2012). It has been previously suggested that intellectual disability can be linked to working memory deficits (Vicari, 2004), however it is arguably not a reliable predictor (Alloway and Alloway, 2010). The heterogenic nature of intellectual disability origins may account for these discrepancies. This drosophila model was the first attempt of replicating NSun2 deficiencies found in humans suggesting that the gene may be involved in higher cognitive function.

The NSun2 model that has provided the most in-depth characterisation is a mouse model with a mutation triggering NSun2 gene truncation. This model has significantly contributed to the current understanding of the pathology caused by RNA hypo-methylation in the absence of NSun2 (Blanco et al., 2014). Blanco *et al*. reported a high number of tRNAs that are methylated by NSun2 in mouse skin cells (194 tRNAs), with a significant overlap with NSun2-mediated methylation detected in human fibroblast cells. tRNAs that do not undergo methylation in the NSun2 knock-out model seem to be more likely to accumulate 5’ tRNA fragments leading to excessive cell apoptosis in hippocampal, striatal and cortical neurons. It has been shown that cleavage of tRNAs is a response to stress stimuli (Thompson et al., 2008), and as a result, NSun2$^{-/-}$ cells are more sensitive towards stressors.

The NSun2$^{-/-}$ mouse model was also shown to have a reduction in protein synthesis, and a significant reduction in brain volume due to diminution of the hippocampus, striatum and cortex (Blanco et al., 2014). Blanco ***et al.’s*** report of a global reduction in translation rates might be key to many of the phenotypes observed in the model, as translation has been shown to be a fundamental requirement for normal development and maturation of neuronal cells (Darnell et

al., 2011). This indicates NSun2 being a prerequisite for normal translation for the maturation of cells, and the neuronal loss observed could be caused by the increased likelihood of apoptosis. A reduction in postsynaptic density-95 (PSD-95), a marker of post synaptic densities in mature neurons was also reported, though there was no change in the presynaptic marker, synapsin (Blanco et al. 2014). Neurological defects were also investigated; altered motor coordination deficits were recorded due to poor performance of NSun2$^{-/-}$ mice in rotarod tests, and discrepancies in an open field test indicated reduced adaptive anxiety. A Y-Maze Spontaneous Alternation Test which involves the use of many brain regions such as the hippocampus, prefrontal cortex and septum also showed a reduction in spontaneous alterations in the NSun2$^{-/-}$ mice, indicative of spatial working memory deficits (Blanco et al. 2014).

A significant amount of our understanding of NSun2's function has been due to Blanco *et al.'s* Nsun2$^{-/-}$ mutant mouse model study. Although, extrapolating a direct physiological function from a model where the protein is absent throughout development and the entire life of the animal is particularly difficult; some of the deficits observed might not be directly attributable to NSun2, but could be due to secondary effects. To uncover direct causality, ideally a Cre/Lox animal model could be utilised to allow NSun2 to be present and fully functional during the animals' development, and then disrupted just prior to experimentation. However, when modelling inherited Mendelian diseases, the use of a constitutive knockout, such as that used by Blanco *et al*., is most appropriate; this is important when studying neurodevelopmental disorders, considering for example that the formation of synaptic plasticity is thought to have a strong early developmental component. The characterised murine constitutive knock-out model of NSun2-deficiency (Blanco et al. 2014) was used for all of the electrophysiology investigations in this thesis work.

1.4.1.3. NSun2s' possible role in neural function

It has been demonstrated that NSun2 localises to the soma and dendrites of cultured human neurons (Hussain and Bashir, 2015). Hussain *et al.* (2013a) also identified a total of 241 postsynaptic proteome mRNAs that were methylation targets of NSun2. A significant proportion of NSun2 methylation targets were also found to be binding targets of the protein disrupted in FXS, FMRP, such targets included mTOR and eIF4F mRNAs (Hussain and Bashir, 2015). Owing to the progress made to understand FMRP-related function, much is known about the target proteins encoded by these transcripts and how they are involved in synaptic plasticity modulation, although the functional consequences of NSun2-mediated methylation of the corresponding target transcripts is not yet known.

A further promising finding that could have implicit relevance for a role of NSun2 in neuronal function came from the evidence that NSun2 can target vault non-coding RNA (vtRNA) 1.1 for methylation (Hussain et al., 2013b). vtRNA1.1 is a non-coding RNA and forms a ribonucleoprotein complex with a protein known as Major Vault Protein; this complex has previously been implicated in the transport of mRNAs along neurites (Paspalas et al., 2009). It has also been shown that vtRNA1.1 can further be processed into small regulatory RNAs, known as small vault RNAs (svRNAs), with microRNA-like properties (Persson et al., 2009). Hussain *et al*. (2013b) exploited the methylation individual nucleotide resolution crosslinking immunoprecipitation (miCLIP) method which identified six NSun2-targetted cytosine locations on vtRNA1.1. Subsequently, using NSun2$^{-/-}$ patient fibroblast cells as controls, they learnt that the vtRNA can normally be processed into svRNAs in an NSun2-dependent manner; whereas the svRNAs were generally downregulated, one specific svRNA, svRNA4, was found to be dramatically increased in NSun2$^{-/-}$ patient cells. svRNA4 targets both CACNG7 and CACNG8 mRNAs which encode TARP γ-7 and TARP γ-8, respectively. TARPs are auxiliary proteins that associate with AMPA receptors, the γ-8 is

found abundantly in the hippocampus and has been shown to regulate AMPA receptor trafficking from the readily-available pool through the use of a TARP γ-8 knock-out model (Rouach et al., 2005). Intriguingly, in the same knock-out model a significant reduction in LTP, but not LTD, was observed in the hippocampal CA1 region (Rouach et al., 2005).

The NSun2 protein is further known to undergo regulation itself, namely by the Aurora B kinase (Sakita-Suto et al., 2007). Thus Aurora B has the capability of phosphorylating NSun2 resulting in two main consequences, firstly suppression of its methylase activity, and secondly causing NSun2s' dissociation from another protein, nucleolar phosphoprotein-1 (NPM1) (Sakita-Suto et al., 2007). Although phosphorylation of NSun2 has been shown to occur at the onset of mitosis (Sakita-Suto et al., 2007), whether phosphorylation of NSun2 occurs within non-dividing cells, such as neurons, remains unknown. It is however quite plausible that this may occur, potentially in response to neural activity, given the observations for example that the Aurora B kinase resides in synaptic regions of hippocampal neurons in rats, and is activated in response to NMDA receptor stimulation (Huang et al., 2002).

1.4.2. RNA methylation

RNA molecules are comprised of the four major bases, adenine (A), cytosine (C), uracil (U) and guanine (G), as well as many non-canonical bases (Garcia and Goodenough-Lashua, 1998). These non-canonical bases are created with post-transcriptional chemical modifications of which there are predicted to be over 130, a stark contrast to the handful of identified DNA modifications (Machnicka et al., 2013). The functionality of the majority of these modifications are unknown, however their conservation in many species suggests important physiological roles (Schaefer et al., 2017).

RNA methylation investigation, sometimes referred to as ‘epitranscriptomics’, is still a relatively young field of molecular genetics. Indeed, only recently has the investigation into RNA modifications received an intense global focus, a shift that can be largely attributed to the development of relevant Next-Generation-Sequencing (NGS) methodologies aimed at the sensitive and accurate detection of these modifications (Hussain and Bashir, 2015). The newly founded procedures include m5C-RNA immunoprecipitation (Edelheit et al., 2013), RNA bisulfite sequencing (Schaefer, 2015), 5-azacytidine-mediated RNA immunoprecipitation (Khoddami and Cairns, 2013) and miCLIP (Hussain et al., 2013a), all of which have been previously implemented allowing contribution to mapping of the epitranscriptome. These tools have led to a burst of research with the aim to create a comprehensive map of RNA modifications and whilst a great deal of positional sites have been identified, work on gaining a functional insight by conducting thorough follow-up experiments has to be undertaken. Reports so far have linked RNA modifications in controlling spatiotemporal protein translation with possible biological outcomes including regulation of circadian rhythms (Fustin et al., 2013) and control of stem cell differentiation (Wang and He, 2014). Several other functional pathways are probably also impacted, and the mounting evidence points towards a large number of physiological roles of these post-transcriptional modifications.

A prominent functional mechanism that is becoming increasingly synonymous with RNA methylation is the control it exerts on protein synthesis. Wang *et al*. (2015) have provided particularly compelling evidence in support of this through their examination of N6-Methyladenosine (m6A) modifications in HeLa cells. The study revealed that the in addition to m6A promoting interaction with the RNA-binding protein, YTHFD2, the RNA modification also promoted a similar interaction with a related reader protein, YTHFD1. Whereas binding of YTHFD2 to m6A sites was found to accelerate mRNA decay, binding of YTHFD1 significantly accelerated the rate of translation. The authors therefore concluded that by enhancing binding of the YTHFD readers, translation occurs acutely from

m6A-modified mRNAs during a time-limited window. It is also quite relevant here that RNA methylation can be a dynamic process, and several proteins that can read, write and erase RNA methylation marks have been identified (Fu et al., 2014; Jia et al., 2011). These, and possible related similar mechanisms, are particularly attractive when considering intracellular postsynaptic signalling processes, where acute local changes in specific protein concentrations are likely important for proper function (Hussain and Bashir, 2015).

1.4.2.1. RNA methylation's influence on neural function

As discussed earlier in this chapter, the suggestions that the m5C RNA modification might be involved in learning and memory have been indicated from relevant observations made from studies of NSun2-deficiency. However, efforts have already been made to provide a connection between RNA methylation and relevant neural function more directly, with progress on this front being made mostly with investigations of RNA m6A modifications (Niu et al., 2013). Walters *et al*. (2017) observed the transient decrease in the Fat Mass and Obesity-Associated (FTO) protein, an m6A demethylase, as a result of fear conditioning, a behaviour heavily dependent on the hippocampus. Furthermore, the group artificially decreased FTO levels specifically in the dorsal region of the hippocampus with a viral vector expressing short hairpin RNA targeted to FTO, which led to an increase in contextual fear memory. Their findings suggest that m6A methylation enhances fear memory and is one of the first confirmations of RNA methylation bearing an influence on memory. Walters *et als*' research supports previous efforts from Widagdo *et al*. (2016) who found that knocking down FTO specifically in the prefrontal cortex also enhanced fear memory.

More recently, Merkurjev *et al*. (2018) established that m6A regulatory proteins reside within dendrites of mouse pyramidal cortical cells and therefore may bind to their RNA targets locally. Furthermore, reducing the expression of the m6A

readers, YTHDF1 or YTHDF3, in dissociated hippocampal neurons, altered neural morphology with an increased spine neck length and decreased spine head width. Alongside the morphological deficits uncovered, a decrease in PSD-95 clustering and surface expression of the GluA1 subunit was concomitant with a decrease in miniature EPSC amplitude. Remarkably, the group found that 85% of proteins found within the synaptic cleft, including CamKIIN1, were encoded by m6A methylated transcripts at both inhibitory and excitatory synapses, thus suggesting prominent roles of the m6A RNA modification in modulating synaptic function.

1.4.3. Regulated translation in neurons, and its functional importance

As mentioned in previous sections, the regulation of protein synthesis via RNA methylation including that catalysed by NSun2, has emerged as a central and common theme within the epitranscriptomics field. It is therefore particularly noteworthy that protein synthesis resulting from activity-induced gene expression is accepted to be a pre-requisite for learning and long-term memory formation (Alberini and Kandel, 2014). However, the timescale for experience-driven transcription is in the range of minutes – hours, whereas the consolidation and maintenance process can be anywhere from days to years. This clear discrepancy of time-frames suggests a non-linear relationship between behavioural adaptation and gene expression (McGaugh, 2000). Further temporal discordance is discernible between the extremely fast signal transduction through ion channels and the metabolic and chemical alteration of macromolecules and smaller molecules resulting in gene-expression (Sweatt, 2016). Because of this, the link between neural firing patterns, activity-induced gene expression and memory formation raises questions about how these processes are connected.

Although most mRNAs are translated within the soma (Doyle and Kiebler, 2011) there is ample evidence supporting the notion of local synaptic translation. The initial findings in the 1960's demonstrated that mRNA (Bodian, 1965) and polyribosomes (Levy and Steward, 1979) can be visualised in synaptic regions followed by supporting evidence that other translational machinery including tRNAs and other important translation factors such as initiation and elongation factors reside distally from the nucleus. Further validation was made by Torre and Steward (1992), whose experiments demonstrated that severing the soma from the dendrites in neural cultures did not prevent translation. There are some clear benefits of mRNA localisation within dendrites. Firstly, the presence of the mRNA rather than the protein means that the protein will be expressed locally and does not have to be recruited from other regions where said protein may have adverse and even harmful effects, for example Tau protein that has been implicated in Alzheimer's Disease (Chong et al., 2018). Secondly, it allows a very high spatial and temporal resolution for control of protein synthesis at an activated synapse that is instrumental in homosynaptic plasticity (Gardiol et al., 1999). Lastly, this microenvironment within the dendrite is independent of the cell body reducing the need for communication over long distances which increases the economy of the cell and improves energy conservation. One of the prominent questions regarding dendritic RNA localisation is, how does the mRNA find its way to where it needs to be?

To answer this, it is important to discuss aspects of the mRNA structure. mRNAs are known to contain what has been dubbed, "molecular zipcodes"; cis-acting elements usually located in the 3'- Untranslated Region (UTR) but also found at the 5'-UTR. These zipcodes are heterogenic in size as well as sequence and can be complex consisting of multiple distinct stem loops causing intricate secondary structures. The cis-acting elements are deemed to have multiple functions, with regulatory-elements in the 5'-UTR proposed to exert posttranscriptional control whereas 3'-UTRs influence a variety of stages such as nuclear export, mRNA stability and trafficking to specific subcellular locations

(Jambhekar and Derisi, 2007). The 3' regions also contain binding sites where miRNAs can attach and activate degradation of the mRNA (Andreassi and Riccio, 2009). The cis-acting elements are targeted by trans-acting factors such as RBPs or non-coding RNA's (Di Liegro et al., 2014). It is considered that RBPs provide the link between the RNA and other molecular machinery to promote transport (Palacios, 2007). For example, RBPs allows active linking to molecular motor proteins (dynein and kinesin) and the cellular cytoskeleton to facilitate diffusion before trapping and anchoring the transcript, it can also protect the transcript from degradation during its transport.

Another important aspect in neural translation is how the translational process is controlled once RNA is at the synapse. It is not uncommon for there to be thousands of synapses per neuron where there is a precise requirement for these connections to be independently maintained and local RNA regulation is fundamental to this. A frequently studied example is FMRP (an RBP) that binds to a subset of targeted mRNA to halt translation (as discussed earlier). RBP's are not the only method of RNA control, as miRNA interaction (Fukao et al., 2015), mRNA phosphorylation (Pierrat et al., 2007), eukaryotic initiation factors (Jackson et al., 2010) and RNA methylation all contribute to the layers of translational control.

Finally, an important feature of protein synthesis within neurons is that it can be triggered in response to neural activity. Early experiments from Weiler and Greenough (1991) depolarised synaptoneurosomes with K^+ ions which led to an increase in polyribosomal complexes, an indicator of translation. Aakalu *et al*. (2001) developed a protein synthesis reporter consisting of GFP flanking 5′ and 3′ UTRs from CAMKII-α allowing it to be visualised in dendrites. The application of BDNF was used to stimulate protein synthesis causing an increase in fluorescence in dendritic regions.

1.4.3. Summary

Until the end of the twentieth century, the dominating view was that the central dogma of biology (DNA → RNA → Protein) occurred centrally within a cell, that is, the nuclei and soma. However, evidence since then has revolutionised this doctrine and advocated a non-linear pathway in neuronal cells that involves peripheral (dendritic) processes partly accomplished through the localisation of non-coding and coding RNA within dendrites and the control on those RNA's. These RNA-centric mechanisms can provide numerous layers of control and allows a neuron to adaptively respond to environmental stimuli (Holt and Schuman, 2013). The localised RNAs are also likely regulated via different mechanisms, one of which is RNA methylation that may play a vital role in learning and plasticity mechanisms. NSun2 is a regulatory protein that catalyses the addition of such methyl groups.

Chapter 1.5. Hypothesis

The main hypothesis of this thesis is that NSun2$^{-/-}$ mice display plasticity deficits in the form of LTP or LTD when compared to their heterozygous littermates. The postulation is based around clinical observations of patients found to have NSun2 gene mutations, previous research involving other intellectual disability models and also current knowledge of NSun2$^{-/-}$ murine and drosophila models. The evidence to support the hypothesis are summarised as follows:

i) An NSun2$^{-/-}$ drosophila model was shown to have deficits in an odour aversion task (Abbasi-Moheb et al., 2012), a task that has been previously associated with an LTP requirement in the hippocampus of rats (Chaillan et al., 1996), however it should be mentioned that this association was not shown to be causative.

ii) Other intellectual disability models, a common phonotype shared with NSun2-deficient patients, have displayed deficits in plasticity. These models include a Ts65Dn knock-out model of Down syndrome (Siarey et al., 1999), Mecp2 knock-out model of Rett syndrome (Moretti et al., 2006), Tsc2$^{+/-}$ mutant rat model of Tuberous sclerosis (von der Brelie et al., 2006), various Huntington Disease models (Lynch et al., 2007; Simmons et al., 2009) and FXS models (Chen et al., 2010; Lauterborn et al., 2007). It is therefore possible that NSun2$^{-/-}$ mice harbour similar deficits.

iii) NSun2 seems to share many similar mRNA targets as FMRP that are found in the postsynaptic proteome involved in intracellular signalling downstream of mGluR activation (Hussain and Bashir, 2015). The FXS mouse model, as explained above, has been shown to have mis-regulated plasticity (Chen et al., 2010; Lauterborn et al., 2007).

iv) Hussain *et al.* (2013) presented data suggesting NSun2-mediated methylation of vtRNA1.1 can influence the RNAs' breakdown into svRNAs that may regulate transcripts encoding TARPs. TARPs have been shown to be vital in the efficacy of AMPA receptors and their trafficking (Rouach et al., 2005).

v) Although a different modification, m6A modifications similarly involves the addition of methyl groups to RNA. Previous research has demonstrated the dynamic nature of methylase activity and its requirement for learning (Walters *et al.* 2017).

vi) Blanco *et al.* (2014) reported a global reduction of translation in the NSun2$^{-/-}$ mice; previous reports of protein synthesis reduction or complete inhibition have resulted in significant plasticity impairments (Huber *et al.* 2001).

Chapter 2. Materials and Methods

Both whole-cell patch clamp and field electrophysiology methods were used to investigate synaptic plasticity and intrinsic properties in CA1 pyramidal neurons of an NSun2 knock-out mouse model; these experiments were all conducted within the Bashir laboratory at the University of Bristol. In addition, immunohistochemistry imaging studies were carried out on a PC12 cell model investigating NSun2 protein subcellular localisation in the Hussain laboratory at the University of Bath.

2.1. Animals

The NSun2 mutant mouse model was generated by the German Gene Trap Consortium and carries a gene trap in intron 8 (GGTC-clone ID: D014D11). They were provided for this study by Dr Michaela Frye (University of Cambridge), within whose laboratory the mutant allele has previously been shown to result in functional NSun2 protein not being produced (Blanco et al., 2011; Hussain et al., 2013a). The mice were mated with C57Bl6/J CBA F1 mice as described previously (Blanco et al., 2011). The mice used for experimentation in this project had to be rederived from the original colonies. All mice were genotyped to determine either a full NSun2 mutation (knock-out mouse), no mutation (wildtype mouse) or one mutated allele (heterozygous mouse). Theoretically, litters containing knock-out and WT mice should be approximately 25% each (Mendelian ratios), this was not the case and resulted in difficulty obtaining mice with the full NSun2 mutation and WT's. For this reason, it was more practical to use the more commonly acquired heterozygous mice as a control allowing regular interleaving of experiments when NSun2$^{-/-}$ mice became

available. There have been no reports of observable phenotypes in carriers of the NSun2 mutation (one NSun2 allele mutation) in the human population. However, the heterozygous mice used in these experiments were not characterised or tested for similar deficits previously observed in NSun2$^{-/-}$mice.

All animals used for experimentation were between 4 and 12 weeks old. Control mice were age-matched *NSun2*$^{+/-}$ littermates and all mice were housed on a 12:12 light/dark cycle with *ad libitum* food and water. Recordings were not conducted blind to genotype. All procedures were carried out in accordance with UK Home Office guidelines set out in the Animals (Scientific Procedures) Act 1986.

2.2. Genotyping

All mice used for experiments were genotyped to determine either a full NSun2 mutation, no mutation or one mutated allele. Ear notches were used for genotyping (see below), and after killing the animals for experimentation, a tail tip was also taken to re-genotype the animal in order to re-confirm the result; no discrepancies were found throughout the duration of the project.

2.2.1. DNA extraction

The DNA extraction was based on Truett *et al*.'s "HotSHOT" method (2000). Ear notches were taken from the mice by the Animal Services Unit breeding team at the Langford site of Bristol University. Ear notches or tail tips were placed in a 0.5ml microfuge tube and 25µl of Alkaline Lysis Reagent (25mM NaOH and 0.2mM EDTA) was added. Each sample was placed in a heat block and incubated for 60 mins. During this time, a tube was removed from the heat block and vortexed for approximately 30 seconds before placing it back to continue

incubation and moving onto the next sample. After the DNA was extracted from the samples, 25µl of Neutralisation Reagent (40mM TRIS-HCL) was added.

2.2.2. DNA Amplification

The genotyping assay was essentially identical to that described previously (Blanco et al., 2011). Polymerase Chain Reaction (PCR) was used to amplify a relevant amplicon of the NSun2 gene using the DNA extracted from ear notches or tail tips. For each reaction 2µl of the DNA sample was diluted with 12.5µl of x2 PCR Master Mix (ThermoFisher), 1µl of 10µM forward and reverse primers, and 8.5µl water. For each sample two reactions were carried out; one used primers for the wild-type NSun2 allele and the other used primers for the mutant NSun2 allele; the primer sequences were:

- WT-R: 5’ - AGGGAGGGTCTGGAAAGATG
- WT- F: 5’ - AAGTAAGGCATAGTAACAGCTAC
- Mut-R: 5’ - CCGTAATGGGATAGGTTACGTTG
- Mut-F: 5’ – CCCAACAGTTGCGCAGCCTGAAT

Samples were loaded into a Bio-Rad PCR machine, and the PCR machines’ lid heated to 95°C, enabling the samples to undergo an initial denaturation phase for 2 minutes. Next, 40 cycles of the following programme was performed: 95°C for 20s, 55°C for 20s, 72°C for 40s. After the final cycle, there was a final extension step for 5 mins at 72°C, after which the samples were maintained at 4°C until the next stage.

2.2.3. Gel Electrophoresis

For gel electrophoresis analysis of the PCR products, Tris-acetate EDTA (TAE) buffer (Sigma) was diluted from 50x stock, 100ml of which was combined with

1g of agarose powder (type II, Sigma-Aldrich) and microwaved to boiling point to dissolve the agarose. The cyanine dye, SYBR Safe (ThermoFisher), was then diluted into the molten agarose (1:10,000), and then left for a minimum of 30 minutes to set in the electrophoresis tray with combes in place. 4.2µl of 6x DNA Gel Loading Dye was combined to each 25µl PCR product, and 10µl of each sample was then loaded into the formed wells of the set gel. Electrophoresis was performed at 95V for 45 minutes in 1X TAE running buffer. PCR products were viewed using a gel documentation system.

2.3. Electrophysiology

2.3.1. Slicing

Animals were killed through anaesthesia by isoflurane inhalation prior to cervical dislocation. Decapitation preceded the removal of the brain (without the prefrontal cortex) and was placed in oxygenated ice-cold sucrose (in mM: sucrose: 189, KCl: 3, $NaHCO_3$: 26, NaH_2PO_4: 1.25, D-glucose: 10, $CaCl_2$: 0.1, $MgSO_4$: 5). The brain was transferred to a metal stage where the dorsal side was glued to the stage surface. The stage was then mounted onto the vibratome (Leica VT 1000S) and submerged in the sucrose buffer. 400µm horizontal slices were made with the vibratome and placed in a beaker consisting of artificial cerebral spinal fluid (aCSF) (in mM: NaCl: 124, KCl: 3, $NaHCO_3$: 24, NaH_2PO_4: 1.25, D-glucose: 10, $CaCl_2$: 2, $MgSO_4$: 1) to incubate for 30 minutes at 32 - 34°C and then for 30 minutes at room temperature. The brain has gone through significant damage through the slicing process, both mechanical and hypoxic, which may lead to release of adenosine (Dale et al., 2000). Adenosine can dampen neuronal signal and modulate plasticity (de Mendonça and Ribeiro, 1997) and so the resting phase can provide time for the brain slices to regulate this.

2.3.2. Extracellular field potential recordings

CA3 region of the hippocampus was removed prior to transferring to the recording chamber. The slice was fully submerged in the chamber where aCSF was continually perfused through at a rate of 2.5-3mL.min^{-1} and maintained at 32 - 34°C. All pharmacological agents were applied to the perfusion system by adding to the aCSF when required. Field recordings were obtained using 2–3 MΩ glass microelectrodes (Harvard Apparatus) filled with aCSF. Microelectrodes were passed through a micropipette puller (P-97 Flaming Brown micropipette puller (Sutter Instrument Co.)). The stimulating electrode was placed in the *stratum radiatum* of the CA1 region, in close proximity to CA2. The recording electrode was also placed in the *stratum radiatum* in the CA1 region but closer to the *subiculum*, as shown in Figure 2.1. The fEPSPs were evoked through the delivery of 0.1ms electrical stimulation via a concentric stimulating electrode connected to an isolated constant current stimulator box (Warner Instruments). The response signals were amplified using an Axopatch 200B and Multiclamp 700B amplifier (Molecular Devices) and digitised with an M, X series acquisition board (National Instruments) at 40kHz and low-pass filtered at 2kHz. The acquired data was stored on a personal computer using WinLTP 2.0 (WinLTP Ltd.).

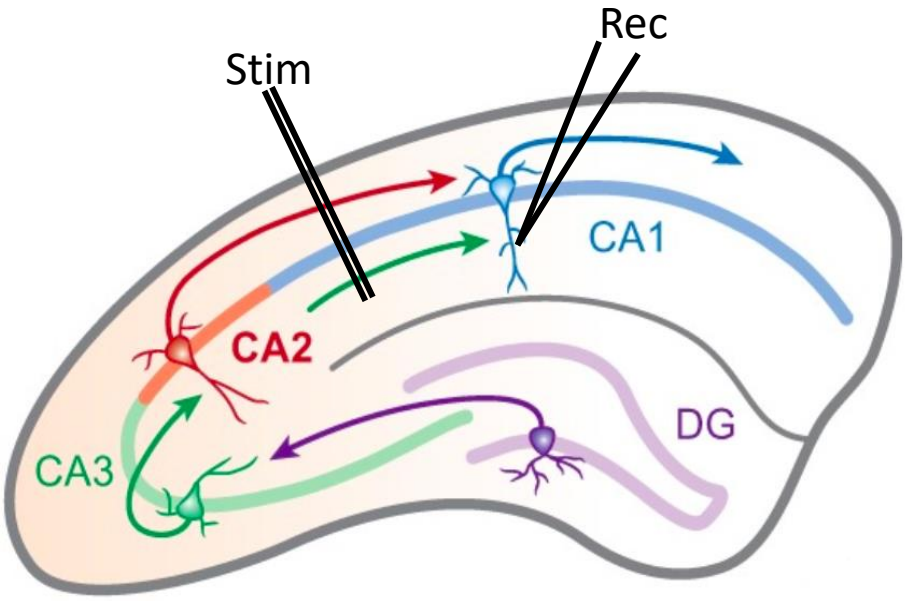

Figure 2.1. Electrode placement in hippocampus for extracellular recordings

Schematic demonstrating electrode placement for extracellular field recordings. A stimulating electrode (Stim) was placed in the stratum radiatum allowing innervation of the schaffer-collateral inputs from CA3. The recording electrode (Rec) was placed in the same layer but closer to the subiculum. Diagram modified from Caruana et al. (2012).

2.3.2.1. Basal transmission

Before field recording experiments for the mGluR-LTD experiments presented in chapter 3.2.2. an input-output curve was generated; initially, the input-threshold was determined by applying a pair of pulses at a minimum viable intensity that resulted in a visually observable fEPSP. This input was then used to stimulate the *Schaffer-collateral* pathway every 15s with increasing intensity every minute (the nine remaining values were taken as multiples of this threshold (2x up to 10x threshold with integers of 1)). Four sweeps were averaged together for the resulting response. The input-output curve was not only used to compare basal

transmission but also to find an appropriate stimulation level for each field experiment. The stimulation intensity range for experiments was between x3 and x5 the threshold for fEPSP response. After input-output responses were determined, a pair of stimuli was applied to the *Schaffer-collateral* pathway separated by pre-determined intervals (10ms, 20ms, 50ms, 100ms and 200ms). The aim of these experiments was to determine basal levels of pre-synaptic glutamate release.

2.3.2.2. Plasticity recordings

3.2.2.2.1. LTD

Chemical-LTD was achieved with a 20-minute bath application of 100µM DHPG (HelloBio) after a stable 30-minute baseline. NMDA receptors were blocked throughout the induction of LTD by bath-application of 50µM D-2-amino-5-phosphonovalerate (D-AP5) (HelloBio) during baseline recording and induction phase of LTD (up to 35 minute after DHPG application). DHPG was washed off and recordings continued for another 60 minutes. Two different protocols of synaptic-LTD induction were used; a paired-pulse protocol and a single-pulse protocol. Both methods applied 900 sweeps at 1Hz to the *Schaffer collateral* pathway, however the paired-pulse sweep consisted of dual electrical pulses with a 50ms inter-stimulus interval whereas the Single-Pulse sweep consisted of only one electrical pulse.

3.2.2.2.2. LTP

The induction of LTP was induced using a theta-burst stimulation (TBS) protocol consisting of 5 bursts (10 pulses at 100Hz) at 5 Hz (theta frequency range) and repeated 4 times separated with 20s intervals. Bursts at this frequency replicate

the endogenous theta rhythm and can induce maximal LTP by maximising post-synaptic depolarisation through disabling feedforward inhibition (Larson and Munkácsy, 2015).

2.3.3. Whole-cell patch clamp recordings

Whole cell recordings were taken from CA1 pyramidal neurons in the current clamp configuration. The 'Blind Patch' technique was implemented due to only having a brightfield microscope available and with no access to DIC optics. The glass micropipette for the recording electrode was filled with K-gluconate solution (in mM: K-gluconate: 145, NaCl: 5, HEPES: 10, EGTA: 0.2, GTP-NA Salt: 0.4, ATP Mg Salt; 4), and once filled, was attached to the head-stage and positive pressure was applied. The electrode was lowered into the chamber in the voltage clamp configuration with a +10mV voltage step to monitor the tip resistance. If the resistance was outside of the range of 3-5 MΩ then the glass was discarded and another used. When the electrode tip was positioned close to the CA1 *stratum pyramidale* a single-axis water hydraulic micromanipulator was used to slowly lower the electrode until a large deflection in the voltage step occurred. The transient voltage change is an indication of resistance being met; in this case the resistance being caused by the proximity to a cell body. A release of the positive pressure at this point combined with a brief application of negative pressure helps form the seal between the micropipette and the cell. When a seal has been formed, the command potential is set to that of an average resting membrane potential of a CA1 pyramidal neuron, -70mV, and electrode capacitance is negated. Once a stable giga-ohm seal is formed, negative pressure can be applied in fast bursts to rupture the cell membrane. To gauge the success of the whole-cell configuration, the capacitance transients in the voltage step (a representation of the cell capacitance) was used to indicate the series resistance. The WinLTP software calculates the series resistance by dividing the voltage step amplitude (10mV) by the peak of the capacitive transient.

Successful entry into the cell was followed by switching to current clamp mode with no current injected into the cell allowing cells to rest at their natural potential. Before the start of all experiments the intracellular and micropipette solutions were given 10 minutes to equilibrate and allow the cell to dialyse. Series resistance was monitored before and after the current clamp experiments. If the series resistance reached over 30MΩ at any point, then the experiment was excluded from analysis. Using the 'blind patch' technique means it is not possible to visually identify the cell types, however if the cell in question exhibited spike-frequency adaptation, fired spikes at a moderate rate (under 10 Hz) and had a relatively low input resistance (under 100 MΩ), then it would be considered a pyramidal neuron (Milior et al., 12). All recordings were obtained using the amplifiers bridge circuit to allow compensation of access resistance. The liquid junction potential created from the used of K-gluconate was -14mV and this was corrected for post-hoc.

2.4. Electrophysiology Data analysis

The bulk of analysis was completed using WinLTP, clampfit10.2 (Axon), Excel (Microsoft Co.) and custom written scripts within MATLAB (MathWorks) (with thanks to Clair Booth for writing the MATLAB scripts). Graphs were created in Prism 6.0 (GraphPad Software) and all statistical analysis was conducted with SPSS statistics 23 software (SPSS Inc.). Details of the statistical tests used to determine statistical significance are provided in each chapter. The magnitudes of any potential effects were unknown prior to experimentation and therefore power analysis prior to experiments was not suitable.

2.4.1. Analysis of extracellular recordings

All field recordings were analysed with WinLTP. The average of every 4 successive sweeps (each minute) was taken and low-pass filtered at 2kHz. The rising phase of the fEPSP was measured between 10–90% of peak amplitude, to prevent possible contamination of the signal from population spikes that may occur with high stimulus intensities.

2.4.1.1. Input-output relationship

With regards to measurements of synaptic efficacy at basal levels, there are several relationships that can be investigated in CA1 hippocampus. For example, the relationship between the fibre volley and the stimulus intensity (indicates the number of presynaptic fibres initiated in response to a given stimulus intensity), the relationship between the fEPSP and the fibre volley (indicates the response of the postsynaptic CA1 PNs to a given pre-synaptic activation) and also the relationship between the fEPSP and the stimulus intensity. Unfortunately, fibre volleys were not always visible, especially during the use of higher stimulus intensities and therefore the third option was used, which is arguably the most commonly reported relationship of basal transmission.

2.4.1.2. Paired Pulse Ratio

Paired Pulse Ratios (PPRs) were recorded after completion of input-output experiments conducted prior to the mGluR-LTD experiment presented in chapter 3.2.2. PPR has been used as a measure of probability of release of neurotransmitter from presynaptic terminals (Hanse and Gustafsson, 2001; Schulz, Cook and Johnston, 1994). During the PPR experiments, the stimulus

interval was increased every minute (intervals used: 10ms, 20ms, 50ms, 100ms, 200ms). The PPR was calculated as slope of the second fEPSP divided by the slope of the first fEPSP.

2.4.2. Current clamp recordings

2.4.2.1. Passive membrane properties

Immediately after switching to the current-clamp configuration the mean resting membrane potential was measured over a 1 second period in the absence of a current injection. For all other membrane properties, all cells were held at -70mV (with junction potential error correction taken into account) with a manually injected steady-state current preceding the hyperpolarising square-current injection of -100pA for 500ms.

Both the membrane charge constant and the input resistance were determined with a single exponential fitted to 10-95% of the membrane charge curve (Kerrigan et al., 2014). The input resistance was calculated using Ohm's law (voltage = current * resistance) applied to the steady state voltage after the "sag" (and therefore includes information from activated HCN channels) which is more conventional then calculating the input resistance from the infinite time extrapolation from the exponential fit. The % sag was calculated from the same voltage response to the -100pA current injection by:
(Extrapolated voltage change (from exponential fit) – steady state voltage change (after sag))/extrapolated voltage change)*100)
Both the negative peak and rebound (as depicted in figure 2.2.) were again measured from the same -100pA current injection.

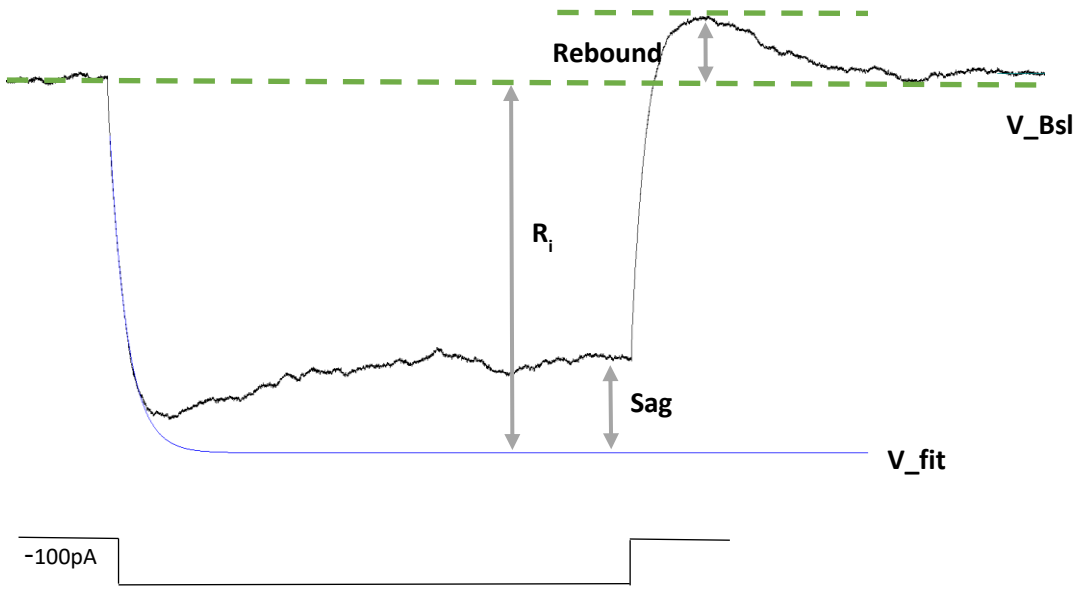

Figure 2.2. Measurements taken of passive membrane properties, rebound potential and sag in response to a -100pA current injection

An example of a voltage response trace from a CA1 pyramidal neuron during a -100pA current injection. V_Bsl is the Baseline voltage, v_fit (blue line) is the single exponential fit to the negative membrane voltage deflection and R_i demonstrates the measurements used for the input resistance. The green dashed lines represent the baseline voltage and the top of the rebound potential peak depicting this measurement. The current injection is depicted at the bottom of the trace.

2.4.2.2. Action potential properties

Due to action potential properties being dependable on the cells membrane potential, all cells were held at the same value with a manual current injection used to maintain the cells at -70mV during the experiments. All action potential properties were obtained from the first spike from the response elicited by a 300pA current injection. All cells fired a train of spikes at this intensity. The

action potential width was measured at 50% of the spike height and the action potential peak was measured relative to the baseline value. Analysis of the action potential threshold was calculated by differentiating the spike trace and using the first derivative that exceeded 20mV.ms^{-1}. The maximum value from the differentiation was used as the maximum rate of rise value (Figure 2.3.). To calculate instantaneous frequency/spike number, the number of spikes were counted from four different depolarising current steps, 100pA, 200pA, 300pA and 400pA.

The medium after-hyperpolarisation (mAHP) was measured as the peak amplitude relative to the resting membrane potential as 58ms after the last spike. For the AHP conversion to ADP experiment, a similar protocol was used to Park et al. (2010), where a burst of action potentials were evoked in response to five large and brief current injections at 2nA and lasting 2ms each. This elicited a reliable AHP. The voltage change was measured at the same time point of each sweep.

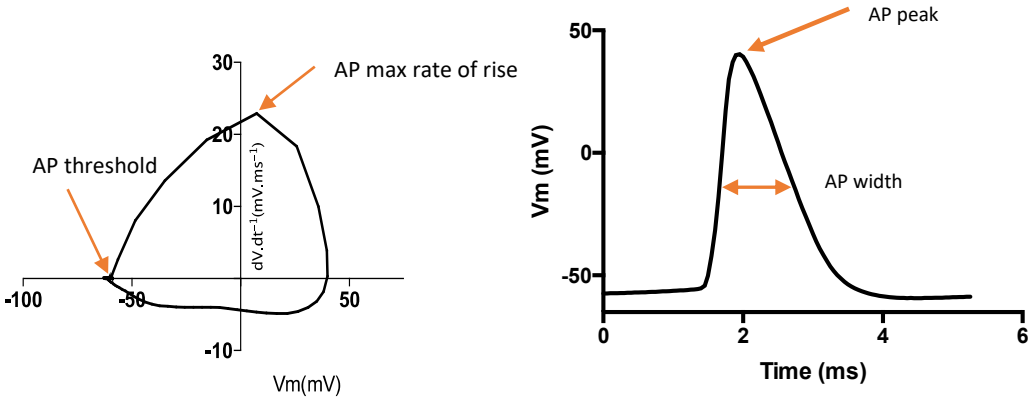

Figure 2.3. Measurement of supra-threshold/action potential properties

Representative phase plot (left) of the corresponding action potential (right) recorded from a CA1 pyramidal neuron response to a 300pA square wave current. The phase plot illustrates the first derivative of the response against the membrane potential.

2.5. PC12 cell cultures and drug treatments

PC12 cells were maintained in growth medium (Roswell Park Memorial Institute (RPMI) with L-Glutamate (Sigma-Aldrich), supplemented with 10% Horse Serum (Thermofisher), 1% penicillin/streptomycin (Thermofisher) and 5% foetal calf serum (Thermofisher) at a temperature of 37°C in a humidified incubator with 5% CO_2. Once cells had reached 80–90% confluency, the media was removed and 3ml of 0.25% trypsin (Sigma) was applied. The cells were then immediately incubated for 2 mins at 37°C to enable cell detachment from the monolayer. 13ml of media was then added to the flasks to neutralise the trypsin, and the cell-media mix was next transferred to a 50ml falcon tube and centrifuged for 4 mins at 1,400rpm at 21°C. The supernatant was removed and the pellet resuspended in 12ml of fresh media. 150µl of the resuspended PC12 cells were applied to coverslip-containing wells of a 6 well plate, which had been coated in 2% collagen (Sigma). This was then incubated for 1-2 days until the cover slips

had a cell monolayer confluency of approximately 60-70%, at which point the media was removed and replaced with growth medium supplemented with nerve growth factor (NGF) (100ng/ml). The cells were then left to differentiate for 24-48 hours before proceeding to immunostaining experiments.

For some experiments, drug treatments in the final growth media were used. The protein phosphatase 2A inhibitor, okadaic acid (Merck Millipore) was used at 1μM (Garcia et al., 2002); incubations were performed for 30 mins at 37^{o}C just prior to immunostaining. The Aurora B Kinase Inhibitor, ZM447439 (Tocris) was used at 20nM (Li et al., 2010); incubations were performed for 30 mins just prior to immunostaining. The eIF4F inhibitor, 4EGI-1 (Merck Millipore) was used at 100μM (Descamps et al., 2012) for 24 hours prior to immunostaining. For the 'No Treatment' control group, a vehicle was not used.

2.5.1. Immunostaining

Coverslips were removed from wells and carefully washed three times with Phosphate Buffered Saline (PBS) (Sigma). Fixation of cells was accomplished with 5% Paraformaldehyde and 5% Acetic acid in water for 10 minutes before permeabalisation with ice-cold methanol for 2 minutes. Methanol was rinsed off by applying PBS several times. The cover slips were then coated in a blocking buffer consisting of 5% foetal calf serum in PBS for 30 mins at room temperature to help prevent non-specific binding. The blocking buffer was then removed and the primary antibody (rabbit NSun2 used at 1:100 (Proteintech), mouse FMRP used at 1:250 (Merck Millipore) or Beta-Actin used at 1:250 (Proteintech)) was applied and left overnight at 4^{o}C. The following day, PBS was used to wash off the primary antibody and this was repeated 5 times. The secondary antibody (Alexa Fluor 555 or 488 (ThermoFisher)) was then applied onto the coverslips and left at room temperature for 1.5 hours. Coverslips were then washed several times with PBS before being left to air-dry. Once dry, coverslips were mounted onto microscope slides with Vectashield containing DAPI (Vector Laboratories).

2.5.2. Image acquisition

Images were acquired with the Zeiss LSM 510 Meta confocal microscope with a 63x oil-immersion objective. Two distinct lasers were used with excitation wavelengths of 488nm and 543nm. The images were acquired at a resolution of 2048x2048, scan speed 6 and with a varying zoom factor. Band-pass filters were used to capture distinct ranges of fluorescence emission; for the 488nm laser a bandpass filter of 480–520nm was used, and for the 543nm laser a bandpass filter of 535–590nm was used.

2.5.3. Image analysis

Background noise levels were estimated by averaging 5 regions around the cell of interest. These values were averaged and subtracted from the image in an attempt to rid any auto-fluorescence that remained after image acquisition. Background fluorescence for colocalisation analysis was automatically calculated with the Coloc2 plugin for Fiji image software. All images were analysed for intensity saturation to ensure there was no over-exposure and therefore no information-clipping. Prior to the image analysis, parameters of image collection were obtained, such as illumination level, detector gain, and exposure time, which enabled detection of the dimmest fluorescence without saturating the signal. Colocalisation analysis was conducted using the Coloc 2 plugin within Fiji software. The separate channels were split and a region of interest drawn around each cell (Figure 2.4.). The Coloc 2 plugin automatically calculates the threshold intensity levels (the lowest intensity permitting colocalisation of two probes) and provides a Pearsons Coefficient (r) for that region; obtained values for r are between -1 (negative correlation) and +1 (positive correlation). The reasoning behind using r is due to its simplicity and robust measurement that is relatively free of experimenter bias. The Pearson’s correlation method calculates the covariance of both variables investigated

divided by their standard deviation. Due to r incorporating variability (termed “noise”), as variability increases in a sample, then the value for r declines. In order to further rule out imaging artefacts, an immunostaining control was implemented in the form of β-actin, a protein that has relatively high expression levels in NGF-treated PC12 cells (Henke et al., 1991) and does not have any known interaction with NSun2 (Zhang et al., 2012). In addition to this, a Costes significance test was employed which involved scrambling blocks of pixels and comparing those images to the those that are unscrambled (the original image) to determine the likelihood of the colocalisation observed being due to chance.

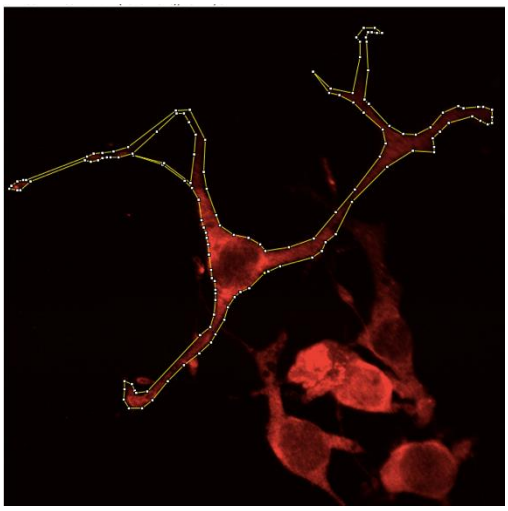

Figure 2.4. Image analysis

An example of a PC12 selected for colocalisation analysis. A region of interest was drawn around each cell prior to running the Coloc2 plugin embedded in Fiji image software.

2.5.4. vtRNA RNA oligonucleotides and transfection

The full vtRNA1.1 sequence was synthesised *in vitro* by Dharmacon in two versions; in the first, cytosine 69 was replaced with methyl-5-cytosine (methylated), and in the second, cytosine 69 was substituted with an adenine (unmethylated). For transfections, 10ng of each vtRNA was diluted in Plus

reagent (6µl), Lipofectamine (4µl), and opti-MEM (20µl) (Thermofisher), and complexes allowed to form at room temperature for 30 mins. This was then applied to the growth medium of PC12 cells. Cells were incubated overnight at 37ºC before proceeding to imaging as described above.

2.6. Statistical analysis

Data was statistically analysed using SPSS and Fiji Image software. The Shapiro-Wilk test was used to determine the distribution of data sets. The outcome determined whether parametric or non-parametric statistical tests were used; the tests used for each data set is stated in the Results chapters. The statistical tests used include: unpaired two-tailed student's t-test, two-way analysis of variance (ANOVA), mann-whitney U test and repeated measures ANOVA. In the case of using the repeated measures ANOVA, if the data set in question violated sphericity from the Mauchly's test then a Greenhouse Geisser correction was used.

The descriptive statistics presented in the results chapters include the mean and the standard error of the mean. In the case of the electrophysiology results sample sizes are expressed as 'n' which represents the number of slices. Parentheses follow each sample size declared containing the number of animals used for that particular experiment.

For the colocalisation analysis, a Pearson correlation coefficient was determined and statistical significance was tested with the costes significance test; all data sets were deemed significant. To determine the significance of the colocalisation data sets against negative controls, a Fisher's r-to-z transformation was used to normalise the data. Due to the natural skew at higher or lower Pearson correlation coefficients, normalisation is required for parametric testing.

Chapter 3. Results: Long Term Depression in NSun2 $^{-/-}$ mice

3.1. Introduction

At time of writing, there have been less than a handful of hippocampal-dependent behavioural studies involving NSun2-deficient models, these include: an olfactory aversion task with an NSun2$^{-/-}$ drosophila model (Abbasi-Moheb et al., 2012) and a Y-maze task with an NSun2$^{-/-}$ mouse model (Blanco et al., 2014). Consistent with learning deficits observed in NSun2$^{-/-}$ human patients, both of the aforementioned tasks further exposed learning deficits in the absence of NSun2, although the underlying relevant physiological mechanisms remain undetermined. As learning disabilities are often associated with mis-regulated synaptic plasticity, the main goals of this thesis work were to characterise potential synaptic plasticity defects in a transgenic murine model of NSun2 deficiency. There are various forms of plasticity involving many different mechanisms and proteins, however mGluR-LTD was the standout candidate as a possible plasticity deficit to investigate. mGluR-LTD is thought to be an essential plasticity mechanism attributed to hippocampal-dependent tasks involving spatial memory (Balschun et al., 1999; Sanderson et al., 2016). The implication of mGluR-LTD in multiple neurodevelopmental disorders phenotypically similar to NSun2-deficiency syndromes (Auerbach et al., 2011; Huber et al., 2002; Osterweil et al., 2010; von der Brelie et al., 2006) highlight the possibility of its dysfunction. Further support arises from the similarities in cellular function between NSun2 and the translational repressor, FMRP; these include their role in protein synthesis through spatial and temporal control of RNA translation (Darnell and Klann, 2013; Hussain and Bashir, 2015; Majumder et al., 2017), albeit likely through different molecular mechanisms. Indeed there are overlapping phenotypes observed between FXS and NSun2 deficiency

patients that include moderate to severe intellectual disability, autistic features, facial dysmorphia and epilepsy in some patients (Abbasi-Moheb et al., 2012; Fahiminiya et al., 2014; Khan et al., 2012; Martinez et al., 2012; Squires et al., 2012). Arguably the most persuasive evidence for NSun2's potential involvement in mGluR-LTD came from Hussain and Bashir (2015) who identified NSun2-targeted mRNA's in HEK-293 cells; 236 of the targets were identified in total with 83 of these also being targeted by FMRP. They include mTOR mRNA and mRNAs for several different eukaryotic translation initiation factors that are involved in the intracellular cascades downstream of group I mGluR activation and have been implicated in behavioural tasks involving mGluR-LTD (Di Prisco et al., 2014). Combining these observations leads to the reasonable speculation that NSun2$^{-/-}$ mice may show deficits in mGluR-LTD in the hippocampus.

As described in the Introduction of this thesis, various forms of LTD exist, as do numerous induction methods that are believed to involve different mechanisms. For example, mGluR-LTD can be triggered pharmacologically with the Group 1 mGluR agonist, DHPG (Palmer et al., 1997) or synaptically by applying a paired pulse LFS (PP-LFS) consisting of 900 paired pulses delivered at 1-3Hz (Huber et al., 2000; Moult et al., 2008). NMDA receptor activation can also instigate LTD and can be induced via an LFS comprising of a single pulse–LFS (SP-LFS) protocol delivered at similar frequencies (Dudek and Bear, 1992; Mulkey and Malenka, 1992; Staubli and Ji, 1996). The mechanisms underlying these forms of plasticity are not well understood at the molecular level, however all three are believed to involve the internalisation of AMPA receptors from post-synaptic contacts (Lüscher and Huber, 2010; Lüscher and Malenka, 2012). This chapter explores these three forms of synaptic plasticity in the NSun2$^{-/-}$ mouse model as well as the possible role of *de-novo* protein synthesis, a controversial component of synaptic plasticity (Abbas, 2016; Huber et al., 2001). The reasons underpinning the investigation into protein synthesis dependency is due to previous reports of PSIs reducing LTD (Huber et al., 2001) and NSun2 playing a

possible role in the spatiotemporal regulation of protein synthesis (Blanco et al., 2014; Hussain et al., 2013b; Hussain and Bashir, 2015).

3.2. Results

3.2.1 Basal synaptic transmission is enhanced in NSun2$^{-/-}$ mice

Prior to the mGluR-LTD experiment presented in the next section, an input-output curve was generated. Not only does this allow for an estimation for use of an appropriate stimulation intensity during experiments (approximately between x3 and x5 of threshold and always below maximal stimulation) but can also indicate synaptic efficacy. As explained in Materials and Methods, ideally the output is compared against the size of the fibre volley rather than the stimulus intensity however obvious visible fibre volleys could not always be discerned. The input-output curve created from CA1 PN extracellular responses of NSun2$^{-/-}$ slices demonstrated significant enhancements when analysed against their *NSun2$^{+/-}$* littermates (*Figure 3.1A*: *NSun2$^{-/-}$: n = 15 (12); NSun2$^{+/-}$: n = 10 (9); Repeated Measure ANOVA with Greenhouse Geisser correction: F = 8.55, p = 0.003).*

PPF was measured by eliciting x2 field responses in succession and dividing the slope resulting from the second pulse by the slope elicited from the first pulse. The measurement of the PPR was completed over 5 different stimuli intervals (10ms, 20ms, 50ms, 100ms and 200ms) to investigate the possible short term plasticity dynamics. No differences could be discerned between NSun2$^{-/-}$ and *NSun2$^{+/-}$* mice (*Figure. 3.1B: NSun2$^{-/-}$: n = 5 (5); NSun2$^{+/-}$: n = 5 (5); Repeated Measure ANOVA with Greenhouse Geisser correction, P > 0.05, F = 1.35*).

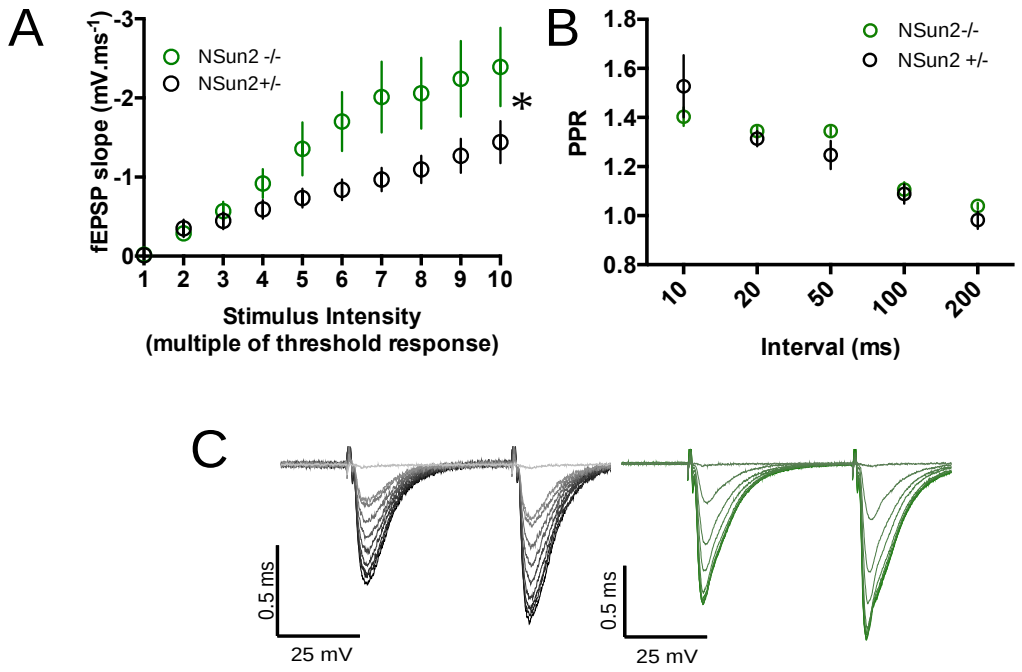

Figure 3.1. Enhanced Input-output curve in NSun2$^{-/-}$ mice

A) *NSun2$^{-/-}$ mice exhibit an enhanced input:ouput relationship compared to heterozygous littermates (NSun2$^{-/-}$: n = 15 (12); NSun2$^{+/-}$: n = 10 (9); Repeated Measure ANOVA with Greenhouse Gesisser correction: F = 8.55, p = 0.003)*
B) *No difference was found in the PPRs between NSun2$^{-/-}$ and NSun2$^{+/-}$ (NSun2$^{-/-}$: n = 5 (5); NSun2$^{+/-}$: n = 5 (5); Repeated Measure ANOVA with Greenhouse Geisser correction, P > 0.05, F = 1.35)*
C) *Example traces from an input-output experiment and demonstrates an example of the PPR at a 50ms interval.*

3.2.2. Initial DHPG-LTD experiment indicates reduced LTD in NSun2$^{-/-}$ mice

The most commonly reported method for induction of mGluR-LTD is with a bath application of 100µM DHPG, and has been used regularly in the context of pathological models such as FXS (Lüscher and Huber, 2010). The results contained in this chapter followed a similar methodology. fEPSPs were recorded in the *stratum radiatum* of the CA1 hippocampus in response to electrical stimulation of the SC pathway every 15 seconds, with the average per minute

analysed (stimulation intensity was low enough to elicit a sub-maximal fEPSP response). NSun2$^{-/-}$ mice exhibited a significant reduction in LTD compared to their heterozygous littermates (*Figure 3.2A-B: NSun2$^{+/-}$: 58.4% ± 2.82, n = 11; NSun2$^{-/-}$: 71.54% ± 2.19, n = 9; unpaired two-tailed student's t-test, p = 0.0023*).

There is an unresolved debate regarding whether DHPG-LTD is a consequence of either pre- or post-synaptic changes, although there is a broad consensus that modifications to both synaptic compartments is likely (Watabe et al., 2002). To appreciate which synaptic compartment may be altered leading to the reduced LTD observation, the PPR was analysed indicating DHPG-induced mGluR-LTD led to an increase in PPR in NSun2$^{-/-}$ mice and therefore inferring a reduction in release probability (Figure 3.2C: *NSun2$^{+/-}$: 123.3% ± 7.65, n = 11 (11); NSun2$^{-/-}$: 161.9% ± 17.65, n = 9 (9); unpaired, two-tailed student's t-test, p = 0.04*).

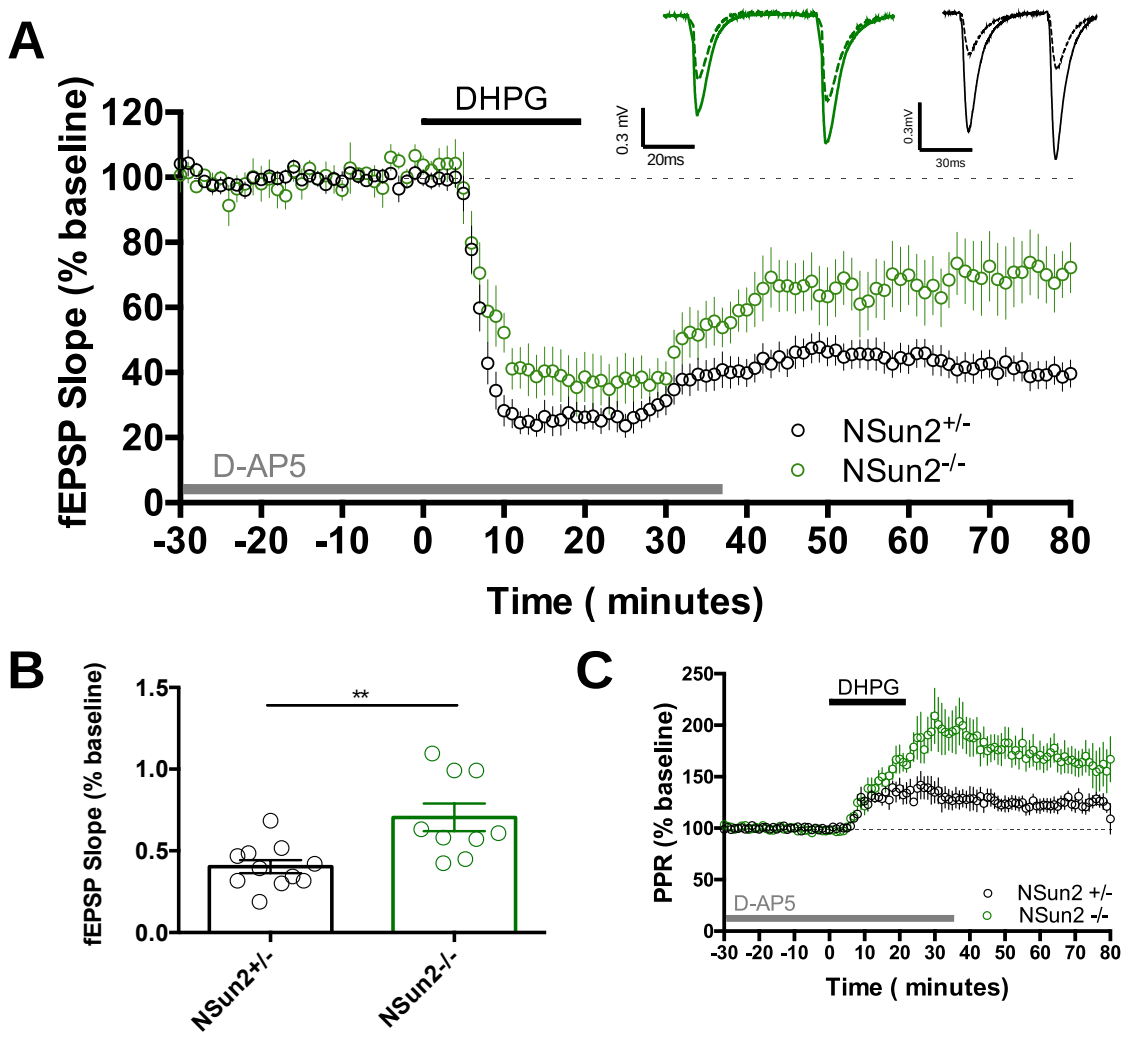

Figure 3.2. Decreased mGluR-LTD in NSun2-/- mice

A) *fEPSP responses, each data point represents an average minute response calculated from 4 responses every 15 seconds. 50μM DAP-5 was applied for the first hour of the experiment to prevent NMDA receptor activation. After a stable 30-minute baseline, 100μM DHPG was bath applied for 20 minutes. Recordings were continued for 1-hour after DHPG wash-off. NSun2$^{-/-}$ mice exhibited significantly less LTD when compared to NSun2$^{+/-}$ mice relative to fEPSP baseline (analysed from the last 10 minutes of baseline which were statistically compared to the last 10 minutes of the experiment). (NSun2$^{+/-}$: 58.4% ± 2.89, n = 11 (11); NSun2$^{-/-}$: 71.54% ± 2.16, n = 9 (9); unpaired two-tailed student's t-test, p = 0.0023). Top right corner: Representative traces (4 consecutive traces averaged), solid line represents fEPSP 1 minute before DHPG application,*

dotted line represents fEPSP responses 1 minute before end of experiment. Green line = NSun2$^{-/-}$. Black line = NSun2$^{+/-}$.
***B)** Bar chart representing the mean fEPSP alterations in response to DHPG and includes individual points to demonstrate spread of data from each experiment.*
***C)** Change in PPR with 20-minute application of 100μM DHPG. A significant increase in the PPR was observed in NSun2$^{-/-}$ compared to NSun2$^{+/-}$ mice (NSun2$^{+/-}$: 123.3% ± 7.65, n = 11 (11); NSun2$^{-/-}$: 161.9% ± 17.65, n = 9 (9); unpaired, two-tailed student's t-test, p = 0.04).*

3.2.3. NSun2$^{-/-}$ CA1 PNs display reduced NMDA-dependent LTD

As well as inducing LTD chemically with DHPG, LTD can also be produced synaptically via electrical stimulation. Previous reports demonstrate that low-frequency stimuli between 1 and 3Hz leads to LTD. For example, 900 single pulse stimuli at 1Hz has been reported to lead to NMDA-dependent LTD (Dudek and Bear, 1992; Mulkey and Malenka, 1992) whereas 900 paired pulse stimuli (separated by 50ms) at 1Hz can induce an mGluR-dependent form of LTD (Kang and Kaang, 2016; Kemp and Bashir, 1999). In order to investigate whether these induction mechanisms are affected in NSun2$^{-/-}$ mice, field experiments were conducted in the CA1 hippocampus by stimulating the SC pathway, in the same manner as the previous section. However, as opposed to bath-washing DHPG onto the slice after a 30-minute baseline, two distinct electrical stimulation patterns were used. Initially, the delivery of a SP-LFS was used with the aim of inducing NMDA receptor-dependent LTD (Figure 3.3A). A significant amount of LTD was observed in heterozygous mice compared to the mutants and the depression in fEPSP responses was blocked by 50μM D-AP5 in the heterozygous mice demonstrating an NMDA receptor component (*Figure 3.3.A: NSun2$^{+/-}$: 68.56% ± 4.94, n = 8 (8); NSun2$^{-/-}$: 100.84% ± 11.13, n =7 (7); NSun2$^{+/-}$ with D-AP5: 113.11 ± 16.39%, n = 5 (5); unpaired two-tailed student's t-test NSun2$^{+/-}$ vs NSun2 $^{-/-}$: p = 0.015; unpaired two-tailed student's t-test NSun2$^{+/-}$ vs NSun2$^{+/-}$ with AP5: p = 0.006*). Investigations were next made into synaptically induced mGluR-dependent LTD by applying a PP-LFS. In order to prevent NMDA receptor-mechanisms contributing to any depression observed,

50µM D-AP5 was administered throughout the baseline, stimulation protocol and 15 minutes after LTD induction (Figure 3.4*).* Unexpectedly, this methodology did not generate LTD in either mouse model (*Figure 3.4: NSun2$^{+/-}$: 99.99% ± 0.4, n = 5 (5); NSun2$^{-/-}$: 100.12% ± 15, n =7 (7); unpaired two-tailed student's t-test, p = 0.37*). The PPR was not altered in either the SP-LFS or PP-LFS protocol in either mouse model (*Figure 3.3C and 3.4C*).

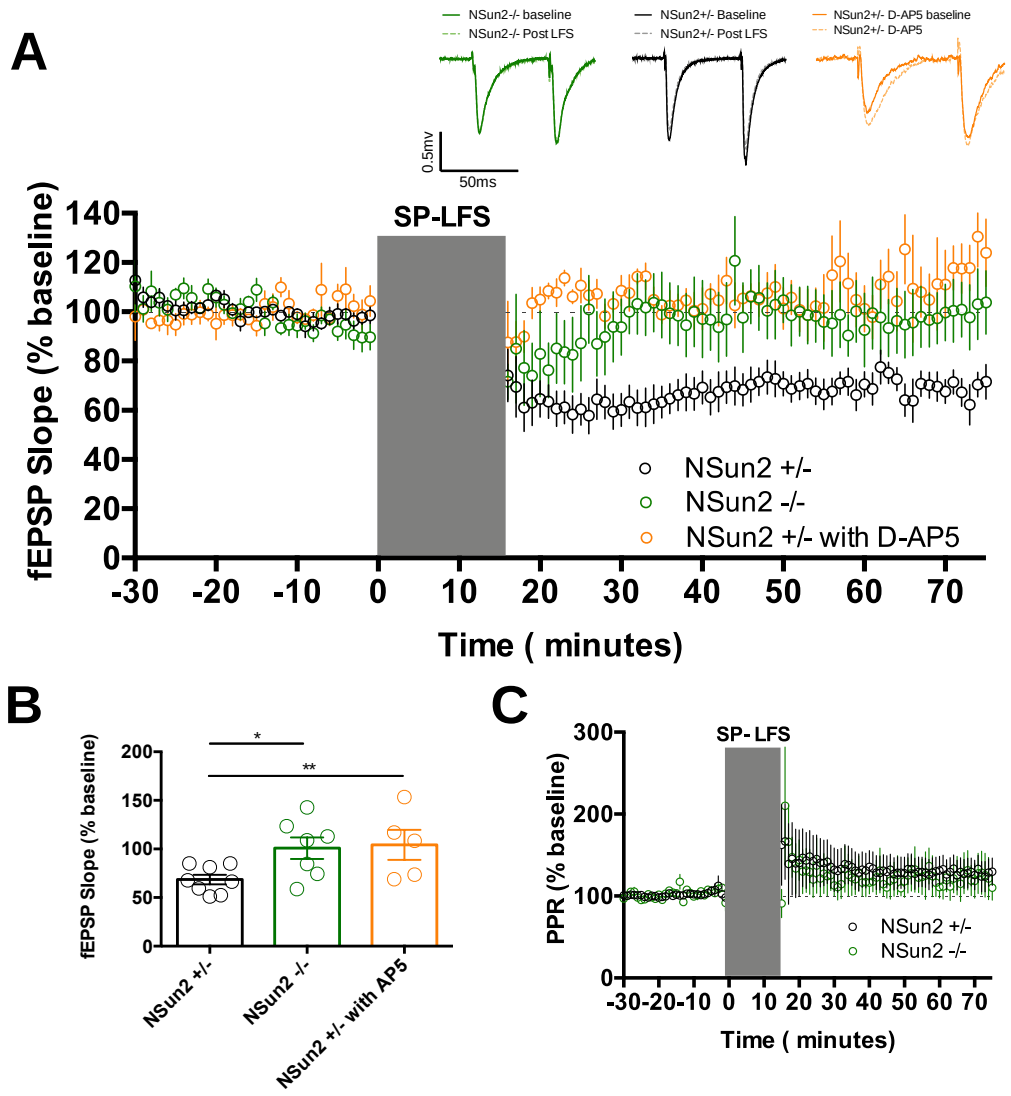

Figure 3.3. NSun2-/- mice exhibit reduced NMDA-dependent LTD

A) *LTD was significantly less in the NSun2$^{-/-}$ mice than NSun2$^{+/-}$. LTD in NSun2$^{+/-}$ mice was also blocked with D-AP5 application. The results were analysed from the last 10 minutes of baseline and compared to the last 10 minutes of the experiment (NSun2$^{+/-}$: 68.56% ± 4.94, n = 8 (8); NSun2$^{-/-}$: 100.84% ± 11.13, n =7 (7); NSun2$^{+/-}$ with AP5: 113.11 ± 16.39%, n = 5 (5); unpaired two-tailed student's t-test NSun2$^{+/-}$ vs NSun2 $^{-/-}$: p = 0.015; unpaired two-tailed student's t-test NSun2$^{+/-}$ vs NSun2$^{+/-}$ with D-AP5: p = 0.006). Top: Representative traces (4 consecutive traces averaged), solid line represents fEPSP 1 minute before DHPG application, dotted line represents fEPSP responses 1 minute before end of experiment. Green line = NSun2$^{-/-}$. Black line = NSun2$^{+/-}$. Grey line = NSun2$^{+/-}$ with D-AP5*

B) *Bar charts depicting spread of data from each experiment.*

C) *No discernible difference in PPR was found between NSun2$^{-/-}$ and NSun2$^{+/-}$ mice resulting from the SP-LFS protocol (NSun2$^{+/-}$: 127.75% ± 17.57, n = 8 (8); NSun2$^{-/-}$: 122.42% ± 22.88, n = 7 (7); unpaired two-tailed student's t-test, p > 0.05).*

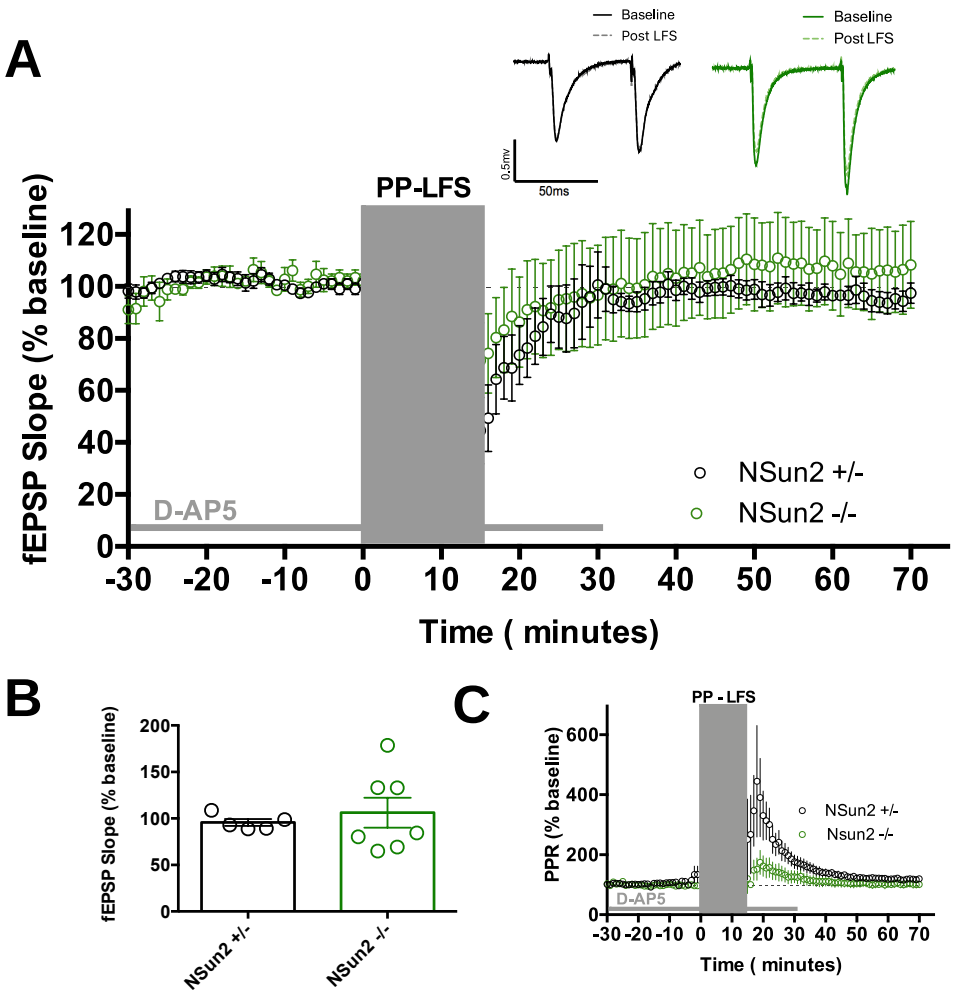

Figure 3.4. ***PP-LTD could not induce LTD in either mouse model***

A) *The first hour of this experiment was completed in the presence of 50μM D-AP5 (during baseline, induction and 15-minutes post-induction) to block NMDAR activation. Both NSun2$^{+/-}$ and NSun2$^{-/-}$ CA1 PNs do not undergo LTD. (NSun2$^{+/-}$: 99.9% ± 4, n = 5 (5); NSun2$^{-/-}$: 112% ± 15, n =7 (7); unpaired two-tailed student's t-test, p = 0.37). Top: Representative traces (4 consecutive traces averaged), solid line represents fEPSP 1 minute before DHPG application, dotted line represents fEPSP responses 1 minute before end of experiment. Green line = NSun2$^{-/-}$. Black line = NSun2$^{+/-}$.*
B) *Bar charts depicting spread of data from individual experiments.*
C) *No discernible difference in PPR was found between NSun2$^{-/-}$ and NSun2$^{+/-}$ mice resulting from the PP-LFS protocol (NSun2$^{+/-}$: 118.85% ± 5.44, n = 5 (5); NSun2$^{-/-}$: 102.97% ± 12.59, n =7 (7); unpaired two-tailed student's t-test, p > 0.05).*

3.2.4. Initial NSun2$^{-/-}$ DHPG-LTD deficits cannot be replicated and DHPG-LTD in both models is protein synthesis dependent

The proposed functionality of NSun2 as a spatiotemporal regulator of protein synthesis (Blanco et al., 2014) combined with the general view that DHPG-LTD is dependent on protein synthesis (Gallagher et al., 2004; Huber et al., 2001, 2000; Moult et al., 2008) led to the question of how decreasing translation might affect DHPG-LTD. A bath application of the potent PSI, CHX, was used at a concentration of 60μM for the duration of experiments. Previous research has shown this concentration of CHX used for a similar duration reliably reduces mGluR-LTD in the CA1 region of hippocampus (Auerbach et al., 2011) and so was expected to reduce the long-term depressive capacity of DHPG. A reduction in the level of DHPG-LTD in *NSun2$^{+/-}$* mice in response to CHX but a more limited effect in NSun2$^{-/-}$ mice was anticipated. This rationale was formed because of the global reduction in translation observed in the absence of NSun2 (Blanco et al., 2014) that could cause a "flooring" effect, whereby CHX cannot limit translation further. The results here suggest that protein synthesis is required in some part for the ordinary expression of DHPG-induced mGluR-LTD in *NSun2$^{+/-}$* mice (*Figure 3.4A: NSun2$^{+/-}$ CTRL: 49% ± 5, n = 9, NSun2$^{+/-}$ CHX: 85% ± 11, n =7; unpaired two-tailed student's t-test, p = 0.012*) and in NSun2$^{-/-}$ mice as a significant reduction in LTD levels were observed (*Figure 3.4B*: *NSun2$^{-/-}$ CTRL: 39% ± 6, n = 13, NSun2$^{-/-}$ CHX: 63% ± 8, n =9; unpaired two-tailed student's t-test, p = 0.04*). In order to statically evaluate the impact of CHX on LTD in each mouse group, a two-way ANOVA was utilised and inferred that there was no interaction between the strain of mouse and CHX (*Two-way ANOVA: F=0.75, P=0.39*).

Although the particular aim of this experiment was to examine protein synthesis dependency of DHPG-LTD in both murine models, it also provided an opportunity to validate the initial DHPG-LTD experiment that suggested a deficit in the SC pathway of NSun2$^{-/-}$ mice (Figure 3.2A). This comparison was

reasonable to make due to the exact experimental protocol and conditions employed previously. Upon executing an unpaired two-tailed student's t-test to statistically analyse the control groups from the CHX experiments, it was clear that the initial DHPG-LTD deficits could not be replicated (*Figure 3.4C: NSun2$^{+/-}$ CTRL: 49% ± 6, n = 13 (13); NSun2$^{-/-}$ CTRL: 39% ± 5, n = 9 (9); unpaired two-tailed student's t-test, p = 0.34*).

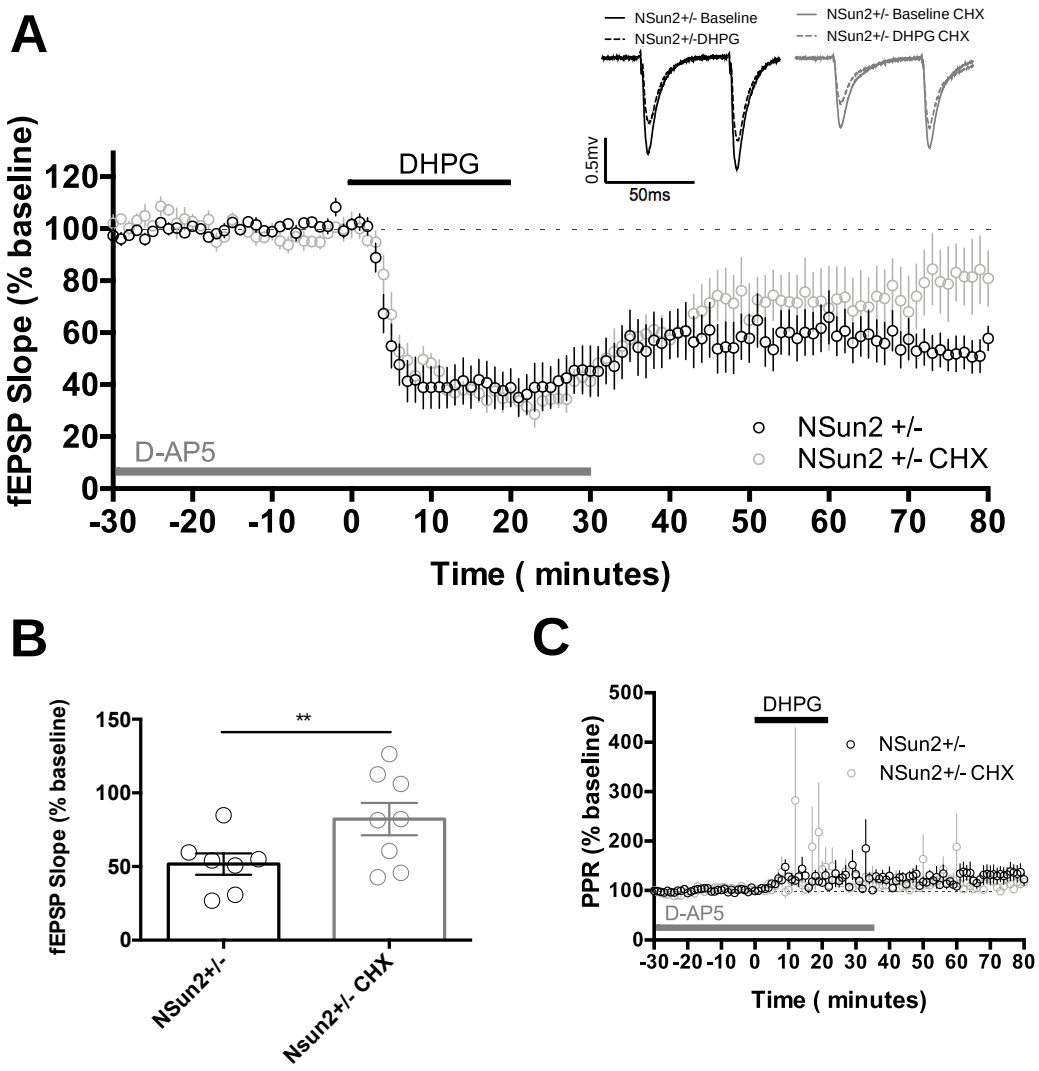

Figure 3.5. DHPG-LTD is reduced in NSun2+/- mice with CHX

A) *Blocking protein synthesis with CHX significantly reduces the extent of LTD in heterozygous NSun2 mice (NSun2$^{+/-}$ CTRL: 49% ± 0.05, n = 9 (9), NSun2$^{+/-}$ CHX: 85% ± 0.10, n =7 (7); unpaired two-tailed student's t-test, p = 0.012).*
B) *Bar chart expressing the spread of data for individual experiments.*
C) *CHX had no effect on the PPR in NSun2$^{+/-}$ mice (CTRL: 132.45% ± 16.58, n = 9 (9); CHX: 112.86% ± 8.73, n = 7 (7); unpaired two-tailed student's t-test, p > 0.05).*

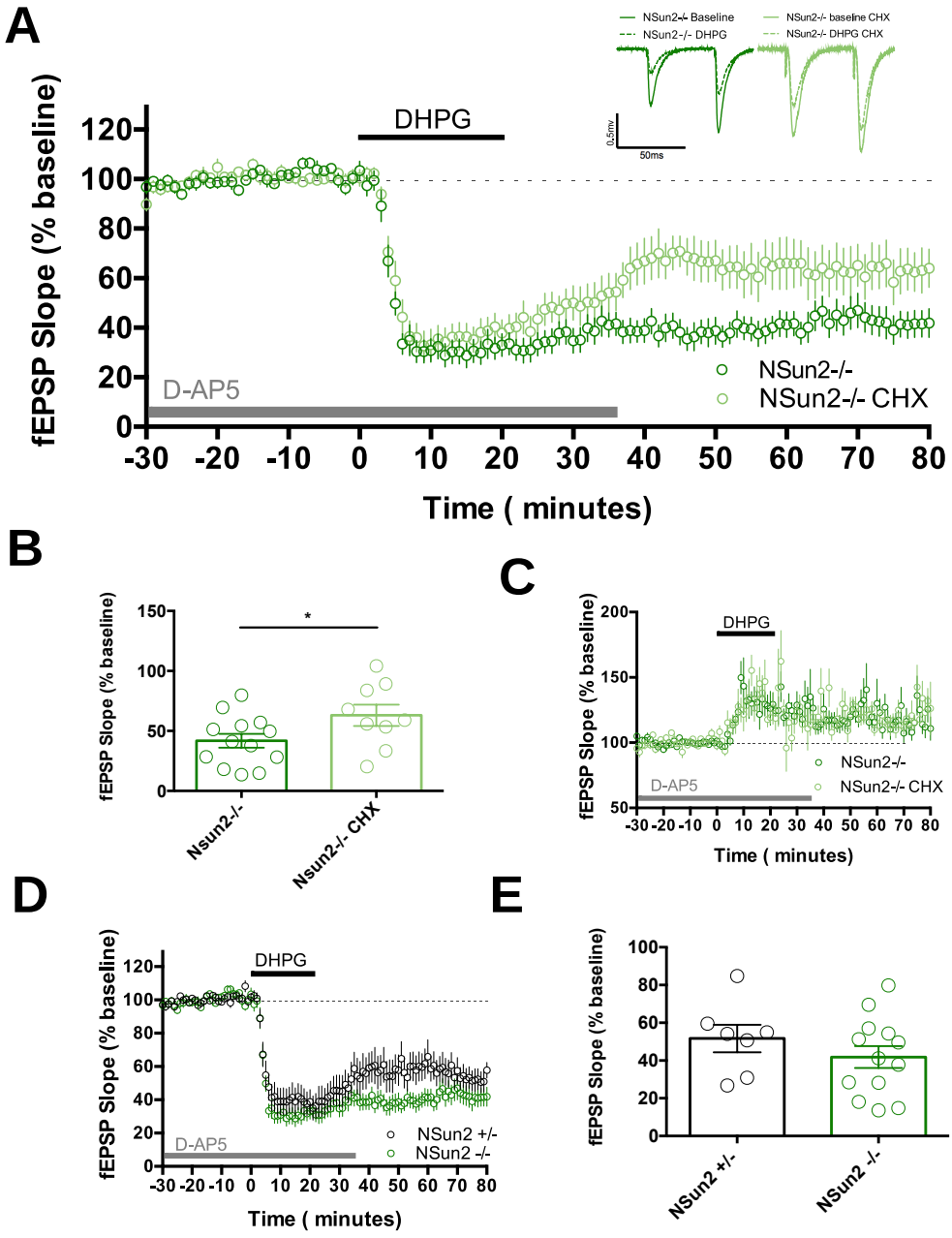

Figure 3.6. DHPG-LTD is reduced in NSun2$^{-/-}$ mice with CHX and previous NSun2$^{-/-}$ DHPG-LTD deficit cannot be replicated

A) *fEPSP recordings in response to a 20-minute application of 100μM DHPG either with or without the presence of 60μM CHX. Each data point represents a minute average from 4 responses. Blocking protein synthesis with CHX reduces the amount of LTD in NSun2$^{-/-}$ mice (NSun2$^{-/-}$ CTRL: 39% ± 6, n = 13 (13), NSun2$^{-/-}$ CHX: 63% ± 8, n =9 (9); unpaired two-tailed student's t-test, p = 0.04).*

To analyse a possible genotype effect on the use of CHX, a two-way ANOVA test was used; no significant strain-drug interaction was observed (Two-way ANOVA: F = 0.75, P= 0.39).
B) *Bar chart expressing the spread of data for individual experiments.*
C) *CHX had no effect on the PPR in NSun2$^{-/-}$ mice (CTRL: 123.32% ± 9.69, n = 13 (13); CHX: 116.72% ± 8.75, n = 9 (9); unpaired two-tailed student's t-test, p > 0.05).*
D) *NSun2$^{+/-}$ and NSun2$^{-/-}$ control experiments were compared and analysed to determine whether the initial DHPG-induced mGluR-LTD deficit in NSun2$^{-/-}$ mice could not be replicated (unpaired two-tailed student's t-test; p = 0.34).*
E) *Bar chart expressing the spread of data for individual experiments.*

3.3. Discussion

The data presented within this chapter describes the first investigations into LTD plasticity and basal transmission in an NSun2$^{-/-}$ model. To summarise, an increase in the input-output relationship was observed in NSun2$^{-/-}$ mice with no alterations found in release probability. Electrically induced mGluR-dependent LTD could not be induced in either model, however synaptically induced NMDA receptor-dependent LTD was reduced significantly in NSun2$^{-/-}$ mice. Initially an NSun2-dependent deficit was found in DHPG-LTD, however repetition of this experiment failed to replicate the initial findings. Finally, DHPG-LTD in both NSun2$^{-/-}$ and *NSun2$^{+/-}$* mice seem to require protein synthesis.

3.3.1. Basal synaptic transmission is enhanced in NSun2$^{-/-}$ mice

NSun2$^{-/-}$ mice have enhanced basal transmission in the CA1 region of the hippocampus (Figure 3.1A*).* While the underlying mechanism is not known, it has previously been shown that there is a reduction in synaptic/PSD-95 puncta in cortical neurons (Blanco et al., 2014) which would logically infer a decrease in basal transmission. However, there are many other factors to bear in mind; the same paper found a large increase in the number of cells within the cortex that, if similar in the hippocampus, could possibly overcompensate for the reduced

puncta leading to enhanced transmission. Also, whether these findings apply to the adult hippocampus is unknown, as the analysis undertaken was from E17.5 embryos and these features may well dramatically change into adulthood. Another factor to consider is the rederivation process of the mice colonies and how this may result in different genes and protein expression compared to Blanco ***et al.s'*** colonies. Although Blanco *et al.'s* (2014) findings would suggest reduced basal transmission, the animals used here may differ significantly and the previously observed reduction in synaptic puncta may not apply to these animals.

Interestingly, this NSun2$^{-/-}$ model has been previously linked to enhanced activation of stress pathways (largely due to increased fragmentation of tRNA) (Blanco et al*.*, 2014) and a report from Kamal *et al.* (2008) discovered that higher stress levels in the rat led to an enhancement of basal transmission in the CA1 *in vivo* and also substantially decreased LTP, suggesting memory deficits may result (Kamal et al., 2008). This could provide a link between enhanced basal transmission and NSun2, though further experimentation is required; examining whether preventing the excessive tRNA cleavage in NSun2$^{-/-}$ mice normalises the augmented transmission may help to confirm this link. No changes were observed in PPR (Figure 3.1B*)* suggesting that release probability of vesicles is not the cause for the changes in basal transmission.

Other possible mechanisms underlying enhanced transmission include changes in intrinsic neuronal properties. A prime candidate for alterations to input-output relationships when recording from dendritic regions (such as the *stratum radiatum* in the hippocampus) could be A-type K^+ currents (I_A). Mediated by K^+ channel $K_V4.2$ subunits (Chen et al., 2006), I_A is active at potentials below that which produces action potentials and is activated in response to EPSPs in dendritic regions. Its activation causes an increase in EPSP attenuation and is an important controller of dendritic excitability (Beck and Yaari, 2008). Western blot analysis could be used to identify any possible reduction in these subunits

that might have contributed to the enhanced output in NSun2$^{-/-}$ mice. It may also prove useful to investigate NMDA:AMPA receptor ratios in whole-cell patch clamp experiments; postsynaptic AMPA receptors are responsible for the majority of the fEPSP observed in response to electrical stimulation. This ratio may be altered if more AMPA receptors are embedded in the postsynaptic membrane of NSun2$^{-/-}$ CA1 pyramidal neurons.

A final aspect to discuss is that the input-output curve presented in in this chapter was a result of experiments prior to the initial mGluR-LTD experiment (Figure 3.2.). Although a statistically significant effect was observed, the fact that the mGluR-LTD results could not be replicated raises questions about the replicability of the input-output results and an attempt to repeat these experiments would aid in the validation of these initial findings.

3.3.2. Reduced NMDA-dependent LTD in CA1 of NSun2$^{-/-}$ mice

Two forms of synaptically-induced LTD were investigated, one induced with a PP-LFS and the other with a SP-LFS. A substantial reduction in SP-LFS-induced LTD was observed in the NSun2$^{-/-}$ mice compared to heterozygous, although distinguishing the physiological relevance of the protocols used is problematic; multiple mechanisms are likely to be involved to some degree but the precise molecular understanding is limited. A layer of complexity is added by the possible developmental changes and conflicting literature. Research from Mulkey and Malenka (1992) established that SP-LFS (900 stimuli at 1Hz) in young rats produces LTD that requires NMDA receptor activation in the CA1 region of the hippocampus, which was validated by Dudek and Bear (1992) and Staubli and Ji (1996). Later, Kemp and Bashir (1997) investigated induction methods in the adult CA1 rat hippocampus and found that a SP-LFS does not induce LTD and that LTD induced by PP-LFS may only partially involve NMDA receptors. Huber *et al*. (2000) later demonstrated that in their experimental set-up PP-LFS solely requires mGluR activation for LTD which agrees with other

findings (Moult et al., 2008) yet previous reports suggested that PP-LFS induced LTD may also involve kainate receptors (Kemp and Bashir, 1999). Deciphering the possible molecular mechanisms resulting from the SP- and PP-LFS protocols in the *NSun2*$^{+/-}$ and NSun2$^{-/-}$ mice is not possible from the data described in this chapter.

These results suggest that firstly, the PP-LFS either doesn't induce LTD in this specific context (i.e. experimental set up, animal species, mouse strain etc.) or it does indeed require NMDA receptor activation; due to the use of the NMDA receptor antagonist, D-AP5, these experiments would need to be repeated in the absence of any NMDA receptor antagonists, however this was not possible due to time constraints. Secondly, the SP-LFS protocol is likely to involve NMDA receptors in this experimental model as D-AP5 abolished LTD in the heterozygous mice (Figure 3.3). For this reason, it is likely that that the lack of LTD from SP-LFS observed in NSun2$^{-/-}$ mice is due to a dysfunction of NMDA receptors or related downstream pathways. Further molecular analysis along the NMDA-activation pathway is required to obtain a deeper understanding of the underlying mechanisms involved in this mis-regulation.

3.3.3. CHX similarly supresses DHPG-induced mGluR-LTD in NSun2$^{+/-}$ *and NSun2*$^{-/-}$ *mice*

Although a full consensus remains to be established, there is considerable evidence supporting the role of *de novo* protein synthesis in DHPG-LTD (Aguilar-Valles et al., 2015; Antar et al., 2005, 2004; Bear et al., 2004; Di Prisco et al., 2014; Gallagher et al., 2004; Narayanan et al., 2007). To investigate whether protein synthesis is involved in the current experimental model, 60µM CHX was bath applied for the duration of the LTD experiment (interleaved with experiments without CHX). CHX interferes with the translocation step of protein synthesis preventing elongation (Schneider-Poetsch et al., 2010) and is routinely used in mGluR-LTD experiments. Given that CHX may have off-target effects,

other PSIs such as anisomycin may help provide evidence of a protein translation-dependent effect with CHX. Earlier work demonstrated that concentrations of CHX between 50-500nM can enhance neural protection by increasing levels of bcl-1 and c-jun (Furukawa et al., 1997). In an ideal situation control experiments with anisomycin would be used, however this was not possible due to time constraints.

The hypothesis proposed the possibility that DHPG-LTD in the NSun2$^{-/-}$ mouse may not be impacted upon by CHX due to the previously described global reductions in protein translation (Blanco et al., 2014). If a flooring effect were to be present i.e. translation is at a lower base level that cannot be reduced further with CHX, then it may help explain the deficit. This was not the case however, as a two-way ANOVA identified that CHX decreased DHPG-LTD similarly between the two mouse groups (Figure 3.6).

3.3.4. Initial DHPG-induced mGluR-LTD reduction in NSun2$^{-/-}$ mice could not be replicated

The data from the CHX experiments was used to statistically analyse the control data from *NSun2*$^{+/-}$ and Nsun2$^{-/-}$ mice, essentially replicating the initial DHPG-experiment that indicated reduced DHPG-LTD in the NSun2$^{-/-}$ mice (Figure 3.2A). Those initial experiments could not be replicated, indicating a possible false-positive result (Figure 3.6D). It is difficult to know which sets of data is more reliable, however pooling the control data from the CHX experiments (Figure 3.6*D*) with the initial mGluR-LTD experiments (Figure 3.2) results in no significant difference between the two mouse groups when statistically tested (data not shown). It is unknown what caused the lack of reproducibility in this case as the experimental set-up remained unchanged, but certainly a large variance in the data can be observed (Figure 3.6E*)*. This suggests any possible genotype effect could well be hidden under the relatively vast spread of data. It should also be noted that the sample sizes used here closely resemble those for

other published field recording experiments, though it could be argued that the relatively small sample sizes used have also negatively affected the statistical power.

3.4. Summary

NSun2$^{-/-}$ mice exhibit enhanced basal transmission in the SC pathway, with no change detected in the PPR. An initial DHPG-LTD deficit in NSun2$^{-/-}$ mice could not be replicated and both *NSun2*$^{+/-}$ and NSun2$^{-/-}$ mice responded equally to protein synthesis inhibition. A SP-LFS induction protocol did not induce LTD in either model, however, a significant reduction in NMDA-dependent LTD was found in NSun2$^{-/-}$ mice compared to the control.

Chapter 4. Results: Investigation of LTP in NSun2$^{-/-}$ mice

4.1 Introduction

In chapter 3, a significant impairment in an NMDA receptor-dependent form of LTD was described in NSun2$^{-/-}$ mice (Figure 3.3A). This somewhat unexpected finding raised the possibility that other forms of NMDA receptor-dependent synaptic plasticity might also in fact be mis-regulated in these mice. NMDA receptor-dependent LTP is a good candidate in such a regard, as previous reports have revealed that the lack of NSun2 leads to deficits in learning, presented by a reduced performance in both the y-maze task (Blanco et al., 2014) and an olfactory aversion behavioural assay (Abbasi-Moheb et al., 2012), which, as previously explained, are behaviours that seem to correlate to LTP. Secondly, LTP deficits have been shown to be major hallmarks of several different intellectual disability murine models whose major phenotype of learning impairment is shared with NSun2-deficient patients. These models include: Ts65Dn knock-out model of Down syndrome (Siarey et al., 1999), Mecp2 knock-out model of Rett syndrome (Moretti et al., 2006), Tsc2+/- mutant rat model of Tuberous sclerosis (von der Brelie et al., 2006), various Huntington Disease models (Lynch et al., 2007; Simmons et al., 2009) and FXS models (Chen et al., 2010; Lauterborn et al., 2007). Lastly, there is evidence proposing that both LTP and SP-LFS-induced LTD require NMDA receptors for its induction (Dudek and Bear, 1992; Ekstrom et al., 2001; Lüscher and Malenka, 2012; Sweatt, 2016). It is possible that the reduced SP-LFS LTD described in NSun2$^{-/-}$ mice (Figure 3.3A) may also involve NMDA receptors, however this has not yet been verified. In order to test the hypothesis of mis-regulated LTP in CA1 PNs of NSun2$^{-/-}$ mice, fEPSPs were recorded in the CA1 region of the hippocampus in response to electrical activation of the SC pathway, as described in the Materials and

Methods chapter. A TBS protocol (described in Materials and Methods) was implemented to induce LTP. Furthermore, pharmacological intervention in the form of CHX and BDNF were administered. Both compounds were used to investigate whether LTP expression in NSun2$^{-/-}$ hippocampal slices would respond similarly to their heterozygous counterparts if protein synthesis was inhibited or enhanced, respectively.

4.2 Results

4.2.1. Reduced LTP in NSun2$^{-/-}$ mice

After achieving a stable 30-minute baseline by recording dendritic CA1 field responses in the *stratum radiatum* in response to SC stimulation, a TBS was applied to elicit a potentiation of the responses. 1-hour post-TBS the fEPSP responses of hippocampal slices from *NSun2$^{+/-}$* mice were enhanced by 163.9% (± 7.18%, n = 6 (6)), relative to baseline. This LTP was completely blocked with 50µM of the NMDA receptor antagonist, D-AP5, when applied for the first 45 minutes of the experiments *(Figure 4.1A-B: 97.69% ± 11.32, n =5 (5), unpaired two-tailed student's t-test: p < 0.001*). Potentiation was significantly less in slices from NSun2$^{-/-}$ mice, with an average increase of 122.4% (± 5.78%, n = 6 (6)) recorded. A depotentiation protocol consisting of LFS (900 single pulses at 1Hz) (Bashir and Collingridge, 1994) was instigated 1 hour after LTP induction in order to study further possible disparities between NSun2 heterozygous and knock-out mice. Analysing fEPSP responses 1-hour after the completion of the LFS demonstrated no meaningful impact on what appeared to be stable LTP in *NSun2$^{+/-}$* mice with an average change of -4.4% (± 9.8, n = 6 (6), p > 0.05) recorded (Figure 4.1A-C*)*. This is in contrast to what was observed in NSun2$^{-/-}$ mice, with an average change of -27.9% (± 7.3, n = 6 (6), p < 0.05) observed. Although there is a significant difference between the groups, it seems extremely unlikely that the LFS has had any effect since LTP appears to be

declining in the NSun2$^{-/-}$ group regardless. For this reason, the experiments were repeated for a longer time frame and without the implementation of an LFS protocol (see next section). Due to Ca^{2+} influx being a major determinant of LTP, any possible changes discovered during LTP induction could indicate a pathological mechanism relating to the LTP deficit in NSun2$^{-/-}$ mice. Although a slight reduction in TBS-fEPSP responses were observed, no significant changes were found in the TBS-fEPSP responses. (*Figure 4.1.D: Repeated measures ANOVA with Greenhouse Geisser correction; F = 1.19, p = 0.13*).

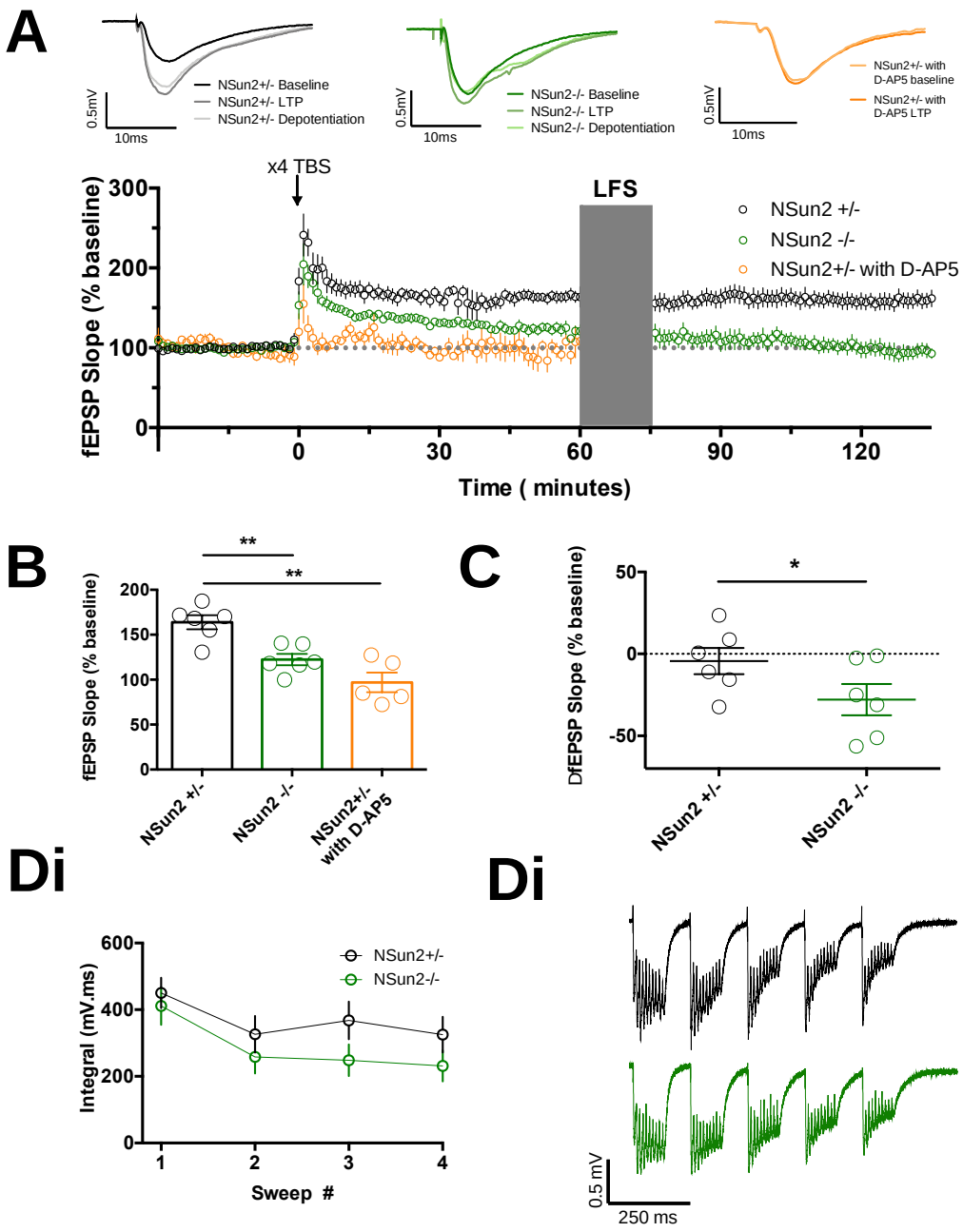

Figure 4.1. NSun2$^{-/-}$ mice exhibit reduced LTP in the SC pathway that is not affected by a de-potentiation protocol

A) *Bottom: fEPSP responses averaged every minute. TBS was applied to the SC pathway to evoke stable LTP in NSun2$^{+/-}$ mice. 60 minutes after the induction of LTP, a LFS was used in an attempt to de-potentiate the LTP. The protocol had no bearing on the level of LTP in NSun2$^{+/-}$ mice. Prior to the LFS,*

LTP in the NSun2$^{-/-}$ mice was greatly reduced (LTP: NSun2$^{+/-}$ = 163.9% ± 7.18%, n = 6 (6); NSun2$^{-/-}$ = 122.4% ± 5.78%, n = 6 (6); unpaired two-tailed student's t-test: p = 0.002; NSun2$^{+/-}$ with D-AP5 = 97.69% ± 11.32, n = 5 (5), unpaired two-tailed student's t-test: p < 0.001. De-potentiation: NSun2$^{+/-}$ = 159.6% ± 9.86%, n = 6 (6); Nsun2$^{-/-}$ = 94.54% ± 8.86%, n = 6 (6); unpaired, two-tailed student's t-test: p = 0.001). Top: LTP and depotentiation example traces.
***B)** Bar chart depicting LTP data spread from each experiment.*
***C)** Data spread of LTP to de-potentiation from each experiment.*
***Di)** Integral of field responses to TBS for each of the four sweeps (NSun2$^{+/-}$: n = 6; sweep 1 = 450.4 mV.ms ± 45.9, sweep 2 = 326.4 mV.ms ± 55, sweep 3 = 367.6 mV.ms ± 56.7, sweep 4 = 325.4 mV.ms ± 53.6; NSun2$^{-/-}$: n = 6 (6); sweep 1 = 411.1 mV.ms ± 56.9, sweep 2 = 258.2 mV.ms ± 49.4, sweep 3 = 248 mV.ms ± 47.9, sweep 4 = 231.3 mV.ms ± 46.7; repeated measures ANOVA with Greenhouse Geisser correction; F = 1.19, p > 0.05).*
***Dii)** Representative traces of first sweep from TBS responses.*

4.2.2. CHX reduces LTP in NSun2$^{+/-}$ *but not in NSun2$^{-/-}$ mice*

Examined at a more detailed level in chapter 1.*3*, there is a marked ambiguity surrounding the protein synthesis dependency of LTP (Abbas et al., 2015). Previous research from Fonseca *et al. (*2006*)* has suggested that LTP may have a greater dependency on protein synthesis with a higher frequency stimulation protocol that was recorded for up to 170 minutes. Using a similar time-frame to Fonseca *et al.*, fEPSP responses were recorded for 3 hours after the induction of LTP (with the previously used TBS protocol) interleaved with and without the protein synthesis inhibitor, CHX (60μM). The extended experimental time-frame used here aided in answering three questions; is the LTP deficit in NSun2$^{-/-}$ mice reproducible? Will the fEPSP responses from NSun2$^{-/-}$ mice continue to run-down irrespective of LFS? Does the NSun2$^{-/-}$ LTP deficit involve protein synthesis? To answer the first question, LTP levels 60-minutes after TBS application were analysed to reveal similar increases in transmission in both *NSun2$^{+/-}$* and NSun2$^{-/-}$ mice when compared to the previous LTP experiment in *section 4.2.1.* (Figure 4.2B: *NSun2$^{+/-}$*: 149.9% ± 5.9; Nsun2$^{-/-}$: 121.2% ± 9.5). This has provided support for the validation of Nsun2 requirement for normal LTP. Referring to the second question of whether the previous de-potentiation

experiment (Figure 4.1A and C) caused the run-down of the NSun2$^{-/-}$ fEPSP responses or if the persistent decrease was independent of the LFS application. By identifying the corresponding time point from the NSun2$^{-/-}$ CTRL group (average taken between 110 – 120 minutes) revealed similar LTP levels (109% ± 9.2%) to the preceding de-potentiation experiment which suggests the LFS protocol bared no influence on LTP levels (Figure 4.1A). The last question queried protein synthesis involvement in LTP; the reasoning behind the hypothesis is identical to that explained in chapter 3. which outlines a possible "flooring" effect. This was hypothesised as NSun2$^{-/-}$ mice are known to exhibit a global reduction in protein synthesis (Blanco et al., 2014), and therefore attempts at reducing protein synthesis pharmacologically might in fact fail to yield the otherwise expected response of the PSI. Blocking protein synthesis pharmacologically significantly reduced LTP in *NSun2*$^{+/-}$ mice. fEPSP measurements were analysed at the final 10 minutes of experiments i.e. between 2 hours 50 minutes and 3 hours (*Figure 4.2Bi: CTRL: n = 6 (6); 127% ± 5.9%, CHX: n = 5 (5); 107% ± 2.43%; unpaired, student's t-test: p = 0.004*), however this effect was not observed in NSun2$^{-/-}$ mice (*Figure 4.2C: CTRL: n =5; 90.85% ± 6.8%, CHX: n =5 (5); 101% ± 3.8%; unpaired, student's t-test: p > 0.05).* In order to compare the effectiveness of the drug between the two mouse groups, a two-way ANOVA was used revealing a significant genotype-CHX interaction suggesting CHX had a vastly greater effect on LTP in *NSun2*$^{+/-}$ than NSun2$^{-/-}$ mice *(Two-way ANOVA, F = 13.54, P = 0.002)*. However, interpreting the meaning of this result is difficult as LTP couldn't be maintained in the NSun2$^{-/-}$ mice regardless of CHX application. CHX did not have an effect on either the PPR (*Figure 4.2Biii*) or on the integral of the TBS response (*Figure 4.2D-E*).

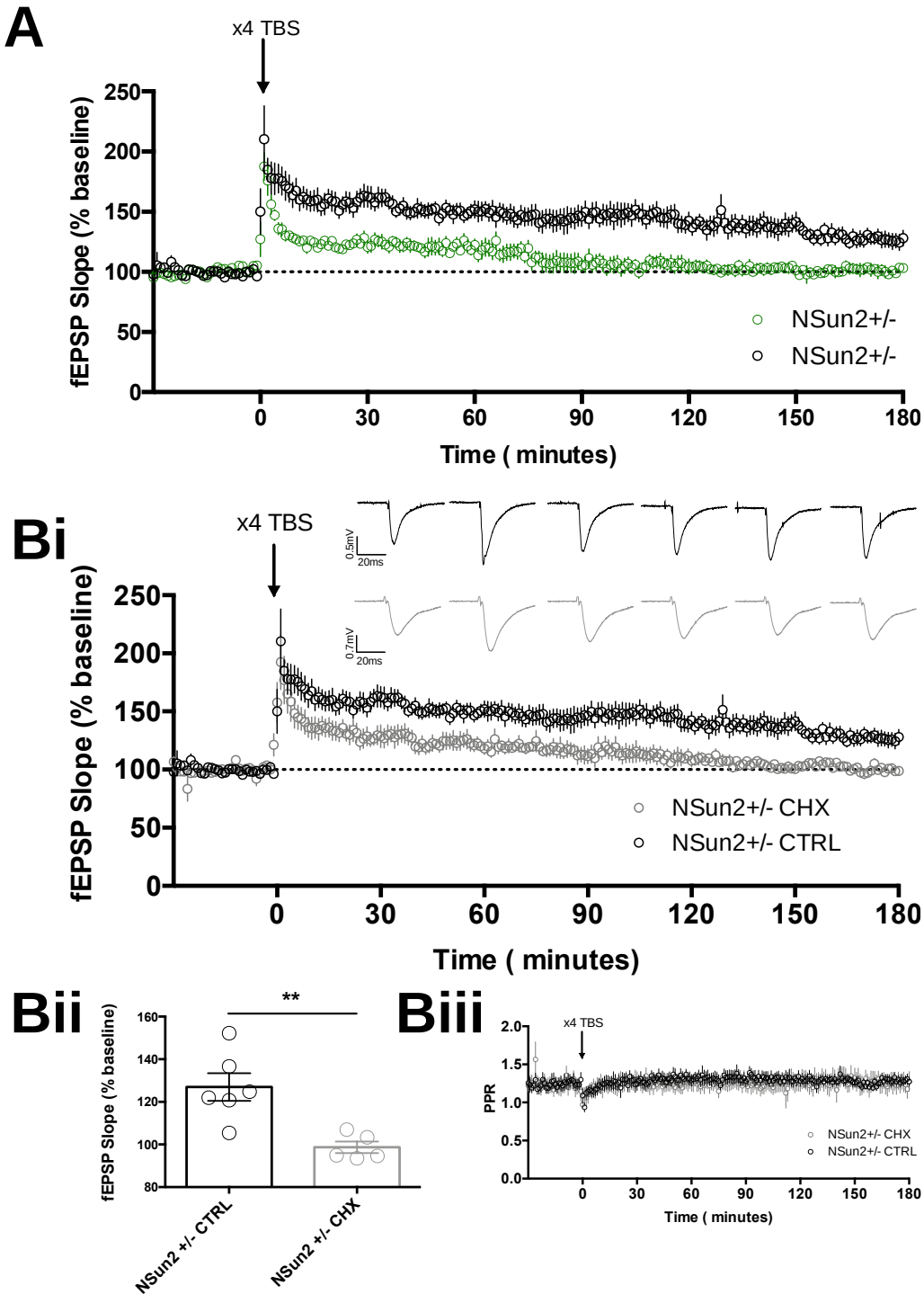
A
x4 TBS
fEPSP Slope (% baseline)
250
200
150
100
50
0
0
30
60
90
120
150
180
Time (minutes)
NSun2+/-
NSun2+/-
Bi
x4 TBS
0.5mV
20ms
0.7mV
20ms
fEPSP Slope (% baseline)
Time (minutes)
NSun2+/- CHX
NSun2+/- CTRL
Bii
**
fEPSP Slope (% baseline)
160
140
120
100
80
NSun2 +/- CTRL
NSun2 +/- CHX
Biii
x4 TBS
PPR
2.0
1.5
1.0
0.5
0.0
Time (minutes)
NSun2+/- CHX
NSun2+/- CTRL

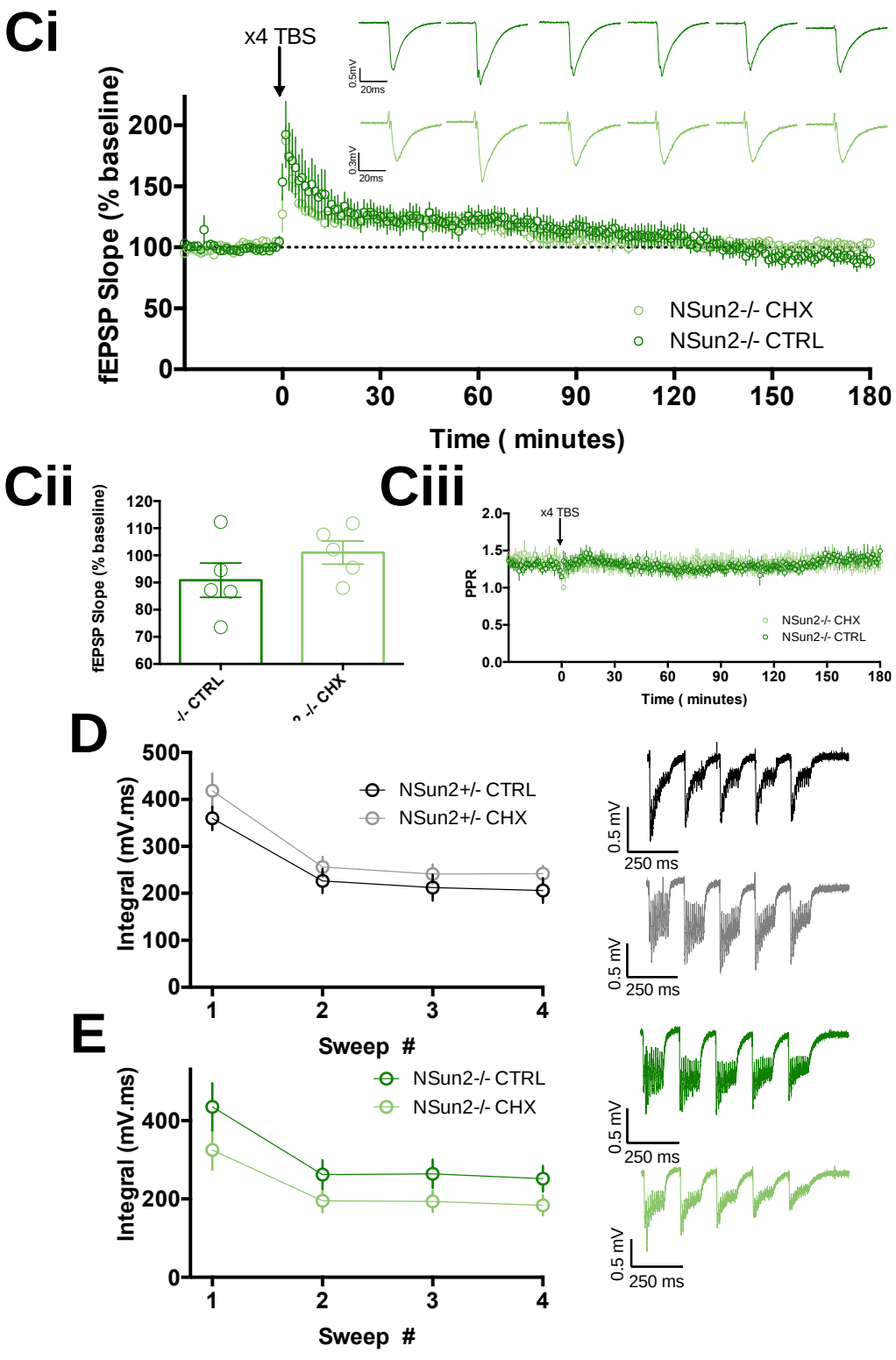
Ci
x4 TBS
0.5mV
20ms
0.3mV
20ms
fEPSP Slope (% baseline)
200
150
100
50
0
0
30
60
90
120
150
180
Time (minutes)
NSun2-/- CHX
NSun2-/- CTRL
Cii
fEPSP Slope (% baseline)
120
110
100
90
80
70
60
Ciii
x4 TBS
PPR
2.0
1.5
1.0
0.5
0.0
0
30
60
90
120
150
180
Time (minutes)
NSun2-/- CHX
NSun2-/- CTRL
D
Integral (mV.ms)
500
400
300
200
100
0
1
2
3
4
Sweep #
NSun2+/- CTRL
NSun2+/- CHX
0.5 mV
250 ms
0.5 mV
250 ms
E
Integral (mV.ms)
400
200
0
1
2
3
4
Sweep #
NSun2-/- CTRL
NSun2-/- CHX
0.5 mV
250 ms
0.5 mV
250 ms

Figure 4.2. The NSun2$^{-/-}$ LTP deficit may be influenced by protein synthesis

A) *TBS-induced LTP of SC pathway recorded for 3 hours post-LTP. Significantly reduced LTP was observed in the NSun2$^{-/-}$ mice (NSun2$^{+/-}$: n =6 (6); 127% ± 5.9%, NSun2$^{-/-}$: n = 5 (5); 90.85% ± 6.8%)*
Bi) *TBS-induced LTP of SC pathway recorded for 3 hours post-LTP either with or without the presence of CHX (60μM). CHX significantly decreased LTP in the NSun2$^{+/-}$ group (CTRL: n =6 (6); 127% ± 5.9%, CHX: n =5 (5); 107% ± 2.43%; unpaired, student's t-test: p = 0.004). A significant genotype-CHX interaction was identified (Two-way ANOVA, F = 13.54, P = 0.002). Top right: example traces from every 30 minutes of experiment post TBS.*
Bii) *Bar charts depicting data spread of LTP from NSun2$^{+/-}$ mice; each data point represents the average of the last 10 minutes of each experiment.*
Biii) *CHX does not affect PPR in NSun2$^{+/-}$ mice (CTRL: n =6 (6); 128.8% ± 6.4%, CHX: n =5 (5); 125% ± 11.9%; unpaired, student's t-test: p > 0.05).*
Ci) *TBS-induced LTP of SC pathway extended to 3 hours either with or without the presence of CHX (60μM). CHX did not alter LTP in the NSun2$^{-/-}$ group (CTRL: n = 5 (5); 90.85% ± 6.8%, CHX: n = 5 (5); 101% ± 3.8%; unpaired, student's t-test: p > 0.05). Top right: example traces from every 30 minutes of experiment.*
Cii) *Bar charts depicting data spread of LTP from NSun2$^{-/-}$ mice; each data point represents the average of the last 10 minutes of each experiment.*
Ciii) *CHX does not affect PPR in NSun2$^{-/-}$ mice (CTRL: n =5 (5); 139.9% ± 9.1%, CHX: n =5 (5); 134% ± 12.3%; unpaired, student's t-test: p > 0.05).*
D) *Integral of response to TBS is not influenced by CHX in NSun2$^{+/-}$ (NSun2$^{+/-}$ CTRL: n = 6 (6); sweep 1 = 359.62 mV.ms ± 25.3, sweep 2 = 226.5 mV.ms ± 25.8, sweep 3 = 212.4 mV.ms ± 28.1, sweep 4 = 206.16 mV.ms ± 26.5; NSun2$^{+/-}$ CHX: n = 5; sweep 1 = 418.58 mV.ms ± 36.5, sweep 2 = 255.9 mV.ms ± 21.8, sweep 3 = 241.2 mV.ms ± 20.9, sweep 4 = 242 mV.ms ± 17) Right: Representative traces of first sweep from TBS responses.*
E) *Integral of response to TBS is not influenced by CHX in NSun2$^{-/-}$ (NSun2$^{-/-}$ CTRL: n = 5 (5); sweep 1 = 435.16 mV.ms ± 60.72, sweep 2 = 262.48 mV.ms ± 37.4, sweep 3 = 264.2 mV.ms ± 36.5, sweep 4 = 251.7 mV.ms ± 33.2; NSun2$^{-/-}$ CHX: n = 5; sweep 1 = 325.4 mV.ms ± 51.1, sweep 2 = 195.4 mV.ms ± 28.9, sweep 3 = 193.8 mV.ms ± 27.1, sweep 4 = 183.7 mV.ms ±25.5). Right: Representative traces of first sweep from TBS responses. No interaction between genotype, sweep number and drug condition was found (Repeated-Measures ANOVA with Greenhouse Geisser correction: F = 2.07, p = 0.17)*

4.2.3. BDNF does not rescue LTP deficit in NSun2$^{-/-}$ mice

BDNF has been shown to enhance mRNA translation rates (Yin, Edelman and Vanderklish, 2002; Gharami and Das, 2014), as detailed further in chapter 1.3., and has been used effectively in a variety of intellectual disability murine models to reverse plasticity dysfunction. These models include: Huntington's disease (Simmons et al., 2009), Rett syndrome (Moretti et al., 2006) and FXS (Lauterborn et al., 2007). Of course, these are heterogeneous disorders in terms of clinical presentation, pathology, and molecular mechanisms, and are indeed dissimilar to NSun2-deficiency. However, intellectual disability is a key characterising phenotype in all the disorders and provides a common link between them. Furthermore, translation/protein synthesis factors modulated by BDNF are also targeted for NSun2-mediated methylation and could therefore impact the efficacy of LTP expression (discussed in *Chapter 4.3.3.*). Thus, in order to investigate whether BDNF-mediated pathways might also be involved in the pathology of the NSun2-deficient model, fEPSP recordings responding to SC pathway stimulation were analysed in the presence of 20nM BDNF, a concentration previously used to reverse LTP deficits in intellectual disability models (Lauterborn et al., 2007).

As was performed for the LTP-CHX experiments (section 4.2.2.), all BDNF field experiments were carried out for 3 hours post-LTP induction. BDNF did not influence levels of LTP in heterozygous mice (*Figure 4.3Aii: CTRL: n = 6 (6); 152.9% ± 12.74%, BDNF: n = 6 (6); 145.5% ± 3.3%; unpaired, student's t-test: p > 0.05*), neither was an effect found in the knock-out mice (*Figure 4.3Bii: CTRL: n = 4; 105.9% ± 7.5%, BDNF: n = 4 (4); 103% ± 20.68%; unpaired, student's t-test: p > 0.05*). In order to statistically evaluate an interaction between the mouse genotype and BDNF on LTP expression, a two-way ANOVA test was implemented; no significant interaction between mouse strain and BDNF application was observed (Figure 4.3Aii and Bii).

To establish whether BDNF affected the release probability or cation influx into the cell during induction of LTP, the PPR and the integral of the TBS response was analysed. BDNF did not have a discernible effect on PPR (Figure 4.3Aiii and Biii*)* or TBS-response (Figure 4.3C-D).

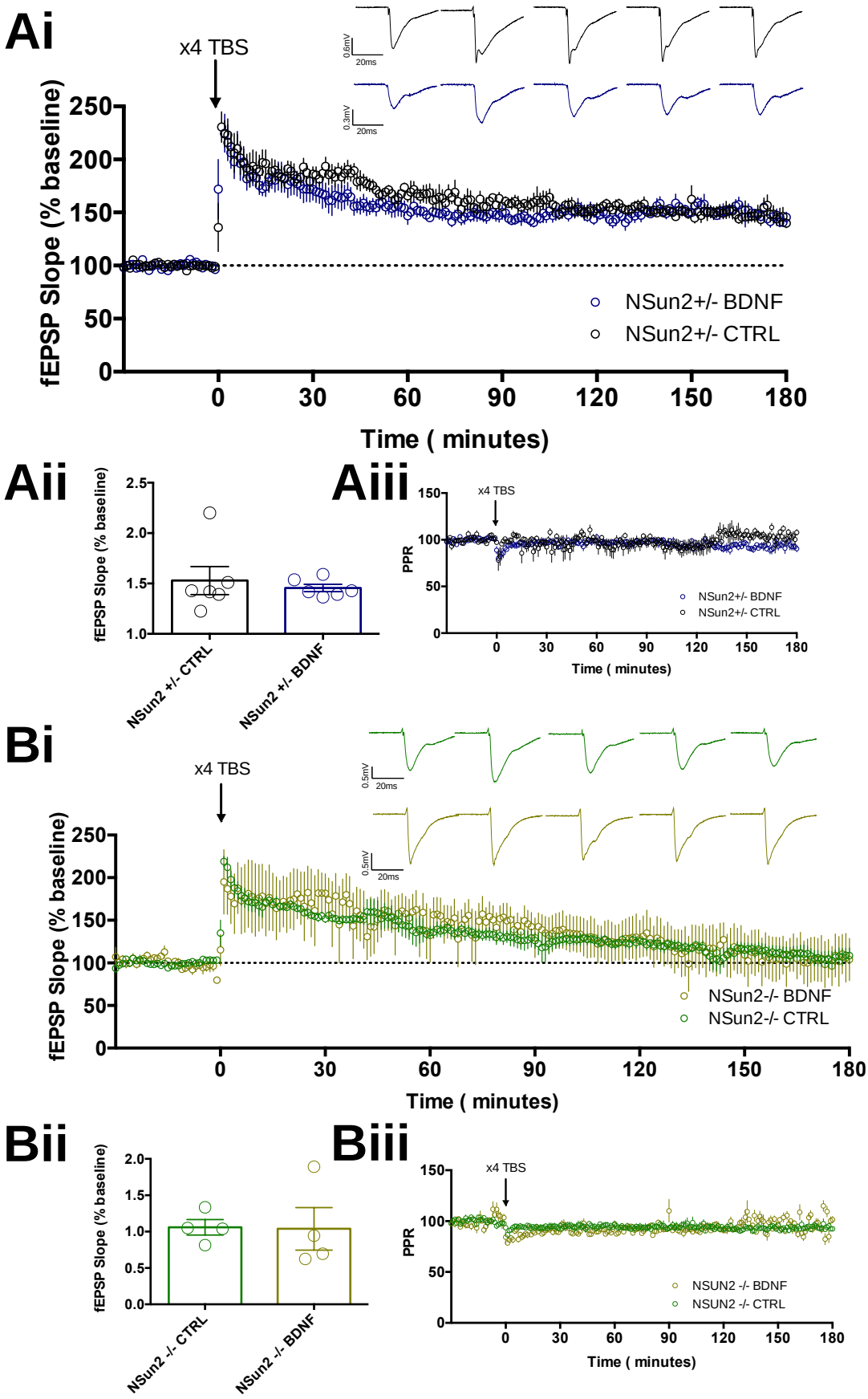
Ai
x4 TBS
0.6mV
20ms
0.3mV
20ms
fEPSP Slope (% baseline)
250
200
150
100
50
0
0
30
60
90
120
150
180
Time (minutes)
NSun2+/- BDNF
NSun2+/- CTRL
Aii
fEPSP Slope (% baseline)
2.5
2.0
1.5
1.0
NSun2 +/- CTRL
NSun2 +/- BDNF
Aiii
x4 TBS
PPR
150
100
50
0
0
30
60
90
120
150
180
Time (minutes)
NSun2+/- BDNF
NSun2+/- CTRL
Bi
x4 TBS
0.5mV
20ms
0.5mV
20ms
fEPSP Slope (% baseline)
250
200
150
100
50
0
0
30
60
90
120
150
180
Time (minutes)
NSun2-/- BDNF
NSun2-/- CTRL
Bii
fEPSP Slope (% baseline)
2.0
1.5
1.0
0.5
0.0
NSun2 -/- CTRL
NSun2 -/- BDNF
Biii
x4 TBS
PPR
150
100
50
0
0
30
60
90
120
150
180
Time (minutes)
NSUN2 -/- BDNF
NSUN2 -/- CTRL

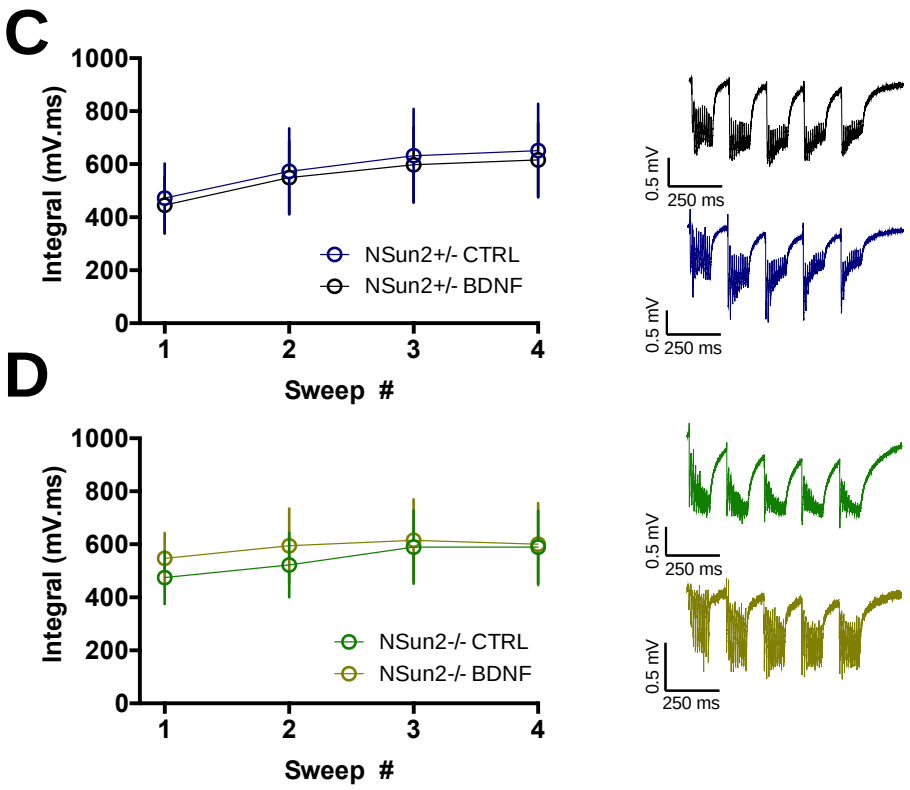

Figure 4.3. BDNF does not rescue LTP deficit in NSun2$^{-/-}$ mice

Ai) *TBS-induced LTP of SC pathway recorded for up to 3 hours post-LTP either with or without the presence of BDNF (20nM). BDNF did not influence LTP in the NSun2$^{+/-}$ group (CTRL: n = 6 (6); 152.9% ± 12.74%, BDNF: n = 6 (6); 145.5% ± 3.3%; unpaired, student's t-test: p > 0.05). Top right: example traces from every 30 minutes of experiment.*
Aii) *Bar charts depicting data spread of LTP from NSun2$^{+/-}$ mice; each data point represents the average of the last 10 minutes of each experiment.*
Aiii) *BDNF does not affect PPR in NSun2$^{+/-}$ mice (CTRL: n =6 (6); 104.2% ± 4.6%, BDNF: n =6 (6); 93.9% ± 4.1%; unpaired, student's t-test: p > 0.05).*
Bi) *TBS-induced LTP of SC pathway recorded for up to 3 hours post-LTP either with or without the presence of BDNF (20nM). BDNF did not have a bearing on LTP in the NSun2$^{-/-}$ group (CTRL: n = 4 (4); 105.9% ± 7.5%, BDNF: n = 4 (4); 103% ± 20.68%; unpaired, student's t-test: p > 0.05). Top right: example traces from every 30 minutes of experiment.*
No significant genotype-BDNF interaction was identified (Two-way ANOVA, F = 0.184, P > 0.05).

Bii) *Bar charts depicting data spread of LTP from NSun2$^{-/-}$ mice; each data point represents the average of the last 10 minutes of each experiment.*
Biii) *BDNF does not affect PPR in NSun2$^{-/-}$ mice (CTRL: n =4 (4); 93.8% ± 2.2%, BDNF: n =4 (4); 97.5% ± 4.4%; unpaired, student's t-test: p > 0.05).*
C) *Integral of response to TBS is not influenced by BDNF in NSun2$^{+/-}$ (NSun2$^{+/-}$ CTRL: n = 6 (6); sweep 1 = 472.3 mV.ms ± 131, sweep 2 = 573.3 mV.ms ± 162.5, sweep 3 = 631.8 mV.ms ± 176.7, sweep 4 = 650.9 mV.ms ± 177.4; NSun2$^{+/-}$ BDNF: n = 6; sweep 1 = 445.2 mV.ms ± 107.8, sweep 2 = 549.3 mV.ms ± 137.5, sweep 3 = 597.8 mV.ms ± 141.4, sweep 4 = 615.9 mV.ms ± 140) Right: Representative traces of first sweep from TBS responses.*
D) *Integral of response to TBS is not influenced by CHX in NSun2$^{-/-}$(NSun2$^{-/-}$ CTRL: n = 4 (4); sweep 1 = 474.5 mV.ms ± 99.9, sweep 2 = 522.3 mV.ms ± 121.9, sweep 3 = 589.9 mV.ms ± 138.9, sweep 4 = 589.6 mV.ms ± 137.4; NSun2$^{-/-}$ BDNF: n = 4; sweep 1 = 547.1 mV.ms ± 96.1, sweep 2 = 594.8 mV.ms ± 140.1, sweep 3 = 615.2 mV.ms ± 154.6, sweep 4 = 600.1 mV.ms ± 155.2). Right: Representative traces of first sweep from TBS responses. No interaction between genotype, sweep number and drug condition was found (Repeated-Measures ANOVA with Greenhouse Geisser correction: F = 2.53, p = 0.13)*

4.3. Discussion

4.3.1. NSun2$^{-/-}$ mice exhibit LTP deficits

The SC pathway was subject to a TBS LTP-induction protocol, as described in the Materials and Methods. This protocol was preferred over others, such as tetanic stimulation, in order to promote physiological relevance; theta rhythms endogenously occur in the hippocampus during rodent exploration (Winson, 1978). A stable LTP resulted from the TBS which enhanced responses in heterozygous mice to 163.9% (± 7.18%). These responses were also able to withstand attempts of de-potentiation using a SP-LFS underlining the stability of the LTP that was induced (Figure 4.1.). This was in stark contrast to NSun2$^{-/-}$ mice where only an increase of 122.4% (± 5.78%) was observed, a statistically significant reduction in LTP when compared to their heterozygous littermates. In order to consider possible depotentiation deficits, a SP-LFS was applied 60-

minutes post-LTP induction. No significant reduction in responses were observed in the heterozygous mice, however 60-minutes post-depotentiation induction, NSun2$^{-/-}$ mouse responses had descended back to baseline measurements. As previously explained, there could be two possibilities for this result, de-potentiation could have caused the LTP-reduction or the LTP may not stabilise in the NSun2$^{-/-}$ mice regardless of the LFS.

Having established a plasticity deficit in this NSun2 neurodevelopmental model, there were several primary questions to answer: can this result be replicated? This is especially relevant due to the previous inability to replicate the initial mGluR-LTD experiments. Did the LFS cause the gradual reduction in LTP in NSun2$^{-/-}$ mice? And lastly, could this LTP deficit involve protein synthesis discrepancies? These questions are addressed in the next section.

4.3.2. CHX decreases LTP in NSun2$^{+/-}$ *mice but not NSun2$^{-/-}$ mice*

In order to explore the aforementioned questions, field experiments were conducted interleaved with and without 60μM CHX for 3 hours post-LTP induction. The reason for this time-frame was two-fold; the length of time could act as a control for the depotentiation in NSun2$^{-/-}$ mice, and also, previous reports have identified protein-synthesis dependency up to this time point and beyond (Fonseca et al., 2006).

CHX significantly decreased LTP in heterozygous mice, eventually reducing responses back to baseline (Figure 4.2). This would suggest that protein synthesis is a requirement for the establishment of normal LTP. These results are both similar to some reports (Fonseca et al., 2006; Vickers et al., 2005) and yet differs to others (Abbas et al., 2009b; Villers et al., 2012). It is, however, conceivable that off-target effects from CHX has caused the LTP deficits. For example, concentrations between 50 – 500nM CHX have been shown to increase mRNA levels of c-jun and bcl-2 in hippocampal cell cultures that are

believed to enhance neural protection (Furukawa et al., 1997). In an ideal situation anisomycin would be used as a control, however this was not possible due to time constraints. It would however, prove useful to flash-freeze slices after an LTP experiment for protein synthesis analysis. For example, conducting surface sensing of translation (SUnSET) to investigate global protein translation changes or western blot assays to identify proteins that are supposedly required to be translated for the normal expression of LTP could determine the molecular effect of CHX. One of the difficulties with this approach is that a detailed view of the local activity-dependent proteome in response to TBS has not been characterised. However there is evidence of proteins including wnt5a (Li et al., 2012) and Arc (Bloomer et al., 2008) to name a couple, that are rapidly synthesised in response to theta burst stimulation, and these for example could be scrutinised to further investigate how CHX might be influencing LTP.

The protein synthesis-dependency of LTP observed in *NSun2*$^{+/-}$ mice is not found in NSun2$^{-/-}$ mice as CHX has no influence on LTP levels; a two-way ANOVA revealed a significant interaction between genotype and CHX. It is possible that the global reduction in translation previously reported in this NSun2 model (Blanco et al., 2014) has produced a “flooring effect” whereby protein synthesis cannot be blocked any further with the application of CHX. On the other hand, the lack of CHX effect is more difficult to interpret as LTP could not be maintained in the NSun2$^{-/-}$ mice regardless of CHX. As previously explained, a SUnSET assay could prove invaluable in determining if any such effect exists (i.e. analyse translation levels before and after CHX application).

The effect of CHX on LTP on the heterozygous control mice described in this section may be considered somewhat surprising. The generally accepted view is that the early phase of LTP (if such a phase does indeed exist (Abbas et al., 2015)) sits between 1–2 hours post-LTP induction and is dependent on modifications to constitutively expressed proteins as well as their trafficking to synaptic regions, rather than new protein synthesis (Bliss and Collingridge,

1993; Lisman et al., 2002; Malenka and Nicoll, 1999; Oliet et al., 1997). If this were the case, then the CHX would not be expected to influence LTP until the beginning of the L-LTP phase (2+ hours post-LTP induction) but an obvious immediate reduction was noticed in these results (Figure 4.2A*)*. It could be that the induction protocol is a determinant of protein synthesis dependency, with reports of the E-LTP phase relying on protein synthesis when a protocol with a faster frequency is used (Fonseca et al., 2006). Another study used a similar TBS-induction protocol to that employed in the experiments detailed in this chapter. Their protocol was applied to organotypic hippocampal CA1 PN cultures which led to enhanced levels of activated nuclear factor kappa-light-chain-enhancer of activated B (NF- κB) cells after only 30 minutes (within the E-LTP range). NF-kB can be used as an indicator of gene expression changes and suggests that TBS could lead to an early dependency of protein synthesis (Sheridan et al., 2014).

It will be important to conduct follow up experiments to support these findings for a multitude of reasons; to gain an appreciation of the full precise effects of CHX on CA1 PNs, how much translation is being inhibited and if so, whether there are LTP-specific proteins being affected. It will also be necessary to understand if these deficits are localised to CA1 PNs or if there are other cells affected within the hippocampus and if this effect has more of a global reach. Investigations into behavioural correlations would aid in the understanding of how protein synthesis influences LTP expression in NSun2$^{-/-}$ mice. Previous research described a deficit in spatial working memory with a Y-maze task in the NSun2$^{-/-}$ model used in this thesis (Blanco et al., 2014) and similar behavioural tasks (in non-genetically modified animals) has demonstrated a reduction in performance, specifically in the encoding phase, when PSIs are applied (Ozawa et al., 2017). It may be possible to replicate the poor performance observed in spatial tasks in NSun2$^{-/-}$ mice in their heterozygous counterparts by applying PSIs *in vivo*. Furthermore, other hippocampal-dependent behaviours are affected by PSIs, including fear conditioning (Yang et al., 2011). It is entirely

plausible that this Nsun2-deficient model may exhibit impaired fear conditioning similar to that of wild-type mice that have been administered PSIs. Though, this is just conjecture at time of writing and requires further examination.

4.3.3. BDNF does not rescue LTP deficit in NSun2$^{-/-}$ mice

It is of particular interest to uncover methods of deficit reversal in order to improve the current understanding of the mechanisms underlying NSun2-deficiency phenotypes that will hopefully lead to potential therapies for NSun2-deficient patients. Knowledge concerning NSun2-deficiency syndromes in the population as well as experimental models is currently limited, however the summation of recent evidence suggests NSun2 is a requirement for normal protein synthesis (Blanco et al., 2014; Hussain et al., 2013a, 2013b; Hussain and Bashir, 2015). One compound that has been intimately linked with translation rates, LTP expression and other intellectual disability models with LTP deficits, is BDNF.

BDNF has been implicated in synaptic transmission and LTP since the 1990's, with acute BDNF applications enhancing synaptic activity and vesicle release *in vitro* (Levine et al., 1995; Takei et al., 1997). It has also previously been demonstrated that knock-out of BDNF via genetic manipulation can cause reduced LTP expression in rodents (Patterson et al., 1996) and that BDNF mRNA levels are increased in response to tetanic stimulation *in-vitro* (Patterson et al., 1992), although enhanced levels of mRNA doesn't necessarily translate to enhanced levels of protein synthesis (Koussounadis et al., 2015). BDNF activates MAPK and PI3K pathways which are involved in both early- and late-phases of LTP (Gottschalk et al., 1999) (although the classic temporal biphasic property of LTP is highly debated (Abbas et al., 2015)) and can lead to the upregulation of the NMDA receptor subunits: NR1, NR2A and NR2B and the AMPA receptor subunit, GluA1, via a protein synthesis dependent mechanism (Caldeira et al., 2007), all of which are vital for LTP expression.

BDNF can enhance the phosphorylation of both eIF4E and eIF4E-BP which can be a rate-limiting step in translation (Ruiz et al., 2014). As an initiation factor, eIF4E forms complexes with other proteins and factors, such as EIF4G1 whose mRNA is an NSun2-mediated methylation target (Hussain and Bashir, 2015). EIF4G1 associates with ribosomes through another factor named eIF3 (Richter and Sonenberg, 2005), whose sub-unit composition also includes NSun2-methylation targets (Hussain and Bashir, 2015). These complexes that interact with eIF4E have been previously implicated in autism disorders (Kelleher and Bear, 2008; Santini et al., 2013), which is also an observable phenotype in NSun2-deficient patients (Abbasi-Moheb *et al.*, 2012; Fahiminiya *et al.*, 2014; Khan *et al.*, 2012). An earlier investigation exploited a transgenic model of monogenic non-syndromic autism via eIF4E overexpression which exaggerated cap-dependent translation (Santini et al., 2013). The mouse model, engineered to mimic a relevant mutation found in a human patient (Neves-Pereira et al., 2009), did indeed display autistic behaviours providing another link between abnormal translation and autistic phenotypes. Although, an important consideration to reflect upon is the vast heterogeneity of causes and mechanisms involved in autism spectrum disorders, two of these diagnoses in the population may have no overlapping molecular mechanisms. BDNF (20nM) was bath-applied to hippocampal slices for the duration of the LTP experiment but had no effect on either mouse model. There could be multiple reasons why BDNF didn't rescue the LTP deficit in NSun2$^{-/-}$ mice. For example, it may be as simple as requiring a higher concentration as cellular BDNF levels were not quantified prior to and after LTP, or that increasing phosphorylation of eIF4E (by increasing BDNF levels) couldn't increase cap-dependent translation because the other requirements (i.e. EIF4G1) may be the limiting factor in BDNF-LTP pathways. It could also be that a completely different mechanism is dysfunctional. Another possible reason for the lack of LTP rescue with BDNF in NSun2$^{-/-}$ mice is that although BDNF itself can regulate activity-dependent gene expression, it's availability is not influenced by the altering of protein synthesis

rates (Gottschalk et al., 1999), ergo NSun2$^{-/-}$ may have normal levels of BDNF. The varying possibilities underscores the necessity for further research; it is currently not known how levels of eIF4G1 are affected in NSun2$^{-/-}$ mice or if this has any bearing on the abnormalities observed. Protein synthesis assays could be used to understand whether BDNF is increasing global mRNA translation levels to provide insight into the BDNF-LTP interaction. Finally, it could prove beneficial to test whether increasing eIF4G1 protein levels or eIF4G1 methylation levels would reverse the LTP deficits observed.

Another possible deficit that could lead to the rapid decaying of LTP in NSun2$^{-/-}$ slices may involve actin polymerisation in dendritic spines, a requirement for the stabilisation of LTP induced via TBS in mice (Lynch et al., 2007). It has been previously communicated that TBS leads to activation of the p21-activated kinase (PAK)/cofilin pathway (Chen et al., 2007). The resulting activation inhibits cofilin and therefore prevents actin-depolymerisation. In order to test if these pathways were indeed deficient, hippocampal slices could receive a TBS and then subjected to fixation to allow for maximal cofilin phosphorylation (Chen et al., 2007). Fixed slices could then be investigated for phosphorylated-cofilin levels and may provide an indicator of dysfunction of this pathway. It may also be constructive to use phalloidin labelling of filamentous actin as increases in this protein is necessary for stable LTP expression (Lauterborn et al., 2007).

A further possible impaired mechanism revolves around the enhanced stress pathways reported in NSun2$^{-/-}$ mice (Blanco *et al.*, 2014). Kamal *et al.* (2008) demonstrated reductions in LTP in stressed animals that are similar to the deficits seen here that could involve similar apoptotic pathways that are enhanced in the NSun2$^{-/-}$ mouse. External stress applied to animals has been previously linked to cell death in the hippocampus (Heine et al., 2004) and also involves tRNA fragment accumulation (Saikia and Hatzoglou, 2015) that is also seen in NSun2 mice. For this reason, it could be possible that the enhanced apoptosis in NSun2$^{-/-}$ mice have contributed to the diminished LTP. To add

weight to this suggestion, Kamal *et al.* (2008) also saw an enhancement of basal synaptic transmission along with the LTP discrepancy; Figure 3.1A of this thesis described a similar increase in basal transmission in the NSun2$^{-/-}$ mice.

As well as not influencing LTP, BDNF did not seem to alter the induction process via Ca^{2+} influx as indicated by no change to the TBS integral (Figure 4.3C-D*).* Although a previous report divulged an increase in AMPA receptor trafficking to the cell surface with BDNF application (Reimers et al., 2014), a more relevant study found no change to the TBS integral using the same BDNF concentration as was used here (Lauterborn *et al.*, 2007). In line with Lauterborn *et al's.* (2007) previous work, BDNF does not alter cation influx through AMPA receptor and NMDA receptors suggesting its influence may be more downstream.

4.4. Summary

To summarise, *NSun2*$^{+/-}$ mice display robust protein-synthesis dependent LTP that is stable enough to withstand a LFS depotentiation protocol. In contrast, stable LTP cannot be induced in NSun2$^{-/-}$ mice and this deficit cannot be reversed with BDNF application. The underlying dysfunctional mechanisms are as of yet unknown with the possibility of aberrant protein synthesis being a factor due to the LTP in NSun2$^{-/-}$ hippocampal slices not responding to the PSI, CHX.

Chapter 5. Results: Intrinsic property modulation in Nsun2$^{-/-}$ mice

5.1. Introduction

In contrast to the extensive endeavours in the field of synaptic plasticity, the plasticity of neural intrinsic properties had only begun to be considered in depth over the past couple of decades. Even now the volume of literature regarding intrinsic modulation pales in comparison to that of synaptic plasticity. The features of intrinsic modulation involves the alteration of the hugely diverse number of ion channels embedded in the plasma membrane. This type of modulation can have an impact on action potential generation and waveform and passive properties of membranes, all of which can influence how neurons may respond to an input. One example of intrinsic alterations causing a physiological impact is the backpropagation of action potentials in dendrites which is important for STDP (Daoudal and Debanne, 2003). A study showed that spike-timing-dependent long-term potentiation (STD-LTP) was complemented with a decrease in excitability of the cell as well as a reduction in R_i; the intrinsic changes were revealed to be caused by the regulation of HCN channels (Fan et al., 2005).

Intrinsic properties are pliable and are subject to alterations that can be determined by the physiological history of the neuron, such as previous synaptic and intrinsic activity (Daoudal and Debanne, 2003; Zhang and Linden, 2003). The aim of the following experiments within this chapter were two-fold, firstly to create a characterisation of both sub- and supra-threshold intrinsic properties. Secondly, to identify if mGluR-dependent intrinsic alterations in NSun2$^{-/-}$ mice exist. Motives behind the latter were prompted by the initial findings that NSun2$^{-/-}$ mice presented with reduced DHPG-LTD (Figure 3.2); mGluR-dependent

intrinsic property modulation could indicate a dysfunctional pathway resulting in the reduction in DHPG-LTD. The experiments in this chapter were carried out prior to the knowledge that the initial DHPG-LTD experiments could not be replicated (chapter 3.4C). Although the initial aim of this current chapter was to investigate possible intrinsic mechanisms responsible for the deficient DHPG-LTD, the creation of an intrinsic characterisation of NSun2$^{-/-}$ CA1 PNs is an important step in understanding the NSun2-deficiency pathology.

In this chapter the whole-cell patch-clamp technique was employed to investigate the intrinsic properties of CA1 PNs in NSun2$^{-/-}$ mice. Data concerning the subthreshold and action potential waveform characterisation are reported before describing mGluR-dependent intrinsic changes via DHPG application.

5.2. Results

5.2.1. Nsun2$^{-/-}$ and NSun2$^{+/-}$ *subthreshold intrinsic properties*

Subthreshold intrinsic membrane properties were obtained and analysed from a total of 54 pyramidal cells. 29 *NSun2*$^{+/-}$ cells (14 animals) and 25 Nsun2$^{-/-}$ cells (12 animals) between 1 and 3 months old. Upon immediate entry of the pipette electrode into the cell the resting membrane potential (RMP) was recorded for 1s. The cell was then allowed to dialyse for 10 minutes before the intrinsic properties were measured. The cells were then held at -70mV and a -100pA square-wave current injection was used to observe several membrane properties: sag, τm, R_i and rebound. Of the five measurements, a genotype effect was only observed in the τm with NSun2$^{-/-}$ cells displaying a faster charge time (14.89ms ± 0.74) when compared to *NSun2*$^{+/-}$ cells (17.92ms ± 0.97) (Figure 5.1). A faster time constant could be due to several factors: a decreased number or increased closure of ion channels, a high series resistance or a

difference in cell size. If there were to be a difference in cell size, this could be reflected by either soma or dendritic changes such as a reduction in branching and complexity (in somatic recordings dendrites still serve as a capacitive load). The series resistance was monitored before and after each experiment, those experiments whereby series resistance increased to over 30MΩ were rejected.

A

	Het (n=29)		NSun2-/- (n=25)		P
	Mean	SEM	Mean	SEM	
RMP (mV)	-62.9	1.3	-63.8	1.4	0.67
τ membrane (ms)	17.9	0.9	14.9	0.7	0.02
Sag (%)	30.8	2.8	31.6	2.3	0.82
Rebound (mV)	1.9	0.2	2.3	0.2	0.32
R_i (MΩ)	104.9	5.9	96.9	5.3	0.32

B

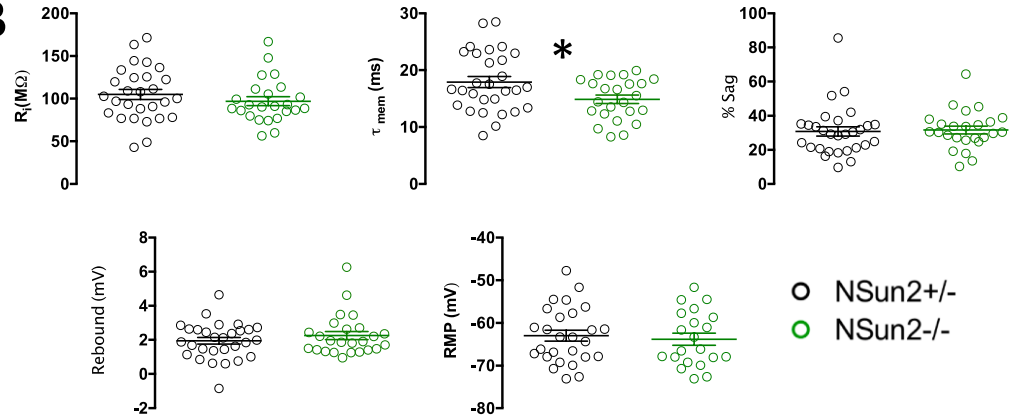

Figure 5.1. Subthreshold intrinsic properties

A) *Table describing the subthreshold properties of CA1 PNs from NSun2$^{-/-}$ and NSun2$^{+/-}$ littermates. Red indicates a P value of <0.05 resulting from unpaired student t-tests.*
B) *Scatter graphs depicting data spread from experiments. Measurements include: RMP, τm, % sag, rebound and R_i. The wide horizontal line is the mean with the two shorter horizontal lines representing the SEM. * = p < 0.05.*

5.2.2. mAHP is not altered in NSun2$^{-/-}$ CA1 PNs

After completing the sub-threshold experiments, an after-hyperpolarisation experiment was conducted; a post-burst mAHP was obtained from cells with a brief application of x5 2nA current pulses, each pulse lasting for 2ms. The mAHP was measured as the peak amplitude relative to the resting membrane potential at 58ms after the last spike, as conducted by Park *et al*. (Park et al., 2010). The motivations for using Park's methodology allowed not only the analysis of the mAHP amplitude but was also utilised as an established method of DHPG-altered mAHP (as shown later in Figure 5.4E). No genotype effect was observed (*Figure 3E; unpaired two-tailed Student's T-Test; p = 0.415; n = 6 NSun2$^{+/-}$, n = 9 Nsun2$^{-/-}$*).

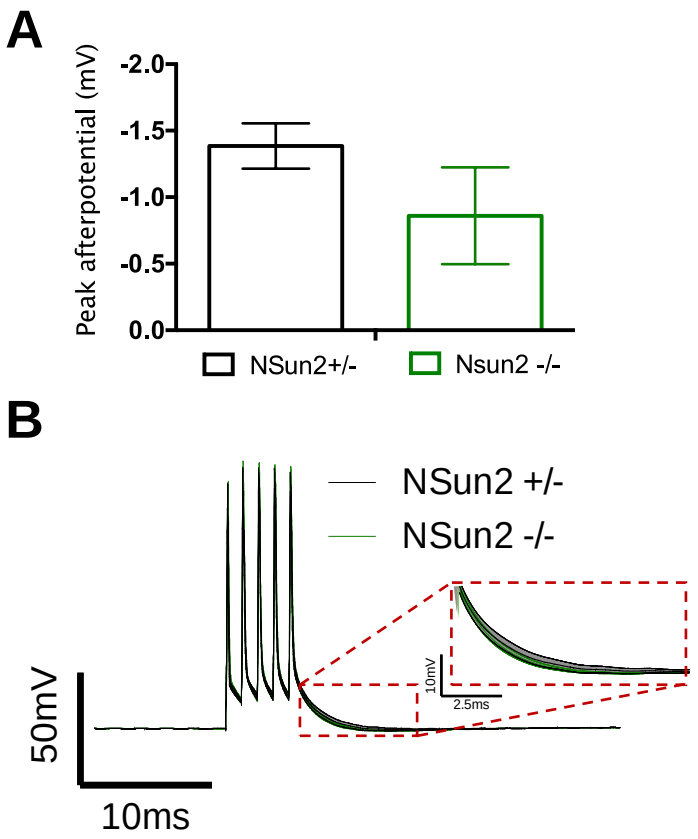

Figure 5.2. mAHP amplitude

A) *There was no genotype effect on post-burst mAHP (NSun2$^{+/-}$: -1.38mV ± 0.17, n = 6 (5), Nsun2$^{-/-}$: -0.86mV ± 0.36. n= 9 (7); unpaired two-tailed students' t-test, p = 0.415)*
B) *Averaged traces for post-burst after-hyperpolarisation with the SEM included. The red box on the trace highlights the region that the mAHP was analysed and the inset image represents the magnification of this region.*

5.2.3. Action potential waveform of NSun2$^{-/-}$ CA1 PNs

Analysing the action potential waveform can indicate possible defects of VG-channels. The action potential waveform was measured from the first spike of a train of spikes elicited from a 300pA square-wave current injection for 500ms with the membrane potential held at -70mV. Five measurements were analysed:

maximum rate of action potential rise, threshold for action potential, action potential peak amplitude and both decay and rise times of the spike (Figure 5.3A). There were no differences observed between genotypes (Figure 5.3A-B).

A

	Het (n=16)		NSun2-/- (n=14)		P
	Mean	SEM	Mean	SEM	
Max rate of rise (V.s-1)	331.0	18.4	324.5	26.6	0.8
Threshold (mv)	-45.3	1.2	-42.8	1.0	0.1
Peak amplitude (mV)	109.9	2.1	108.6	2.8	0.7
Rise time (ms)	4.0	0.01	4.0	0.01	0.4
Decay time (ms)	5.3	0.1	5.3	0.1	0.8

B

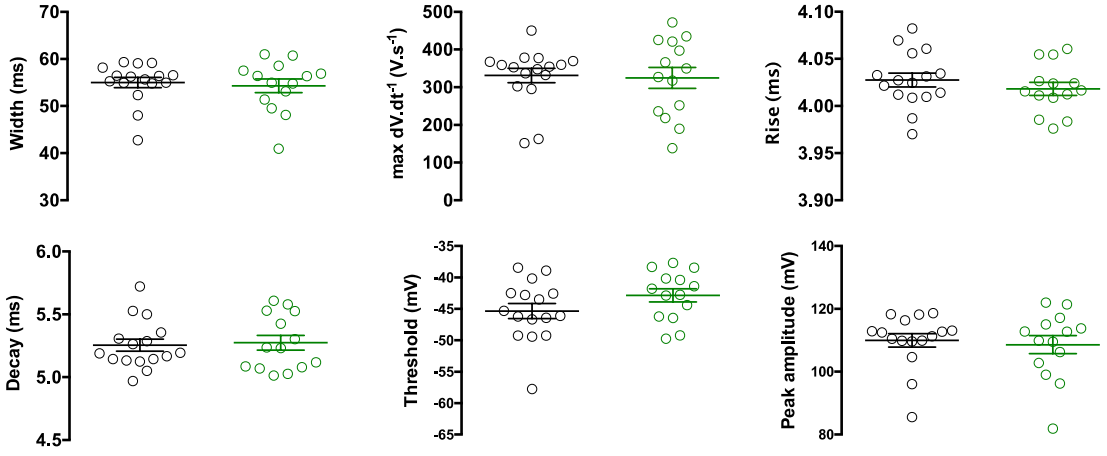

C

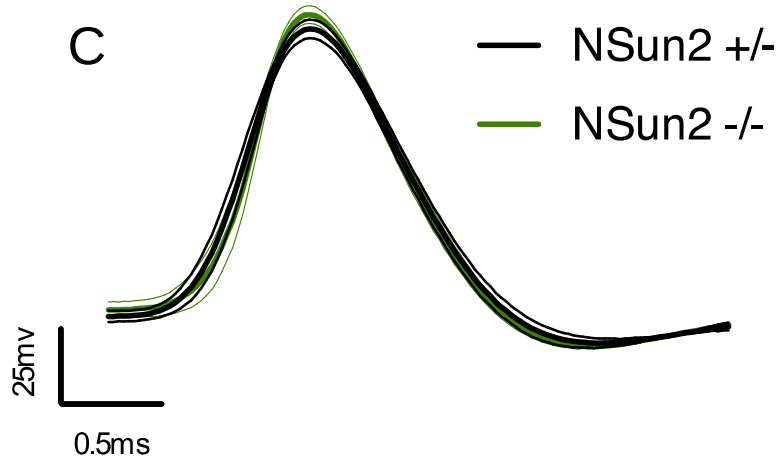

Figure 5.3. Action potential waveform analysis in NSun2$^{-/-}$ mice

A) *Table describing the action potential properties of CA1 PNs from NSun2$^{-/-}$ mice (n = 16 (11)) and their NSun2$^{+/-}$ littermates (n = 14 (13)). No genotype*

differences were found between the five characteristics as determined by unpaired student t-tests.
B) *Scatter graphs depicting spread of data from each experiment: maximum rate of action potential rise, threshold for action potential, action potential peak amplitude and both decay and rise times of the action potential. The wide horizontal line is the mean with the two shorter horizontal lines representing the SEM.*
C) *Action potential waveforms averaged from first spike elicited from 300pA current injection. Thick line represents the mean, the thin lines either side represent the SEM.*

5.2.4. Firing rate analysis of CA1 PNs in Nsun2$^{-/-}$ mice

CA1 PN firing patterns were observed by injecting a 500ms depolarising square-wave current injection at varying magnitudes; between 100pA and 400pA with 100pA intervals. The number of action potentials per 500ms period at the different current intensities were analysed for each cell and uncovered a propensity for NSun2$^{-/-}$ cells to fire more spikes. Therefore, the NSun2$^{-/-}$ CA1 PNs fire at a greater frequency (*Figure 5.4: Repeated-measures ANOVA; F = 6.86, p = 0.049; NSun2$^{+/-}$: n = 15 (11); NSun2$^{-/-}$: n = 15 (14)*).

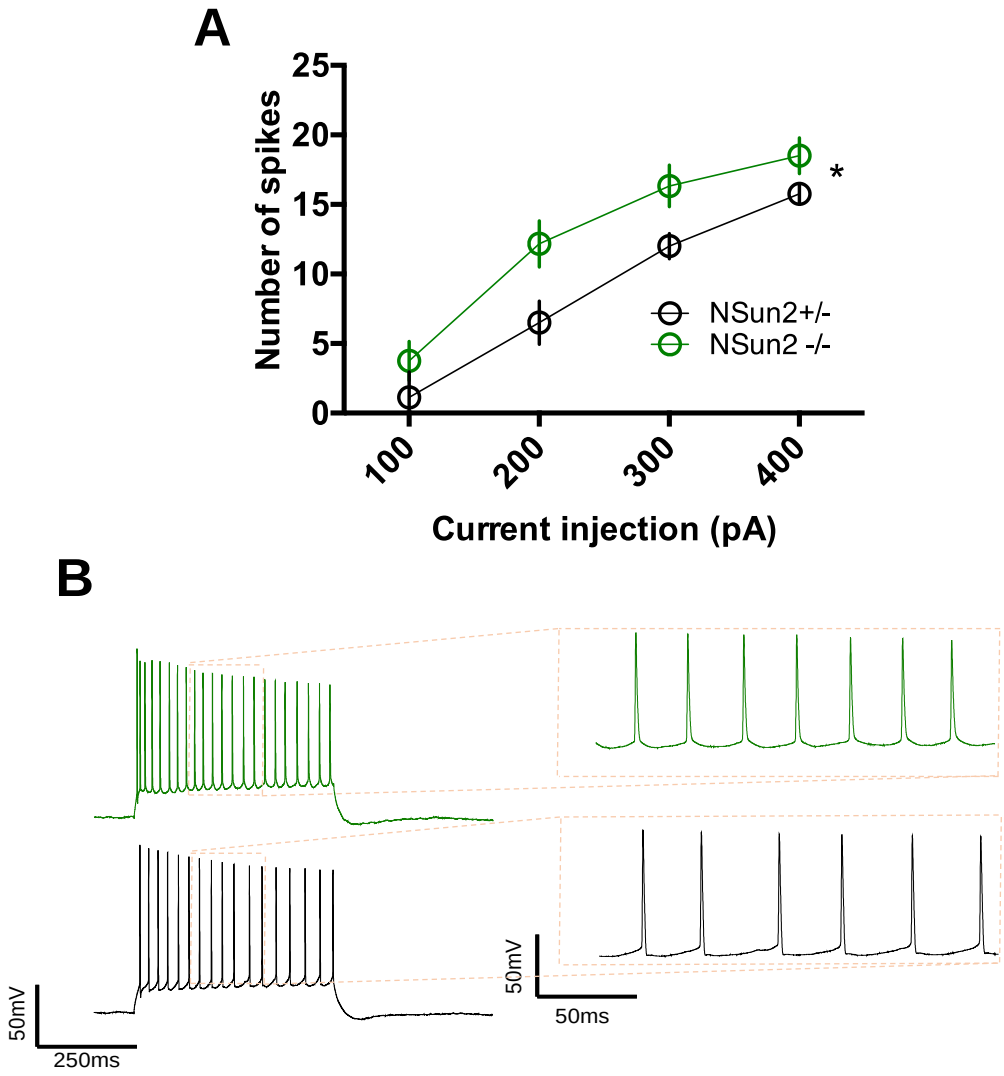

Figure 5.4. Action potential firing rate of NSun2$^{-/-}$ CA1 PNs

A) *Mean number of action potentials fired for each current injection (100-400pA) with SEM. (NSun2$^{+/-}$: 100pA: 1.636 ± 1.267, 200pA: 7.363 ± 1.267, 300pA: 13 ± 5.238, 400pA: 16.384 ± 1.291, n =15 (11); Nsun2$^{-/-}$: 100pA: 2.53 ± 0.76, 200pA: 10.47 ± 1.08, 300pA: 14.667 ± 1.11, 400pA: 16.974 ± 1.06, n=15 (14); Repeated Measures ANOVA: F = 6.856, P = 0.049).*
B) *Example traces of action potential firing in response to a 500ms 300pA current injection. The red box on the spiking trace highlights a region that is then magnified in inset image.*

5.2.5. Group 1 mGluR-modulated intrinsic properties

It has been documented that certain intrinsic factors are modulated with DHPG application and these factors are investigated here. These include: an increase in R_i (Ireland and Abraham, 2002; Tateno et al., 2004), instantaneous frequency (Shirasaki et al., 1994) and RMP (El-Hassar et al., 2011) and a decrease in action potential peak (Carlier et al., 2006) as well as a conversion of a post-burst hyperpolarisation to a depolarisation (Park et al., 2010).

After baseline measurements were achieved, 100µM DHPG was bath-applied and membrane potential recorded for 15 minutes. During this period of time the membrane voltage was not clamped allowing the membrane potential to fluctuate freely. Although the NSun2$^{-/-}$ CA1 PNs demonstrated a strong trend for less depolarisation compared to heterozygous neurons, this was deemed non-significant (*Figure 5.4A; two-tailed unpaired student's t-test; p = 0.051; NSun2$^{+/-}$:* 0.86mV ± 0.02*, n = 17; NSun2$^{-/-}$:* 0.92mV ± 0.02, *n = 11).* After a 15-minute recording of the membrane potential, several intrinsic properties were recorded and analysed as outlined above. The experiments exploring RMP response to DHPG were interleaved with experiments to determine the change in post-burst hyperpolarisation (Figure 5.5A). Similar to the other intrinsic properties, no significant DHPG-genotype effect was observed in the post-burst hyperpolarisation response to DHPG (*Figure 5.5E: NSun2$^{+/-}$: Baseline: -0.99mV ± 0.38, DHPG: 2.32mV ± 0.52, n = 6 (5); Nsun2$^{-/-}$: Baseline: -1.33mV ± 0.17, DHPG: 0.92mV ± 0.29, n = 6 (6); Repeated Measures ANOVA: F = 0.58, P = 0.458*).

Following either the RMP or post-burst hyperpolarisation experiments, intrinsic properties were again analysed in order to investigate how they may be influenced by DHPG and possible differences between the two mouse groups. These included measuring the change in instantaneous frequency of a train of spikes in response to a 300pA square-wave current injection after exposure to

100μM DHPG. No differences were observed (*Figure 5.5B: Repeated Measures ANOVA, F = 0.097, P = 0.759*). From the spike train elicited, the first action potential was isolated and its peak was analysed, again no significant differences between the two mouse groups were observed (*Figure 5.5C: NSun2$^{+/-}$: Baseline: 107.32mV ± 2.649, DHPG: 97.22mV ± 3.65, n =15 (11); Nsun2$^{-/-}$: Baseline: 108.72mV ± 2, DHPG: 99.98mV ± 2.4, n = 15 (14); Repeated Measures ANOVA: F = 0.187, P = 0.67*). Finally, a -100pA current was then injected into the neurons allowing the measurement of the R_i (see Materials and Methods). The genotype had no bearing on R_i in response to DHPG (*Figure 5.4D: NSun2$^{+/-}$: Baseline: 96.12MΩ ± 5.13, DHPG: 105.85MΩ ± 10.2, n = 13 (11); Nsun2$^{-/-}$: Baseline: 101.79MΩ ± 8.45, DHPG: 110.22MΩ ± 7.03. n = 13 (13); Repeated Measures ANOVA, F = 0.086, P = 0.773*).

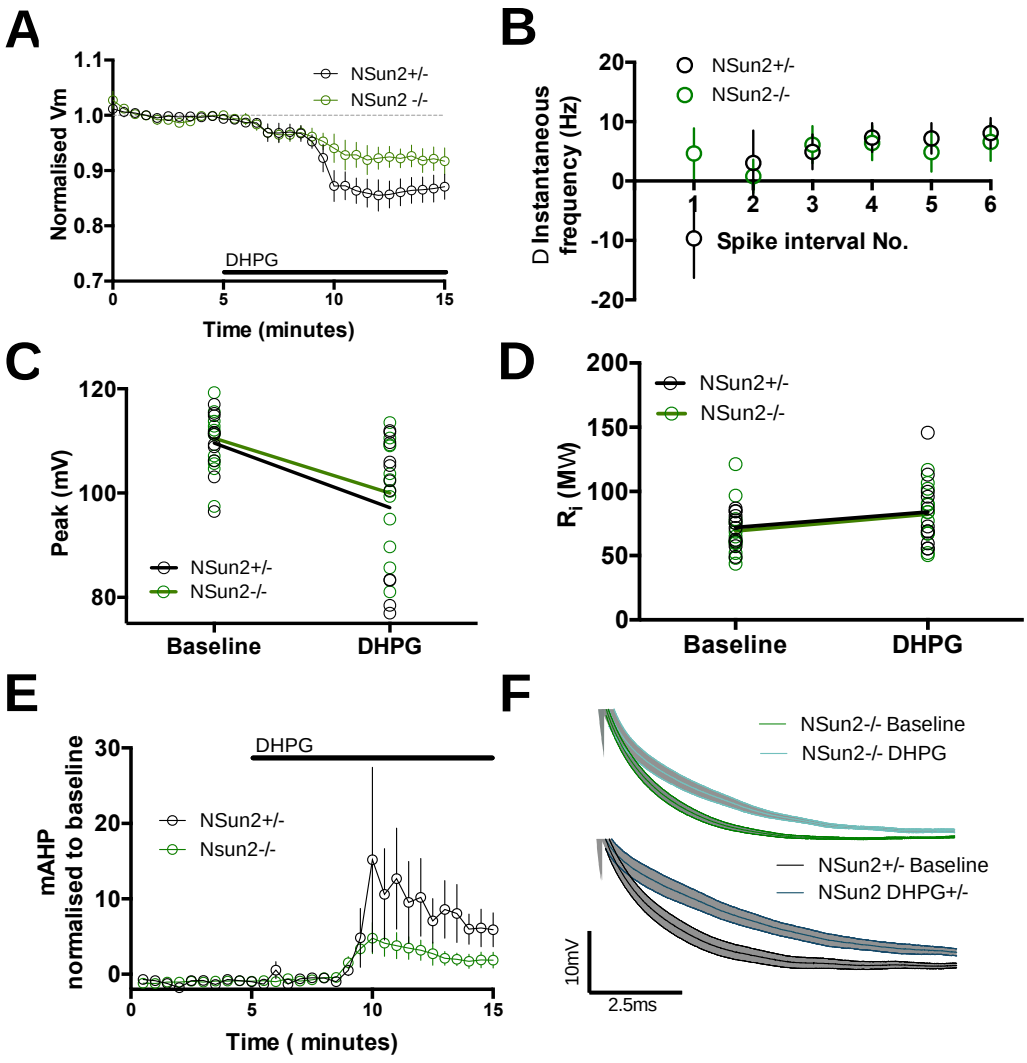

Figure 5.5. Intrinsic properties modulated by DHPG

A) *Resting membrane potential in response to 10-minute bath application of 100μM DHPG. No significant genotype effect was observed ($NSun2^{+/-}$: 0.86 mV ± 0.02, n = 17 (14); $NSun2^{-/-}$: 0.92 ± 0.02, n = 11 (10); unpaired two-tailed student's t-test: p = 0.051; n = 17 $NSun2^{+/-}$, n = 11 $Nsun2^{-/-}$).*
B) *The change in instantaneous frequency in response to 100μM DHPG plotted for each spike interval to a maximum of 6 intervals. ($NSun2^{+/-}$: interval 1 = 1.702Hz ± 6.819, interval 2 = 4.081 Hz ± 4.769. interval 3 = 7.89 Hz ± 3.41, interval 4 = 9.031 Hz ± 2.675, interval 5 = 8.032 Hz ± 2.6, interval 6 = 9.367 Hz ±*

2.457, n = 13; Nsun2$^{-/-}$: interval 1 = -11.46 Hz ± 12.84, interval 2 = 2.05 Hz ± 9.58, interval 3 = 3.887 Hz ± 6.87, interval 4 = 6.51 ± 5.04 Hz, interval 5 = 5.891 Hz ± 4.87, interval 6 = 7.144 Hz ± 5.031, n = 10; Repeated Measures ANOVA, F = 0.097, P = 0.759)
C) *Action potential peak height values of the first action potential from a 300pA square-wave current injection before and after 100μM DHPG bath application (NSun2$^{+/-}$: Baseline: 107.32mV ± 2.649, DHPG: 97.22mV ± 3.65, n =15 (11); Nsun2$^{-/-}$: Baseline: 108.72mV ± 2, DHPG: 99.98mV ± 2.4, n = 15 (14); Repeated Measures ANOVA: F = 0.187, P = 0.67)*
D) *Input resistance values calculated from a 500ms 100pA current injection before and after 100μM DHPG bath application (NSun2$^{+/-}$: Baseline: 96.12MΩ ± 5.13, DHPG: 105.85MΩ ± 10.2, n = 13 (11); Nsun2$^{-/-}$: Baseline: 101.79MΩ ± 8.45, DHPG: 110.22MΩ ± 7.03. n = 13 (13); Repeated Measures ANOVA, F = 0.086, P = 0.773)*
E) *Post-burst after-potentials before and after 100μM DHPG bath application (NSun2$^{+/-}$: Baseline: -0.99mV ± 0.38, DHPG: 2.32mV ± 0.52, n = 6 (5); Nsun2-/: Baseline: -1.33mV ± 0.17, DHPG: 0.92mV ± 0.29, n =6 (6); Repeated Measures ANOVA: F = 0.58, P = 0.458)*
F) *Averaged traces of post-burst after-hyperpolarisation conversion into an after-depolarisation. Grey area represents SEM.*

5.3. Discussion

In this chapter, data examining both subthreshold intrinsic properties and their DHPG-dependent plastic properties as well as the action potential waveform of NSun2$^{-/-}$ and *NSun2$^{+/-}$* CA1 PNs are presented. An often overlooked aspect of neural physiology, intrinsic modulation can have ramifications on synaptic plasticity and has been described as a metaplastic mechanism for learning and memory (Sehgal et al., 2013). The key findings were as follows: (i) CA1 PNs from NSun2$^{-/-}$ mice exhibit a faster membrane time constant, (ii) a reduction in spike accommodation/increase in spike frequency, (iii) no alterations to the action potential waveform and (iv) no changes to intrinsic properties modulated by mGluR activation were observed.

5.3.1. Membrane time constant is reduced in NSun2$^{-/-}$ mice

Five subthreshold intrinsic properties were investigated: RMP, τm, sag, rebound and R_i. They were acquired as described in chapter 2. Materials and Methods. R_i is closely related to the membrane resistance and has been described as the membrane resistance plus the electrode resistance (Barbour, 2014) and as current injections leading to a voltage drop across the electrode resistance (which should remain constant throughout an experiment) was compensated for with a bridge balance, any differences observed could be indicators of the ion channel density and those that are constitutively open. Sag and rebound can be an indirect indicator of density or activation of channels active at hyperpolarised potentials, such as HCN channels (Robinson and Siegelbaum, 2003); no statistically significant differences were observed in these properties although an extensive reduction in mAHP amplitude was observed in NSun2$^{-/-}$ mice (Figure 5.2A). Nor were significant differences found between *NSun2*$^{+/-}$ and NSun2$^{-/-}$ mice in RMP, however a significant difference was observed in the membrane time constant (Figure 5.1A), which reflects a combination of the resistance and capacitance of the cell ($\tau m = R_m * C_m$). The faster τm, could result from a range of morphological deviations, for example, a reduction in soma size, dendritic complexity, spine size, axon diameter or spine number. Previous morphological characterisation of cortical cells from NSun2$^{-/-}$ mice revealed a reduction in both spine number and soma size, no other morphology was investigated, nor were hippocampal neurons considered (Blanco *et al.*, 2014). If these features that were previously analysed also apply to hippocampal neurons, then it could explain the faster membrane time constant. However, extensive morphological characterisation of NSun2$^{-/-}$ hippocampal neurons is required such as a Sholl analysis to analyse dendritic complexity.

5.3.2 NSun2$^{-/-}$ CA1 PNs exhibit a reduction in SFA

As is the case for subthreshold intrinsic properties, the action potential wave form and spiking information is governed by ion channels. With the huge diversity of VG-ion channels per single neuron, commonly including several Na^+ and Ca^{2+} current components as well as up to five different K^+ current components (Bean, 2007), alterations to these channels such as their kinetics can be reflected in changes to the action potential waveform. For example, differences in the maximum rate of rise and action potential peak may vary depending on VG-Na^+ channel kinetics or density. The threshold for firing can also be influenced by Na^+ and K^+ conductance (Bean, 2007).

Measurements were taken from the first action potential in a spike train in response to a 500ms 300pA square-wave current injection, they included: threshold for action potential, max rate of rise, peak amplitude and rise and decay times. No changes to these properties were observed in NSun2$^{-/-}$ mice compared to *NSun2*$^{+/-}$ (Figure 5.3). From these current injections, spike accommodation, also known as SFA, can be investigated. SFA is a phenomena observed in many types of neurons which describes a reduction in the number of action potentials fired over the course of a constant current injection applied to the cell. The NSun2$^{-/-}$ CA1 PNs exhibit less SFA by consistently firing significantly more action potentials (Figure 5.4). There could be several reasons for this change. Firstly, the VG-Na^+ channels responsible for generating action potentials recover slowly after inactivation resulting from an action potential, and so for the subsequent spike, less VG-Na^+ channels will be available increasing the delay for the next spike. They are also responsible for the continuing decrease in action potential height through the course of the current injection (La Camera et al., 2006). The possibility of alterations to these channel types is made less likely because they also influence action potential height which remained unchanged between the two mouse groups (Figure 5.3). Secondly, the activity-dependent activation of the AHP current may be a root cause of the

deficit. VG-K^+ currents such as I_M are activated slowly during depolarisation and leading to a decrease in probability of spiking, and also the I_{AHP} current which is activated by the influx of Ca^{2+} at the peak of the action potential triggering the opening of Ca^{2+}-dependent K^+ channels (La Camera et al., 2006). These type of channels have been shown to be influenced by NMDA receptor activation in the medial prefrontal cortex and could be a consideration for this NSun2 mutant model (Faber, 2010). Thirdly, it is possible that HCN channels could alter spike pattern; if a neuron has a higher density or conductivity through HCN channels then the AHP may be enhanced and take an extended amount of time to recover to a membrane potential that is depolarised enough to fire another action potential. The mAHP amplitude was analysed in NSun2$^{-/-}$ mice (in Figure 5.2*)* with no significant decrease observed suggesting that this scenario may be unlikely. Finally, recent research has implicated ANO2 channels in hyperpolarisation of CA1 PNs with ANO2 knock-down animals exhibiting reduced SFA (Ha and Cheong, 2017). Although the implication of these channels have also been shown to influence the action potential waveform in CA1 PNs (Huang et al., 2012) which was not observed here (Figure 5.3).

It is not currently understood which contributing mechanism may be altered causing the decrease SFA in the NSun2$^{-/-}$ CA1 PNs. A more detailed analysis is required such as specific single-channel recordings of a channel of interest to scrutinise possible conductive differences or assays to quantify ion channel densities. Importantly, SFA has been correlated to behaviour; specifically fear conditioning with reports concluding a decrease in spike accommodation coinciding with the conditioning (Sehgal et al., 2014). For this reason, it would be of particular interest to investigate fear-conditioning in the NSun2$^{-/-}$ mice as current evidence may suggest deficits in this type of behavioural task.

5.3.3. No mGluR-dependent intrinsic modulation deficits were observed in NSun2$^{-/-}$ CA1 PNs

It has been established that pharmacological activation of Group I mGluRs with DHPG impacts intrinsic properties. Although there is a general acceptance that the alteration of these intrinsic properties causes a rise in neural excitability, any physiological relevance remains unknown. In order to understand if the initial mGluR-LTD deficit in NSun2$^{-/-}$ was influenced by differential intrinsic changes in response to DHPG, several characteristics were investigated.

Intrinsic properties known to be modulated in response to Group I mGluRs include: decreases in SFA due to a repression of the I_{AHP} (Gereau and Conn, 1995; Netzeband et al., 1997), a decrease in action potential peak due to a downregulation of VG-Na^+ responsible for the upstroke of a spike *(Carlier et al.*, 2006), a depolarisation of the RMP resulting from a suppression of intracellular Ca^{2+} release (El-Hassar et al., 2011), and finally a decrease in R_i (Ireland and Abraham, 2002) possible from the DHPG-induced closure of channels such as TRPC (El-Hassar et al., 2011). Alterations of these properties in NSun2$^{-/-}$ mice in response to DHPG could have provided useful mechanistic information regarding mGluR-LTD deficits. Nevertheless, no differences were found between NSun2$^{-/-}$ and *NSun2*$^{+/-}$ mice suggesting there are no differential effects of chemical mGluR activation on intrinsic properties in CA1 PNs.

5.4. Summary

Both subthreshold intrinsic properties and action potential waveform measurements were investigated as well as mGluR-modulating intrinsic properties in CA1 PNs of NSun2$^{-/-}$ mice. Only two significant alterations were found; a reduction in SFA and an increase in the membrane time constant. The former could be caused by alterations to a multitude of different channels and

requires further electrophysiological experimentation to identify the possible channels. The latter discrepancy necessitates detailed morphological analysis of CA1PNs from NSun2$^{-/-}$ mice to classify distinct regions and parameters affected within the neuron.

Chapter 6. Results: Localisation of NSun2 and its spatial relationship with FMRP in PC12 cells

6.1. Introduction

Understanding the subcellular localisation of proteins can yield useful information which provides an essential step towards appreciating their functions. Preliminary research from Hussain and Bashir (2015) presented NSun2 immunohistochemistry data from neurons differentiated in culture from human foetal brain-derived neural stem cells which showed localisation of NSun2 within dendritic locations. As previous relevant research had looked at the cellular location of NSun2 only in cultured non-neuronal cells, where it localises to the nucleus as well as the cytoplasm (Hussain et al., 2009; Sakita-Suto et al., 2007; Yang et al., 2017), this novel finding was of considerable interest, especially given the neurological phenotype of human patients with mutations in NSun2.

The current assumption of NSun2's function is that it likely controls translation both spatially and temporally (Blanco *et al.*, 2014; Hussain *et al.*, 2013), although further research is required to understand how NSun2-mediated methylation exerts this control and the physiological outcome. A recent finding has highlighted a nuclear function (Yang et al., 2017); NSun2-mediated methylation can be detected by mRNA-adapter proteins to promote export of mRNA from the nucleus to the cytoplasm. The transport of RNA is a necessary process for all cell types but is further emphasised in neuronal cells due to their highly polarised structure that requires translational machinery at synapses for vital cellular processes including plasticity (Bramham and Wells, 2007).

The results described in this chapter utilised an immunohistochemistry methodology to identify the proportion of NSun2 localisation within pre-defined regions (such as the nucleus, soma and neurites) of PC12 cells, which is a robustly cultured cell line originally derived from the neural crest lineage. The regional expression levels are also compared to FMRP, a protein that, as previously discussed, may have some similar functional properties to NSun2. The immunohistochemistry-detected colocalisation of the two proteins initially identified by Hussain and Bashir (2015) are investigated in this chapter using a more objective form of analysis, i.e. via employment of Pearson's correlation rather than counting fluorescent puncta to aid in the elimination of human bias and increase accuracy.

Both NSun2 and FMRP are regulated by other proteins such as the Aurora B Kinase which phosphorylates NSun2 (Sakita-Suto et al., 2007) and PP2A that dephosphorylates FMRP (Narayanan et al., 2008, 2007). How the phosphorylation status of the proteins in question influences their localisation as well as their colocalisation with each other is currently unknown; this would be intriguing to investigate, particularly since phosphorylation/dephosphorylation cascades are known to be prominent in neuritic/dendritic locations (Crino et al., 1998; Heise et al., 2014; Urbanska et al., 2017) and are modulated by external factors, i.e. experience. This chapter explores the possibility of whether phosphorylation/dephosphorylation events might regulate the co-localisation of NSun2 and FMRP, through the use of the relevant chemical compounds ZM447439 and Okadaic Acid. The translation inhibitor, 4EGFI-1 was also used to investigate whether neuritic colocalisation of FMRP and NSun2 was translation-dependent. The last section of this chapter very briefly touches upon the vtRNA, a methylation target of NSun2 (Hussain et al. 2013), focussing on how its methylation status may affect its subcellular localisation in PC12 cells. Investigation of this previously reported NSun2 target would be of some

relevance to the current studies, as these vtRNAs along with associated proteins are known to undergo neuritic transport (Li et al., 1999).

The ZM447439 compound has previously been shown to constrain Aurora B activity (Sakita-Suto et al., 2007), a kinase that can positively affect NSun2s' methylase activity and its association with other proteins, such as NPM-1 (Sakita-Suto et al., 2007). Okadaic Acid is a PP2A inhibitor; PP2A is a phosphatase that targets FMRP, thus removing a phosphate group from the protein. PP2A's activity on FMRP can be enhanced by mGluR activation leading to alterations of FMRPs capacity to bind to mRNAs (Narayanan et al., 2007). 4EGI-1 on the other hand does not directly impact phosphorylation levels, it is known to be an inhibitor of cap-dependent translation by preventing the formation of the eIF4 complex (Descamps et al., 2012). FMRP can form a complex by binding with Cytoplasmic FMR1-interacting protein 1 (CYFIP1) which then sequesters eIF4E which inhibits cap-dependent translation (Majumder et al., 2016; Napoli et al., 2008). There is evidence supporting the notion that NSun2 targets mRNAs encoding proteins that affect the eIF4E complex, for example mTOR (Hussain and Bashir, 2015); a known phosphatase of 4E binding proteins (Hay and Sonenberg, 2004), mTOR upregulates cap-dependent translation by releasing translational repression. The initiation of mRNA translation can be disrupted by subjecting cells to 4EGI-1, a compound that prevents eIF4E binding to EIF4G, a vital step required for translation (Majumder et al., 2017; Santini et al., 2017). Although a rather large leap in supposition, exposing cells to 4EGI-1 may be comparable to cells lacking NSun2; the lack of NSun2 may lead to reduced levels of mTOR through a reduction of mTOR mRNA methylation causing a decline in phosphorylation of 4E-BPs decreasing translational activity.

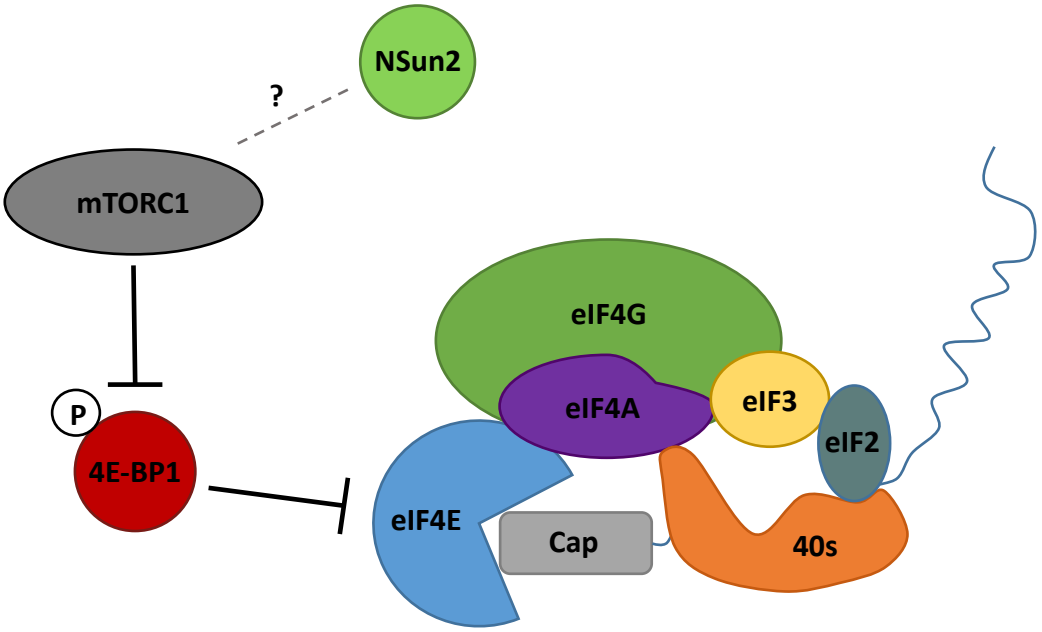

Figure 6.1. Initiation translation complex 4F and possible regulation by NSun2

A simplified schematic illustration depicting the initiation translation complex. The availability of eIF4E, the RNA helicase, eIF4A, as well as the scaffolding protein eIF4G are essential for the formation of the eukaryotic initiation complex 4F (Kosciuczuk et al., 2017). eIF4G interacts with eIF4E which binds directly to the mRNA 5'-cap and is vital for recruitment of the small ribosomal subunit (40s) (Aitken and Lorsch, 2012). The mTOR pathway is a key regulator of eIF4E; mTORC1 is a kinase that targets the substrate 4E-BP1, a translational repressor. If mTORC1 were to be negatively affected then inhibition on translation is increased (Raught et al., 2004). As an RNA methylation target of Nsun2 (Hussain and Bashir, 2015), mTOR protein expression may be affected in the absence of NSun2. If this were the case then it is possible that mTORC1 levels are reduced in NSun2$^{-/-}$ mice and may contribute to the global reduction of translation previously observed (Blanco et al., 2014).

6.2. Results

6.2.1. Localisation of NSun2 and FMRP

Immunohistochemistry was used on a PC12 cell model differentiated into NGF-induced neural-type cells in order to identify where the proteins, NSun2 and FMRP, localise. Pre-defined regions of the cell were determined: nucleus, soma and neurite, and the protein localisation is reported as the proportion of each protein within each region. In the nucleus, fluorescence of NSun2 was greater than FMRP (*Figure 6.2*: *NSun2: 26.95% ± 1.98, n = 17; FMRP: 19.61% ± 2.6, n =17: two-tailed unpaired student's t-test: p = 0.012*). Similar fluorescent levels of NSun2 and FMRP were found in the soma and neurites (*Figure 6.2: NSun2 soma: 60.16% ± 2.56, n =17; FMRP soma: 64.44% ± 2.75, n =17, two-tailed unpaired student's t-test: p = 0.27; Nsun2 neurite: 12.89 ± 1.69, n = 17; FMRP neurite: 15.95 ± 1.93, two-tailed unpaired student's t-test: p = 0.68*).

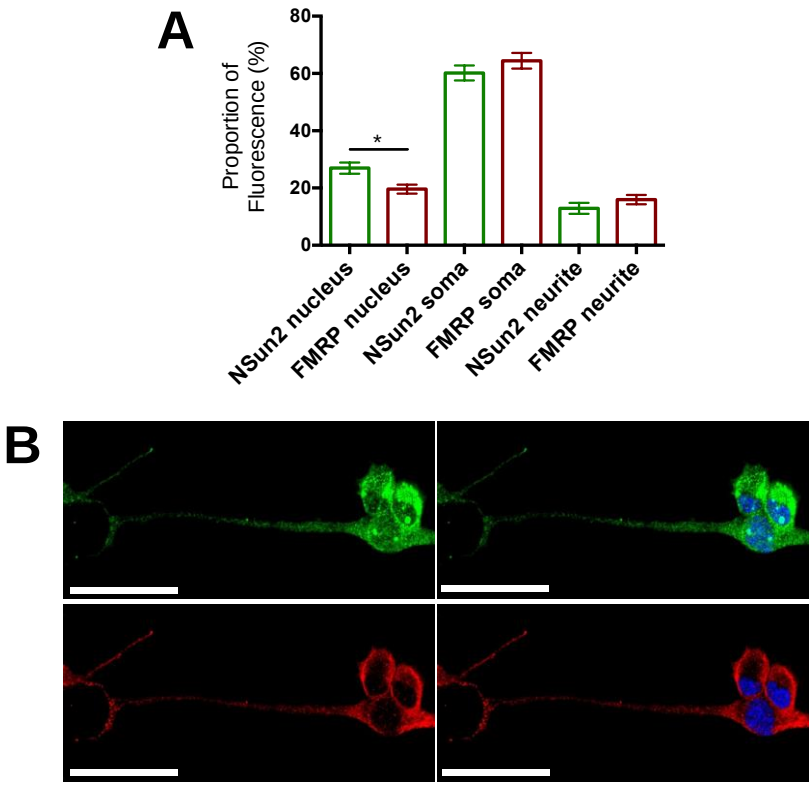

Figure 6.2. NSun2 localises primarily in the cell body, with a greater proportion localising to the nucleus relative to FMRP

A) *Both NSun2 and FMRP are similarly distributed throughout PC12 cells with the exception of the nucleus where NSun2 has a higher proportion of protein (Nucleus: NSun2: 26.95% ± 1.98, n = 17; FMRP: 19.61% ± 2.6, n = 17, two-tailed unpaired student's t-test: p = 0.012; Soma: NSun2: 60.16% ± 2.56, n =17; FMRP: 64.44% ± 2.75, n =17, two-tailed unpaired student's t-test: p = 0.27; Neurite: Nsun2: 12.89% ± 1.69, n = 17, FMRP: 15.95% ± 1.93, n = 17, two-tailed unpaired student's t-test: p = 0.68)*
B) *Representative confocal images. NSun2 = green, FMRP = red, Dapi = blue. Scale bars = 25μm.*

6.2.2. Influence of phosphatase activity on NSun2 and FMRP localisation

The dynamic addition and removal of phosphate groups to proteins is integral for numerous aspects of cell physiology and provides a layer of control for many

complex intracellular cascades, such as those involved in both LTP and LTD (Lee, 2006; Lee et al., 2003; Pi and Lisman, 2008). In order to investigate if phosphorylation may influence NSun2 and FMRPs sub-cellular localisation two compounds were tested (ZM447439 (20nM), Okadaic Acid (1μM)) that have been shown to influence the proteins' phosphorylation status. The third and final compound probed was 4EGI-1 (100μM) that affects cap-dependent translation.

For this experiment, the pre-defined regions remained the same as beforehand (soma, nucleus, neurite) and fluorescent levels were analysed from images captured via confocal microscope. None of the three treatments altered NSun2 localisation throughout the cell, however, FMRP localisation was significantly increased in the neurites and decreased in the soma in response to Okadaic acid treatment (Figure 6.3F).

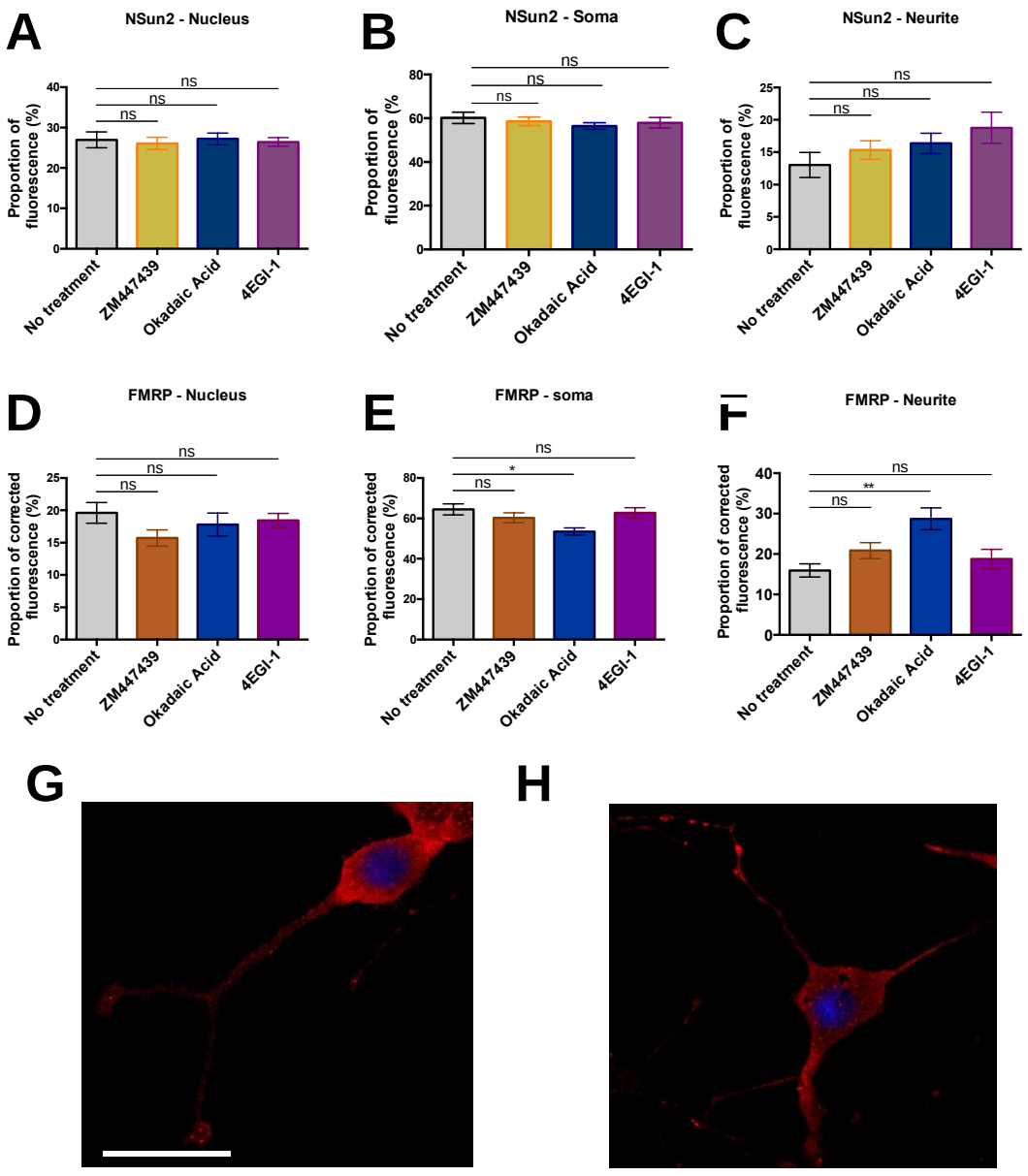

Figure 6.3. Influence of phosphorylation on NSun2 and FMRP localisation

A) *NSun2 localisation in nucleus does not change with treatments (No treatment: 26.95% ± 1.98, n = 17; ZM447439: 26.08% ± 1.49, n =16; Okadaic Acid: 27.2% ± 1.46, n = 10; 4EGI-1 = 25.43% ± 1.01, n = 13; Mann-Whitney U tests: ZM447439: p = 0.65, Okadaic Acid: p = 0.80, 4EGI-1: p = 0.78)*
B) *NSun2 localisation in soma does not change with treatments (No treatment = 60.16 ± 2.59, n = 17; ZM447439 = 58.58% ± 1.97, n =16; Okadaic Acid =*

56.43% ± 1.51, n = 10; 4EGI-1 = 56.86% ± 2.39, n = 13; Mann-Whitney U tests: ZM447439: p = 0.61, Okadaic Acid: p = 0.20, 4EGI-1: p = 0.54)
***C)** NSun2 localisation in neurite does not change with treatments (No treatment = 12.89% ± 1.69, n = 17; ZM447439 = 15.34% ± 1.43, n =16; Okadaic Acid = 16.37% ± 1.57%, n = 10; 4EGI-1 = 17.71% ± 2.41, n = 13; Mann-Whitney U tests: ZM447439: P = 0.19, Okadaic Acid: p = 0.17, 4EGI-1: P = 0.10)*
***D)** FMRP localisation in nucleus does not change with treatments (No treatment = 19.61% ± 1.59, n = 17; ZM447439 = 15.72% ± 1.25, n =16; Okadaic Acid = 17.79% ± 1.79, n = 8; 4EGI-1 = 18.44% ± 1.09, n = 13; Mann-Whitney U tests: ZM447439: P = 0.07, Okadaic Acid: p = 0.43, 4EGI-1: p = 0.64)*
***E)** FMRP localisation in soma is decreased with Okadaic Acid (means: no treatment = 64.44% ± 2.73, n = 17; ZM447439 = 60.27% ± 2.4, n =16; Okadaic Acid = 53.48% ± 1.79, n = 8; 4EGI-1 = 62.79% ± 2.51, n = 13; Mann-Whitney U tests: ZM447439: p = 0.35, Okadaic Acid: p = 0.02, 4EGI-1: p = 0.80)*
***F)** FMRP localisation in neurite is increased with Okadaic Acid treatment (means: no treatment = 15.95% ± 1.63, n = 17; ZM447439 = 24.01% ± 2.61, n =16; Okadaic Acid = 28.73% ± 2.71, n = 8; 4EGI-1 = 18.77% ± 2.4, n = 13; Mann-Whitney U tests: ZM447439: p = 0.1, Okadaic Acid: p = 0.001, 4EGI-1: p = 0.44)*
***G)** Representative image of FMRP localisation in PC12 cell with no treatment. Scale bar = 25μm.*
***H)** Representative image of FMRP localisation in PC12 cell with Okadaic Acid. Scale bar = 25μm*

6.2.3. NSun2 and FMRP colocalise in PC12 cells

Using confocal microscopy, antibodies conjugated with different fluorescent molecules allowed the detection of NSun2 and FMRP to be distinguished during co-staining experiments. Application of the required excitation wavelengths to the imaged samples identified the location of distinct proteins, and overlap/colocalisation was calculated using Pearsons correlation (as detailed in Materials and Methods). NSun2 and FMRP colocalise in whole-cell measurements (*Figure 6.3: 0.7 +/- 0.02, n = 10*). A Costes significance test was used; this test scrambles blocks of pixels in the same image 100 times and determines whether the Pearsons correlation coefficient (PCC) observed from the original images is significantly greater than random overlap of two channels

(Costes et al., 2004). Every sample passed the Costes test. A negative control was also used to scrutinise the possibility of artificially inflated correlation values from microscope artefacts. The colocalisation between NSun2 and FMRP was significantly greater than the colocalisation of both NSun2 and Beta-actin and FMRP and Beta-Actin. In order to statistically compare the conditions, a Fisher's r-to-z transformation was used to normalise the PCC values (see Figure 6.4 legend).

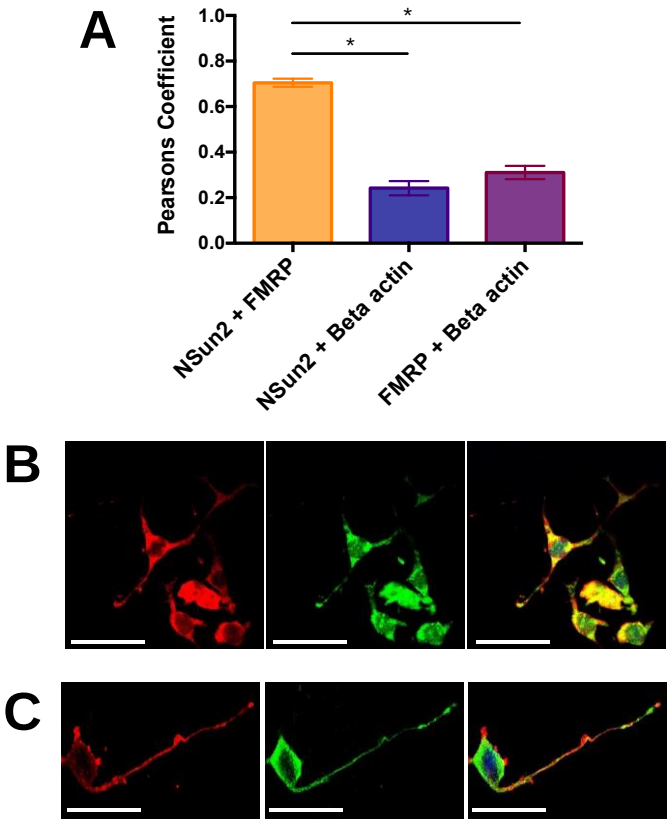

Figure 6.4. NSun2 and FMRP colocalise in whole cell measurement of PC12 cells

A) *Colocalisation using whole cell measurements (FMRP and NSun2: 0.7 ± 0.02, n = 17; NSun2 and Beta actin: mean: 0.24 ± 0.03, n = 17; FMRP and Beta actin: 0.31 ± 0.03, n = 17. Fisher's r-to-z transformation: FMRP and NSun2 vs Nsun2 and Beta actin, z = 1.65, p = 0.049, FMRP and NSun2 vs FMRP and Beta actin, z =1.64 p = 0.048)*
B) *Representative images. (Red = FMRP, green = NSun2, blue = Dapi. All scale bars = 25μm)*
C) *Representative images. (Red = Beta-actin, green = FMRP, blue = Dapi. All scale bars = 5μm)*

6.2.4. NSun2 and FMRP colocalisation is not affected by ZM447439, Okadaic Acid or 4EGFI-1

The compounds used in the preceding section (ZM447439, Okadaic Acid or 4EGFI-1) were next used to investigate the possibility of their influence on NSun2 and FMRP colocalisation. None of the three treatments influenced the colocalisation of NSun2 and FMRP (Figure 6.5).

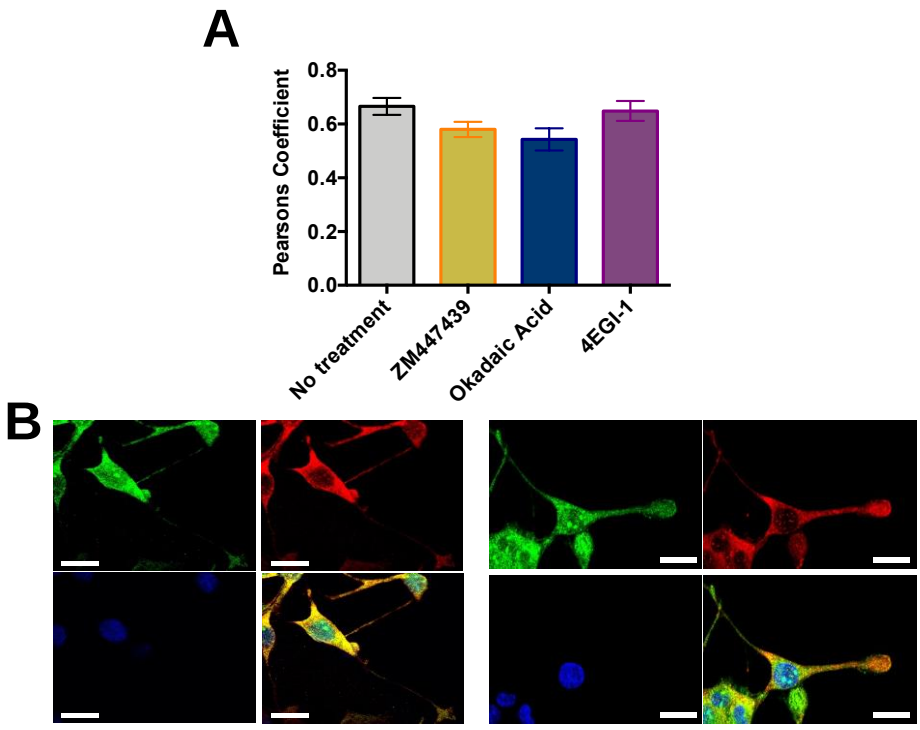

Figure 6.5. ZM447439, Okadaic Acid and 4EGFI-1 do not influence Nsun2 and FMRP colocalisation

A) *None of the treatments induced changes to NSun2 and FMRP colocalisation within the entire cell. Left: (No treatment = 0.67 ± 0.031, n = 16; ZM447439 = 0.58 ± 0.03, n =22, Fisher's r-to-z transformation: P = 0.19; Okadaic Acid = 0.54 ± 0.01, n = 17, Fisher's r-to-z transformation: P = 0.2; 4EGFI-1 = 0.65 ± 0.04, n = 20, Fisher's r-to-z transformation: P = 0.32).*

B) *Left: Representative images without any treatments. (Red = FMRP, green = NSun2, blue = Dapi. Bottom-right image is overlay of all channels. Scale bars for all images = 25μm). Right: Representative images with Okadaic Acid treatment. (Red = FMRP, green = NSun2, blue = Dapi. Bottom-right image is overlay of all channels. Scale bars for all images = 25μm).*

6.2.5. vault RNA does not differentially localise to cellular regions dependent on its methylation status.

Previous work had shown that NSun2 methylates position C69 of the Vault RNA (Hussain et al. 2013) (see Figure 6.6A). An *in vitro*-synthesised constitutive C69-methylated form of the vault RNA was thus generated, along with a mutant C69 form unable to undergo methylation. Fluorophore-conjugated methylated and unmethylated vtRNA oligonucleotides were transfected into PC12 cells and analysed as the soma-neurite ratio of RNA puncta per μm^2. The two forms of transfected vtRNA seemingly localise in a similar proportion throughout the cell with a higher percentage found in cell body regions (*Figure 6.6A: methylated = 2.28 ± 0.4, n = 11; unmethylated = 1.91 ± 0.32, n = 9; unpaired two-tailed student's t-test, p = 0.5*). These findings suggest that, within this PC12 system, methylation status of the Vault RNA does not affect its cellular localisation.

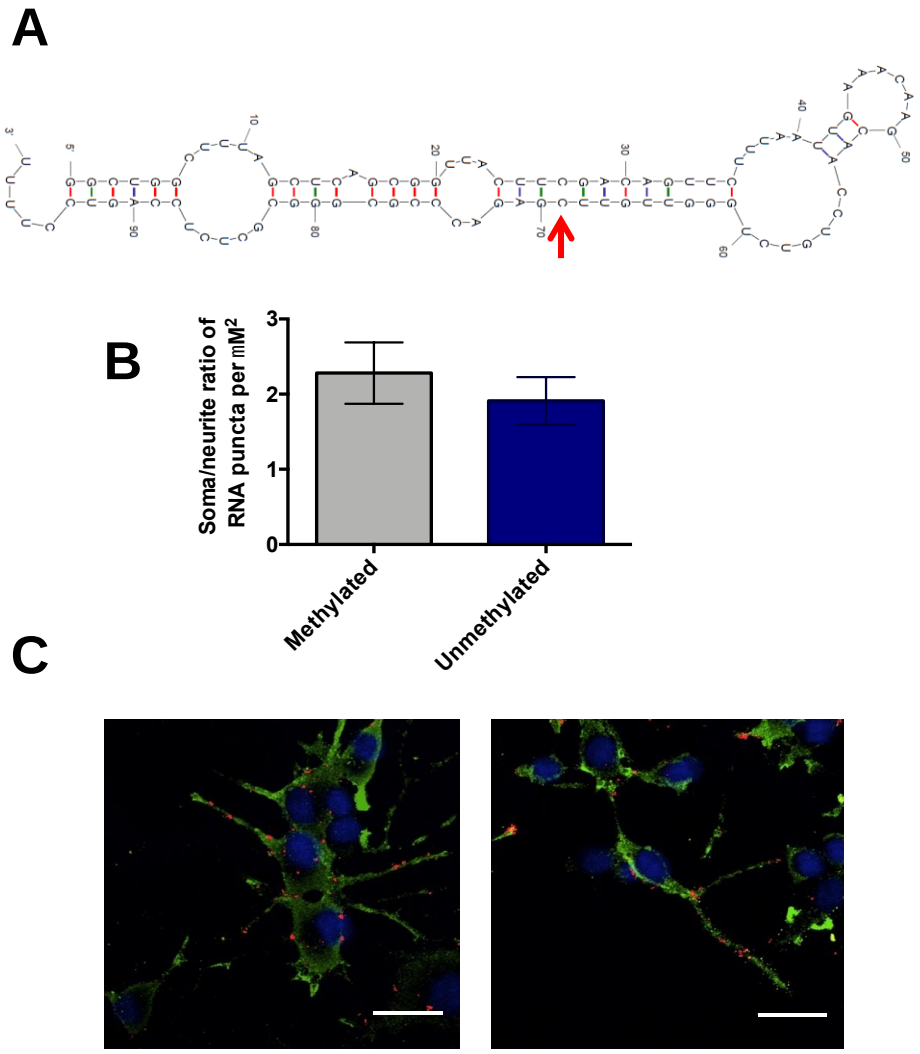

Figure 6.6. Methylated and unmethylated vtRNA do not differentially localise to cellular compartments in PC12 cell

A) *Prediction of vtRNA secondary structure using the M-fold programme. The previously reported cytosine which NSun2 targets for m5C methylation is indicated with a red arrow. The C69 mutant unmethylated vtRNA oligonucleotide had a mutation introduced at cytosine 69 to prevent methylation occurring within cells. The C69 methylated vtRNA instead contained an m5C methyl group conjugated to the corresponding cytosine position.*
B) *Ratio of soma/neurite puncta per μm^2 for both the methylated and unmethylated version of the vtRNA. No significant differences were found*

(methylated: 2.28 ± 0.4, n = 11; unmethylated: 1.91 ± 0.32, n = 9; unpaired two-tailed student's t-test, p = 0.5).
C) *Representative images. Left: PC12 transfected with C69 methylated vtRNA (Green = MAPT, blue = DAPI, red puncta = C69 methylated vtRNA. Scale bar = 20μm). Right: PC12 transfected with unmethylated C69 mutant vtRNA (Green = MAPT, blue = DAPI, red puncta = unmethylated C69 mutant vtRNA. Scale bar = 20μm).*

6.3. Discussion

The data presented in this chapter describe the localisation of NSun2 and FMRP to selected cellular compartments of PC12 cells differentiated into neuronal-type cells and investigates how these are affected by the application of compounds that alter phosphorylation and translation. Data is also presented demonstrating the relatively high colocalisation of NSun2 and FMRP and the influence of the same compounds on the spatial relationship of these two proteins. The main findings are as follows: (i) Both NSun2 and FMRP have similar relative levels of expression throughout the pre-determined cellular locations with the majority of expression being in the soma, followed by the nucleus and then the neurites. However, NSun2 differs from FMRP with higher localisation in the nucleus. (ii) ZM447439, Okadaic Acid and 4EGI-1 do not influence NSun2 localisation but Okadaic Acid increases localisation of FMRP to the neurites. (iii) NSun2 and FMRP colocalisation is not affected by any of the compounds used. (iv) Exogenous vtRNA does not differentially localise depending on its methylation status.

6.3.1. PC12 cells as a molecular model

PC12 cell cultures provide a model of study for molecular localisation. The cell line is a monoclonal population, with a robustness and reliability with the capability to efficiently differentiate with NGF. However, extracting a physiological relevance is problematic as they do not behave as a mammalian

neuron would. For example, PC12 cells do not release glutamate in response to DHPG (Li et al., 2003) and these cells are therefore lacking vital physiological machinery. These neural-type cells also do not form connections with each other preventing any network activity. The advantage of PC12 cells over other cell lines is that they are robust with a high survival rate and relatively low maintenance. They also only form neuronal-like cells with the application of NGF rather than other non-neural type cells (Belliveau et al., 2006).

6.3.2. The localisation and colocalisation of Nsun2 and FMRP

Immunohistochemistry was used on PC12 cells to identify where the proteins, NSun2 and FMRP, localise. The analysis was conducted on pre-defined regions of the cell: the nucleus, soma and neurite. A greater proportion of NSun2 fluorescence was observed in the nucleus than FMRP which is unsurprising as NSun2 has been previously described as a nuclear protein on several occasions (Sakita-Suto et al., 2007; Hussain et al*.*, 2013; Yang et a*l.*, 2017). However, these findings also indicate that although substantial levels of NSun2 reside in the nucleus, even higher expression levels were found in the soma and a significant, albeit lower expression in PC12 neurites were found.

Preliminary experiments from Hussain and Bashir (2015) illustrated the potential link between NSun2 and FMRP, notably the large overlap of postsynaptic mRNA targets, several of which are involved in AMPA receptor trafficking and synaptic plasticity. The results defined in this chapter support those previous findings in neurons produced in culture from human foetal brain-derived neural stem cells. Though, it is important to state that no information regarding functionality or interaction of proteins can be assimilated; spatial overlap of proteins could be insignificant in the context of understanding a functional relationship between NSun2 and FMRP. On the other hand, it is possible that the large number of RNA targets shared between the two proteins could be the foremost cause for their close proximity observed in this investigation.

6.3.3. Okadaic Acid increases FMRP localisation to neurites but has no effect on NSun2 and FMRP colocalisation

Phosphorylation provides an additional layer of control over proteins altering their functionality and localisation within a cell with direct links made between efficacy of synaptic plasticity and the phosphorylation status of various molecules (Li et al., 2016; Pi and Lisman, 2008). In this chapter efforts were made to understand whether compounds influencing phosphorylation of FMRP or NSun2 affected where the respective proteins localise within subcellular compartments and whether phosphorylation state changes their colocalisation.

Two compounds were applied to PC12 cells to inhibit phosphatases known to modulate either NSun2 or FMRP activity. ZM447439 is a compound that has been shown to inhibit Aurora B activity (Sakita-Suto *et al.*, 2007), a kinase involved in the regulation of NSun2 activity that has previously been shown to command phosphorylation activity in PC12 cells (Carpinelli et al., 2007). Not only is NSun2s' methylase activity supressed with Aurora B inhibition but it also induces association of NSun2 with the nuclear protein, NPM-1 (Sakita-Suto *et al.*, 2007). This change in association could suggest an increase in nuclear localisation of the protein however the nuclear fluorescence values did not significantly change across all three cellular regions (Figure 6.3). As expected, the cellular localisation of FMRP was also not influenced by the application of ZM447439.

FMRP is another protein influenced by phosphorylation. Previous research from Narayanan *et al.* (2007) revealed how activity-dependent changes alter the phosphorylation status of FMRP bi-directionally. They established an increase in FMRP dephosphorylation due to greater PP2A enzymatic activity within the first minute of mGluR activation. An increase in re-phosphorylation of FMRP was then observed due to mTOR-mediated suppression of PP2A within 1-5 minutes

of mGluR activation. Evidence proposes phosphorylation of FMRP permits the protein to bind to mRNAs undergoing translation to halt the ribosome and repress translation, its predominant function (Darnell and Klann, 2013).

To examine how phosphorylation may alter the localisation of FMRP the PP2A inhibitor, Okadaic Acid, was applied to PC12 cells. This treatment ought to increase the phosphorylation levels of FMRP, however as was the case with ZM447439, phosphorylation levels were not verified and this highlights a caveat of this methodology. The assumed increase in FMRP phosphorylation significantly decreased its localisation to the soma and increased its localisation to the neurites of the cell with fluorescence levels in the nucleus unchanged. The cause of these changes are unknown but it could consequently lead to an increase in intracellular efficiency; only phosphorylated FMRP seems to have an active role at synaptic regions (Nalavadi et al., 2012) and therefore FMRP may only be required in these regions when phosphorylated.

As explained previously, the colocalisation observed between FMRP and NSun2 (Figure 6.4) could be caused by the dozens of shared mRNA targets. Due to existing evidence supporting phosphatase-state dependent control of both FMRP and NSun2 functionality (Ceman et al., 2003; Coffee et al., 2012; Sakita-Suto et al., 2007) as well as being a key regulator of synaptic plasticity (Pi and Lisman, 2008), this chapter investigated whether influencing this layer of control pharmacologically affects the colocalisation of the proteins. Similar to the protein localisation analysis, there was no significant alteration in FMRP-NSun2 colocalisation. This is fairly unsurprising as the two proteins seem to inhabit fairly similar locations irrespective of phosphorylation alteration.

6.3.4. Reducing translation does not affect NSun2 and FMRP colocalisation or sub-cellular localisation

As well as exploring phosphorylation-dependent colocalisation, the modification of cap-dependent translation was also investigated via the application of the 4E-BP inhibitor, 4EGI-1. Previous research studying a FXS mouse model revealed that 4EGI-1 normalised the two commonly reported deficits, a reversal in exaggerated mGluR-LTD and rescue of aberrant actin dynamics, providing a mechanism that could be targeted for future therapeutic relief of patients with FXS (Santini et al., 2017). As previously elucidated, the addition of 4EGI-1 may have a similar consequence as the absence of NSun2, although this is purely conjecture. The results here indicate that reducing translation with 4EGI-1 did not influence either colocalisation of NSun2 and FMRP or where the proteins localise within the cell.

There could be multiple reasons for this, firstly, the 4EGI-1 treatment or methodology used may not have adequately interfered with the binding of EIF4E to EIF4G to prevent translation, however, this was not directly tested. Secondly, the relatively small sample size obtained combined with a low resolution confocal microscope may mean that small changes were not detectable via statistical analysis. Thirdly, molecular mechanisms may react and interact differently in the PC12 model used when compared to other widely used *ex vivo* animal models. Lastly, and arguably the most likely, inhibiting translation does not influence where FMRP and NSun2 localise or their colocalisation.

6.3.5. Exogenous vtRNA does not differentially localise in sub-cellular compartments

VtRNAs are something of an enigma; they were first described in 1986 by Kedersha and Rome as a component of RNP complexes known as vaults that are highly conserved among many species. With an unknown function, they

have been associated with chemotherapy resistance (Mossink et al., 2003) and later found to localise to neurite terminals (Slesina et al., 2006), although their means of transport allowing their localisation remains unknown. More recently it was uncovered that they may be a target of NSun2 (Hussain et al., 2013). This interaction could have implications for synaptic plasticity; Hussain *et al*. (2013) demonstrated how the processing of vault RNA1.1 into five svRNAs is heavily influenced by NSun2. In NSun2$^{-/-}$ human fibroblast cells, svRNA4 levels were radically increased which may lead to downregulation of CACNG7 and CACNG8 transcripts that encode TARP γ-7 and TARP γ-8, respectively.

TARP γ-8 are proteins that associate to AMPA receptors and are found exclusively in the hippocampus. A previous TARP γ-8 knock-out model exhibited mis-regulated AMPA receptor delivery to post synaptic membranes from intracellular pools. The model also showed a reduction in GluR2 subunit levels in CA1 PNs which altered Ca^{2+} permeability of the AMPA receptors and produced a deficit in both basal transmission and LTP (Rouach et al., 2005). It's fair to suggest that compared to the widely studied TARP γ-2, also known as Stargazin, TARP γ-8 has not received much attention since Rouach *et al's*. work (2005). TARP γ-8 could provide a link between NSun2 and correlates of memory such as synaptic plasticity.

In order to acquire preliminary data surrounding localisation of vtRNA1.1 dependent on its methylation status, PC12 cells were transfected with either an unmethylated or methylated version of the RNA (Figure 6.6) prior to fixation and visualisation. No differences could be discerned between the vtRNA types indicating that the methylation of vtRNA doesn't influence where it localises within subcellular compartments.

Examinations into vtRNA localisation in animal models has not been conducted, neither has its possible involvement in experience-dependent plasticity. Previous research indicates that vtRNA localises to neuronal terminals with unidentified

cargo (Suprenant, 2002) where synaptic changes required for learning and memory occur (Herrmann et al., 1999, 1996) and is also involved in interactions with mRNAs encoding proteins required for regular AMPA receptor trafficking and plasticity (Rouach *et al.*, 2005).

The PC12 model is a reductionist one and regulation of transport throughout a neuron should be investigated further in an animal model. Due to the limited understanding of vtRNA1.1 that includes a possible indirect link to AMPA receptor trafficking, further work should be undertaken to clarify the connection between the two. A knock-out mouse model has been investigated previously (Kickhoefer et al., 2001; Mossink et al., 2002) and *in vitro* electrophysiological studies may help uncover a possible role in synaptic plasticity. Another possibility could be to apply a plasticity-inducing stimulus to a brain slice prior to flash freezing and homogenisation to use for a northern blot assay to test the possibility of vtRNA levels and interactions in response to the plasticity-inducing stimulus.

6.3.6. Colocalisation analysis and limitations

Colocalisation can be defined as the spatial overlap of two probes, in this case the fluorescent molecules conjugated to the secondary antibody. The ability to quantitatively analyse colocalisation with appropriate software provides a more objective evaluation compared to the more subjective process of human visual interpretation of different coloured images. The subjective nature of analysing colocalisation via visual interpretation is much more open to human bias.

All images in this chapter were taken with the Zeiss LSM510 confocal microscope. This confocal microscope lacks “super-resolution” capabilities, and therein lies the first limitation of this data. A conventional confocal microscope is limited to a theoretical resolution of 200nm that could drop to between 400–600nm in practical scenarios due to a diffraction limit (possibly caused by lens

imperfection or misalignment) and as a result colocalisation could be over-estimated (Wu et al., 2012). Another significant limitation includes possible bleed-through artefacts which is a concern due to the fluorophores used. Both Alexa Fluor 488 and 555 were chosen because of the limited excitation lasers available (488nm and 543nm) however band-pass filters, 480–520nm and 535–590, should have aided in blocking the emission detected from the other fluorophore.

A PCC was used as a method for quantifying the colocalisation of FMRP and NSun2. The PCC outputs a value between 1 and -1; a value of 1 would indicate a perfect positive correlation whereby every pixel of fluorescence from one protein (from the conjugated antibodies) is in the same position as all pixels from the other protein. A value of -1 would indicate perfect negative correlation whereby there is a complete lack of overlap between the pixels. A Fisher's r-to-z transformation was used to test significance between two PCC values. The reason being that correlation is bounded (between -1 and 1) and therefore the data distribution is likely to be skewed especially when the correlation coefficient is larger. In essence, the transformation normalises the data allowing parametric statistical tests to be implemented (Fisher, 1915).

There are clear benefits of using a PCC over other methods, for example, the mean intensity of the image is subtracted from every pixel's intensity. This provides an analysis that is independent of both background (signal offset) and signal levels, therefore the analyst does not have to conduct any pre-processing which eliminates a large amount of user-bias and error (Dunn et al., 2011).

With regards to analysing protein localisation, there are notable caveats with the methodology employed. A more ideal situation for investigating the change in protein localisation would involve live-cell imaging where the compounds can be applied during recording allowing the analysis of paired-data. As is the case here, by analysing independent data the between-cell variability is combined

with the compound response variability, therefore any potential effects caused by these compounds may be required to be powerful in order to filter out the background (i.e. noise). This can result in false negative results. Also, there is a possibility that all of the compounds used might influence the ability for antibodies to bind to their respective proteins. This would affect the fluorescence levels observed and consequently these results might not suggest changes in FMRP localisation with Okadaic Acid, rather it might reflect the change in antibody binding to the protein. Another possibility is the concentrations used, as higher doses of the compounds may have been required to observe a significant effect. It is also impossible to infer if the concentrations used influenced phosphorylation of the proteins without using a Western Blot or similar assay for clarification.

It should be noted that a large caveat of this experimental design was that the 'No Treatment' control condition did not contain a suitable vehicle that, in this case, would have been ethanol. Therefore, any changes that were identified (i.e. okadaic acid altering FMRP localisation) could be a direct result of the ethanol used to dilute kinase inhibitor, rather than the inhibitor itself.

6.4. Summary

To summarise, a PC12 model was used to investigate cellular localisation of FMRP and NSun2. The proteins are similarly distributed throughout the cells and have a high level of colocalisation which does not seem to be influenced by phosphorylation status of either protein. The application of Okadaic acid increases neuritic FMRP localisation but has no impact on NSun2. Blocking protein synthesis also had no effect on the localisation or colocalisation of either protein. Finally, the methylation status of vtRNA1.1 does not influence its subcellular localisation.

Chapter 7. Final discussion and future work

The research presented in this thesis aimed to investigate the underlying neurological mechanisms that may contribute to the learning and memory discrepancies previously reported in patients with NSun2-deficiency syndromes. *Ex-vivo* electrophysiology methods utilising a murine NSun2-deficiency model revealed deficits in several physiological processes.

Chapter 3 demonstrated that the NSun2$^{-/-}$ mice exhibit enhanced synaptic basal transmission that is likely caused by post-synaptic, rather than pre-synaptic deficits (due to no change in the PPR). Two possible explanations were proposed. Firstly, it is possible that the increased number of cells observed in cortical neurons (Blanco et al., 2014) applies to the hippocampus and could contribute to the increase in transmission. To explore this idea, future experimentation using *in vitro* hippocampal slices, as used in this thesis, could prove useful. In the first instance, repeating the input-output experiments is necessary to validate the findings presented in chapter 3.1A. due to inability to reproduce the initial mGluR-LTD experiments (Figure 3.2.). If the input-output differences can be reproduced, then stimulation of the SC pathway whilst recording from CA1 PNs in a whole-cell voltage clamp configuration could be used. If basal transmission in NSun2$^{-/-}$ neurons is indistinguishable from the heterozygous controls then an increased number of hippocampal cells may be the cause, and cell quantification experiments could provide validation. If, however, the recordings reveal an enhanced EPSC in individual neurons responding to the SC stimulation, then mis-regulation of postsynaptic AMPA receptors may be the cause. Immunohistochemistry assays investigating surface densities or electrophysiology experiments to analyse unitary conductance of AMPA receptors may provide a possible answer. Another beneficial avenue to evaluate could be the excessive activation of apoptotic pathways in the NSun2$^{-/-}$ mouse; other research reported an increase in basal synaptic transmission caused by high stress levels in the rat (Kamal et al.,

2008). For this reason, it would be of interest to inhibit stress pathways in NSun2$^{-/-}$ mice, possibly by inhibiting angiogenin stress pathways to test whether this would impact basal transmission and reverse fEPSPs back to baseline. Conversely, initiating excessive cleavage of tRNA in control animals and investigating if this increases basal transmission would be of interest.

In the same chapter it was shown that the NSun2$^{-/-}$ mice display normal levels of DHPG-LTD but a significant reduction in NMDA-dependent LTD. The cause of this synaptic plasticity deficit is unknown and could involve mis-regulation of any component along the NMDA-LTD pathway, from NMDA receptors to gene expression resulting from the activation of complex intracellular cascades. Investigating the cause and mechanism underlying the deficit would be of interest for future work. One of the difficulties is that there are few clues as to what stage may be altered along the NMDA receptor-gene expression pathway, not only because the effect of NSun2-mediated methylation is unknown, but because the understanding of the neurodevelopmental condition of NSun2-deficiency is still in its infancy. A possible future experiment could involve pharmacological intervention during CA1 hippocampal field recordings to manipulate mTOR activation/inhibition during LTD and comparing fEPSP responses after LTD induction. One of the problems with this is that there is not an obvious indication that mTOR is affected in NSun2$^{-/-}$ mice; NSun2 does target mTOR mRNA for methylation but the mTOR protein may well be unaffected in the mice as this has not yet been investigated. This highlights the difficulty in understanding the mechanisms of the plasticity deficits observed here. For this reason, the initial step of using northern and western blot assays with NSun2$^{-/-}$ hippocampal neurons to determine protein and mRNA levels of NSun2-methylation targets that are also known to be involved in LTD, is essential. Once relevant targets have been identified then manipulating their activity pharmacologically during the *in vitro* hippocampal experiments, as previously explained, would provide a greater chance of success in understanding how NSun2 is affecting this plasticity process.

The reduced NMDA-LTD led to the hypothesis that other NMDA-dependent forms of synaptic plasticity may be affected in NSun2$^{-/-}$ mice. LTP in the CA1 hippocampus was investigated for this reason. Results showed that the absence of NSun2 does indeed also reduce LTP. It is possible that the reduced global translation of the NSun2$^{-/-}$ mouse (Blanco et al., 2014) may contribute to this pathology. It was shown in chapter 4 that CHX blocks LTP in the control mouse but has no effect on their NSun2$^{-/-}$ littermates. The “flooring effect” described previously could be an explanation for this deficit, however LTP could not be maintained in the NSun2$^{-/-}$ mouse regardless of CHX application, and so extracting meaning is difficult. As in the case of the NMDA-LTD deficits, future work to elucidate causes and mechanisms of the LTP deficit in NSun2$^{-/-}$ mice will be important. In both the NMDA-LTD and LTP forms of plasticity, it would be particularly useful to explore NMDA:AMPA receptor ratios as it is possible that a mis-regulation of AMPA receptor trafficking to postsynaptic membranes exists. It was previously reported by Hussain *et al.* (2013) that NSun2$^{-/-}$ may indirectly influence TARPs via vtRNA methylation. It is therefore plausible to suggest that the trafficking of AMPA receptors might be disturbed in the NSun2$^{-/-}$ neurons, and NMDA:AMPA receptor ratios could reveal a deficit, especially if conducted both pre- and post-LTP induction. If these receptor ratios were investigated, it would not reveal the cause leading to AMPA receptor deficits. To further scrutinise the vtRNA theory, TARPs will need to be further analysed in the NSun2$^{-/-}$ mice. Firstly, a western blot assay of hippocampal tissue to evaluate TARP levels relative to control animals should be done. If a deficit were to be observed then a more comprehensive examination would be required, ideally in the form of an in situ hybridisation study to understand where a potential TARP deficit may exist within a cell. Another possible cause that may contribute to the reduced LTP is that the excessive apoptotic pathways that, as explained above, may contribute to the enhanced basal transmission in the NSun2$^{-/-}$ mice reported, may also have a bearing on the reduced LTP. Kamal *et al.* (2018)

demonstrated that excessive stress can lower LTP levels as well as increase basal synaptic transmission. It would be interesting to test whether blocking apoptotic signalling pathways with inhibitors such as anigogenin inhibitor 1 could alleviate some of the plasticity dysfunctions. The possible contribution to stress pathways may involve noradrenaline, a compound released in response to stress from neurons primarily originating in the locus coeruleus (Glavin, 1985) that is a known modulator of LTP (Katsuki et al., 1997). Of note, noradrenaline application to brain slices enhances the translation of a sub-set of mRNAs during LTP (Maity et al., 2015) and it would be worth examining which mRNAs are regulated by noradrenaline and whether they are also methylation targets of NSun2. Rather than investigate the effect of exogenous noradrenaline on LTP in hippocampal slices from NSun2$^{-/-}$ mice, it would be more useful to undertake quantification assays to identify possible deficits; western blot analysis of adrenergic receptors in the hippocampus as well as anatomical study through fluorescence imaging of noradrenergic efferents from the locus coeruleus could provide useful clues.

Aside from dysfunctional TARPs and stress pathways, there could be a whole host of other aspects to investigate. One problem is that currently there is a lack of information available regarding NSun2 and its function; further exploration of the cause of the plasticity deficits are a stab in the dark as any receptor or neuron type in the hippocampus (or other brain regions) may be contributing to the LTP deficit in NSun2$^{-/-}$ mice. Other than monoamine or acetylcholine-containing neurons, another possible candidate for future investigation are GABAergic interneurons, not only because they form a significant proportion of the hippocampal neuronal population, but because previous reports have linked interneurons to plasticity deficits in other intellectual disability models. For example, the FXS mouse model has been found to have a reduction in GABA production, GABA receptor density and an increase in GABA catabolism (Lozano et al., 2014). In fact, GABA modulation is the focus of patient therapy in several intellectual disability disorders including FXS (Lozano et al., 2014),

Down Syndrome (Contestabile et al., 2017) and Rett Syndrome (Chao et al., 2010). As well as this, GABAergic interneurons are explicitly involved in LTP generation via TBS protocols as the feed-forward inhibition is supressed (Larson and Munkácsy, 2015) aiding in the LTP formation in the control mice examined in this thesis. For these reasons, examining GABA receptor levels, GABA reabsorption or GABA catabolism in the hippocampus may provide insights as to whether this system is affected in the NSun2$^{-/-}$ mice. If a deficiency in the GABA system were to be observed, then the next logical step may be to apply exogenous GABA or GABA inhibitors such as picrotoxin to hippocampal slices during LTP induction in an attempt to reverse the deficit.

It is clear that the two forms of plasticity discussed above need to be further investigated, both to understand the molecular mechanisms causing the mis-regulation and to further appreciate how these deficits may affect learning and memory in NSun2-deficient models. Chapter 6 utilised PC12 cell cultures to investigate basic protein behaviour of NSun2. The results verified previous findings that NSun2 and FMRP have high levels of colocalisation (Hussain and Bashir, 2015) in postsynaptic compartments. While such findings are intriguing, a much more detailed study is required to investigate whether any functionally relevant molecular interplay between the proteins actually exists. It would first of all perhaps be important to perform co-immunoprecipitation experiments to confirm physical interaction between the two proteins. miCLIP/iCLIP experiments could also be performed from relevant tissue (i.e. hippocampal) to determine whether NSun2 and FMRP share relevant RNA targets; thus are mRNA targets that are methylated by NSun2 also bound by FMRP? The fact that NSun2 is a protein synthesis promoter (Blanco et al. 2016) while FMRP is a protein synthesis repressor (Darnell et al. 2011), is certainly also interesting; there might also potentially be some investigation into whether FMRP and NSun2 co-operate to regulate the translation of common relevant mRNA targets. Further behavioural studies on the NSun2$^{-/-}$ mouse could also be carried out; a sensible starting point may be by using a fear conditioning paradigm as well as

spatial-learning tasks owing to the previously reports of disruption to protein synthesis leading to impaired performance in spatial memory tasks and fear conditioning (Ozawa, et al., 2017; Yang et al., 2011). The disruption to protein synthesis in Nsun2$^{-/-}$ models previously reported combined with the deficits in LTP observed in this thesis suggests that impairments in these learning tasks are probable in the NSun2$^{-/-}$ mutant mouse model.

Chapter 5 considered intrinsic properties in the NSun2$^{-/-}$ CA1 PNs. The results indicated a faster membrane time constant. This observation could be a result of morphological differences in the CA1 PNs. For example, a membrane may charge faster if there is a decrease in dendritic branching or complexity, a smaller soma or a decrease in spine size or number; further detailed morphological analysis would need to be conducted, for example Golgi staining of CA1 PNs followed by Sholl analysis would provide useful insights into dendrite complexity and branching or measuring the cell body density. Even more useful would be to perform whole cell recordings and fill the cell under examination with biocytin to evaluate the correlation between dendrite complexity and the membrane time constant. Another observation in this chapter was the reduction in SFA in NSun2$^{-/-}$ CA1 PNs. A number of ion channels can contribute to alterations in this property and so a granular analysis of these specific channel densities or their conductance may provide answers to mechanisms causing the increased firing rate. For example, physiological or anatomical examination of KCNQ, HCN1 or ANO2 channels (as discussed in chapter 1.3) may provide an answer to the reduction in SFA observed in NSun2$^{-/-}$ mice.

The findings presented in this thesis provide evidence for mis-regulated plasticity mechanisms and altered intrinsic properties in the hippocampus that might contribute to the symptoms of NSun2-deficiency syndrome. Further extensive research must be carried out to elucidate possible mechanisms

causing the aforementioned deficits, and to determine their actual impact on associated learning and memory phenotypes.

References

Aakalu, G., Smith, W.B., Nguyen, N., Jiang, C., Schuman, E.M., 2001. Dynamic visualization of local protein synthesis in hippocampal neurons. Neuron 30, 489–502.

Abbas, A.K., 2016. Protein Synthesis Inhibitors Did Not Interfere with Long-Term Depression Induced either Electrically in Juvenile Rats or Chemically in Middle-Aged Rats. PLoS One 11, e0161270. https://doi.org/10.1371/journal.pone.0161270

Abbas, A.K., Dozmorov, M., Li, R., Huang, F.S., Hellberg, F., Danielson, J., Tian, Y., Ekström, J., Sandberg, M., Wigström, H., 2009a. Persistent LTP without triggered protein synthesis. Neurosci Res 63, 59–65. https://doi.org/10.1016/j.neures.2008.10.008

Abbas, A.K., Dozmorov, M., Li, R., Huang, F.S., Hellberg, F., Danielson, J., Tian, Y., Ekström, J., Sandberg, M., Wigström, H., 2009b. Persistent LTP without triggered protein synthesis. Neurosci Res 63, 59–65. https://doi.org/10.1016/j.neures.2008.10.008

Abbas, A.K., Villers, A., Ris, L., 2015. Temporal phases of long-term potentiation (LTP): myth or fact? Rev Neurosci 26, 507–46. https://doi.org/10.1515/revneuro-2014-0072

Abbasi-Moheb, L., Mertel, S., Gonsior, M., Nouri-Vahid, L., Kahrizi, K., Cirak, S., Wieczorek, D., Motazacker, M.M., Esmaeeli-Nieh, S., Cremer, K., Weißmann, R., Tzschach, A., Garshasbi, M., Abedini, S.S., Najmabadi, H., Ropers, H.H., Sigrist, S.J., Kuss, A.W., 2012. Mutations in NSUN2 cause autosomal-recessive intellectual disability. Am J Hum Genet 90, 847–55. https://doi.org/10.1016/j.ajhg.2012.03.021

Abdul-Ghani, M.A., Valiante, T.A., Carlen, P.L., Pennefather, P.S., 1996. Metabotropic glutamate receptors coupled to IP3 production mediate inhibition of IAHP in rat dentate granule neurons. J Neurophysiol 76, 2691–700. https://doi.org/10.1152/jn.1996.76.4.2691

Agris, P.F., 2008. Bringing order to translation: the contributions of transfer RNA anticodon-domain modifications. EMBO Rep 9, 629–35. https://doi.org/10.1038/embor.2008.104

Aguilar-Valles, A., Matta-Camacho, E., Khoutorsky, A., Gkogkas, C., Nader, K., Lacaille, J.C., Sonenberg, N., 2015. Inhibition of Group I Metabotropic Glutamate Receptors Reverses Autistic-Like Phenotypes Caused by Deficiency of the Translation Repressor eIF4E Binding Protein 2. J Neurosci 35, 11125–32. https://doi.org/10.1523/JNEUROSCI.4615-14.2015

Aitken, C.E., Lorsch, J.R., 2012. A mechanistic overview of translation initiation in eukaryotes. Nat Struct Mol Biol 19, 568–76. https://doi.org/10.1038/nsmb.2303

Alberini, C.M., Kandel, E.R., 2014. The regulation of transcription in memory consolidation. Cold Spring Harb Perspect Biol 7, a021741. https://doi.org/10.1101/cshperspect.a021741

Alloway, T.P., Alloway, R.G., 2010. Investigating the predictive roles of working memory and IQ in academic attainment. J Exp Child Psychol 106, 20–9. https://doi.org/10.1016/j.jecp.2009.11.003
Amara, S.G., Kuhar, M.J., 1993. Neurotransmitter transporters: recent progress. Annu Rev Neurosci 16, 73–93. https://doi.org/10.1146/annurev.ne.16.030193.000445
Amort, T., Rieder, D., Wille, A., Khokhlova-Cubberley, D., Riml, C., Trixl, L., Jia, X.Y., Micura, R., Lusser, A., 1. Distinct 5-methylcytosine profiles in poly(A) RNA from mouse embryonic stem cells and brain. Genome Biol 18, 1. https://doi.org/10.1186/s13059-016-1139-1
Anderson, P., 2007. The Hippocampus Book. Oxford University Press, Oxford.
Andreassi, C., Riccio, A., 2009. To localize or not to localize: mRNA fate is in 3'UTR ends. Trends Cell Biol 19, 465–74. https://doi.org/10.1016/j.tcb.2009.06.001
Antar, L.N., Afroz, R., Dictenberg, J.B., Carroll, R.C., Bassell, G.J., 2004. Metabotropic glutamate receptor activation regulates fragile x mental retardation protein and FMR1 mRNA localization differentially in dendrites and at synapses. J Neurosci 24, 2648–55. https://doi.org/10.1523/JNEUROSCI.0099-04.2004
Antar, L.N., Dictenberg, J.B., Plociniak, M., Afroz, R., Bassell, G.J., 2005. Localization of FMRP-associated mRNA granules and requirement of microtubules for activity-dependent trafficking in hippocampal neurons. Genes Brain Behav 4, 350–9. https://doi.org/10.1111/j.1601-183X.2005.00128.x
Anwyl, R., 1999. Metabotropic glutamate receptors: electrophysiological properties and role in plasticity. Brain Res Brain Res Rev 29, 83–120.
Ashburner, M., Ball, C.A., Blake, J.A., Botstein, D., Butler, H., Cherry, J.M., Davis, A.P., Dolinski, K., Dwight, S.S., Eppig, J.T., Harris, M.A., Hill, D.P., Issel-Tarver, L., Kasarskis, A., Lewis, S., Matese, J.C., Richardson, J.E., Ringwald, M., Rubin, G.M., Sherlock, G., 2000. Gene ontology: tool for the unification of biology. The Gene Ontology Consortium. Nat Genet 25, 25–9. https://doi.org/10.1038/75556
Auerbach, B.D., Osterweil, E.K., Bear, M.F., 2011. Mutations causing syndromic autism define an axis of synaptic pathophysiology. Nature 480, 63–8. https://doi.org/10.1038/nature10658
Azouz, R., Jensen, M.S., Yaari, Y., 1996. Ionic basis of spike after-depolarization and burst generation in adult rat hippocampal CA1 pyramidal cells. J Physiol 492 (Pt 1), 211–23.
Balschun, D., Manahan-Vaughan, D., Wagner, T., Behnisch, T., Reymann, K.G., Wetzel, W., 1999. A specific role for group I mGluRs in hippocampal LTP and hippocampus-dependent spatial learning. Learn Mem 6, 138–52.
Banko, J.L., Hou, L., Klann, E., 2004. NMDA receptor activation results in PKA- and ERK-dependent Mnk1 activation and increased eIF4E phosphorylation in hippocampal area CA1. J Neurochem 91, 462–70. https://doi.org/10.1111/j.1471-4159.2004.02734.x
Barbour, B., 2014. Electronics for electrophysiologists.

Barondes, S.H., Cohen, H.D., 1967. Delayed and sustained effect of acetoxycycloheximide on memory in mice. Proc Natl Acad Sci U A 58, 157–64.
Barria, A., Muller, D., Derkach, V., Griffith, L.C., Soderling, T.R., 1997. Regulatory phosphorylation of AMPA-type glutamate receptors by CaM-KII during long-term potentiation. Science 276, 2042–5.
Bartlett, T.E., Bannister, N.J., Collett, V.J., Dargan, S.L., Massey, P.V., Bortolotto, Z.A., Fitzjohn, S.M., Bashir, Z.I., Collingridge, G.L., Lodge, D., 2007. Differential roles of NR2A and NR2B-containing NMDA receptors in LTP and LTD in the CA1 region of two-week old rat hippocampus. Neuropharmacology 52, 60–70. https://doi.org/10.1016/j.neuropharm.2006.07.013
Bashir, Z., Kemp, N., 1997. NMDA receptor-dependent and -independent long-term depression in the CA1 region of the adult rat hippocampus in vitro. Neuropharmacology 397–399.
Bashir, Z.I., Collingridge, G.L., 1994. An investigation of depotentiation of longterm potentiation in the CA1 region of the hippocampus. Exp. Brain Res. 100, 437–443. https://doi.org/10.1007/bf02738403
Bassell, G.J., Warren, S.T., 2008. Fragile X syndrome: loss of local mRNA regulation alters synaptic development and function. Neuron 60, 201–14. https://doi.org/10.1016/j.neuron.2008.10.004
Bean, B.P., 2007. The action potential in mammalian central neurons. Nat Rev Neurosci 8, 451–65. https://doi.org/10.1038/nrn2148
Bear, M.F., Huber, K.M., Warren, S.T., 2004. The mGluR theory of fragile X mental retardation. Trends Neurosci 27, 370–7. https://doi.org/10.1016/j.tins.2004.04.009
Beck, H., Yaari, Y., 2008. Plasticity of intrinsic neuronal properties in CNS disorders. Nat Rev Neurosci 9, 357–69. https://doi.org/10.1038/nrn2371
Belliveau, D.J., Bani-Yaghoub, M., McGirr, B., Naus, C.C., Rushlow, W.J., 2006. Enhanced neurite outgrowth in PC12 cells mediated by connexin hemichannels and ATP. J Biol Chem 281, 20920–31. https://doi.org/10.1074/jbc.M600026200
Bellone, C., Lüscher, C., Mameli, M., 2008. Mechanisms of synaptic depression triggered by metabotropic glutamate receptors. Cell Mol Life Sci 65, 2913–23. https://doi.org/10.1007/s00018-008-8263-3
Blanco, S., Dietmann, S., Flores, J.V., Hussain, S., Kutter, C., Humphreys, P., Lukk, M., Lombard, P., Treps, L., Popis, M., Kellner, S., Hölter, S.M., Garrett, L., Wurst, W., Becker, L., Klopstock, T., Fuchs, H., Gailus-Durner, V., Hrabě de Angelis, M., Káradóttir, R.T., Helm, M., Ule, J., Gleeson, J.G., Odom, D.T., Frye, M., 2014. Aberrant methylation of tRNAs links cellular stress to neuro-developmental disorders. EMBO J 33, 2020–39. https://doi.org/10.15252/embj.201489282
Blanco, S., Kurowski, A., Nichols, J., Watt, F.M., Benitah, S.A., Frye, M., 2011. The RNA-methyltransferase Misu (NSun2) poises epidermal stem cells to differentiate. PLoS Genet. 7, e1002403–e1002403. https://doi.org/10.1371/journal.pgen.1002403

Bliss, T.V., Collingridge, G.L., 2013. Expression of NMDA receptor-dependent LTP in the hippocampus: bridging the divide. Mol Brain 6, 5. https://doi.org/10.1186/1756-6606-6-5
Bliss, T.V., Collingridge, G.L., 1993. A synaptic model of memory: long-term potentiation in the hippocampus. Nature 361, 31–9. https://doi.org/10.1038/361031a0
Bliss, T.V., Collingridge, G.L., Morris, R.G., 2014. Synaptic plasticity in health and disease: introduction and overview. Philos Trans R Soc Lond B Biol Sci 369, 20130129. https://doi.org/10.1098/rstb.2013.0129
Bliss, T.V., Lømo, T., 1973. Long-lasting potentiation of synaptic transmission in the dentate area of the unanaestetized rabbit following stimulation of the perforant path. J Physiol 232, 357–74.
Bloomer, W.A., VanDongen, H.M., VanDongen, A.M., 2008. Arc/Arg3.1 translation is controlled by convergent N-methyl-D-aspartate and Gs-coupled receptor signaling pathways. J Biol Chem 283, 582–92. https://doi.org/10.1074/jbc.M702451200
Bodian, D., 1965. A suggestive relationship of nerve cell RNA with specific synaptic sites. Proc Natl Acad Sci U A 53, 418–25.
Bolhuis, J.J., Stewart, C.A., Forrest, E.M., 1994. Retrograde amnesia and memory reactivation in rats with ibotenate lesions to the hippocampus or subiculum. Q J Exp Psychol B 47, 129–50.
Bortolotto, Z.A., Nistico, R., More, J.C., Jane, D.E., Collingridge, G.L., 2005. Kainate receptors and mossy fiber LTP. Neurotoxicology 26, 769–77. https://doi.org/10.1016/j.neuro.2005.02.004
Bramham, C.R., Wells, D.G., 2007. Dendritic mRNA: transport, translation and function. Nat Rev Neurosci 8, 776–89. https://doi.org/10.1038/nrn2150
Bredt, D.S., Nicoll, R.A., 2003. AMPA receptor trafficking at excitatory synapses. Neuron 40, 361–79.
Brigman, J.L., Wright, T., Talani, G., Prasad-Mulcare, S., Jinde, S., Seabold, G.K., Mathur, P., Davis, M.I., Bock, R., Gustin, R.M., Colbran, R.J., Alvarez, V.A., Nakazawa, K., Delpire, E., Lovinger, D.M., Holmes, A., 2010. Loss of GluN2B-containing NMDA receptors in CA1 hippocampus and cortex impairs long-term depression, reduces dendritic spine density, and disrupts learning. J Neurosci 30, 4590–600. https://doi.org/10.1523/JNEUROSCI.0640-10.2010
Brown, D.A., Passmore, G.M., 2009. Neural KCNQ (Kv7) channels. Br J Pharmacol 156, 1185–95. https://doi.org/10.1111/j.1476-5381.2009.00111.x
Brown, J.T., Booth, C.A., Randall, A.D., 2011. Synaptic activation of mGluR1 generates persistent depression of a fast after-depolarizing potential in CA3 pyramidal neurons. Eur J Neurosci 33, 879–89. https://doi.org/10.1111/j.1460-9568.2010.07565.x
Brown, J.T., Randall, A.D., 2009. Activity-dependent depression of the spike after-depolarization generates long-lasting intrinsic plasticity in hippocampal CA3 pyramidal neurons: Persistent plasticity of the hippocampal ADP. J. Physiol. 587, 1265–1281. https://doi.org/10.1113/jphysiol.2008.167007

Brun, V.H., Otnass, M.K., Molden, S., Steffenach, H.A., Witter, M.P., Moser, M.B., Moser, E.I., 2002. Place cells and place recognition maintained by direct entorhinal-hippocampal circuitry. Science 296, 2243–6. https://doi.org/10.1126/science.1071089

Bull, R., Ferrera, E., Orrego, F., 1976. Effects of anisomycin on brain protein synthesis and passive avoidance learning in newborn chicks. J Neurobiol 7, 37–49. https://doi.org/10.1002/neu.480070105

Caldeira, M.V., Melo, C.V., Pereira, D.B., Carvalho, R., Correia, S.S., Backos, D.S., Carvalho, A.L., Esteban, J.A., Duarte, C.B., 2007. Brain-derived neurotrophic factor regulates the expression and synaptic delivery of alpha-amino-3-hydroxy-5-methyl-4-isoxazole propionic acid receptor subunits in hippocampal neurons. J Biol Chem 282, 12619–28. https://doi.org/10.1074/jbc.M700607200

Carlier, E., Sourdet, V., Boudkkazi, S., Déglise, P., Ankri, N., Fronzaroli-Molinieres, L., Debanne, D., 2006. Metabotropic glutamate receptor subtype 1 regulates sodium currents in rat neocortical pyramidal neurons. J Physiol 577, 141–54. https://doi.org/10.1113/jphysiol.2006.118026

Castrén, E., Pitkänen, M., Sirviö, J., Parsadanian, A., Lindholm, D., Thoenen, H., Riekkinen, P.J., 1993. The induction of LTP increases BDNF and NGF mRNA but decreases NT-3 mRNA in the dentate gyrus. Neuroreport 4, 895–8.

Ceman, S., O'Donnell, W.T., Reed, M., Patton, S., Pohl, J., Warren, S.T., 2003. Phosphorylation influences the translation state of FMRP-associated polyribosomes. Hum Mol Genet 12, 3295–305. https://doi.org/10.1093/hmg/ddg350

Chapman, E.R., 2008. How does synaptotagmin trigger neurotransmitter release? Annu Rev Biochem 77, 615–41. https://doi.org/10.1146/annurev.biochem.77.062005.101135

Charpak, S., Gähwiler, B.H., Do, K.Q., Knöpfel, T., 1990. Potassium conductances in hippocampal neurons blocked by excitatory amino-acid transmitters. Nature 347, 765–7. https://doi.org/10.1038/347765a0

Chen, L.Y., Rex, C.S., Babayan, A.H., Kramár, E.A., Lynch, G., Gall, C.M., Lauterborn, J.C., 2010. Physiological activation of synaptic Rac>PAK (p-21 activated kinase) signaling is defective in a mouse model of fragile X syndrome. J Neurosci 30, 10977–84. https://doi.org/10.1523/JNEUROSCI.1077-10.2010

Chen, L.Y., Rex, C.S., Casale, M.S., Gall, C.M., Lynch, G., 2007. Changes in synaptic morphology accompany actin signaling during LTP. J Neurosci 27, 5363–72. https://doi.org/10.1523/JNEUROSCI.0164-07.2007

Chen, X., Yuan, L.L., Zhao, C., Birnbaum, S.G., Frick, A., Jung, W.E., Schwarz, T.L., Sweatt, J.D., Johnston, D., 2006. Deletion of Kv4.2 gene eliminates dendritic A-type K+ current and enhances induction of long-term potentiation in hippocampal CA1 pyramidal neurons. J Neurosci 26, 12143–51. https://doi.org/10.1523/JNEUROSCI.2667-06.2006

Choi, S., Lovinger, D.M., 1996. Metabotropic glutamate receptor modulation of voltage-gated Ca2+ channels involves multiple receptor subtypes in cortical neurons. J Neurosci 16, 36–45.

Chong, F.P., Ng, K.Y., Koh, R.Y., Chye, S.M., 2018. Tau Proteins and Tauopathies in Alzheimer's Disease. Cell Mol Neurobiol 38, 965–980. https://doi.org/10.1007/s10571-017-0574-1
Chuang, S.C., Bianchi, R., Wong, R.K., 2000. Group I mGluR activation turns on a voltage-gated inward current in hippocampal pyramidal cells. J Neurophysiol 83, 2844–53. https://doi.org/10.1152/jn.2000.83.5.2844
Clark, R.E., Broadbent, N.J., Zola, S.M., Squire, L.R., 2002. Anterograde amnesia and temporally graded retrograde amnesia for a nonspatial memory task after lesions of hippocampus and subiculum. J Neurosci 22, 4663–9.
Coan, E.J., Collingridge, G.L., 1985. Magnesium ions block an N-methyl-D-aspartate receptor-mediated component of synaptic transmission in rat hippocampus. Neurosci Lett 53, 21–6.
Coffee, R.L., Williamson, A.J., Adkins, C.M., Gray, M.C., Page, T.L., Broadie, K., 2012. In vivo neuronal function of the fragile X mental retardation protein is regulated by phosphorylation. Hum Mol Genet 21, 900–15. https://doi.org/10.1093/hmg/ddr527
Cohen, H.D., Ervin, F., Barondes, S.H., 1966. Puromycin and cycloheximide: different effects on hippocampal electrical activity. Science 154, 1557–8.
Collingridge, G.L., Isaac, J.T., Wang, Y.T., 2004. Receptor trafficking and synaptic plasticity. Nat Rev Neurosci 5, 952–62. https://doi.org/10.1038/nrn1556
Collingridge, G.L., Kehl, S.J., Loo, R., McLennan, H., 1983. Effects of kainic and other amino acids on synaptic excitation in rat hippocampal slices: 1. Extracellular analysis. Exp Brain Res 52, 170–8.
Collingridge, G.L., Peineau, S., Howland, J.G., Wang, Y.T., 2010. Long-term depression in the CNS. Nat Rev Neurosci 11, 459–73. https://doi.org/10.1038/nrn2867
Connors, B.W., Gutnick, M.J., 1990. Intrinsic firing patterns of diverse neocortical neurons. Trends Neurosci 13, 99–104.
Costes, S.V., Daelemans, D., Cho, E.H., Dobbin, Z., Pavlakis, G., Lockett, S., 2004. Automatic and quantitative measurement of protein-protein colocalization in live cells. Biophys J 86, 3993–4003. https://doi.org/10.1529/biophysj.103.038422
Coultrap, S.J., Bayer, K.U., 2012. CaMKII regulation in information processing and storage. Trends Neurosci 35, 607–18. https://doi.org/10.1016/j.tins.2012.05.003
Crino, P., Khodakhah, K., Becker, K., Ginsberg, S., Hemby, S., Eberwine, J., 1998. Presence and phosphorylation of transcription factors in developing dendrites. Proc Natl Acad Sci U A 95, 2313–8.
Cummings, J.A., Mulkey, R.M., Nicoll, R.A., Malenka, R.C., 1996. Ca2+ signaling requirements for long-term depression in the hippocampus. Neuron 16, 825–33.
Dale, N., Pearson, T., Frenguelli, B.G., 2000. Direct measurement of adenosine release during hypoxia in the CA1 region of the rat hippocampal slice. J Physiol 526 Pt 1, 143–55.

Dale, N., Roberts, A., 1985. Dual-component amino-acid-mediated synaptic potentials: excitatory drive for swimming in Xenopus embryos. J Physiol 363, 35–59.
Dan, Y., Poo, M.M., 2006. Spike timing-dependent plasticity: from synapse to perception. Physiol Rev 86, 1033–48. https://doi.org/10.1152/physrev.00030.2005
Daoudal, G., Debanne, D., 2003. Long-term plasticity of intrinsic excitability: learning rules and mechanisms. Learn Mem 10, 456–65. https://doi.org/10.1101/lm.64103
Darnell, J.C., Klann, E., 2013. The translation of translational control by FMRP: therapeutic targets for FXS. Nat Neurosci 16, 1530–6. https://doi.org/10.1038/nn.3379
Darnell, J.C., Van Driesche, S.J., Zhang, C., Hung, K.Y., Mele, A., Fraser, C.E., Stone, E.F., Chen, C., Fak, J.J., Chi, S.W., Licatalosi, D.D., Richter, J.D., Darnell, R.B., 2011. FMRP stalls ribosomal translocation on mRNAs linked to synaptic function and autism. Cell 146, 247–61. https://doi.org/10.1016/j.cell.2011.06.013
de Mendonça, A., Ribeiro, J.A., 1997. Adenosine and neuronal plasticity. Life Sci 60, 245–51.
Descamps, G., Gomez-Bougie, P., Tamburini, J., Green, A., Bouscary, D., Maïga, S., Moreau, P., Le Gouill, S., Pellat-Deceunynck, C., Amiot, M., 2012. The cap-translation inhibitor 4EGI-1 induces apoptosis in multiple myeloma through Noxa induction. Br J Cancer 106, 1660–7. https://doi.org/10.1038/bjc.2012.139
Di Liegro, C.M., Schiera, G., Di Liegro, I., 2014. Regulation of mRNA transport, localization and translation in the nervous system of mammals (Review). Int J Mol Med 33, 747–62. https://doi.org/10.3892/ijmm.2014.1629
Di Prisco, G.V., Huang, W., Buffington, S.A., Hsu, C.C., Bonnen, P.E., Placzek, A.N., Sidrauski, C., Krnjević, K., Kaufman, R.J., Walter, P., Costa-Mattioli, M., 2014. Translational control of mGluR-dependent long-term depression and object-place learning by eIF2α. Nat Neurosci 17, 1073–82. https://doi.org/10.1038/nn.3754
Diamond, J.S., Bergles, D.E., Jahr, C.E., 1998. Glutamate release monitored with astrocyte transporter currents during LTP. Neuron 21, 425–33.
Dickerson, B., Eichenbaum, H., 2010. The episodic memory system: neurocircuitry and disorders. Neuropsychopharmacology 35, 86–104.
Dingledine, R., Borges, K., Bowie, D., Traynelis, S.F., 1999. The glutamate receptor ion channels. Pharmacol Rev 51, 7–61.
Dobrunz, L.E., Stevens, C.F., 1997. Heterogeneity of release probability, facilitation, and depletion at central synapses. Neuron 18, 995–1008.
Dölen, G., Carpenter, R.L., Ocain, T.D., Bear, M.F., 2010. Mechanism-based approaches to treating fragile X. Pharmacol Ther 127, 78–93. https://doi.org/10.1016/j.pharmthera.2010.02.008
Dolphin, A.C., Errington, M.L., Bliss, T.V., 1982. Long-term potentiation of the perforant path in vivo is associated with increased glutamate release. Nature 297, 496–8.

Doyle, M., Kiebler, M.A., 2011. Mechanisms of dendritic mRNA transport and its role in synaptic tagging. EMBO J 30, 3540–52. https://doi.org/10.1038/emboj.2011.278
Drachman, D.A., 2005. Do we have brain to spare? Neurology 64, 2004–5. https://doi.org/10.1212/01.WNL.0000166914.38327.BB
Drake, C.T., Milner, T.A., Patterson, S.L., 1999. Ultrastructural localization of full-length trkB immunoreactivity in rat hippocampus suggests multiple roles in modulating activity-dependent synaptic plasticity. J Neurosci 19, 8009–26.
Dudek, S.M., Alexander, G.M., Farris, S., 2016. Rediscovering area CA2: unique properties and functions. Nat Rev Neurosci 17, 89–102. https://doi.org/10.1038/nrn.2015.22
Dudek, S.M., Bear, M.F., 1992. Homosynaptic long-term depression in area CA1 of hippocampus and effects of N-methyl-D-aspartate receptor blockade. Proc Natl Acad Sci U A 89, 4363–7.
Duffy, S., Labrie, V., Roder, J.C., 2008. D-serine augments NMDA-NR2B receptor-dependent hippocampal long-term depression and spatial reversal learning. Neuropsychopharmacology 33, 1004–18. https://doi.org/10.1038/sj.npp.1301486
Dunn, K.W., Kamocka, M.M., McDonald, J.H., 2011. A practical guide to evaluating colocalization in biological microscopy. Am J Physiol Cell Physiol 300, C723-42. https://doi.org/10.1152/ajpcell.00462.2010
Eales, K.L., Palygin, O., O'Loughlin, T., Rasooli-Nejad, S., Gaestel, M., Müller, J., Collins, D.R., Pankratov, Y., Corrêa, S.A., 2014. The MK2/3 cascade regulates AMPAR trafficking and cognitive flexibility. Nat Commun 5, 4701. https://doi.org/10.1038/ncomms5701
Edelheit, S., Schwartz, S., Mumbach, M.R., Wurtzel, O., Sorek, R., 2013. Transcriptome-wide mapping of 5-methylcytidine RNA modifications in bacteria, archaea, and yeast reveals m5C within archaeal mRNAs. PLoS Genet 9, e1003602. https://doi.org/10.1371/journal.pgen.1003602
Ekstrom, A.D., Meltzer, J., McNaughton, B.L., Barnes, C.A., 2001. NMDA receptor antagonism blocks experience-dependent expansion of hippocampal "place fields." Neuron 31, 631–8.
El-Hassar, L., Hagenston, A.M., D'Angelo, L.B., Yeckel, M.F., 2011. Metabotropic glutamate receptors regulate hippocampal CA1 pyramidal neuron excitability via Ca^{2+} wave-dependent activation of SK and TRPC channels. J Physiol 589, 3211–29. https://doi.org/10.1113/jphysiol.2011.209783
Faber, E.S., 2010. Functional interplay between NMDA receptors, SK channels and voltage-gated Ca2+ channels regulates synaptic excitability in the medial prefrontal cortex. J Physiol 588, 1281–92. https://doi.org/10.1113/jphysiol.2009.185645
Faber, E.S., Sah, P., 2003. Ca2+-activated K+ (BK) channel inactivation contributes to spike broadening during repetitive firing in the rat lateral amygdala. J Physiol 552, 483–97. https://doi.org/10.1113/jphysiol.2003.050120

Fahiminiya, S., Almuriekhi, M., Nawaz, Z., Staffa, A., Lepage, P., Ali, R., Hashim, L., Schwartzentruber, J., Abu Khadija, K., Zaineddin, S., Gamal, H., Majewski, J., Ben-Omran, T., 2014. Whole exome sequencing unravels disease-causing genes in consanguineous families in Qatar. Clin Genet 86, 134–41. https://doi.org/10.1111/cge.12280

Fan, Y., Fricker, D., Brager, D.H., Chen, X., Lu, H.C., Chitwood, R.A., Johnston, D., 2005. Activity-dependent decrease of excitability in rat hippocampal neurons through increases in I(h). Nat Neurosci 8, 1542–51. https://doi.org/10.1038/nn1568

Fisher, R.A., 1915. On the “probable error” of a coefficient of correlation deduced from a small sample. METRON 1.

Fitzjohn, S.M., Kingston, A.E., Lodge, D., Collingridge, G.L., 1999. DHPG-induced LTD in area CA1 of juvenile rat hippocampus; characterisation and sensitivity to novel mGlu receptor antagonists. Neuropharmacology 38, 1577–83.

Fitzjohn, S.M., Palmer, M.J., May, J.E., Neeson, A., Morris, S.A., Collingridge, G.L., 2001. A characterisation of long-term depression induced by metabotropic glutamate receptor activation in the rat hippocampus in vitro. J Physiol 537, 421–30.

Flexner, J.B., Flexner, L.B., Stellar, E., 1963. Memory in mice as affected by intracerebral puromycin. Science 141, 57–9.

Flexner, L.B., Flexner, J.B., 1966. Effect of acetoxycycloheximide and of an acetoxycycloheximide-puromycin mixture on cerebral protein synthesis and memory in mice. Proc Natl Acad Sci U A 55, 369–74.

Fonseca, R., Nägerl, U.V., Bonhoeffer, T., 2006. Neuronal activity determines the protein synthesis dependence of long-term potentiation. Nat Neurosci 9, 478–80. https://doi.org/10.1038/nn1667

Francesconi, A., Duvoisin, R.M., 2004. Divalent cations modulate the activity of metabotropic glutamate receptors. J Neurosci Res 75, 472–9. https://doi.org/10.1002/jnr.10853

Frye, M., Watt, F.M., 2006. The RNA methyltransferase Misu (NSun2) mediates Myc-induced proliferation and is upregulated in tumors. Curr Biol 16, 971–81. https://doi.org/10.1016/j.cub.2006.04.027

Fu, Y., Dominissini, D., Rechavi, G., He, C., 2014. Gene expression regulation mediated through reversible m^6A RNA methylation. Nat Rev Genet 15, 293–306. https://doi.org/10.1038/nrg3724

Fukao, A., Aoyama, T., Fujiwara, T., 2015. The molecular mechanism of translational control via the communication between the microRNA pathway and RNA-binding proteins. RNA Biol 12, 922–6. https://doi.org/10.1080/15476286.2015.1073436

Furukawa, K., Estus, S., Fu, W., Mark, R.J., Mattson, M.P., 1997. Neuroprotective action of cycloheximide involves induction of bcl-2 and antioxidant pathways. J Cell Biol 136, 1137–49.

Fustin, J.M., Doi, M., Yamaguchi, Y., Hida, H., Nishimura, S., Yoshida, M., Isagawa, T., Morioka, M.S., Kakeya, H., Manabe, I., Okamura, H., 2013. RNA-methylation-dependent RNA processing controls the speed of the

circadian clock. Cell 155, 793–806. https://doi.org/10.1016/j.cell.2013.10.026
Fyhn, M., Hafting, T., Witter, M.P., Moser, E.I., Moser, M.B., 2008. Grid cells in mice. Hippocampus 18, 1230–8. https://doi.org/10.1002/hipo.20472
Gallagher, A., Hallahan, B., 2012. Fragile X-associated disorders: a clinical overview. J Neurol 259, 401–13. https://doi.org/10.1007/s00415-011-6161-3
Gallagher, S.M., Daly, C.A., Bear, M.F., Huber, K.M., 2004. Extracellular signal-regulated protein kinase activation is required for metabotropic glutamate receptor-dependent long-term depression in hippocampal area CA1. J Neurosci 24, 4859–64. https://doi.org/10.1523/JNEUROSCI.5407-03.2004
Garcia, G.A., Goodenough-Lashua, D.M., 1998. Mechanisms of RNA-Modifying and -Editing Enzymes, in Modification and Editing of RNA. Am. Soc. Microbiol.
Garcia, L., Garcia, F., Llorens, F., Unzeta, M., Itarte, E., Gómez, N., 2002. PP1/PP2A phosphatases inhibitors okadaic acid and calyculin A block ERK5 activation by growth factors and oxidative stress. FEBS Lett 523, 90–4.
Gardiol, A., Racca, C., Triller, A., 1999. Dendritic and postsynaptic protein synthetic machinery. J Neurosci 19, 168–79.
Garner, C.C., Tucker, R.P., Matus, A., 1988. Selective localization of messenger RNA for cytoskeletal protein MAP2 in dendrites. Nature 336, 674–7. https://doi.org/10.1038/336674a0
Gereau, R.W., Conn, P.J., 1995. Roles of specific metabotropic glutamate receptor subtypes in regulation of hippocampal CA1 pyramidal cell excitability. J Neurophysiol 74, 122–9. https://doi.org/10.1152/jn.1995.74.1.122
Gereau, R.W., Conn, P.J., 1994. A cyclic AMP-dependent form of associative synaptic plasticity induced by coactivation of beta-adrenergic receptors and metabotropic glutamate receptors in rat hippocampus. J Neurosci 14, 3310–8.
Giese, K.P., Fedorov, N.B., Filipkowski, R.K., Silva, A.J., 1998. Autophosphorylation at Thr286 of the alpha calcium-calmodulin kinase II in LTP and learning. Science 279, 870–3.
Gladding, C.M., Fitzjohn, S.M., Molnár, E., 2009. Metabotropic glutamate receptor-mediated long-term depression: molecular mechanisms. Pharmacol Rev 61, 395–412. https://doi.org/10.1124/pr.109.001735
Gong, R., Park, C.S., Abbassi, N.R., Tang, S.J., 2006. Roles of glutamate receptors and the mammalian target of rapamycin (mTOR) signaling pathway in activity-dependent dendritic protein synthesis in hippocampal neurons. J Biol Chem 281, 18802–15. https://doi.org/10.1074/jbc.M512524200
González-Sánchez, P., Del Arco, A., Esteban, J.A., Satrústegui, J., 2017. Store-Operated Calcium Entry Is Required for mGluR-Dependent Long Term Depression in Cortical Neurons. Front Cell Neurosci 11, 363. https://doi.org/10.3389/fncel.2017.00363

Gottschalk, W.A., Jiang, H., Tartaglia, N., Feng, L., Figurov, A., Lu, B., 1999. Signaling mechanisms mediating BDNF modulation of synaptic plasticity in the hippocampus. Learn Mem 6, 243–56.
Gu, N., Vervaeke, K., Hu, H., Storm, J.F., 2005. Kv7/KCNQ/M and HCN/h, but not KCa2/SK channels, contribute to the somatic medium after-hyperpolarization and excitability control in CA1 hippocampal pyramidal cells. J Physiol 566, 689–715. https://doi.org/10.1113/jphysiol.2005.086835
Gu, N., Vervaeke, K., Storm, J.F., 2007. BK potassium channels facilitate high-frequency firing and cause early spike frequency adaptation in rat CA1 hippocampal pyramidal cells. J Physiol 580, 859–82. https://doi.org/10.1113/jphysiol.2006.126367
Ha, G.E., Cheong, E., 2017. Spike Frequency Adaptation in Neurons of the Central Nervous System. Exp Neurobiol 26, 179–185. https://doi.org/10.5607/en.2017.26.4.179
Hamilton, A., Esseltine, J.L., DeVries, R.A., Cregan, S.P., Ferguson, S.S., 2014. Metabotropic glutamate receptor 5 knockout reduces cognitive impairment and pathogenesis in a mouse model of Alzheimer's disease. Mol Brain 7, 40. https://doi.org/10.1186/1756-6606-7-40
Hay, N., Sonenberg, N., 2004. Upstream and downstream of mTOR. Genes Dev 18, 1926–45. https://doi.org/10.1101/gad.1212704
Hebb, D., 1950. The organization of behavior: A neuropsychological theory 378.
Heine, V.M., Maslam, S., Zareno, J., Joëls, M., Lucassen, P.J., 2004. Suppressed proliferation and apoptotic changes in the rat dentate gyrus after acute and chronic stress are reversible. Eur J Neurosci 19, 131–44.
Heise, C., Gardoni, F., Culotta, L., di Luca, M., Verpelli, C., Sala, C., 2014. Elongation factor-2 phosphorylation in dendrites and the regulation of dendritic mRNA translation in neurons. Front Cell Neurosci 8, 35. https://doi.org/10.3389/fncel.2014.00035
Henke, R.C., Tolhurst, O., Sentry, J.W., Gunning, P., Jeffrey, P.L., 1991. Expression of actin and myosin genes during PC12 cell differentiation. Neurochem Res 16, 675–9.
Hermans, E., Challiss, R.A., 2001. Structural, signalling and regulatory properties of the group I metabotropic glutamate receptors: prototypic family C G-protein-coupled receptors. Biochem J 359, 465–84.
Herrmann, C., Golkaramnay, E., Inman, E., Rome, L., Volknandt, W., 1999. Recombinant major vault protein is targeted to neuritic tips of PC12 cells. J Cell Biol 144, 1163–72.
Herrmann, C., Volknandt, W., Wittich, B., Kellner, R., Zimmermann, H., 1996. The major vault protein (MVP100) is contained in cholinergic nerve terminals of electric ray electric organ. J Biol Chem 271, 13908–15.
Hitti, F.L., Siegelbaum, S.A., 2014. The hippocampal CA2 region is essential for social memory. Nature 508, 88–92. https://doi.org/10.1038/nature13028
Hodgkin, A.L., Huxley, A.F., 1952. A quantitative description of membrane current and its application to conduction and excitation in nerve. J Physiol 117, 500–44.

Hollmann, M., Heinemann, S., 1994. Cloned glutamate receptors. Annu Rev Neurosci 17, 31–108. https://doi.org/10.1146/annurev.ne.17.030194.000335
Holt, C.E., Schuman, E.M., 2013. The central dogma decentralized: new perspectives on RNA function and local translation in neurons. Neuron 80, 648–57. https://doi.org/10.1016/j.neuron.2013.10.036
Hou, L., Klann, E., 2004. Activation of the phosphoinositide 3-kinase-Akt-mammalian target of rapamycin signaling pathway is required for metabotropic glutamate receptor-dependent long-term depression. J Neurosci 24, 6352–61. https://doi.org/10.1523/JNEUROSCI.0995-04.2004
Huang, C.C., You, J.L., Wu, M.Y., Hsu, K.S., 2004. Rap1-induced p38 mitogen-activated protein kinase activation facilitates AMPA receptor trafficking via the GDI.Rab5 complex. Potential role in (S)-3,5-dihydroxyphenylglycene-induced long term depression. J Biol Chem 279, 12286–92. https://doi.org/10.1074/jbc.M312868200
Huang, W.C., Xiao, S., Huang, F., Harfe, B.D., Jan, Y.N., Jan, L.Y., 2012. Calcium-activated chloride channels (CaCCs) regulate action potential and synaptic response in hippocampal neurons. Neuron 74, 179–92. https://doi.org/10.1016/j.neuron.2012.01.033
Huang, Y.S., Jung, M.Y., Sarkissian, M., Richter, J.D., 2002. N-methyl-D-aspartate receptor signaling results in Aurora kinase-catalyzed CPEB phosphorylation and alpha CaMKII mRNA polyadenylation at synapses. EMBO J 21, 2139–48. https://doi.org/10.1093/emboj/21.9.2139
Huber, K.M., Gallagher, S.M., Warren, S.T., Bear, M.F., 2002. Altered synaptic plasticity in a mouse model of fragile X mental retardation. Proc Natl Acad Sci U A 99, 7746–50. https://doi.org/10.1073/pnas.122205699
Huber, K.M., Kayser, M.S., Bear, M.F., 2000. Role for rapid dendritic protein synthesis in hippocampal mGluR-dependent long-term depression. Science 288, 1254–7.
Huber, K.M., Roder, J.C., Bear, M.F., 2001. Chemical induction of mGluR5- and protein synthesis--dependent long-term depression in hippocampal area CA1. J Neurophysiol 86, 321–5.
Hussain, S., Aleksic, J., Blanco, S., Dietmann, S., Frye, M., 2013a. Characterizing 5-methylcytosine in the mammalian epitranscriptome. Genome Biol 14, 215. https://doi.org/10.1186/gb4143
Hussain, S., Bashir, Z.I., 2015. The epitranscriptome in modulating spatiotemporal RNA translation in neuronal post-synaptic function. Front Cell Neurosci 9, 420. https://doi.org/10.3389/fncel.2015.00420
Hussain, S., Benavente, S.B., Nascimento, E., Dragoni, I., Kurowski, A., Gillich, A., Humphreys, P., Frye, M., 2009. The nucleolar RNA methyltransferase Misu (NSun2) is required for mitotic spindle stability. J Cell Biol 186, 27–40. https://doi.org/10.1083/jcb.200810180
Hussain, S., Sajini, A.A., Blanco, S., Dietmann, S., Lombard, P., Sugimoto, Y., Paramor, M., Gleeson, J.G., Odom, D.T., Ule, J., Frye, M., 2013b. NSun2-mediated cytosine-5 methylation of vault noncoding RNA

determines its processing into regulatory small RNAs. Cell Rep 4, 255–61. https://doi.org/10.1016/j.celrep.2013.06.029
Insausti, R., 1993. Comparative anatomy of the entorhinal cortex and hippocampus in mammals. Hippocampus 3 Spec No, 19–26.
Ireland, D.R., Abraham, W.C., 2002. Group I mGluRs increase excitability of hippocampal CA1 pyramidal neurons by a PLC-independent mechanism. J Neurophysiol 88, 107–16. https://doi.org/10.1152/jn.2002.88.1.107
Ito, M., 1986. Long-term depression as a memory process in the cerebellum. Neurosci Res 3, 531–9.
Jackson, R.J., Hellen, C.U., Pestova, T.V., 2010. The mechanism of eukaryotic translation initiation and principles of its regulation. Nat Rev Mol Cell Biol 11, 113–27. https://doi.org/10.1038/nrm2838
Jacquemont, S., Berry-Kravis, E., Hagerman, R., von Raison, F., Gasparini, F., Apostol, G., Ufer, M., Des Portes, V., Gomez-Mancilla, B., 2014. The challenges of clinical trials in fragile X syndrome. Psychopharmacol. Berl 231, 1237–50. https://doi.org/10.1007/s00213-013-3289-0
Jambhekar, A., Derisi, J.L., 2007. Cis-acting determinants of asymmetric, cytoplasmic RNA transport. RNA 13, 625–42. https://doi.org/10.1261/rna.262607
Jia, G., Fu, Y., Zhao, X., Dai, Q., Zheng, G., Yang, Y., Yi, C., Lindahl, T., Pan, T., Yang, Y.G., He, C., 2011. N6-methyladenosine in nuclear RNA is a major substrate of the obesity-associated FTO. Nat Chem Biol 7, 885–7. https://doi.org/10.1038/nchembio.687
Johnstone, V.P., Raymond, C.R., 2011. A protein synthesis and nitric oxide-dependent presynaptic enhancement in persistent forms of long-term potentiation. Learn Mem 18, 625–33. https://doi.org/10.1101/lm.2245911
Jung, M.W., McNaughton, B.L., 1993. Spatial selectivity of unit activity in the hippocampal granular layer. Hippocampus 3, 165–82. https://doi.org/10.1002/hipo.450030209
Kamal, A., Urban, I., Hendrik Gispen, W., 2008. Stress Affects Synaptic Plasticity and Basal Synaptic Transmission in the Rat Hippocampus In Vivo. Adv. Cogn. Neurodynamics ICCN 2007 37–41.
Kandel, E., 2013. Principles of neural science, 5th ed. McGraw-Hill Medical, New York.
Kang, H., Schuman, E.M., 1996. A requirement for local protein synthesis in neurotrophin-induced hippocampal synaptic plasticity. Science 273, 1402–6.
Kang, S.J., Kaang, B.K., 2016. Metabotropic glutamate receptor dependent long-term depression in the cortex. Korean J Physiol Pharmacol 20, 557–564. https://doi.org/10.4196/kjpp.2016.20.6.557
Kato, H.K., Kassai, H., Watabe, A.M., Aiba, A., Manabe, T., 2012. Functional coupling of the metabotropic glutamate receptor, InsP3 receptor and L-type Ca2+ channel in mouse CA1 pyramidal cells. J Physiol 590, 3019–34. https://doi.org/10.1113/jphysiol.2012.232942
Katz, B., Miledi, R., 1968. The role of calcium in neuromuscular facilitation. J Physiol 195, 481–92.

Kauderer, B.S., Kandel, E.R., 2000. Capture of a protein synthesis-dependent component of long-term depression. Proc Natl Acad Sci U A 97, 13342–7. https://doi.org/10.1073/pnas.97.24.13342
Kedersha, N.L., Rome, L.H., 1986. Isolation and characterization of a novel ribonucleoprotein particle: large structures contain a single species of small RNA. J Cell Biol 103, 699–709.
Kelleher, R.J., Bear, M.F., 2008. The autistic neuron: troubled translation? Cell 135, 401–6. https://doi.org/10.1016/j.cell.2008.10.017
Kelso, S.R., Ganong, A.H., Brown, T.H., 1986. Hebbian synapses in hippocampus. Proc Natl Acad Sci U A 83, 5326–30.
Kemp, N., Bashir, Z.I., 1999. Induction of LTD in the adult hippocampus by the synaptic activation of AMPA/kainate and metabotropic glutamate receptors. Neuropharmacology 38, 495–504.
Kerrigan, T.L., Brown, J.T., Randall, A.D., 2014. Characterization of altered intrinsic excitability in hippocampal CA1 pyramidal cells of the Aβ-overproducing PDAPP mouse. Neuropharmacology 79, 515–24. https://doi.org/10.1016/j.neuropharm.2013.09.004
Khan, M.A., Rafiq, M.A., Noor, A., Hussain, S., Flores, J.V., Rupp, V., Vincent, A.K., Malli, R., Ali, G., Khan, F.S., Ishak, G.E., Doherty, D., Weksberg, R., Ayub, M., Windpassinger, C., Ibrahim, S., Frye, M., Ansar, M., Vincent, J.B., 2012. Mutation in NSUN2, which encodes an RNA methyltransferase, causes autosomal-recessive intellectual disability. Am J Hum Genet 90, 856–63. https://doi.org/10.1016/j.ajhg.2012.03.023
Khoddami, V., Cairns, B.R., 2013. Identification of direct targets and modified bases of RNA cytosine methyltransferases. Nat Biotechnol 31, 458–64. https://doi.org/10.1038/nbt.2566
Kickhoefer, V.A., Liu, Y., Kong, L.B., Snow, B.E., Stewart, P.L., Harrington, L., Rome, L.H., 2001. The Telomerase/vault-associated protein TEP1 is required for vault RNA stability and its association with the vault particle. J Cell Biol 152, 157–64.
Kim, J.J., Foy, M.R., Thompson, R.F., 1996. Behavioral stress modifies hippocampal plasticity through N-methyl-D-aspartate receptor activation. Proc Natl Acad Sci U A 93, 4750–3.
Kita, T., Kita, H., Kitai, S.T., 1984. Passive electrical membrane properties of rat neostriatal neurons in an in vitro slice preparation. Brain Res 300, 129–39.
Klyubin, I., Cullen, W.K., Hu, N.W., Rowan, M.J., 2012. Alzheimer's disease Aβ assemblies mediating rapid disruption of synaptic plasticity and memory. Mol Brain 5, 25. https://doi.org/10.1186/1756-6606-5-25
Kole, M.H., Stuart, G.J., 2012. Signal processing in the axon initial segment. Neuron 73, 235–47. https://doi.org/10.1016/j.neuron.2012.01.007
Komara, M., Al-Shamsi, A.M., Ben-Salem, S., Ali, B.R., Al-Gazali, L., 2015. A Novel Single-Nucleotide Deletion (c.1020delA) in NSUN2 Causes Intellectual Disability in an Emirati Child. J Mol Neurosci 57, 393–9. https://doi.org/10.1007/s12031-015-0592-8

Korte, M., Carroll, P., Wolf, E., Brem, G., Thoenen, H., Bonhoeffer, T., 1995. Hippocampal long-term potentiation is impaired in mice lacking brain-derived neurotrophic factor. Proc Natl Acad Sci U A 92, 8856–60.
Kosciuczuk, E.M., Saleiro, D., Platanias, L.C., 2017. Dual targeting of eIF4E by blocking MNK and mTOR pathways in leukemia. Cytokine 89, 116–121. https://doi.org/10.1016/j.cyto.2016.01.024
Koussounadis, A., Langdon, S.P., Um, I.H., Harrison, D.J., Smith, V.A., 2015. Relationship between differentially expressed mRNA and mRNA-protein correlations in a xenograft model system. Sci Rep 5, 10775. https://doi.org/10.1038/srep10775
Kramár, E.A., Lin, B., Lin, C.Y., Arai, A.C., Gall, C.M., Lynch, G., 2004. A novel mechanism for the facilitation of theta-induced long-term potentiation by brain-derived neurotrophic factor. J Neurosci 24, 5151–61. https://doi.org/10.1523/JNEUROSCI.0800-04.2004
Kumar, A., Dhull, D.K., Mishra, P.S., 2015. Therapeutic potential of mGluR5 targeting in Alzheimer's disease. Front Neurosci 9, 215. https://doi.org/10.3389/fnins.2015.00215
Kumar, A., Foster, T.C., 2007. Shift in induction mechanisms underlies an age-dependent increase in DHPG-induced synaptic depression at CA3 CA1 synapses. J Neurophysiol 98, 2729–36. https://doi.org/10.1152/jn.00514.2007
Kwapis, J.L., Helmstetter, F.J., 2014. Does PKM(zeta) maintain memory? Brain Res Bull 105, 36–45. https://doi.org/10.1016/j.brainresbull.2013.09.005
La Camera, G., Rauch, A., Thurbon, D., Lüscher, H.R., Senn, W., Fusi, S., 2006. Multiple time scales of temporal response in pyramidal and fast spiking cortical neurons. J Neurophysiol 96, 3448–64. https://doi.org/10.1152/jn.00453.2006
Lancaster, B., Adams, P.R., 1986. Calcium-dependent current generating the afterhyperpolarization of hippocampal neurons. J Neurophysiol 55, 1268–82. https://doi.org/10.1152/jn.1986.55.6.1268
Lauterborn, J.C., Rex, C.S., Kramár, E., Chen, L.Y., Pandyarajan, V., Lynch, G., Gall, C.M., 2007. Brain-derived neurotrophic factor rescues synaptic plasticity in a mouse model of fragile X syndrome. J Neurosci 27, 10685–94. https://doi.org/10.1523/JNEUROSCI.2624-07.2007
Lebeau, G., Miller, L.C., Tartas, M., McAdam, R., Laplante, I., Badeaux, F., DesGroseillers, L., Sossin, W.S., Lacaille, J.C., 2011. Staufen 2 regulates mGluR long-term depression and Map1b mRNA distribution in hippocampal neurons. Learn Mem 18, 314–26. https://doi.org/10.1101/lm.2100611
Lee, H.K., 2006. Synaptic plasticity and phosphorylation. Pharmacol Ther 112, 810–32. https://doi.org/10.1016/j.pharmthera.2006.06.003
Lee, H.K., Kameyama, K., Huganir, R.L., Bear, M.F., 1998. NMDA induces long-term synaptic depression and dephosphorylation of the GluR1 subunit of AMPA receptors in hippocampus. Neuron 21, 1151–62.
Lee, H.K., Takamiya, K., Han, J.S., Man, H., Kim, C.H., Rumbaugh, G., Yu, S., Ding, L., He, C., Petralia, R.S., Wenthold, R.J., Gallagher, M., Huganir, R.L., 2003. Phosphorylation of the AMPA receptor GluR1 subunit is

required for synaptic plasticity and retention of spatial memory. Cell 112, 631–43.
Lee, J.Y., Lee, L.J., Fan, C.C., Chang, H.C., Shih, H.A., Min, M.Y., Chang, M.S., 2017. Important roles of Vilse in dendritic architecture and synaptic plasticity. Sci Rep 7, 45646. https://doi.org/10.1038/srep45646
Lenz, R.A., Wagner, J.J., Alger, B.E., 1998. N- and L-type calcium channel involvement in depolarization-induced suppression of inhibition in rat hippocampal CA1 cells. J Physiol 512 (Pt 1), 61–73.
Lessmann, V., Gottmann, K., Malcangio, M., 2003. Neurotrophin secretion: current facts and future prospects. Prog Neurobiol 69, 341–74.
Leung, L.S., Fu, X.W., 1994. Factors affecting paired-pulse facilitation in hippocampal CA1 neurons in vitro. Brain Res 650, 75–84.
Levine, E.S., Dreyfus, C.F., Black, I.B., Plummer, M.R., 1995. Brain-derived neurotrophic factor rapidly enhances synaptic transmission in hippocampal neurons via postsynaptic tyrosine kinase receptors. Proc Natl Acad Sci U A 92, 8074–7.
Levy, W.B., Steward, O., 1979. Synapses as associative memory elements in the hippocampal formation. Brain Res 175, 233–45.
Li, H., Ding, J.H., Hu, G., 2003. Group I mGluR ligands fail to affect 6-hydroxydopamine- induced death and glutamate release of PC12 cells. Acta Pharmacol Sin 24, 641–5.
Li, J., Wilkinson, B., Clementel, V.A., Hou, J., O'Dell, T.J., Coba, M.P., 2016. Long-term potentiation modulates synaptic phosphorylation networks and reshapes the structure of the postsynaptic interactome. Sci Signal 9, rs8. https://doi.org/10.1126/scisignal.aaf6716
Li, J.Y., Volknandt, W., Dahlstrom, A., Herrmann, C., Blasi, J., Das, B., Zimmermann, H., 1999. Axonal transport of ribonucleoprotein particles (vaults). Neuroscience 91, 1055–65.
Li, M., Jung, A., Ganswindt, U., Marini, P., Friedl, A., Daniel, P.T., Lauber, K., Jendrossek, V., Belka, C., 2010. Aurora kinase inhibitor ZM447439 induces apoptosis via mitochondrial pathways. Biochem Pharmacol 79, 122–9. https://doi.org/10.1016/j.bcp.2009.08.011
Li, Y., Li, B., Wan, X., Zhang, W., Zhong, L., Tang, S.J., 2012. NMDA receptor activation stimulates transcription-independent rapid wnt5a protein synthesis via the MAPK signaling pathway. Mol Brain 5, 1. https://doi.org/10.1186/1756-6606-5-1
Liao, D., Hessler, N.A., Malinow, R., 1995. Activation of postsynaptically silent synapses during pairing-induced LTP in CA1 region of hippocampal slice. Nature 375, 400–404. https://doi.org/10.1038/375400a0
Lisman, J., Schulman, H., Cline, H., 2002. The molecular basis of CaMKII function in synaptic and behavioural memory. Nat Rev Neurosci 3, 175–90. https://doi.org/10.1038/nrn753
Lisman, J., Yasuda, R., Raghavachari, S., 2012. Mechanisms of CaMKII action in long-term potentiation. Nat Rev Neurosci 13, 169–82. https://doi.org/10.1038/nrn3192
Lu, W., Man, H., Ju, W., Trimble, W.S., MacDonald, J.F., Wang, Y.T., 2001. Activation of synaptic NMDA receptors induces membrane insertion of

new AMPA receptors and LTP in cultured hippocampal neurons. Neuron 29, 243–54.
Lujan, R., Nusser, Z., Roberts, J.D., Shigemoto, R., Somogyi, P., 1996. Perisynaptic location of metabotropic glutamate receptors mGluR1 and mGluR5 on dendrites and dendritic spines in the rat hippocampus. Eur J Neurosci 8, 1488–500.
Lüscher, C., Huber, K.M., 2010. Group 1 mGluR-dependent synaptic long-term depression: mechanisms and implications for circuitry and disease. Neuron 65, 445–59. https://doi.org/10.1016/j.neuron.2010.01.016
Lüscher, C., Malenka, R.C., 2012. NMDA receptor-dependent long-term potentiation and long-term depression (LTP/LTD). Cold Spring Harb Perspect Biol 4. https://doi.org/10.1101/cshperspect.a005710
Lüscher, C., Malenka, R.C., Nicoll, R.A., 1998. Monitoring glutamate release during LTP with glial transporter currents. Neuron 21, 435–41.
Lüthi, A., Wikström, M.A., Palmer, M.J., Matthews, P., Benke, T.A., Isaac, J.T., Collingridge, G.L., 2004. Bi-directional modulation of AMPA receptor unitary conductance by synaptic activity. BMC Neurosci 5, 44. https://doi.org/10.1186/1471-2202-5-44
Lyford, G.L., Yamagata, K., Kaufmann, W.E., Barnes, C.A., Sanders, L.K., Copeland, N.G., Gilbert, D.J., Jenkins, N.A., Lanahan, A.A., Worley, P.F., 1995. Arc, a growth factor and activity-regulated gene, encodes a novel cytoskeleton-associated protein that is enriched in neuronal dendrites. Neuron 14, 433–45.
Lynch, G., Kramar, E.A., Rex, C.S., Jia, Y., Chappas, D., Gall, C.M., Simmons, D.A., 2007. Brain-derived neurotrophic factor restores synaptic plasticity in a knock-in mouse model of Huntington's disease. J Neurosci 27, 4424–34. https://doi.org/10.1523/JNEUROSCI.5113-06.2007
Lynch, G., Larson, J., Kelso, S., Barrionuevo, G., Schottler, F., 1983. Intracellular injections of EGTA block induction of hippocampal long-term potentiation. Nature 305, 719–21.
Lynch, M.A., 2004. Long-term potentiation and memory. Physiol Rev 84, 87–136. https://doi.org/10.1152/physrev.00014.2003
Machnicka, M.A., Milanowska, K., Osman Oglou, O., Purta, E., Kurkowska, M., Olchowik, A., Januszewski, W., Kalinowski, S., Dunin-Horkawicz, S., Rother, K.M., Helm, M., Bujnicki, J.M., Grosjean, H., 2013. MODOMICS: a database of RNA modification pathways--2013 update. Nucleic Acids Res 41, D262-7. https://doi.org/10.1093/nar/gks1007
Magee, J.C., 1999. Dendritic lh normalizes temporal summation in hippocampal CA1 neurons. Nat Neurosci 2, 508–14. https://doi.org/10.1038/9158
Majumder, P., Chatterjee, B., Shen, C.-K.J., 2017. Epitranscriptome and FMRP Regulated mRNA Translation. Epigenomes 1.
Majumder, P., Chu, J.F., Chatterjee, B., Swamy, K.B., Shen, C.J., 2016. Co-regulation of mRNA translation by TDP-43 and Fragile X Syndrome protein FMRP. Acta Neuropathol 132, 721–738. https://doi.org/10.1007/s00401-016-1603-8
Malenka, R.C., Nicoll, R.A., 1999. Long-term potentiation--a decade of progress? Science 285, 1870–4.

Malinow, R., Miller, J.P., 1986. Postsynaptic hyperpolarization during conditioning reversibly blocks induction of long-term potentiation. Nature 320, 529–30. https://doi.org/10.1038/320529a0
Manahan-Vaughan, D., Braunewell, K.H., 2005. The metabotropic glutamate receptor, mGluR5, is a key determinant of good and bad spatial learning performance and hippocampal synaptic plasticity. Cereb Cortex 15, 1703–13. https://doi.org/10.1093/cercor/bhi047
Manita, S., Suzuki, T., Inoue, M., Kudo, Y., Miyakawa, H., 2007. Paired-pulse ratio of synaptically induced transporter currents at hippocampal CA1 synapses is not related to release probability. Brain Res 1154, 71–9. https://doi.org/10.1016/j.brainres.2007.03.089
Martinez, F.J., Lee, J.H., Lee, J.E., Blanco, S., Nickerson, E., Gabriel, S., Frye, M., Al-Gazali, L., Gleeson, J.G., 2012. Whole exome sequencing identifies a splicing mutation in NSUN2 as a cause of a Dubowitz-like syndrome. J Med Genet 49, 380–5. https://doi.org/10.1136/jmedgenet-2011-100686
May-Britt Moser, D.C.R., and Edvard I. Moser, 2015. Place Cells, Grid Cells, and Memory. Perspect. Biol.
McGaugh, J.L., 2000. Memory--a century of consolidation. Science 287, 248–51.
McKee, R.D., Squire, L.R., 1993. On the development of declarative memory. J Exp Psychol Learn Mem Cogn 19, 397–404.
McNaughton, B., 1982. Long-term synaptic enhancement and short-term potentiation in rat fascia dentata act through different mechanisms. J. Physiol. 324, 249–262.
McNaughton, B.L., Barnes, C.A., Meltzer, J., Sutherland, R.J., 1989. Hippocampal granule cells are necessary for normal spatial learning but not for spatially-selective pyramidal cell discharge. Exp Brain Res 76, 485–96.
McNaughton, B.L., Barnes, C.A., O'Keefe, J., 1983. The contributions of position, direction, and velocity to single unit activity in the hippocampus of freely-moving rats. Exp Brain Res 52, 41–9.
McNaughton, B.L., Douglas, R.M., Goddard, G.V., 1978. Synaptic enhancement in fascia dentata: cooperativity among coactive afferents. Brain Res 157, 277–93.
Merkurjev, D., Hong, W.T., Iida, K., Oomoto, I., Goldie, B.J., Yamaguti, H., Ohara, T., Kawaguchi, S.Y., Hirano, T., Martin, K.C., Pellegrini, M., Wang, D.O., 2018. Author Correction: Synaptic N. Nat Neurosci 21, 1493. https://doi.org/10.1038/s41593-018-0219-9
Milior, G., Di Castro, M.A., Sciarria, L.P., Garofalo, S., Branchi, I., Ragozzino, D., Limatola, C., Maggi, L., 12. Electrophysiological Properties of CA1 Pyramidal Neurons along the Longitudinal Axis of the Mouse Hippocampus. Sci Rep 6, 38242. https://doi.org/10.1038/srep38242
Minichiello, L., Korte, M., Wolfer, D., Kühn, R., Unsicker, K., Cestari, V., Rossi-Arnaud, C., Lipp, H.P., Bonhoeffer, T., Klein, R., 1999. Essential role for TrkB receptors in hippocampus-mediated learning. Neuron 24, 401–14.

Mishkin, M., 1978. Memory in monkeys severely impaired by combined but not by separate removal of amygdala and hippocampus. Nature 273, 297–8.
Mockett, B.G., Guévremont, D., Wutte, M., Hulme, S.R., Williams, J.M., Abraham, W.C., 2011. Calcium/calmodulin-dependent protein kinase II mediates group I metabotropic glutamate receptor-dependent protein synthesis and long-term depression in rat hippocampus. J Neurosci 31, 7380–91. https://doi.org/10.1523/JNEUROSCI.6656-10.2011
Moretti, P., Levenson, J.M., Battaglia, F., Atkinson, R., Teague, R., Antalffy, B., Armstrong, D., Arancio, O., Sweatt, J.D., Zoghbi, H.Y., 2006. Learning and memory and synaptic plasticity are impaired in a mouse model of Rett syndrome. J Neurosci 26, 319–27. https://doi.org/10.1523/JNEUROSCI.2623-05.2006
Morishita, W., Connor, J.H., Xia, H., Quinlan, E.M., Shenolikar, S., Malenka, R.C., 2001. Regulation of synaptic strength by protein phosphatase 1. Neuron 32, 1133–48.
Moser, E.I., Kropff, E., Moser, M.B., 2008. Place cells, grid cells, and the brain's spatial representation system. Annu Rev Neurosci 31, 69–89. https://doi.org/10.1146/annurev.neuro.31.061307.090723
Mossink, M.H., van Zon, A., Fränzel-Luiten, E., Schoester, M., Kickhoefer, V.A., Scheffer, G.L., Scheper, R.J., Sonneveld, P., Wiemer, E.A., 2002. Disruption of the murine major vault protein (MVP/LRP) gene does not induce hypersensitivity to cytostatics. Cancer Res 62, 7298–304.
Mossink, M.H., van Zon, A., Scheper, R.J., Sonneveld, P., Wiemer, E.A., 2003. Vaults: a ribonucleoprotein particle involved in drug resistance? Oncogene 22, 7458–67. https://doi.org/10.1038/sj.onc.1206947
Moult, P.R., Corrêa, S.A., Collingridge, G.L., Fitzjohn, S.M., Bashir, Z.I., 2008. Co-activation of p38 mitogen-activated protein kinase and protein tyrosine phosphatase underlies metabotropic glutamate receptor-dependent long-term depression. J Physiol 586, 2499–510. https://doi.org/10.1113/jphysiol.2008.153122
Mulkey, R.M., Endo, S., Shenolikar, S., Malenka, R.C., 1994. Involvement of a calcineurin/inhibitor-1 phosphatase cascade in hippocampal long-term depression. Nature 369, 486–8. https://doi.org/10.1038/369486a0
Mulkey, R.M., Herron, C.E., Malenka, R.C., 1993. An essential role for protein phosphatases in hippocampal long-term depression. Science 261, 1051–5.
Mulkey, R.M., Malenka, R.C., 1992. Mechanisms underlying induction of homosynaptic long-term depression in area CA1 of the hippocampus. Neuron 9, 967–75.
Mumby, D.G., Wood, E.R., Duva, C.A., Kornecook, T.J., Pinel, J.P., Phillips, A.G., 1996. Ischemia-induced object-recognition deficits in rats are attenuated by hippocampal ablation before or soon after ischemia. Behav Neurosci 110, 266–81.
Murthy, V.N., De Camilli, P., 2003. Cell biology of the presynaptic terminal. Annu Rev Neurosci 26, 701–28. https://doi.org/10.1146/annurev.neuro.26.041002.131445

Naie, K., Tsanov, M., Manahan-Vaughan, D., 2007. Group I metabotropic glutamate receptors enable two distinct forms of long-term depression in the rat dentate gyrus in vivo. Eur J Neurosci 25, 3264–75. https://doi.org/10.1111/j.1460-9568.2007.05583.x

Nalavadi, V.C., Muddashetty, R.S., Gross, C., Bassell, G.J., 2012. Dephosphorylation-induced ubiquitination and degradation of FMRP in dendrites: a role in immediate early mGluR-stimulated translation. J Neurosci 32, 2582–7. https://doi.org/10.1523/JNEUROSCI.5057-11.2012

Napoli, I., Mercaldo, V., Boyl, P.P., Eleuteri, B., Zalfa, F., De Rubeis, S., Di Marino, D., Mohr, E., Massimi, M., Falconi, M., Witke, W., Costa-Mattioli, M., Sonenberg, N., Achsel, T., Bagni, C., 2008. The fragile X syndrome protein represses activity-dependent translation through CYFIP1, a new 4E-BP. Cell 134, 1042–54. https://doi.org/10.1016/j.cell.2008.07.031

Narayanan, U., Nalavadi, V., Nakamoto, M., Pallas, D.C., Ceman, S., Bassell, G.J., Warren, S.T., 2007. FMRP phosphorylation reveals an immediate-early signaling pathway triggered by group I mGluR and mediated by PP2A. J Neurosci 27, 14349–57. https://doi.org/10.1523/JNEUROSCI.2969-07.2007

Narayanan, U., Nalavadi, V., Nakamoto, M., Thomas, G., Ceman, S., Bassell, G.J., Warren, S.T., 2008. S6K1 phosphorylates and regulates fragile X mental retardation protein (FMRP) with the neuronal protein synthesis-dependent mammalian target of rapamycin (mTOR) signaling cascade. J Biol Chem 283, 18478–82. https://doi.org/10.1074/jbc.C800055200

Netzeband, J.G., Parsons, K.L., Sweeney, D.D., Gruol, D.L., 1997. Metabotropic glutamate receptor agonists alter neuronal excitability and Ca2+ levels via the phospholipase C transduction pathway in cultured Purkinje neurons. J Neurophysiol 78, 63–75. https://doi.org/10.1152/jn.1997.78.1.63

Neves-Pereira, M., Müller, B., Massie, D., Williams, J.H., O'Brien, P.C., Hughes, A., Shen, S.B., Clair, D.S., Miedzybrodzka, Z., 2009. Deregulation of EIF4E: a novel mechanism for autism. J Med Genet 46, 759–65. https://doi.org/10.1136/jmg.2009.066852

Nicholls, R.E., Alarcon, J.M., Malleret, G., Carroll, R.C., Grody, M., Vronskaya, S., Kandel, E.R., 2008. Transgenic mice lacking NMDAR-dependent LTD exhibit deficits in behavioral flexibility. Neuron 58, 104–17. https://doi.org/10.1016/j.neuron.2008.01.039

Nisticò, R., Mori, F., Feligioni, M., Nicoletti, F., Centonze, D., 2014. Synaptic plasticity in multiple sclerosis and in experimental autoimmune encephalomyelitis. Philos Trans R Soc Lond B Biol Sci 369, 20130162. https://doi.org/10.1098/rstb.2013.0162

Niswender, C.M., Conn, P.J., 2010. Metabotropic glutamate receptors: physiology, pharmacology, and disease. Annu Rev Pharmacol Toxicol 50, 295–322. https://doi.org/10.1146/annurev.pharmtox.011008.145533

Niu, Y., Zhao, X., Wu, Y.S., Li, M.M., Wang, X.J., Yang, Y.G., 2013. N6-methyl-adenosine (m6A) in RNA: an old modification with a novel epigenetic function. Genomics Proteomics Bioinformatics 11, 8–17. https://doi.org/10.1016/j.gpb.2012.12.002

Nolan, M.F., Malleret, G., Dudman, J.T., Buhl, D.L., Santoro, B., Gibbs, E., Vronskaya, S., Buzsáki, G., Siegelbaum, S.A., Kandel, E.R., Morozov, A., 2004. A behavioral role for dendritic integration: HCN1 channels constrain spatial memory and plasticity at inputs to distal dendrites of CA1 pyramidal neurons. Cell 119, 719–32. https://doi.org/10.1016/j.cell.2004.11.020

Nosyreva, E.D., Huber, K.M., 2005. Developmental switch in synaptic mechanisms of hippocampal metabotropic glutamate receptor-dependent long-term depression. J Neurosci 25, 2992–3001. https://doi.org/10.1523/JNEUROSCI.3652-04.2005

Nouranifar, R., Blitzer, R.D., Wong, T., Landau, E., 1998. Metabotropic glutamate receptors limit adenylyl cyclase-mediated effects in rat hippocampus via protein kinase C. Neurosci Lett 244, 101–5.

Nowak, L., Bregestovski, P., Ascher, P., Herbet, A., Prochiantz, A., 1984. Magnesium gates glutamate-activated channels in mouse central neurones. Nature 307, 462–5.

O'Keefe, J., 1999. Do hippocampal pyramidal cells signal non-spatial as well as spatial information? Hippocampus 9, 352–64. https://doi.org/10.1002/(SICI)1098-1063(1999)9:4<352::AID-HIPO3>3.0.CO;2-1

O'Keefe, J., Dostrovsky, J., 1971. The hippocampus as a spatial map. Preliminary evidence from unit activity in the freely-moving rat. Brain Res 34, 171–5.

Oliet, S.H., Malenka, R.C., Nicoll, R.A., 1997. Two distinct forms of long-term depression coexist in CA1 hippocampal pyramidal cells. Neuron 18, 969–82.

O'Mara, S., 2006. Controlling hippocampal output: the central role of subiculum in hippocampal information processing. Behav Brain Res 174, 304–12. https://doi.org/10.1016/j.bbr.2006.08.018

Osterweil, E.K., Krueger, D.D., Reinhold, K., Bear, M.F., 2010. Hypersensitivity to mGluR5 and ERK1/2 leads to excessive protein synthesis in the hippocampus of a mouse model of fragile X syndrome. J Neurosci 30, 15616–27. https://doi.org/10.1523/JNEUROSCI.3888-10.2010

Ostroff, L.E., Cain, C.K., Bedont, J., Monfils, M.H., Ledoux, J.E., 2010. Fear and safety learning differentially affect synapse size and dendritic translation in the lateral amygdala. Proc Natl Acad Sci U A 107, 9418–23. https://doi.org/10.1073/pnas.0913384107

Ozawa, T., Yamada, K., Ichitani, Y., 2017. Differential requirements of hippocampal de novo protein and mRNA synthesis in two long-term spatial memory tests: Spontaneous place recognition and delay-interposed radial maze performance in rats. PLoS One 12, e0171629. https://doi.org/10.1371/journal.pone.0171629

Palacios, I.M., 2007. How does an mRNA find its way? Intracellular localisation of transcripts. Semin Cell Dev Biol 18, 163–70. https://doi.org/10.1016/j.semcdb.2007.01.008

Palmer, C.L., Cotton, L., Henley, J.M., 2005. The molecular pharmacology and cell biology of alpha-amino-3-hydroxy-5-methyl-4-isoxazolepropionic acid receptors. Pharmacol Rev 57, 253–77. https://doi.org/10.1124/pr.57.2.7
Palmer, M.J., Irving, A.J., Seabrook, G.R., Jane, D.E., Collingridge, G.L., 1997. The group I mGlu receptor agonist DHPG induces a novel form of LTD in the CA1 region of the hippocampus. Neuropharmacology 36, 1517–32.
Pang, P.T., Teng, H.K., Zaitsev, E., Woo, N.T., Sakata, K., Zhen, S., Teng, K.K., Yung, W.H., Hempstead, B.L., Lu, B., 2004. Cleavage of proBDNF by tPA/plasmin is essential for long-term hippocampal plasticity. Science 306, 487–91. https://doi.org/10.1126/science.1100135
Paoletti, P., Bellone, C., Zhou, Q., 2013. NMDA receptor subunit diversity: impact on receptor properties, synaptic plasticity and disease. Nat Rev Neurosci 14, 383–400. https://doi.org/10.1038/nrn3504
Park, J.Y., Remy, S., Varela, J., Cooper, D.C., Chung, S., Kang, H.W., Lee, J.H., Spruston, N., 2010. A post-burst after depolarization is mediated by group i metabotropic glutamate receptor-dependent upregulation of Ca(v)2.3 R-type calcium channels in CA1 pyramidal neurons. PLoS Biol 8, e1000534. https://doi.org/10.1371/journal.pbio.1000534
Paspalas, C.D., Perley, C.C., Venkitaramani, D.V., Goebel-Goody, S.M., Zhang, Y., Kurup, P., Mattis, J.H., Lombroso, P.J., 2009. Major vault protein is expressed along the nucleus-neurite axis and associates with mRNAs in cortical neurons. Cereb Cortex 19, 1666–77. https://doi.org/10.1093/cercor/bhn203
Pastalkova, E., Serrano, P., Pinkhasova, D., Wallace, E., Fenton, A.A., Sacktor, T.C., 2006. Storage of spatial information by the maintenance mechanism of LTP. Science 313, 1141–4. https://doi.org/10.1126/science.1128657
Patterson, M.A., Szatmari, E.M., Yasuda, R., 2010. AMPA receptors are exocytosed in stimulated spines and adjacent dendrites in a Ras-ERK-dependent manner during long-term potentiation. Proc Natl Acad Sci U A 107, 15951–6. https://doi.org/10.1073/pnas.0913875107
Patterson, S.L., Abel, T., Deuel, T.A., Martin, K.C., Rose, J.C., Kandel, E.R., 1996. Recombinant BDNF rescues deficits in basal synaptic transmission and hippocampal LTP in BDNF knockout mice. Neuron 16, 1137–45.
Patterson, S.L., Grover, L.M., Schwartzkroin, P.A., Bothwell, M., 1992. Neurotrophin expression in rat hippocampal slices: a stimulus paradigm inducing LTP in CA1 evokes increases in BDNF and NT-3 mRNAs. Neuron 9, 1081–8.
Pedarzani, P., McCutcheon, J.E., Rogge, G., Jensen, B.S., Christophersen, P., Hougaard, C., Strøbaek, D., Stocker, M., 2005. Specific enhancement of SK channel activity selectively potentiates the afterhyperpolarizing current I(AHP) and modulates the firing properties of hippocampal pyramidal neurons. J Biol Chem 280, 41404–11. https://doi.org/10.1074/jbc.M509610200
Peineau, S., Nicolas, C.S., Bortolotto, Z.A., Bhat, R.V., Ryves, W.J., Harwood, A.J., Dournaud, P., Fitzjohn, S.M., Collingridge, G.L., 2009. A systematic investigation of the protein kinases involved in NMDA receptor-dependent

LTD: evidence for a role of GSK-3 but not other serine/threonine kinases. Mol Brain 2, 22. https://doi.org/10.1186/1756-6606-2-22
Persson, H., Kvist, A., Vallon-Christersson, J., Medstrand, P., Borg, A., Rovira, C., 2009. The non-coding RNA of the multidrug resistance-linked vault particle encodes multiple regulatory small RNAs. Nat Cell Biol 11, 1268–71. https://doi.org/10.1038/ncb1972
PhysiologyWeb, 2000. Time course of sodium and potassium permeability during the neuronal action potential [WWW Document]. URL (accessed 1.1.18).
Pi, H.J., Lisman, J.E., 2008. Coupled phosphatase and kinase switches produce the tristability required for long-term potentiation and long-term depression. J Neurosci 28, 13132–8. https://doi.org/10.1523/JNEUROSCI.2348-08.2008
Pierrat, O.A., Mikitova, V., Bush, M.S., Browning, K.S., Doonan, J.H., 2007. Control of protein translation by phosphorylation of the mRNA 5'-cap-binding complex. Biochem Soc Trans 35, 1634–7. https://doi.org/10.1042/BST0351634
Pin, J.P., Galvez, T., Prézeau, L., 2003. Evolution, structure, and activation mechanism of family 3/C G-protein-coupled receptors. Pharmacol Ther 98, 325–54.
Purves D, A.G., Fitzpatrick D, et al., 2001. Neuroscience, 2nd edition. Sinauer Associates.
Racine, R.J., Milgram, N.W., Hafner, S., 1983. Long-term potentiation phenomena in the rat limbic forebrain. Brain Res 260, 217–31.
Rall, W., 1959. Branching dendritic trees and motoneuron membrane resistivity. Exp Neurol 1, 491–527.
Rall, W., 1957. Membrane time constant of motoneurons. Science 126, 454.
Raught, B., Peiretti, F., Gingras, A.C., Livingstone, M., Shahbazian, D., Mayeur, G.L., Polakiewicz, R.D., Sonenberg, N., Hershey, J.W., 2004. Phosphorylation of eucaryotic translation initiation factor 4B Ser422 is modulated by S6 kinases. EMBO J 23, 1761–9. https://doi.org/10.1038/sj.emboj.7600193
Rehbein, M., Wege, K., Buck, F., Schweizer, M., Richter, D., Kindler, S., 2002. Molecular characterization of MARTA1, a protein interacting with the dendritic targeting element of MAP2 mRNAs. J Neurochem 82, 1039–46.
Reimers, J.M., Loweth, J.A., Wolf, M.E., 2014. BDNF contributes to both rapid and homeostatic alterations in AMPA receptor surface expression in nucleus accumbens medium spiny neurons. Eur J Neurosci 39, 1159–69. https://doi.org/10.1111/ejn.12422
Reymann, K.G., Malisch, R., Schulzeck, K., Brödemann, R., Ott, T., Matthies, H., 1985. The duration of long-term potentiation in the CA1 region of the hippocampal slice preparation. Brain Res Bull 15, 249–55.
Richter, J.D., Sonenberg, N., 2005. Regulation of cap-dependent translation by eIF4E inhibitory proteins. Nature 433, 477–80. https://doi.org/10.1038/nature03205

Robinson, R.B., Siegelbaum, S.A., 2003. Hyperpolarization-activated cation currents: from molecules to physiological function. Annu Rev Physiol 65, 453–80. https://doi.org/10.1146/annurev.physiol.65.092101.142734
Rodrigues, S.M., Farb, C.R., Bauer, E.P., LeDoux, J.E., Schafe, G.E., 2004. Pavlovian fear conditioning regulates Thr286 autophosphorylation of Ca2+/calmodulin-dependent protein kinase II at lateral amygdala synapses. J Neurosci 24, 3281–8. https://doi.org/10.1523/JNEUROSCI.5303-03.2004
Rouach, N., Byrd, K., Petralia, R.S., Elias, G.M., Adesnik, H., Tomita, S., Karimzadegan, S., Kealey, C., Bredt, D.S., Nicoll, R.A., 2005. TARP gamma-8 controls hippocampal AMPA receptor number, distribution and synaptic plasticity. Nat Neurosci 8, 1525–33. https://doi.org/10.1038/nn1551
Ruiz, C.R., Shi, J., Meffert, M.K., 2014. Transcript specificity in BDNF-regulated protein synthesis. Neuropharmacology 76 Pt C, 657–63. https://doi.org/10.1016/j.neuropharm.2013.05.004
Sabuncu, M.R., Buckner, R.L., Smoller, J.W., Lee, P.H., Fischl, B., Sperling, R.A., Initiative, A.D.N., 2012. The association between a polygenic Alzheimer score and cortical thickness in clinically normal subjects. Cereb Cortex 22, 2653–61. https://doi.org/10.1093/cercor/bhr348
Saikia, M., Hatzoglou, M., 2015. The Many Virtues of tRNA-derived Stress-induced RNAs (tiRNAs): Discovering Novel Mechanisms of Stress Response and Effect on Human Health. J Biol Chem 290, 29761–8. https://doi.org/10.1074/jbc.R115.694661
Sakita-Suto, S., Kanda, A., Suzuki, F., Sato, S., Takata, T., Tatsuka, M., 2007. Aurora-B regulates RNA methyltransferase NSUN2. Mol Biol Cell 18, 1107–17. https://doi.org/10.1091/mbc.E06-11-1021
Salter, M.W., Kalia, L.V., 2004. Src kinases: a hub for NMDA receptor regulation. Nat Rev Neurosci 5, 317–28. https://doi.org/10.1038/nrn1368
Sanderson, T.M., Hogg, E.L., Collingridge, G.L., Corrêa, S.A., 2016. Hippocampal metabotropic glutamate receptor long-term depression in health and disease: focus on mitogen-activated protein kinase pathways. J Neurochem 139 Suppl 2, 200–214. https://doi.org/10.1111/jnc.13592
Santini, E., Huynh, T.N., Longo, F., Koo, S.Y., Mojica, E., D'Andrea, L., Bagni, C., Klann, E., 2017. Reducing eIF4E-eIF4G interactions restores the balance between protein synthesis and actin dynamics in fragile X syndrome model mice. Sci Signal 10. https://doi.org/10.1126/scisignal.aan0665
Santini, E., Huynh, T.N., MacAskill, A.F., Carter, A.G., Pierre, P., Ruggero, D., Kaphzan, H., Klann, E., 2013. Exaggerated translation causes synaptic and behavioural aberrations associated with autism. Nature 493, 411–5. https://doi.org/10.1038/nature11782
Sargolini, F., Fyhn, M., Hafting, T., McNaughton, B.L., Witter, M.P., Moser, M.B., Moser, E.I., 2006. Conjunctive representation of position, direction, and velocity in entorhinal cortex. Science 312, 758–62. https://doi.org/10.1126/science.1125572

Saugstad, J.A., Marino, M.J., Folk, J.A., Hepler, J.R., Conn, P.J., 1998. RGS4 inhibits signaling by group I metabotropic glutamate receptors. J Neurosci 18, 905–13.
Schaefer, M., 2015. RNA 5-Methylcytosine Analysis by Bisulfite Sequencing. Methods Enzym. 560, 297–329. https://doi.org/10.1016/bs.mie.2015.03.007
Schaefer, M., Kapoor, Jantsch, M.F., 2017. Understanding RNA modifications: the promises and technological bottlenecks of the 'epitranscriptome.' Open Biol. 7.
Schikorski, T., Stevens, C.F., 1997. Quantitative ultrastructural analysis of hippocampal excitatory synapses. J Neurosci 17, 5858–67.
Schnabel, R., Palmer, M.J., Kilpatrick, I.C., Collingridge, G.L., 1999. A CaMKII inhibitor, KN-62, facilitates DHPG-induced LTD in the CA1 region of the hippocampus. Neuropharmacology 38, 605–8.
Schneider-Poetsch, T., Ju, J., Eyler, D.E., Dang, Y., Bhat, S., Merrick, W.C., Green, R., Shen, B., Liu, J.O., 2010. Inhibition of eukaryotic translation elongation by cycloheximide and lactimidomycin. Nat Chem Biol 6, 209–217. https://doi.org/10.1038/nchembio.304
Schoepp, D.D., Jane, D.E., Monn, J.A., 1999. Pharmacological agents acting at subtypes of metabotropic glutamate receptors. Neuropharmacology 38, 1431–76.
Schuman, E.M., Dynes, J.L., Steward, O., 2006. Synaptic regulation of translation of dendritic mRNAs. J Neurosci 26, 7143–6. https://doi.org/10.1523/JNEUROSCI.1796-06.2006
Scoville, W.B., Milner, B., 1957. Loss of recent memory after bilateral hippocampal lesions. J Neurol Neurosurg Psychiatry 20, 11–21.
Sehgal, M., Ehlers, V.L., Moyer, J.R., 2014. Learning enhances intrinsic excitability in a subset of lateral amygdala neurons. Learn Mem 21, 161–70. https://doi.org/10.1101/lm.032730.113
Sehgal, M., Song, C., Ehlers, V.L., Moyer, J.R., 2013. Learning to learn - intrinsic plasticity as a metaplasticity mechanism for memory formation. Neurobiol Learn Mem 105, 186–99. https://doi.org/10.1016/j.nlm.2013.07.008
Shang, Y., Wang, H., Mercaldo, V., Li, X., Chen, T., Zhuo, M., 2009. Fragile X mental retardation protein is required for chemically-induced long-term potentiation of the hippocampus in adult mice. J Neurochem 111, 635–46. https://doi.org/10.1111/j.1471-4159.2009.06314.x
Sharp, P.E., Green, C., 1994. Spatial correlates of firing patterns of single cells in the subiculum of the freely moving rat. J Neurosci 14, 2339–56.
Sheng, M., Kim, M.J., 2002. Postsynaptic signaling and plasticity mechanisms. Science 298, 776–80. https://doi.org/10.1126/science.1075333
Sheridan, G.K., Moeendarbary, E., Pickering, M., O'Connor, J.J., Murphy, K.J., 2014. Theta-burst stimulation of hippocampal slices induces network-level calcium oscillations and activates analogous gene transcription to spatial learning. PLoS One 9, e100546. https://doi.org/10.1371/journal.pone.0100546

Shirasaki, T., Harata, N., Akaike, N., 1994. Metabotropic glutamate response in acutely dissociated hippocampal CA1 pyramidal neurones of the rat. J Physiol 475, 439–53.
Siarey, R.J., Carlson, E.J., Epstein, C.J., Balbo, A., Rapoport, S.I., Galdzicki, Z., 1999. Increased synaptic depression in the Ts65Dn mouse, a model for mental retardation in Down syndrome. Neuropharmacology 38, 1917–20.
Simmons, D.A., Rex, C.S., Palmer, L., Pandyarajan, V., Fedulov, V., Gall, C.M., Lynch, G., 2009. Up-regulating BDNF with an ampakine rescues synaptic plasticity and memory in Huntington's disease knockin mice. Proc Natl Acad Sci U A 106, 4906–11. https://doi.org/10.1073/pnas.0811228106
Slesina, M., Inman, E.M., Moore, A.E., Goldhaber, J.I., Rome, L.H., Volknandt, W., 2006. Movement of vault particles visualized by GFP-tagged major vault protein. Cell Tissue Res 324, 403–10. https://doi.org/10.1007/s00441-006-0158-8
Soderling, T.R., Derkach, V.A., 2000. Postsynaptic protein phosphorylation and LTP. Trends Neurosci 23, 75–80.
Song, I., Huganir, R.L., 2002. Regulation of AMPA receptors during synaptic plasticity. Trends Neurosci 25, 578–88.
Springer, A.D., Schoel, W.M., Klinger, P.D., Agranoff, B.W., 1975. Anterograde and retrograde effects of electroconvulsive shock and of puromycin on memory formation in the goldfish. Behav Biol 13, 467–81.
Squires, J.E., Patel, H.R., Nousch, M., Sibbritt, T., Humphreys, D.T., Parker, B.J., Suter, C.M., Preiss, T., 2012. Widespread occurrence of 5-methylcytosine in human coding and non-coding RNA. Nucleic Acids Res 40, 5023–33. https://doi.org/10.1093/nar/gks144
Stanton, P.K., Winterer, J., Bailey, C.P., Kyrozis, A., Raginov, I., Laube, G., Veh, R.W., Nguyen, C.Q., Müller, W., 2003. Long-term depression of presynaptic release from the readily releasable vesicle pool induced by NMDA receptor-dependent retrograde nitric oxide. J Neurosci 23, 5936–44.
Staubli, U.V., Ji, Z.X., 1996. The induction of homo- vs. heterosynaptic LTD in area CA1 of hippocampal slices from adult rats. Brain Res 714, 169–76.
Su, S.C., Seo, J., Pan, J.Q., Samuels, B.A., Rudenko, A., Ericsson, M., Neve, R.L., Yue, D.T., Tsai, L.H., 2012. Regulation of N-type voltage-gated calcium channels and presynaptic function by cyclin-dependent kinase 5. Neuron 75, 675–87. https://doi.org/10.1016/j.neuron.2012.06.023
Suprenant, K.A., 2002. Vault ribonucleoprotein particles: sarcophagi, gondolas, or safety deposit boxes? Biochemistry (Mosc.) 41, 14447–54.
Sweatt, J.D., 2016. Neural plasticity and behavior - sixty years of conceptual advances. J Neurochem 139 Suppl 2, 179–199. https://doi.org/10.1111/jnc.13580
Takei, N., Sasaoka, K., Inoue, K., Takahashi, M., Endo, Y., Hatanaka, H., 1997. Brain-derived neurotrophic factor increases the stimulation-evoked release of glutamate and the levels of exocytosis-associated proteins in cultured cortical neurons from embryonic rats. J Neurochem 68, 370–5.
Tateno, T., Harsch, A., Robinson, H.P., 2004. Threshold firing frequency-current relationships of neurons in rat somatosensory cortex: type 1 and type 2

dynamics. J Neurophysiol 92, 2283–94. https://doi.org/10.1152/jn.00109.2004
Thandi, S., Blank, J.L., Challiss, R.A., 2002. Group-I metabotropic glutamate receptors, mGlu1a and mGlu5a, couple to extracellular signal-regulated kinase (ERK) activation via distinct, but overlapping, signalling pathways. J Neurochem 83, 1139–53.
Thompson, D.M., Lu, C., Green, P.J., Parker, R., 2008. tRNA cleavage is a conserved response to oxidative stress in eukaryotes. RNA 14, 2095–103. https://doi.org/10.1261/rna.1232808
Todman, D., 2008. Henry Dale and the discovery of chemical synaptic transmission. Eur Neurol 60, 162–4. https://doi.org/10.1159/000145336
Tomita, S., Stein, V., Stocker, T.J., Nicoll, R.A., Bredt, D.S., 2005. Bidirectional synaptic plasticity regulated by phosphorylation of stargazin-like TARPs. Neuron 45, 269–77. https://doi.org/10.1016/j.neuron.2005.01.009
Torre, E.R., Steward, O., 1992. Demonstration of local protein synthesis within dendrites using a new cell culture system that permits the isolation of living axons and dendrites from their cell bodies. J Neurosci 12, 762–72.
Truett, G.E., Heeger, P., Mynatt, R.L., Truett, A.A., Walker, J.A., Warman, M.L., 2000. Preparation of PCR-quality mouse genomic DNA with hot sodium hydroxide and tris (HotSHOT). Biotechniques 29, 52, 54.
Urbanska, A.S., Janusz-Kaminska, A., Switon, K., Hawthorne, A.L., Perycz, M., Urbanska, M., Bassell, G.J., Jaworski, J., 2017. ZBP1 phosphorylation at serine 181 regulates its dendritic transport and the development of dendritic trees of hippocampal neurons. Sci Rep 7, 1876. https://doi.org/10.1038/s41598-017-01963-2
Vasuta, C., Caunt, C., James, R., Samadi, S., Schibuk, E., Kannangara, T., Titterness, A.K., Christie, B.R., 2007. Effects of exercise on NMDA receptor subunit contributions to bidirectional synaptic plasticity in the mouse dentate gyrus. Hippocampus 17, 1201–8. https://doi.org/10.1002/hipo.20349
Vicari, S., 2004. Memory development and intellectual disabilities. Acta Paediatr Suppl 93, 60–3; discussion 63-4.
Vickers, C.A., Dickson, K.S., Wyllie, D.J., 2005. Induction and maintenance of late-phase long-term potentiation in isolated dendrites of rat hippocampal CA1 pyramidal neurones. J Physiol 568, 803–13. https://doi.org/10.1113/jphysiol.2005.092924
Villers, A., Godaux, E., Ris, L., 2012. Long-lasting LTP requires neither repeated trains for its induction nor protein synthesis for its development. PLoS One 7, e40823. https://doi.org/10.1371/journal.pone.0040823
Volk, L.J., Daly, C.A., Huber, K.M., 2006. Differential roles for group 1 mGluR subtypes in induction and expression of chemically induced hippocampal long-term depression. J Neurophysiol 95, 2427–38. https://doi.org/10.1152/jn.00383.2005
von der Brelie, C., Waltereit, R., Zhang, L., Beck, H., Kirschstein, T., 2006. Impaired synaptic plasticity in a rat model of tuberous sclerosis. Eur J Neurosci 23, 686–92. https://doi.org/10.1111/j.1460-9568.2006.04594.x

Walters, B.J., Mercaldo, V., Gillon, C.J., Yip, M., Neve, R.L., Boyce, F.M., Frankland, P.W., Josselyn, S.A., 2017. The Role of The RNA Demethylase FTO (Fat Mass and Obesity-Associated) and mRNA Methylation in Hippocampal Memory Formation. Neuropsychopharmacology 42, 1502–1510. https://doi.org/10.1038/npp.2017.31

Wang, X., He, C., 2014. Dynamic RNA modifications in posttranscriptional regulation. Mol Cell 56, 5–12. https://doi.org/10.1016/j.molcel.2014.09.001

Wang, X., Zhao, B.S., Roundtree, I.A., Lu, Z., Han, D., Ma, H., Weng, X., Chen, K., Shi, H., He, C., 2015. N(6)-methyladenosine Modulates Messenger RNA Translation Efficiency. Cell 161, 1388–99. https://doi.org/10.1016/j.cell.2015.05.014

Watabe, A.M., Carlisle, H.J., O'Dell, T.J., 2002. Postsynaptic induction and presynaptic expression of group 1 mGluR-dependent LTD in the hippocampal CA1 region. J Neurophysiol 87, 1395–403. https://doi.org/10.1152/jn.00723.2001

Weeber, E.J., Jiang, Y.H., Elgersma, Y., Varga, A.W., Carrasquillo, Y., Brown, S.E., Christian, J.M., Mirnikjoo, B., Silva, A., Beaudet, A.L., Sweatt, J.D., 2003. Derangements of hippocampal calcium/calmodulin-dependent protein kinase II in a mouse model for Angelman mental retardation syndrome. J Neurosci 23, 2634–44.

Weiler, I.J., Greenough, W.T., 1991. Potassium ion stimulation triggers protein translation in synaptoneurosomal polyribosomes. Mol Cell Neurosci 2, 305–14.

Weiler, I.J., Irwin, S.A., Klintsova, A.Y., Spencer, C.M., Brazelton, A.D., Miyashiro, K., Comery, T.A., Patel, B., Eberwine, J., Greenough, W.T., 1997. Fragile X mental retardation protein is translated near synapses in response to neurotransmitter activation. Proc Natl Acad Sci U A 94, 5395–400.

Whitlock, J.R., Heynen, A.J., Shuler, M.G., Bear, M.F., 2006. Learning induces long-term potentiation in the hippocampus. Science 313, 1093–7. https://doi.org/10.1126/science.1128134

Widagdo, J., Zhao, Q.Y., Kempen, M.J., Tan, M.C., Ratnu, V.S., Wei, W., Leighton, L., Spadaro, P.A., Edson, J., Anggono, V., Bredy, T.W., 2016. Experience-Dependent Accumulation of N6-Methyladenosine in the Prefrontal Cortex Is Associated with Memory Processes in Mice. J Neurosci 36, 6771–7. https://doi.org/10.1523/JNEUROSCI.4053-15.2016

Winson, J., 1978. Loss of hippocampal theta rhythm results in spatial memory deficit in the rat. Science 201, 160–3.

Wittstock, S., Kaatz, H.H., Menzel, R., 1993. Inhibition of brain protein synthesis by cycloheximide does not affect formation of long-term memory in honeybees after olfactory conditioning. J Neurosci 13, 1379–86.

Wittstock, S., Menzel, R., 1994. Color learning and memory in honey bees are not affected by protein synthesis inhibition. Behav Neural Biol 62, 224–9.

Wong, H.H., Lin, J.Q., Ströhl, F., Roque, C.G., Cioni, J.M., Cagnetta, R., Turner-Bridger, B., Laine, R.F., Harris, W.A., Kaminski, C.F., Holt, C.E., 2017.

RNA Docking and Local Translation Regulate Site-Specific Axon Remodeling In Vivo. Neuron 95, 852-868.e8. https://doi.org/10.1016/j.neuron.2017.07.016

Woo, N.H., Teng, H.K., Siao, C.J., Chiaruttini, C., Pang, P.T., Milner, T.A., Hempstead, B.L., Lu, B., 2005. Activation of p75NTR by proBDNF facilitates hippocampal long-term depression. Nat Neurosci 8, 1069–77. https://doi.org/10.1038/nn1510

Wu, Y., Zinchuk, V., Grossenbacher-Zinchuk, O., Stefani, E., 2012. Critical evaluation of quantitative colocalization analysis in confocal fluorescence microscopy. Interdiscip Sci 4, 27–37. https://doi.org/10.1007/s12539-012-0117-x

Xu, J., Zhu, Y., Contractor, A., Heinemann, S.F., 2009. mGluR5 has a critical role in inhibitory learning. J Neurosci 29, 3676–84. https://doi.org/10.1523/JNEUROSCI.5716-08.2009

Yang, C.H., Huang, C.C., Hsu, K.S., 2011. Generalization of fear inhibition by disrupting hippocampal protein synthesis-dependent reconsolidation process. Neuropsychopharmacology 36, 1992–2008. https://doi.org/10.1038/npp.2011.87

Yang, X., Yang, Y., Sun, B.F., Chen, Y.S., Xu, J.W., Lai, W.Y., Li, A., Wang, X., Bhattarai, D.P., Xiao, W., Sun, H.Y., Zhu, Q., Ma, H.L., Adhikari, S., Sun, M., Hao, Y.J., Zhang, B., Huang, C.M., Huang, N., Jiang, G.B., Zhao, Y.L., Wang, H.L., Sun, Y.P., Yang, Y.G., 2017. 5-methylcytosine promotes mRNA export - NSUN2 as the methyltransferase and ALYREF as an m. Cell Res 27, 606–625. https://doi.org/10.1038/cr.2017.55

Yoshii, A., Constantine-Paton, M., 2010. Postsynaptic BDNF-TrkB signaling in synapse maturation, plasticity, and disease. Dev Neurobiol 70, 304–22. https://doi.org/10.1002/dneu.20765

Yue, C., Remy, S., Su, H., Beck, H., Yaari, Y., 2005. Proximal persistent Na+ channels drive spike afterdepolarizations and associated bursting in adult CA1 pyramidal cells. J Neurosci 25, 9704–20. https://doi.org/10.1523/JNEUROSCI.1621-05.2005

Zalfa, F., Giorgi, M., Primerano, B., Moro, A., Di Penta, A., Reis, S., Oostra, B., Bagni, C., 2003. The fragile X syndrome protein FMRP associates with BC1 RNA and regulates the translation of specific mRNAs at synapses. Cell 112, 317–27.

Zhang, W., Linden, D.J., 2003. The other side of the engram: experience-driven changes in neuronal intrinsic excitability. Nat Rev Neurosci 4, 885–900. https://doi.org/10.1038/nrn1248

Zhang, X., Liu, Z., Yi, J., Tang, H., Xing, J., Yu, M., Tong, T., Shang, Y., Gorospe, M., Wang, W., 2012. The tRNA methyltransferase NSun2 stabilizes p16INK^4 mRNA by methylating the 3'-untranslated region of p16. Nat Commun 3, 712. https://doi.org/10.1038/ncomms1692

Zhao, M.G., Toyoda, H., Ko, S.W., Ding, H.K., Wu, L.J., Zhuo, M., 2005. Deficits in trace fear memory and long-term potentiation in a mouse model for fragile X syndrome. J Neurosci 25, 7385–92. https://doi.org/10.1523/JNEUROSCI.1520-05.2005

Zola, M., Squire, L., Amaral, D., Suzuki, W., 1989. Lesions of perirhinal and parahippocampal cortex that spare the amygdala and hippocampal formation produce severe memory impairment. J. Neurosci. 9, 4355–4370.
Zola, S.M., Squire, L.R., Teng, E., Stefanacci, L., Buffalo, E.A., Clark, R.E., 2000. Impaired recognition memory in monkeys after damage limited to the hippocampal region. J Neurosci 20, 451–63.